Atmospheric General Circulation and Transport of Radioactive Debris

By
J.D. Mahlman

Technical Paper No. 103
Department of Atmospheric Science
Colorado State University
Fort Collins, Colorado

Colorado State University

Department of Atmospheric Science

Paper No. 103

ATMOSPHERIC GENERAL CIRCULATION AND TRANSPORT OF RADIOACTIVE DEBRIS

by
J. D. Mahlman
Colorado State University

This Report was Prepared with Support from
Contract AT(11-1)-1340 with the
U. S. Atomic Energy Commission,
Principal Investigator, Elmar R. Reiter

Department of Atmospheric Science
Colorado State University
Fort Collins, Colorado

September 1966

Atmospheric Science Paper No. 103

ABSTRACT

In this study an attempt is made to explain the physical bases for seasonal and short-term radioactive fallout variations. Previous investigations have shown that large amounts of contaminated stratospheric air enter the troposphere in association with pronounced cyclogenesis at jet stream level. The validity of this mechanism is verified by a statistical analysis of fallout changes compared with 300 mb circulation variations over a two-year period. These analyses also demonstrated that it is not possible to explain the spring fallout peaks on the basis of increased stratospheric-tropospheric mass exchange at that time of the year. It is concluded that the seasonal variation results from characteristics of the stratospheric circulation.

As a way of examining the above conclusion, various aspects of the stratospheric transport problem are investigated. Detailed eddy covariance values at 50°, 60°, and 70°N are computed from 10 January to 20 February 1958 with particular emphasis on the correlation between eddy meridional and vertical wind components. The results indicate that this eddy correlation becomes strongly negative after the polar night vortex breakdown, thus providing a powerful mechanism for northward and downward debris transport in late winter.

In order to examine the effect of mean debris transport relative to the above eddy mechanism, a computation of the mean meridional cell in the polar night stratosphere is performed by employing a heat budget method. This computation reveals that the mean cell operates in the indirect sense over the chosen period. It is shown conclusively that eddy temperature flux provides the predominate mechanism for the large temperature increases during the breakdown of the polar night vortex. A computation of mean vertical velocities using a curvilinear

system oriented along a line of maximum circulation shows that the mean cell operates in the direct sense relative to this reference frame.

As an approach to problems of vertical transport in the lower stratosphere, a comparison is made between the mean amplitude of the vertical motion field at 100 mb and circulation changes at 300 mb. It is shown that the more zonal the circulation at 300 mb, the greater the mean absolute value of the vertical motion field at 100 mb.

In order to investigate the contributions of different motion scales to total stratospheric debris transport, trajectories are determined for the period during and after the polar night vortex breakdown. It is seen that a pronounced descending motion is associated with northward displacements. Also, trajectory calculations demonstrate that directional wind shear with height may provide a dynamical mechanism for the apparent total ozone maximum at the base of troughs in the stratosphere.

Finally, a linear model incorporating the combined dynamic effects of lateral and vertical shear is constructed to analyze the behavior of the polar night vortex. The results show that a necessary condition for instability is that the meridional gradient of potential vorticity must vanish somewhere on an isentropic surface. This criterion is then applied to the polar vortex for each month from July 1957 to February 1958 and it is shown that this circulation becomes quasi-unstable after October 1957. A comparison is made between the Arctic and Antarctic vortices and reveals that the Antarctic vortex is considerably more stable. It is concluded that this theory may help to explain the differences between the Arctic and Antarctic stratospheric circulations.

J. D. Mahlman
Department of Atmospheric Science
Colorado State University
August 1966

ACKNOWLEDGEMENTS

The author particularly welcomes the opportunity to express his appreciation and gratitude to Professor Elmar R. Reiter for the continuing guidance and inspiration he gave over the several years that this study was in progress. He especially wishes to thank Sandra Olson who assisted in computations and typed the manuscript, Howard Hubbs who performed the drafting, and William Ehrman who assisted with a large portion of the computations and programming. Over the period of the study various aspects of the computations were performed by Donald Beran, Donald Davidson, Marilyn Davidson, Richard Dirks, Marvin Glasser, and Gene Wooldridge.

This research was sponsored by the Atomic Energy Commission under Contract Number AT(11-1)-1340. Most of the material in Chapter IV was also contained in Mahlman (1965a), a portion of the yearly report under Contract No. AT(11-1)-1340 to the Atomic Energy Commission.

This material is based upon a dissertation submitted as partial fulfillment of the requirements for the Doctor of Philosophy degree at Colorado State University.

TABLE OF CONTENTS

Table of Contents - Cont.

LIST OF TABLES

LIST OF FIGURES

List of Figures - Cont.

List of Figures - Cont.

LIST OF SYMBOLS

a = wave amplitude

A^* = area between two latitude circles

$A(y, \ln\theta)$, $B(y, \ln\theta)$, $C(y, \ln\theta)$, $D(y, \ln\theta)$ = coefficients to exponential wave solutions

$c = c_r + i c_r$ = wave speed

C = cyclone index

c_p = specific heat of air at constant pressure

dd = wind direction

f = Coriolis parameter

g = constant of gravitation

h = heat per unit mass

hl = radioactive half life

$i = (-1)^{\frac{1}{2}}$

I = radioactive fallout intensity

L = wavelength

$M = c_p T + gz$ = Montgomery stream function

n = coordinate direction normal to streamline

p = pressure

$$P = \text{potential vorticity} = -\frac{\frac{\partial v}{\partial x_\theta} - \frac{\partial u}{\partial y_\theta} + f}{\frac{\partial p}{\partial \ln\theta}}$$

$P^* = \theta P$

r = correlation coefficient

R = gas constant for dry air

R_s = radius of curvature of streamline

s = coordinate direction along streamline

t = time

T = temperature

$u = \frac{dx}{dt}$ = zonal wind component

$\bar{u}$ = zonal wind component averaged around a latitude circle

$v = \frac{dy}{dt}$ = meridional wind component

$\bar{v}$ = meridional wind component averaged around a latitude circle

$\vec{V} = (u^2 + v^2)^{\frac{1}{2}}$ = horizontal vector wind

$V^2/2$ = kinetic energy per unit mass

V_s = wind component along streamline

$w = \frac{dz}{dt}$ = vertical wind component

$\bar{w}$ = mean w around a latitude circle

$\tilde{w}$ = mean w over an area

x, y, z = Cartesian coordinates

Z = percentage of long-lived radioactivity in sample

α = specific volume

$\beta = \frac{\partial f}{\partial y}$ = Rossby parameter

γ = dd - 270^{o}

$\Gamma = -\frac{g}{c_p}$ = adiabatic lapse rate

ζ_a = absolute vorticity

θ = potential temperature

$\kappa = \frac{R}{c_p}$

$\mu = \frac{2\pi}{L}$ = wave number

$\xi_1 = (u - c_r)/[(u - c_r)^2 + c_i^2]$

$\xi_2 = c_i/[(u - c_r)^2 + c_i^2]$

π = 3.14159···.

ϕ = latitude

$\omega = \frac{dp}{dt}$ = vertical motion in a pressure coordinate system

Ω = earth's angular velocity = 7.29×10^{-5} radian sec^{-1}

∇ = two-dimensional del operator

$\overline{}$ = average around a latitude circle

$\sim$ = average over an area

$\rightarrow$ = denotes a vector when used above a symbol

INTRODUCTION

I. REVIEW OF RELEVANT MEASUREMENTS

With the advent of nuclear weapons testing in the atmosphere, it was noted that the resultant distribution of nuclear debris from these tests displayed characteristics of a highly varied and unusual nature. At that time the observations could not be explained on the basis of known properties of the atmosphere's general circulation. Furthermore, due to the sporadic nature of the tests and the incomplete monitoring of the released radioactivity on a global scale, mean transport characteristics could not be established on either a seasonal or short-term basis. With the increased capabilities of the radioactivity monitoring networks in recent years, it now appears feasible to deduce mean debris transport properties on a seasonal and planetary scale.

During the first thermonuclear weapons tests, large amounts of radioactive debris were injected into the stratosphere for the first time. At that time it was assumed that this debris would remain within the stratosphere for long periods of time before being depleted by small-scale diffusion process and natural radioactive decay. However, unexpectedly large concentrations of fallout continued to appear at the earth's surface for long periods of time after thermonuclear testing had terminated. By calculating ratios of strontium-89 (half-life 50.5 days) and strontium-90 (half-life 10,120 days) Stewart et al. (1957) argued that these fallout peaks contained debris which must have recently been in the stratosphere. This inference was based on the assumption that the mean debris residence time is of the order of 30-40 days in the troposphere (Stewart, Crooks, and Fisher, 1955).

This necessitated that the mean residence time of debris in the stratosphere be somewhat shorter than originally believed. One of the first values was given by Libby (1956) who estimated that the mean stratospheric debris time was of the order of five to ten years. This figure was based on the assumption that the debris would be completely and uniformly mixed in the stratosphere soon after debris release. It was then stated that the debris enters the troposphere by "uniform mixing" and by consequence its deposition is highly correlated with precipitation regions. It will be demonstrated that this hypothesis is untenable on many accounts. Through actual flight measurements Machta and List (1959) were able to show that debris concentrations are extremely variable in the stratosphere. On this basis they postulated a mean residence time of less than five years. They did acknowledge, however, that this model is too simple and that one must take differences in season, altitude, and latitude into account. On the basis of more complete information, Libby (1959) altered his earlier estimate to a figure of five years for the tropical stratosphere and one year for the polar regions. Without considering altitude of debris injection this estimate seems to be reasonable in terms of current evidence.

Because radioactivity measurements were only taken at isolated places prior to the 1960's, the results determined from them may lack generality as far as the entire globe is concerned. This is particularly true if it is found that mass and debris are not uniformly mixed into the troposphere as postulated by Libby but enter discretely as a result of dynamic processes (Staley, 1960). In spite of this, however, in 1955, 1956, 1957, well-pronounced spring maxima were measured at Milford Haven, Wales (Machta, 1957). Machta also showed that the mean debris deposition was very strongly-latitude dependent with a pronounced peak at 40^{o}N with a peak of lesser intensity at 40^{o}S. Martell (1959) deduced

that this sharp peak at 40°N was simply the result of preferential injection of debris at these latitudes and that a mid-latitude peak would not occur after a debris injection in the tropical stratosphere. On the other hand, more recent measurements indicate that a mid-latitude maximum also exists for ozone mixing ratio at the earth's surface (Hering, 1964). Since most ozone is produced photochemically in low latitudes, it appears that Martell's hypothesis in untenable and that the mid-latitude maximum is a fundamental characteristic of planetary scale debris deposition. Also, Lockhart et al. (1960) show a pronounced peak in gross fission products at 35°N during 1959. The mid-latitude maximum was further substantiated by Tauber (1961) who demonstrated that a mid-latitude maximum of carbon-14 probably existed as a regular feature before the advent of nuclear testing.

Studies of cesium-137 (half-life 11,150 days) measurements taken at Rijswijk, The Netherlands, documented spring increases for every year from 1957 to 1960 (Bleichrodt, Blok, and Dekker, 1961; Bleichrodt, Blok, and Van Abkoude, 1961). As a result of the wide variation in amplitude of the fallout measurements from year to year, the authors concluded that the spring peak is meteorologically produced but that the actual intensities are dependent upon yearly variations in the stratospheric burden.

Libby and Palmer (1960) showed that a striking spring peak existed in 1959 as a result of the Soviet October tests during the previous year. They also noted a pronounced latitudinal maximum at 35°N. Utilizing chemical dating methods, Fry, Jew, and Kuroda (1960) concluded that the 1959 spring peak contained debris which was older than could be explained by the Soviet tests. At Argonne National Laboratory measurements of cesium-137 revealed a pronounced increase from April to June 1960, although no nuclear tests had taken place the previous year (Gustafson, Brar, and Kerrigan, 1961) (Fig. 1). Also, analysis of bomb-produced tritium revealed

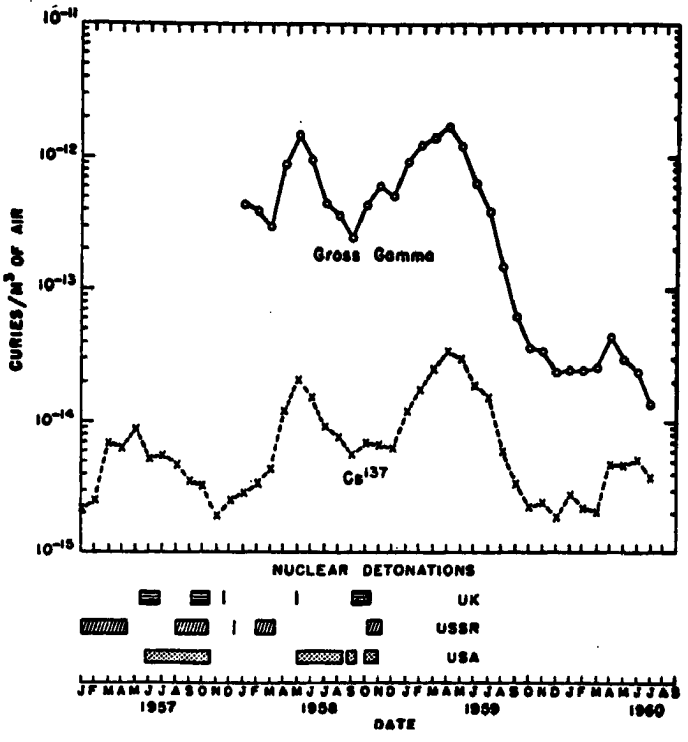

FIG. 1. Concentration of fission products in surface air at Argonne National Laboratory (Gustafson, Brar, and Kerrigan, 1961).

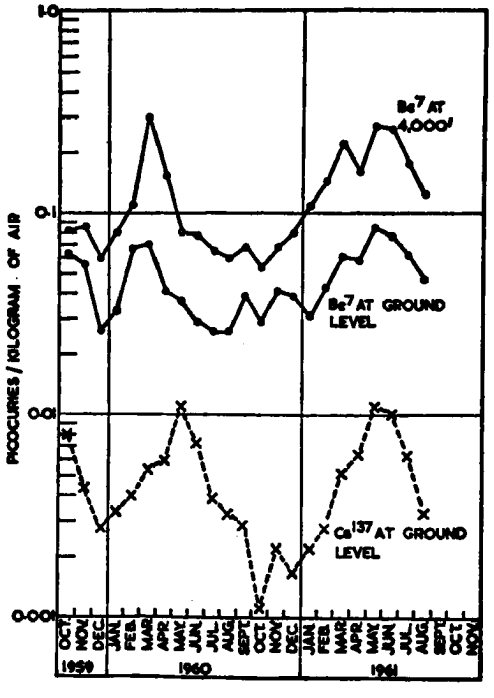

FIG. 2. Seasonal concentration of beryllium-7 and cesium-137 in picocuries per kilogram of air over Great Britain (Peirson, 1963).

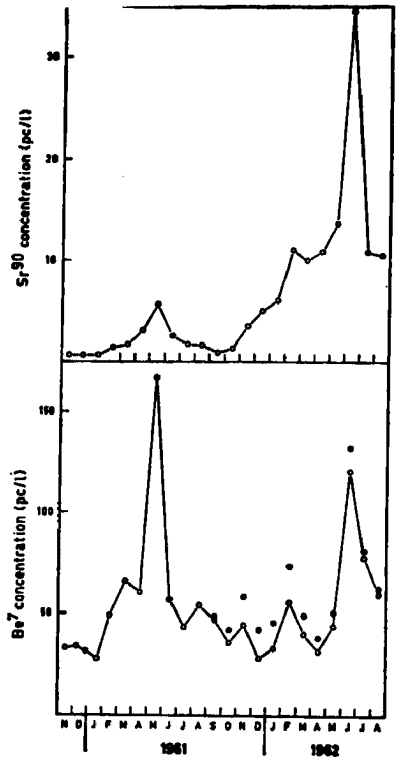

FIG. 3. Seasonal concentration of beryllium-7 and strontium-90 in rain water at Rijswijk, The Netherlands. Total beryllium-7 is represented by solid circles, natural beryllium-7 by open circles (Bleichrodt and Van Abkoude, 1963).

spring peaks in 1958, 1959, and 1960, which are very similar to profiles from the strontium-90 measurements (Libby, 1961). Pierson (1963) showed distinct peaks in beryllium-7 and cesium-137 over Great Britain in March 1960 and May 1961 (Fig. 2).

A study by Bleichrodt and Van Abkoude (1963) at Rijswijk, The Netherlands, was concerned with seasonal variations in intensity of beryllium-7. A well-pronounced seasonal dependence was noted for this naturally produced isotope, with an unmistakable spring maximum (Fig. 3). This is particularly significant because natural beryllium-7 is produced only in the upper atmosphere by cosmic ray bombardment. Thus, it may be concluded that the surface seasonal variation of this tracer element is directly dependent upon the atmospheric mechanisms acting to transport mass within the stratosphere, through the vicinity of the tropopause and within the troposphere.

Thus, it appears almost without doubt that the mid-latitude peak and the spring fallout maximum are distinct physical phenomena resulting from seasonal and short-term characteristics of the general circulation of the stratosphere.

II. PURPOSE

In view of the above mentioned characteristics of fallout deposition at the earth's surface, it is evident that these geophysical phenomena require an explanation in terms of the characteristics of the environment which produces them. As a consequence of this necessity, the purpose of this research is to explain on a physically consistent basis the above fallout deposition characteristics. This investigation will be in terms of a rather comprehensive investigation of general circulation properties in the upper troposphere and lower to middle stratosphere which are thought to be of particular relevance to this problem. The paper will be divided into two main sections. The first section will review previous results and deal with the problem of mass exchange between the stratosphere and troposphere. No attempt whatsoever will be made in this work to reconcile the micro- and meso-scale characteristics of surface fallout deposition and their relation to precipitation processes. This is an area of sufficient complexity to deserve a separate complete treatment.

The second section will be concerned with the problems of debris transport within the stratosphere itself. Special emphasis will be placed upon the transport properties and energetics of the polar stratosphere, the behavior of the lower stratosphere during times of maximum stratospheric-tropospheric mass exchange, mean meridional cells in the stratosphere, the breakdown of the polar night vortex, and ozone transport mechanisms. Also an attempt will be made to find a consistent physical and mathematical theory capable of satisfactorily explaining the breakdown of the polar night vortex.

Finally, an attempt will be made to unify the results obtained into a consistent physical explanation of the observed fallout deposition

characteristics. It is hoped that this will contribute to an improvement and more thorough understanding of mathematical fallout and ozone models similar to those originally attempted on semi-empirical bases by Friend et al. (1961, 1962), Friend and Feely (1962), Prabhakara (1963), Lettau and Lettau (1964), and Prawitz (1964).

PART A

MASS EXCHANGE BETWEEN STRATOSPHERE AND TROPOSPHERE

III. MECHANISMS OF STRATOSPHERIC-TROPOSPHERIC MASS EXCHANGE

Since it was first realized that surface fallout peaks occurring long periods of time after cessation of thermonuclear testing must be of stratospheric origin (Stewart et al., 1955, 1957), several diverse opinions as to the predominate physical mechanisms have been advanced. Libby (1956) assumed that stratospheric debris enters the troposphere at uniform rates and is then removed by precipitation scavenging processes (Greenfield, 1957; Kruger and Hosler, 1963; Engelmann, 1965; Reiter and Mahlman, 1965a).

According to Stewart et al. (1957) the spring peak is due to a more rapid downward mixing through the tropopause at this time of year. Also, the mid-latitude peak is alleged to be due to a "selective zone of downward mixing at middle latitudes". Martell and Drevinsky (1960) contended that debris is removed from the stratosphere by subsidence or intensified mixing in the spring and that the large difference between subtropical and polar rains results from precipitation scavenging along the polar front.

By correlating surface radioactivity increases with mid-tropospheric weather types, Miyake et al. (1960, 1962, 1963) discovered that a strong relationship existed between fallout increases and a cyclone aloft at 500 mb. As a result of this, they hypothesized that descent of stratospheric air occurs to the rear of high level cyclones.

It was first demonstrated by Reed and Sanders (1953) and by Reed (1955) that stratospheric air can enter the troposphere in association with intense frontal zones in the vicinity of jet streams. This was further substantiated by numerous other authors with

detailed analyses of air motions in the vicinity of the "jet stream front" (Endlich and McLean, 1957; Danielsen, 1959a, b, 1964a, b; Danielsen, Bergman, and Paulson, 1962; Reed and Danielsen, 1959; Staley, 1960, 1962; Reiter, 1963a, b, 1964; Reiter and Mahlman, 1964, 1965b; Mahlman, 1964a, b).

By consideration of their "waterspout" model of the upper tropospheric frontal zone, Reed and Danielsen (1959) concluded that a "folding" of the tropopause was the mechanism which produced intrusions of stratospheric air into the troposphere. Reiter (1963b) studied this type of exchange through the "jet stream front" and corroborated the validity of this transport process through an actual trajectory analysis. Some investigators (Staley, 1962; Danielsen, Bergman, and Paulson, 1962; Danielsen, 1964b) have shown through flight measurements that higher values of radioactivity are associated with this high level frontal zone.

In a paper by Storebø (1959) it was suggested that the exchange might be due to cyclonic eddies in the subtropical jet stream, thus creating maximum transport in late winter. He later altered this stand to state that the spring fallout maximum is due to the winter breakdown of the polar night vortex in the upper stratosphere (Storebø, 1960). This view is in accord with that presented by Libby and Palmer (1960).

Staley (1960) traced trajectories of air parcels along isentropic surfaces which were common to both stratosphere and troposphere. This study clearly documented that it is physically possible for air parcels to leave the stratosphere and descend to within a short distance from the surface of the earth. This mechanism is the same as proposed by other investigators (Reed and Sanders, 1953; Reed, 1955; Reed and Danielsen, 1959; Danielsen, 1959a, b; Reiter, 1963a) but Staley further states that the descent is associated with high level cyclones. He also notes that the tropopause reforming at a higher

altitude will result in a net transport of stratospheric air into the troposphere. If these hypotheses are correct, it is conceivable that either or both of the above mechanisms could account for the observed seasonal radioactivity changes.

As a way of testing Staley's (1960, 1962) hypothesis that the transport of mass into the troposphere is associated with high level cyclones, a pronounced surface increase of long-lived (age > 100 days) radioactivity was studied by the author (Mahlman, 1964a, b, 1965). To determine the origin of the air producing the increase, backward isentropic trajectories were traced from the region by an objective method similar to that first suggested by Danielsen (1961).

The trajectory analysis revealed that the fallout producing air was stratospheric in origin. The air had descended from the cyclonic stratosphere into the troposphere in the vicinity of the "jet stream front" under quasi-conservation of potential vorticity. It was noted that the sinking phenomenon occurs in association with pronounced cyclogenesis at tropopause level. This characteristic of the exchange process was also noted by Danielsen (1964a) at the same time that the above results were first published.

The cyclogenetic mechanism was put on a still firmer basis with subsequent case studies (Reiter and Mahlman, 1964, 1965b, c). It was also noted that the amount of mass involved in the descent appears to be related to the intensity of cyclogenetic activity at this level.

IV. STATISTICAL CHARACTERISTICS OF THE EXCHANGE PROCESS

As noted in Chapter III, surface increases of long-lived radioactivity appear to be related to intense cyclogenesis at tropopause level. Because the intended goal of this research is to explain satisfactorily the seasonal as well as the shorter fallout variations, it appears worthwhile to investigate the statistical properties of the stratospheric-tropospheric exchange process on a long-term basis.

As a result of the apparent dependence of individual fallout maxima upon upper tropospheric cyclones, one might inquire whether the yearly fluctuations in mean fallout intensity are in part or completely due to seasonal changes in cyclonic activity. Also, since the correspondence of fallout with upper cyclones is based on only a few case studies, it is of interest to determine if shorter period peaks are statistically related to tropopause-level cyclonic activity throughout the year. A way to examine these problems would be to develop an index parameter that describes the relative amount of tropopause-level cyclonic activity in mid-latitudes, and then compare the seasonal and short-term variations of this index with those of the mean fallout intensity (Mahlman, 1964c, d).

Development of the Cyclone Index

Some of the initial attempts toward the development of a simple quantitative description of the state of atmospheric flow at a given level were made by Rossby (1939) and by Allen et al. (1940). These efforts to produce numerical indices which would reduce the complexities of atmospheric notions resulted in the well-known zonal index. Utilization of this index for description of atmospheric motions on a global basis has proved to be highly valuable in many areas of

atmospheric research. However, for certain specialized problems, this index fails to provide a sufficiently reliable description of the state of atmospheric motions (Namias, 1950; Riehl, Yeh and LaSeur, 1950). Also, if hand computation is necessary, the time required to calculate a series of zonal index values may be prohibitive.

It has been mentioned earlier that possible correlations between the formation of extratropical cyclones and increases in the surface radioactive fallout might be established by using atmospheric indices. The type of index parameter employed should provide an adequate description of the relative amount of cyclogenetic activity in the atmosphere. In estimating cyclonic activity a difficulty arises in the use of the zonal index because the increasing kinetic energy of the current (produced by the release of available potential energy) tends to minimize any decrease in index resulting from the deformation of the pressure field in a growing cyclonic disturbance. Furthermore, a strong seasonal dependence appears in the zonal index due to the decreasing meridional pressure gradient in the summer months. Because cyclonic disturbances strongly influence the direction of the upper wind field, it appears feasible that the derived index parameter be determined by the deviation of the mean wind vector from westerly flow. It also will be advantageous to restrict the index to a non-dimensional and normalized form. With such a restriction, a purely zonal westerly current will be arbitrarily defined to possess an index of 1.0 and a purely meridional current will be defined to be 0.0. (These index values may then be used in the same sense as the "high" and "low index" concepts derived from the original definition of zonal index.)

In order to simplify the mathematical approach as much as possible, one may assume a time-independent sinusoidal velocity field at a given height which is everywhere tangent to the isobars and which is projected on a plane earth. The normal distance (y)

of a given wave from the x-axis in such a system is then given by

$$y = a \sin \frac{2\pi x}{L} \tag{1}$$

where a is the amplitude of the wave, and L is the wave length. The slope of the current at any point in this system is thus

$$\frac{dy}{dx} = \frac{2\pi a}{L} \cos \frac{2\pi x}{L} \quad . \tag{2}$$

The mean value of an arbitrary function $\chi(\xi)$ over the interval (a, b) is defined to be

$$\bar{\chi} = \frac{1}{b-a} \int_a^b \chi(\xi)\, d\xi \quad . \tag{3}$$

By using Eq. (3) the mean slope of the sinusoidal current over one-fourth of a wavelength is given by

$$\overline{\frac{dy}{dx}} = \frac{2\pi a}{L\,(nL + L/4 - nL)} \int_{nL}^{nL+L/4} \cos\left(\frac{2\pi x}{L}\right) dx \tag{4a}$$

or upon reduction,

$$\overline{\frac{dy}{dx}} = \frac{4a}{L} \quad , \tag{4b}$$

where n = 1, 2, 3 $\cdots$. Due to the assumed symmetry of the current, by integrating over any nL/4 wavelengths the mean <u>absolute value</u> of the slope is thus

$$\overline{\left|\frac{dy}{dx}\right|} = \frac{4a}{L} \quad . \tag{5}$$

Also, by definition,

$$\overline{\left|\frac{dy}{dx}\right|} = \tan \overline{|\gamma|} \quad . \tag{6}$$

Here, $\overline{|\gamma|}$ is defined to be the absolute value of the mean deviation from a pure west wind (γ = dd - 270^{o}, where dd is the wind direction). By substituting Eq. (6) into Eq. (5) and solving for $\overline{|\gamma|}$, one obtains

$$\overline{|\gamma|} = \arctan \frac{4a}{L} \qquad (7)$$

which is an expression for the absolute value of the mean deviation from westerly flow of a sinusoidal current of arbitrary amplitude and wavelength.

Now, if a cyclone index is defined in terms of the previously specified conditions for zonal (C = 1.0) and meridional (C = 0.0) flow one may write

$$C = 1 - \frac{\overline{|\gamma|}}{90^{o}} . \qquad (0^{o} \leq \overline{|\gamma|} \leq 90^{o}) \qquad (8)$$

If this derived index is to describe adequately the state of the flow of any given current, the value of $\overline{|\gamma|}$ calculated from the given sinusoidal current must be comparable to the theoretical value obtained from Eq. (7). The calculated values of $\overline{|\gamma|}$ were obtained from plotted examples of this given sinusoidal current by measuring $\overline{|\gamma|}$ at particular points along a discrete grid interval. This grid distance must necessarily be less than one-half wavelength so that a reliable sample can be obtained. The theoretical value of $\overline{|\gamma|}$ from the given sinusoidal current was then compared with the measured values of $\overline{|\gamma|}$ obtained from the same ideal current. The comparison between the measured and the theoretical values was then analyzed statistically by employing a Student's "t" test. This analysis revealed that the value of $\overline{|\gamma|}$ measured from the given sinusoidal current was significantly lower (at the 95% probability level) than its comparable theoretical value. This resulted from the bias introduced by measuring the slope of the current at grid points along the latitude circle rather than along the wave itself. This difficulty was readily circumvented, however, because the statistical analysis also showed that the

measured root-mean-square value of $\overline{|\gamma|}$, ($\overline{|\gamma^2|}^{\frac{1}{2}}$), is an excellent approximation to the theoretical value of $\overline{|\gamma|}$. Thus, one may replace $\overline{|\gamma|}$ in Eq. (8) by $\overline{|\gamma^2|}^{\frac{1}{2}}$ to obtain

$$C = 1 - \frac{\overline{|\gamma^2|}^{\frac{1}{2}}}{90} . \tag{9}$$

Recalling that $\gamma = dd - 270^{\circ}$, Eq. (9) may be defined in terms directly applicable to atmospheric measurement so that

$$C = 1 - \frac{1}{90}\left[\frac{\sum_{i=1}^{n}(dd - 270^{\circ})^2}{n}\right]^{\frac{1}{2}} , \tag{10}$$

where n is the number of measurements along the chosen latitude circle. The index C is now in a form in which its measured value (computed by measuring γ along a discrete grid interval) compares favorably with the theoretical value of the given ideal current. This is advantageous because a value of C can now be calculated from the data for any current, regardless of its complexity, with reasonable assurance that the calculated value agrees well with the possibly unobtainable theoretical value.

Application of the Cyclone Index

In the present study the possible correlations between the derived cyclone index C near tropopause level and fluctuations of radioactive fallout at the surface were examined. Because the peaks of radioactive debris that result from recent atmospheric tests tend to mask the fallout of older stratospheric debris, one has to investigate such correlations over a period in which no nuclear testing has taken place. Also, this chosen period must be long enough after the cessation of nuclear testing so that the influence of tropospheric debris is minimized.

To satisfy these restrictions the period following the last atmospheric test in December 1962 was chosen for the analysis. This was an especially suitable period because the stratospheric debris intensity was relatively high as a result of heavy testing prior to the moratorium.

Since, as noted previously, fallout maxima tend to appear in relation to tropopause-level cyclones, 300 mb was chosen as the most representative level for the calculation. Because the maximum cyclonic intensity generally occurs within the latitude band 40° to 60°N, 50°N was chosen to be an appropriate latitude for the calculation of a series of cyclone index values. Also, since the United States provides the only fallout network which gives values representative over a large area, the index was calculated between 70°W and 180°W longitude, and not around the entire hemisphere.

If Eq. (10) is applied to the atmosphere under the previously specified conditions, a difficulty arises because the flow direction is frequently non-symmetrical with respect to a given longitude line. In theory this could be avoided by deriving the cyclone index in terms of a more complicated atmospheric current which incorporates the tilting of troughs (Machta, 1949; Arakawa, 1953). Such considerations would, however, make the derivation of C considerably more complex. These difficulties resulting from the asymmetry of the current were in part avoided by measuring a meandd over the 10 degree latitude interval 45° to 55°N, instead of taking a point value at 50°N.

The cyclone index was calculated at 24-hour intervals for the period January 1963 to December 1964. Computational noise and the higher frequency components were filtered from the time series by using a weighted smoothing technique (Blackman and Tukey, 1958; Holloway, 1958) (Fig. 4). From independent successive calculations the cyclone index was seen to provide a statistically reliable indication

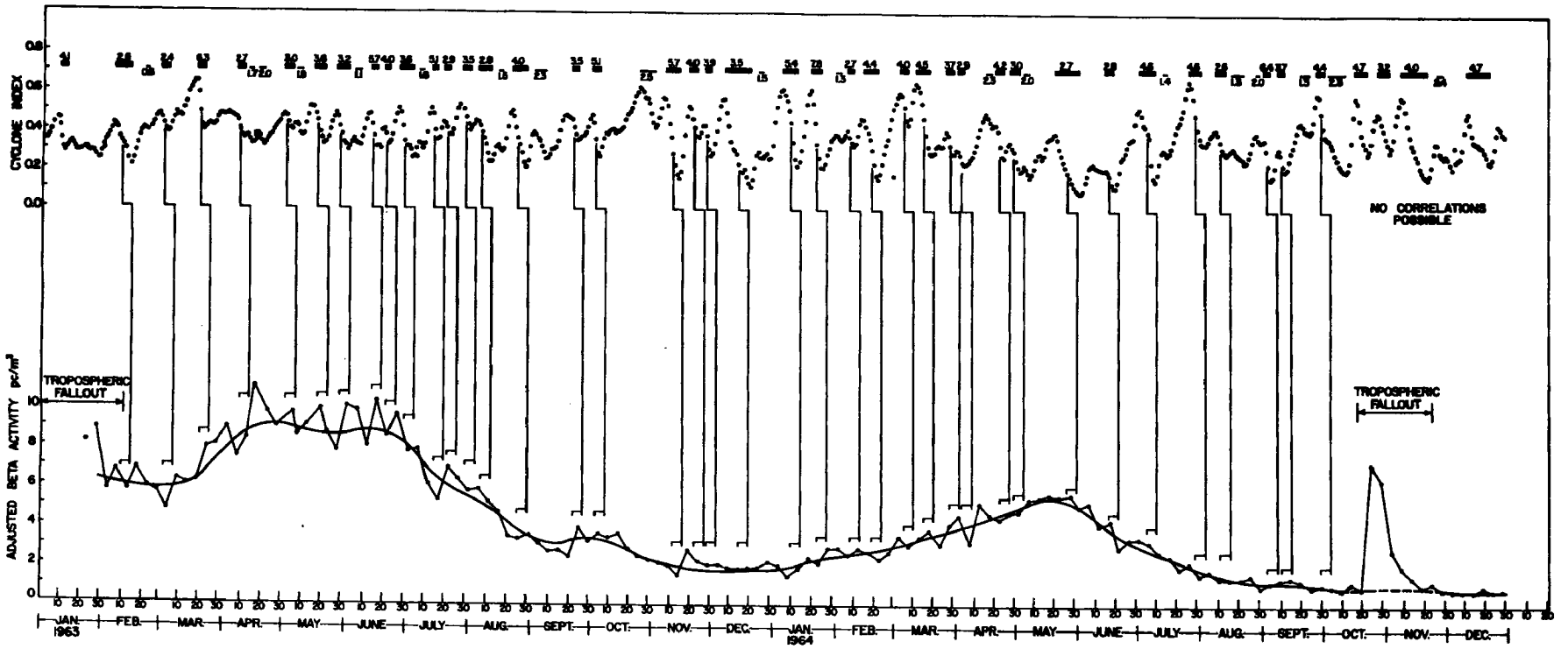

FIG. 4. Time series of comparison between cyclone index and shorter period fallout fluctuations. Upper part of diagram is smoothed cyclone index series. In the lower part: thin connected lines are five-day mean age-adjusted gross beta activity; heavy smooth line gives mean monthly fallout values. Vertical lines from cyclone index show the high percentage of fallout increases within five days after rapid cyclone index decreases. Numbers across top of figure are values of $100\ (C_1 - C_2)/\Delta t$ computed during each cyclone index decrease. Numbers above heavy bars are greater than critical value of 2.5 and numbers below thin bars are less than or equal to 2.5.

of the relative amount of cyclonic activity in the atmosphere. The index was also checked by calculating separate time series for the first four months of the sample using the 0000 GMT and 1200 GMT data, respectively. The major fluctuations in the two resultant smoothed time series were observed to be identical. The calculated filtered index time series for the indicated period showed a succession of index increases terminated by index drops of equal magnitude (Fig. 4).

Relation of the Index Series to Fallout Fluctuations

The time distribution of age-adjusted fallout in air over the United States was determined by computing area-weighted averages of gross beta activity in picocuries per cubic meter of air from the U. S. Public Health Radiation Surveillance Network Data. Two distinct scales of fallout intensity with respect to time were obtained by calculating five-day and monthly averages of the mean area-weighted fallout intensity (Fig. 4). This figure shows that an irregular fallout fluctuation of short duration is superimposed upon the seasonal oscillation as determined from the monthly averages. Because of the large number of observations that determine these five-day means and the relatively small variance between the individual measurements, even small fluctuations of fallout intensity become statistically significant. Fig. 4 shows that a very pronounced increase in mean fallout characterized the spring of 1963, and that a spring peak also occurred in 1964. It is also evident from Fig. 4 that the effectiveness of the moratorium was essentially terminated in late October 1964 due to tropospheric debris from the first Chinese nuclear test at that time. The 1964 maximum is in agreement with the observed spring fallout peak in 1960--more than a year after the voluntary test moratorium of 1959 (Gustafson, Brar, and Kerrigan, 1961).

Since radioactive debris in the stratosphere will decrease with time as a result of natural decay, one should express fallout values in terms of intensities adjusted to an arbitrary age. This has the advantage that similar mass transport processes at different times will produce a comparable "measured" radioactive debris intensity in the troposphere. Such an adjustment may also lead to a more accurate determination of the time rate of depletion of the stratospheric-debris inventory as a result of stratospheric-tropospheric exchange mechanisms.

The rate of decay of the 1963 debris was determined by analyzing the time change of the relative contribution of each specific nuclide and taking into account the resultant change in mean half-life of the debris as time progressed (see Table 1). The debris sample was assumed to consist of two portions--an almost non-decaying part (Sr-90 and Cs-137) and a rapidly decaying part. The decay of this mixed sample was determined by assuming no decay of the long-lived portion and decay according to the mean half-life of the other part. This was done for each month so that the rate of decay of a given fallout sample could be obtained by computing the mean half-life from the available data (Fig. 5). An approximate formula stating these physical conditions (valid for slowly decaying debris) is

$$\text{Final Intensity (I)} = I_o \left[1 - \frac{30\,(1-Z)}{hl_1 + hl_2} \right] \qquad (11)$$

where Z is the percentage of very long-lived debris; hl_1 and hl_2 are the computed half-lives of the original and final samples; and I_o is the original intensity. The measured fallout intensities were then adjusted to an age of 100 days by taking simple ratios from Fig. 5, thus yielding the age-adjusted fallout intensities of Fig. 4.

TABLE 1. Percentage contribution of particular nuclides in radioactive debris measured in total monthly rainfall at Westwood, New Jersey. Half-life of each nuclide in days is given in parentheses.

	PERCENTAGE CONTRIBUTION OF NUCLIDE					
	Sr - 90 (10,120d)	Sr - 89 (50.5d)	Ce - 144 (285d)	Zr - 95 (65.0d)	Cs - 137 (11,140d)	Ce - 141 (33.1d)
January 1963	0.9%	26.3%	21.5%	44.8%	1.4%	5.1%
February	1.2	23.8	34.2	34.2	1.6	5.0
March	1.6	18.0	36.8	30.8	2.3	10.5
April	2.0	15.2	49.7	25.8	2.8	4.5
May	2.2	11.4	44.8	28.2	3.2	10.2
June	2.8	10.3	51.6	26.2	4.1	5.0
July	4.0	9.6	55.6	25.6	5.2	
August	3.0	5.5	65.2	20.0	6.3	
September	3.9	4.9	69.4	15.4	6.4	
October	3.9	3.9	72.6	13.2	6.4	
November	3.5	2.1	75.3	12.3	6.8	
December	3.8	1.3	78.8	11.8	4.3	
January 1964	3.8	0.9	80.9	7.1	7.3	

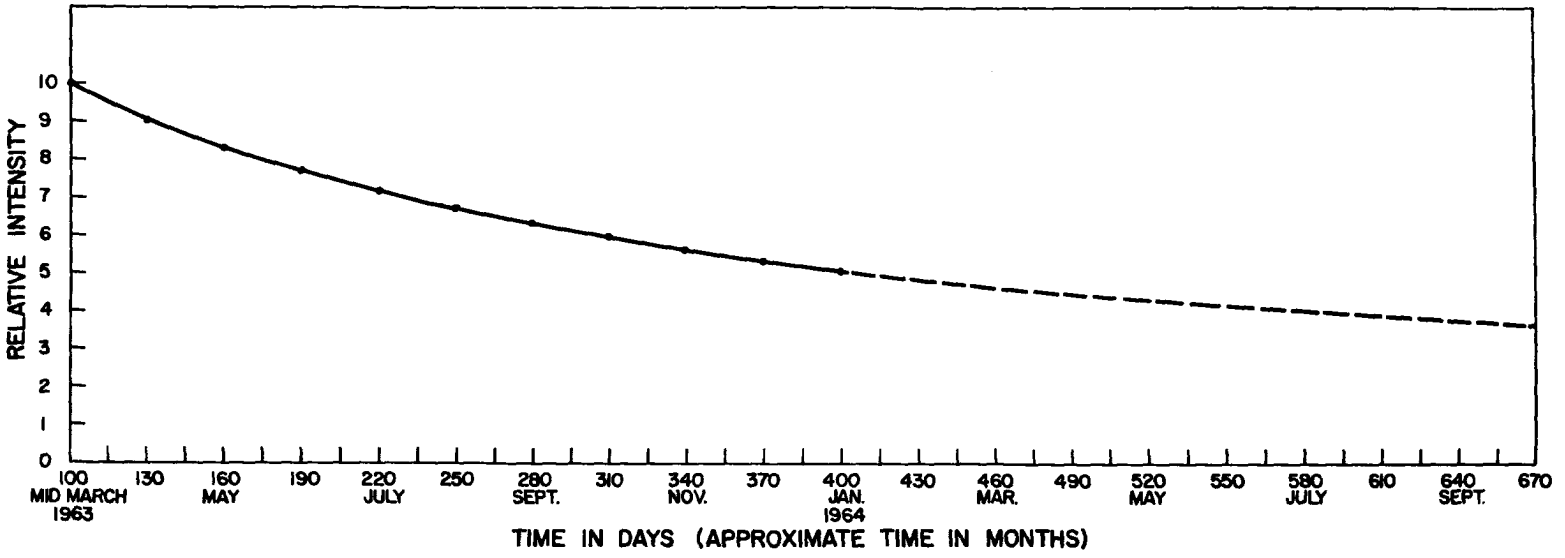

FIG. 5. Natural decay curve for a mixed debris sample computed from relative intensities in Table 1. Source intensity at time 100 days (mid-March 1963) is assumed to be 10 picocuries per cubic meter. Abscissa is in days with the approximate time in months. Black dots represent measured decay; dashed line is extrapolated decay curve.

A comparison of the index time series with that of the mean age-adjusted monthly fallout of Fig. 4 was then attempted. This analysis revealed that no significant relation appeared to exist between these two quantities. Although there were general index breakdowns preceding the April 1963 and May 1964 fallout peaks seen in Fig. 4, equally large breakdowns at other times did not produce similar trends in mean fallout distribution. It thus appears that a simple causal relationship cannot be established between the seasonal changes of the index and the spring fallout maximum.

An attempt was then made to construct a comparison between the cyclone index and the mean age-adjusted five-day fallout (Fig. 4). In this case a certain relationship between the two time series was noted. Fig. 4 suggests that the shorter period fallout fluctuations--superimposed upon the mean monthly curve--are possibly related to rapid decreases of the cyclone index. It is qualitatively evident from Fig. 4 that a high percentage of fallout increases occur within five days after the center point of the index decrease. Because a fallout increase did not occur within five days after all observed decreases in cyclone index, an attempt was made to differentiate between index decreases with and without subsequent fallout increases. It was determined empirically that the parameter $100\ (C_1 - C_2)/\Delta t$ provided a probable method for separating the index decreases associated with fallout from the others (C_1 and C_2 are the initial and final values of cyclone index over the period of decrease and Δt is the time in days over which the decrease occurred) (see Table 2). It was hypothesized from the data given in Table 2 that any value of $100\ (C_1 - C_2)/\Delta t$ greater than 2.5 would most likely produce an increase of surface fallout larger than the mean seasonal value within five days after the center point of the index decrease.

The hypothesis that short term fallout increases are statistically related to discrete decreases in the cyclone index was examined

TABLE 2a. Values of $100\ (C_1 - C_2)/\Delta t$ computed from index drops in Fig. 4. Calculated values are arranged in chronological sequence. The word "fallout" signifies that a fallout increase occurred within five days after the index decrease and a "none" denotes that no subsequent increase was observed.

Dates of Index Drop	$\frac{100\ (C_1-C_2)}{\Delta t}$	Dates of Index Drop	$\frac{100\ (C_1-C_2)}{\Delta t}$
(1963)		Nov. 27-30	3.9 Fallout
Feb. 5-13	2.6 Fallout	Dec. 7-20	3.5 Fallout
Feb. 20-22	0.6 None		
Feb. 28-Mar. 4	2.4 Fallout	(1964)	
Mar. 18-22	6.3 Fallout	Jan. 5-12	5.4 Fallout
Apr. 7-10	2.7 Fallout	Jan. 19-24	7.8 Fallout
Apr. 13-15	1.7 None	Jan. 31-Feb. 3	1.3 None
Apr. 18-21	2.0 None	Feb. 6-9	2.7 Fallout
May 1-5	3.0 Fallout	Feb. 14-21	4.4 Fallout
May 7-10	1.8 Fallout	Mar. 3-7	4.0 Fallout
May 16-21	3.6 Fallout	Mar. 11-19	4.5 Fallout
May 27-June 1	3.2 Fallout	Mar. 26-29	3.7 Fallout
June 5-8	1.1 None	Mar. 31-Apr. 4	2.9 Fallout
June 13-16	5.7 Fallout	Apr. 15-18	2.3 None
June 20-22	4.0 Fallout	Apr. 20-24	4.2 Fallout
June 27-July 4	3.6 Fallout	Apr. 27-May 2	3.0 Fallout
July 7-9	1.6 None	May 4-7	2.0 Fallout
July 13-16	5.1 Fallout	May 27-June 1	2.7 Fallout
July 19-22	2.9 Fallout	June 15-18	2.8 Fallout
July 28-Aug. 1	3.5 Fallout	July 1-9	4.6 Fallout
Aug. 4-11	2.8 None	July 13-15	1.4 None
Aug. 15-17	1.5 None	July 26-Aug. 1	4.6 Fallout
Aug. 22-29	4.0 Fallout	Aug. 8-13	2.6 Fallout
Sept. 2-8	2.3 None	Aug. 16-22	1.3 Fallout
Sept. 20-24	3.5 Fallout	Aug. 28-30	2.0 None
Oct. 1-5	5.1 Fallout	Sept. 1-4	6.4 Fallout
Oct. 25-Nov. 2	2.5 Fallout	Sept. 8-11	3.7 Fallout
Nov. 7-14	5.7 Fallout	Sept. 19-23	1.3 None
Nov. 19-24	4.0 Fallout	Sept. 28-Oct. 10	3.8 Fallout

TABLE 2b. Values of $100 (C_1 - C_2)/\Delta t$ computed from index drops in Fig. 4. Calculated values are arranged in ascending order of $100 (C_1 - C_2)/\Delta t$. The word "fallout" signifies that a fallout increase occurred within five days after the index decrease and a "none" denotes that no subsequent increase was observed.

Value of $\frac{100 (C_1 - C_2)}{\Delta t}$	Fallout Occurrence	Value of $\frac{100 (C_1 - C_2)}{\Delta t}$	Fallout Occurrence
0.6	None	3.0	Fallout
1.1	None	3.2	Fallout
1.3	None	3.5	Fallout
1.3	None	3.5	Fallout
1.3	Fallout	3.5	Fallout
1.4	None	3.6	Fallout
1.5	None	3.6	Fallout
1.6	None	3.7	Fallout
1.7	None	3.7	Fallout
1.8	None	3.9	Fallout
2.0	None	4.0	Fallout
2.0	None	4.0	Fallout
2.0	Fallout	4.0	Fallout
2.3	None	4.0	Fallout
2.3	None	4.2	Fallout
2.4	Fallout	4.4	Fallout
2.5	None	4.5	Fallout
2.6	Fallout	4.6	Fallout
2.6	Fallout	4.6	Fallout
2.7	Fallout	5.1	Fallout
2.7	Fallout	5.1	Fallout
2.7	Fallout	5.4	Fallout
2.8	Fallout	5.7	Fallout
2.8	Fallout	5.7	Fallout
2.9	Fallout	6.3	Fallout
2.9	Fallout	6.4	Fallout
3.0	Fallout	7.8	Fallout
3.0	Fallout		

by a test known as the "superposed epoch method" (Panofsky and Brier, 1958). To test the reality of this hypothesis, the sign (+ or -) of the change in fallout was tabulated as a function of lag distance in days from the center point of a critical ($100\ (C_1 - C_2)/\Delta t > 2.5$) decrease in the cyclone index. This was done for 32 occurrences of $100\ (C_1 - C_2)/\Delta t > 2.5$ and is given in Fig. 6 in terms of the sum of the deviation of fallout increases from an even distribution of plus and minus values. Fig. 6 shows a marked tendency for a peak of plus values (fallout increases) to occur four days after the center point (lag = 0 days) in the index decrease. This is compatible with the physical hypothesis that fallout increases are controlled by cyclogenetic processes at tropopause level. It is also evident from the figure that a pronounced period of fallout decrease occurs about 14 to 18 days after t = 0. The decreases of fallout intensity in the figure are also consistent with this model because of the quasi-periodic nature of the index changes--evident from the cyclone index time series given in Fig. 4.

The statistical reality of this observation was tested by computing linear correlation coefficients (r) between equal samples from the 32 values of $100\ (C_1 - C_2)/\Delta t > 2.5$ as a function of lag from 0 to 18 days. To do this the 32 values were divided into two samples of 16 each. The summation of positive values of fallout change from each sample of 16 was then noted for each day from t = 0 to 18 days. The cross correlation between these two samples of 16 was then computed by pairing the sum of the positive values of fallout change from the two samples for each day from 0 to 18 days.

By choosing samples randomly from the 32 values of $100\ (C_1 - C_2)/\Delta t > 2.5$, values of r were obtained by the above

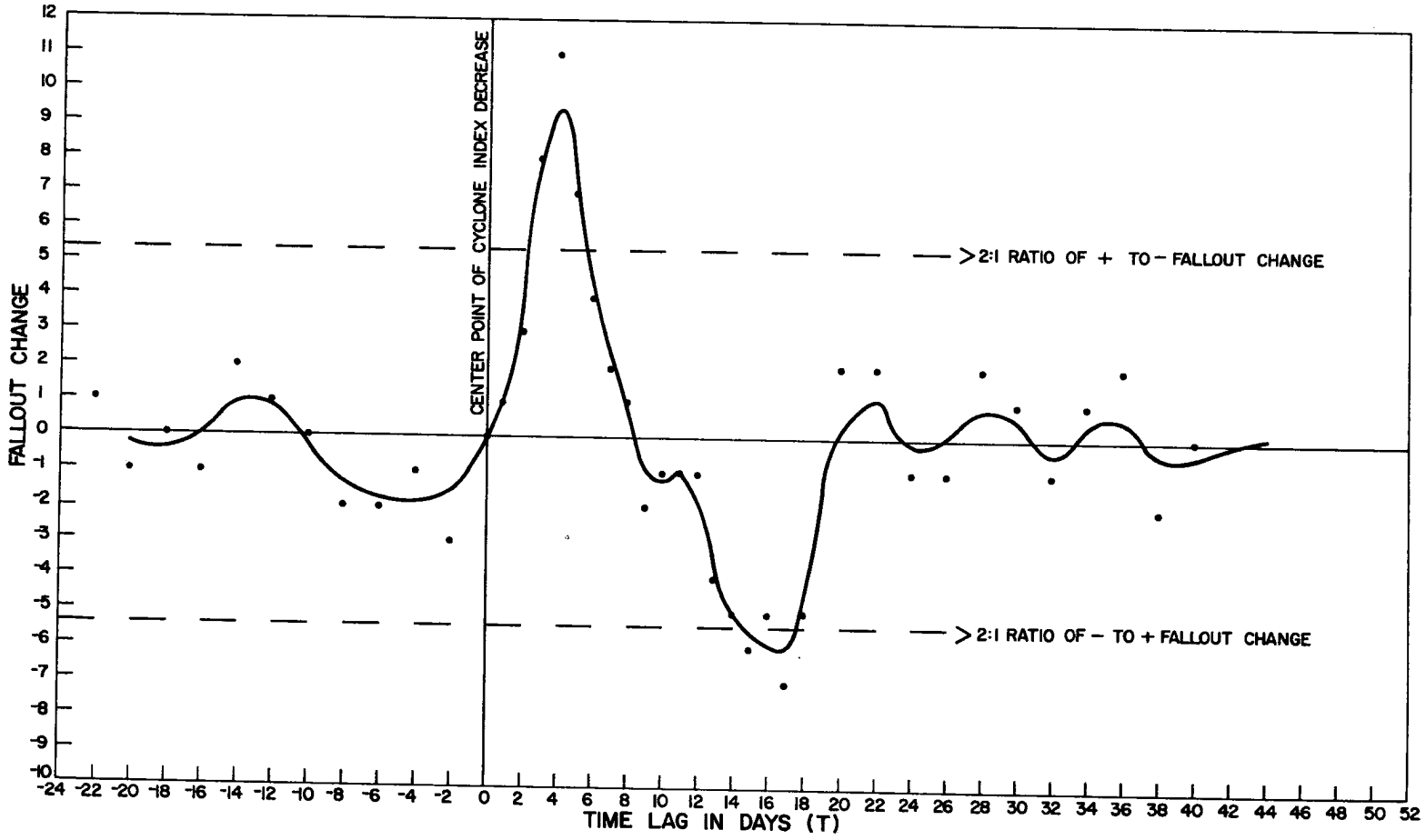

FIG. 6. Time distribution of excess of positive values of fallout change from an even distribution of plus and minus values from sample of 32 occurrences of $100\ (C_1 - C_2)/\Delta t > 2.5$ taken from Fig. 1. Time = 0 days was taken to be the center point of the critical cyclone index decreases. Solid line represents smoothing of points by 1-2-1 weighting method.

procedure. This was repeated five times to give the values

$$r = +0.695$$
$$r = +0.545$$
$$r = +0.551$$
$$r = +0.686$$
$$r = +0.583$$
$$\overline{r} = +0.61 .$$

In addition to this, correlations were calculated between the first and last 16 values to determine whether or not the relationship was in any way different as the half-life of the debris became progressively greater. The value of r from this type of pairing was calculated to be + 0.531. Furthermore, to detect possible seasonal effects, a value of r was computed by pairing critical occurrences of $100\ (C_1 - C_2)/\Delta t$ from 15 October-15 April against those between 15 April and 15 October. In this case r was found to be + 0.626.

Because of the obvious non-independent nature of the data (see Fig. 4), comparison of these values of r with those given in critical correlation coefficient tables can seriously exaggerate the significance of the results. This difficulty was circumvented by generating values of 0 to 18 days, as before, from the same time series but from starting dates selected at <u>random</u>. A machine program was then prepared which computed values of r between all "randomly" generated data sets. This procedure produced a sample of 1764 random values of r for comparison with the values obtained above from the "critical" index decreases. The program output showed that 138 or 7.8% of all values of <u>random</u> r were greater than + 0.5 and 60 or 3.4% were greater than + 0.60. Thus, even with the use of highly time-dependent data, the hypothesis is verified at a relatively high probability level.

The statistical evidence in favor of this hypothesis implies that a quite reliable surface forecasting model for stratospheric debris could be developed from our knowledge of the types of upper flow patterns which produce descents of mass (and radioactivity) from the stratosphere. Furthermore, the geographic location of these predicted maxima could be estimated from the knowledge of trajectory behavior in these regions of descending motions (Danielsen, 1959b, 1961, 1964a, b; Staley, 1960, 1962; Danielsen, Bergman, and Paulson, 1962; Mahlman, 1964a; Reiter, 1963a; Reiter and Mahlman, 1964, 1965b).

Seasonal Mass Exchange from Index and Fallout Data

In view of the discrete nature of the investigated stratospheric-tropospheric transport mechanism, it is of interest to arrive at independent measurements of seasonal mass transport and stratospheric residence half-times from the data presented in the previous sections. Estimates of this type are especially relevant in terms of the general circulation problem and in view of comparison with previous estimates.

Measurements of surface fallout from Fig. 4 show that the age-adjusted mean gross beta intensity in 1964 is slightly less than 50% of the mean 1963 value. This suggests a stratospheric particle residence half-time of about one year for the period after the voluntary test moratorium of December 1962.

The largest portion of the late 1962 stratospheric debris burden was due to mid- and high-latitude weapons testing. Consequently, this estimate is limited by these specialized input conditions and by the immensely complicated nature of the entire physical problem. Because of its inherent statistical nature, a more meaningful determination of residence half-time should be expressed in terms of height, season, circulation type, and latitude of injection into the stratosphere.

By employing the arguments presented in previous sections, from the index data it was possible to arrive at quantitative estimates of seasonal transport of mass from the stratosphere into the troposphere--valid only for the injection conditions mentioned in the previous paragraph. This was crudely accomplished by noting the number of critical index decreases from Fig. 4 ($100 (C_1 - C_2)/\Delta t > 2.5$) which occurred within the 1963 and 1964 time periods. There were found to be 22 and 23 such decreases, respectively. In view of previous estimates for individual cases of mass transport from the stratosphere (Danielsen, 1959a; Mahlman, 1964a, 1965; Reiter and Mahlman, 1964, 1965c), a value of 0.6×10^{12} metric tons of mass transported per critical index decrease was assumed. Because the index described cyclogenetic activity over only one-third of the hemispheric circumference, the number of critical occurrences was multiplied by a factor of 3. Also, since the index described only cyclogenesis between 40 and 60°N, a factor of 2 was introduced to take into account the possibility of transport due to this process at other latitudes. This factor of 2 is roughly compatible with measurements of mean latitudinal fallout distribution by other investigators (Libby and Palmer, 1960; Libby, 1959; Martell, 1959; Lockhart et al. 1960). By employing these assumptions a seasonal mass transport value of 80×10^{12} metric tons of air per year is obtained. This is equivalent to about one-sixth of the total mass of the stratosphere for one hemisphere or approximately one-half of the polar stratosphere. The estimated yearly depletion rate of one-half the mass of the polar stratosphere agrees well with the value obtained above from the fallout data. Furthermore, the rough compatibility of these results suggests that the large majority of seasonal mass transport from the stratosphere is directly attributable to the cyclogenetic mechanism proposed here and elsewhere (Danielsen, 1964a, b; Mahlman, 1964a, b, 1965).

The investigation thus quantitatively documents the hypothesis that tropopause-level cyclogenesis provides the predominate mechanism leading to stratospheric-tropospheric mass exchange. However, the results do not indicate that these cyclogenetic processes are directly responsible for the spring fallout peaks.

On the other hand, this mechanism does give a satisfactory explanation of the mid-latitude peak in fallout intensity. Because the location of the highest frequencies of cyclogenetic activity occur at about 50°N, maximum stratospheric-tropospheric exchange will be expected here. In view of the mean southward trend in trajectory behavior following such intrusions, a mean fallout maximum is anticipated to be at approximately $35\text{-}45^{\circ}$N. Since this corresponds to the latitude belt of the observed fallout maximum, one must regard the cyclogenetic process as the predominate mechanism producing this peak.

Because the spring peak cannot be explained by the cyclogenetic mechanism, this lends support to the contention by Newell (1961, 1963, 1964a), that annual fallout and ozone variations result from seasonal changes in eddy- and energy exchange processes in the stratosphere. Consequently, a thorough analysis of such stratospheric processes is necessary before a physically consistent fallout model can be devised.

PART B

TRANSPORT PROCESSES IN THE STRATOSPHERE

V. REVIEW OF STRATOSPHERIC CIRCULATIONS

As deduced from the work performed in Part A, the existence of seasonal fallout variations must be due to differences in the behavior of the stratospheric circulation throughout the year. Since the most pronounced feature of the mean seasonal fallout distribution is the spring maximum, it appears reasonable to investigate the circulation characteristics of the stratosphere prior to this peak. This is also in accordance with the suggestions by Storebø (1960) and by Libby and Palmer (1960) that the spring fallout peak is attributable to the late winter breakdown of the polar night vortex.

The polar night vortex breakdown (or "sudden warming") is a phenomenon which has attracted much attention in the past ten years. It was first documented by Scherhag (1952) who noted a very sharp temperature rise in a short period of time in the winter stratosphere over Berlin. Subsequently, many investigators have made rather thorough synoptic investigations of the behavior and characteristics of this phenomenon (Lee and Godson, 1957; Teweles, 1958; Teweles and Finger, 1958; Craig and Hering, 1959; Craig and Lateef, 1962; Palmer, 1959a; Hare, 1960; Conover, 1961; Boville, Wilson, and Hare, 1961; Belmont, 1962; Miers, 1963; Morris and Miers, 1964).

In general the wintertime circulation of the polar stratosphere is characterized by strong westerlies increasing as the winter progresses. Usually a slight asymmetry may be seen in the structure of the vortex itself. As noted by the above authors, in many winters this vortex begins to deform into a two- or three-wave pattern leading to the "sudden warming" phenomenon. The warming acts to destroy the strong north-south temperature gradient along with a large decrease in the mean kinetic energy of the vortex. Since this process often

occurs in mid-winter, the westerlies often weakly re-establish themselves. Eventually, however, with the return of the sun the westerlies completely disappear and a weak summertime easterly regime sets in.

Because of the abrupt nature of the vortex breakdown, it is natural to investigate properties of the polar night vortex in late winter which could conceivably produce the spring fallout maximum. In accordance with this, the period January-February 1958 will be studied in detail. This is advantageous in that one can study characteristics of the polar night vortex for periods before, during, and after the breakdown and still remain within a relatively short time period. Since this selected period was during the International Geophysical Year (IGY), the basic data coverage is as good as can be hoped for at this time. Furthermore, for the IGY period the United States Weather Bureau (1961) prepared an excellent and detailed series of 100, 50, and 30 mb maps of the Northern Hemisphere. The data for this map series has been rather thoroughly checked so that measurement and analysis errors are greatly reduced.

The selection of January-February 1958 for investigations is also advantageous in that many quite thorough dynamical and energetical studies have been performed for this time period (Dickenson, 1962; Miyakoda, 1963; Oort, 1963; Sekiguchi, 1963; Muench, 1964; Murakami, 1965). These studies have shown that a complicated sequence of energy transformations characterizes the behavior of the polar night stratosphere during the sudden warming period of early 1958. It is generally found that prior to the onset of the warming (25 January), the total kinetic energy (K) is increasing while the total available potential energy (A) in the stratosphere is decreasing thus suggesting a release of baroclinic energy (Miyakoda, 1963; Sekiguchi, 1963; Muench, 1964). This is

during the period when the polar vortex is in the deformation stage. After the onset of the warming itself, these authors found that the total kinetic energy decreases very rapidly with no significantly pronounced increase in total available potential energy. According to Miyakoda, the excess energy is vertically propagated downward into the troposphere. He also showed a quite remarkable indication of a relationship between blocking action in the troposphere and the breakdown of the polar night vortex.

Another justification for concentrating upon this shorter time period is that the Massachusetts Institute of Technology Planetary Circulations Project has been undertaking a massive project to document thoroughly the climatic properties of the stratosphere. This is an especially valuable and relevant study for the problem of determining seasonal quantitative values of mass and debris transport in these regions. In contrast, the emphasis in this research will be more toward isolating the applicable physical mechanisms leading to the observed seasonal accumulations.

VI. MEAN TRANSPORT PROPERTIES OF THE POLAR NIGHT STRATOSPHERE

As an introduction to the general problem of determining the physical characteristics of the polar night vortex and its relevance to the fallout problem, the transport properties of the polar night circulation during the January-February 1958 period have been measured. This, of course, necessitated a detailed knowledge of the u, v, w, and T fields over the area of computation. In most previous studies of the stratosphere (Jensen, 1961; Murakami, 1962; Dickenson, 1962; Oort, 1962, 1963; Molla and Loisel, 1962; Miller, 1966) all computations were made from the original station data. The hemispheric mean values of all transport quantities were then obtained by taking the arithmetic average of all the stations in a given latitude belt. This is advantageous in that the computations can be immediately made on an electronic computer. A disadvantage that has always been recognized by the above investigators is that this type of averaging procedure can produce inaccuracies due to the unequal weighting. This objection is particularly valid when virtually the entire effect of a particular computation might depend upon the contribution from a limited longitudinal region.

In order to circumvent the possibility of error due to the above averaging method, all values of u, v, w, and T were calculated at 100 and 50 mb and at intervals of 10° longitude at the respective latitudes 50°, 60°, and 70° North. At 80°N the latitudinal circumference is small, and the data coverage does not seem to be adequate; at lower latitudes the effect of the breakdown does not appear to be significant (see Fig. 14). All values of vector wind and temperature are taken from the analyses given in the U. S. Weather Bureau Daily 100-Millibar and 50-Millibar and

Three Times Monthly 30-Millibar Synoptic Weather Maps (1961). Actual wind values were used whenever possible, but geostrophic winds were used when no other data were available.

Since vertical velocity is a derived quantity, many difficulties are often encountered in the attempt to obtain spatially consistent w fields. Because the static stability is very high in the stratosphere and the radiative heat loss is generally thought to be low in these regions, the adiabatic method for computing vertical velocity was chosen to be the most desirable. The equation to be used in the computations is given by

$$w = \frac{1}{\frac{\partial T}{\partial z} - \Gamma} \left[\frac{1}{c_p} \frac{dh}{dt} - \frac{\partial T}{\partial t} - \vec{V}_2 \cdot \nabla T \right], \qquad (12)$$

where h is heat per unit mass and $\Gamma = -g/c_p$. The details of the derivation are given in Chapter VII.

Strictly speaking, this equation is somewhat ambiguous because it computes the vertical motion relative to the pressure surface and not the true vertical velocity. It has been found, however, that the difference between these two values is considerably smaller than the usual uncertainties inherent in the computational procedure. Computing w instead of ω (dp/dt) is advantageous because the amount of adiabatic heating due to compression is then explicitly given in terms of the magnitude of w. In accordance with the findings of Ohring (1958), Davis (1963), and Kennedy (1964), the diabatic term was assumed to be a constant value of 1°C cooling per day. The local time derivative ($\partial T/\partial t$) term was evaluated by taking the average of the 24-hour local temperature change on each side of the given observation time. Finally, the advection term ($\vec{V} \cdot \nabla T$) was determined at each grid point in natural coordinates by evaluating $V_s \, \partial T/\partial s$ from the analysis. Although this procedure is considerably more laborious

than the single station method, it is thought that the greater reliability of the computations merits the extra effort required.

In order to put the u, v, w, and T quantities in more meaningful form in terms of transport quantities, they are broken up into the following definitions:

$$\begin{aligned} u &= \bar{u} + u' \\ v &= \bar{v} + v' \\ w &= \bar{w} + w' \\ T &= \bar{T} + T' \ . \end{aligned} \tag{13}$$

The bar represents an average around a given latitude circle, and the prime denotes the point deviation from this value. From this one can write expressions for the latitudinal means of all the cross correlations

$$\begin{aligned} \overline{uv} &= \bar{u}\bar{v} + \overline{u'v'} \\ \overline{uw} &= \bar{u}\bar{w} + \overline{u'w'} \\ \overline{uT} &= \bar{u}\bar{T} + \overline{u'T'} \\ \overline{vw} &= \bar{v}\bar{w} + \overline{v'w'} \\ \overline{vT} &= \bar{v}\bar{T} + \overline{v'T'} \\ \overline{wT} &= \bar{w}\bar{T} + \overline{w'T'} \end{aligned} \tag{14}$$

where all terms of the nature $\overline{\bar{u}v'}$, $\overline{u'\bar{w}}$, $\overline{\bar{v}T'}$, etc. vanish as a result of the averaging procedure. The barred products may then be thought of as terms arising from the mean circulation and prime products give the effect of the eddies. As noted by Newell (1964) a great deal of the observed ozone and fallout transport can be explained if,in the general circulation of the stratosphere, northward moving parcels are sinking and southward moving air is rising. This relationship necessitates a negative correlation for the quantity $\overline{vw}$, particularly during the late winter when the build-up occurs.

The other terms are often important in determination of the statistical and physical characteristics of general circulation processes.

$\overline{uv}$ is indicative of the meridional transport of zonal momentum and $\overline{uw}$ is the vertical transport of zonal momentum. The meridional transport of temperature is given by $\overline{vT}$ and the zonal transport of T is $\overline{uT}$. The $\overline{wT}$ term indicates the conversion of potential to kinetic energy. Since each of these products has some physical significance, a machine program was prepared to compute all of them even though the term of most direct interest was the $\overline{vw}$ product. This program was designed so that the eddy correlation coefficients, eddy covariance, means, and products of means of all combinations of u, v, w, and T were computed from 10 January to 20 February 1958 at 100 and 50 mb for latitudes 50, 60, and 70°N. The numerical values of all these quantities are included in Appendix A. It is not to be expected that the mean values of the quantities v and w have any true significance. In both cases the actual mean values are considerably smaller than their mean absolute value. Thus, any determination of $\bar{v}$ or $\bar{w}$ is strongly subject to computational uncertainties in the analysis. In fact, the chief merit in calculating $\bar{v}$ and $\bar{w}$ fields directly is that they often give a definite indication of errors in the initial tabulations. As a result of this, it appears that the best procedure for determining $\bar{v}$ and $\bar{w}$ is by indirect techniques. This will be performed in Chapter VIII.

In order to visualize properly the sequence of physical events during this period, the eddy correlation coefficients

$$r_{k,\ell} = \frac{\overline{k'\ell'}}{\sqrt{\overline{k'^2}}\sqrt{\overline{\ell'^2}}} = \frac{\text{covariance of k, } \ell}{\text{variance of k, } \ell} \qquad (15)$$

are plotted as a function of time in Figs. 7-13 (k and ℓ are arbitrary dummy variables). Fig. 7 is a time series of $\frac{\overline{v'w'}}{\sqrt{\overline{v'^2}}\sqrt{\overline{w'^2}}}$ at 50 mb, 60°N for the extended period 1 January to 28 February. This figure shows that prior to the warming $\overline{v'w'}$ becomes strikingly negative

and remains so from 27 January to 24 February. This shows rather conclusively that the breakdown is capable of initiating dynamic processes which produce a consistent northward and downward transport of ozone and radioactive debris for a significant period of time. This is also demonstrated in Fig. 8 which shows v'w' correlation coefficients at 100 and 50 mb, 50°, 60°, and 70°N from 10 January to 20 February 1958. The negative v'w' correlations are present at 60° and 70°N for both 100 and 50 mb. This result indicates that the eddy structure probably plays an extremely important role in determining the transport properties in the lower stratosphere. At this stage it is not possible to evaluate the relative importance of this eddy transport until the role of mean circulations in the stratosphere have also been determined. This will be done in the next chapter.

Fig. 9 gives the v'T' eddy correlation coefficient at the same levels and latitudes as Fig. 8. At 50 mb the v'T' correlation coefficients are consistently positive prior to and during the warming. After the warming a pronounced decrease in the v'T' correlation is evident beginning on 9 February. Following that, the values become rather strongly positive again. From Fig. 14 in the next chapter it is evident that after the warming the eddy processes act to transport heat against the mean gradient. This phenomenon has been noted previously by other investigators (Priestly, 1949; White, 1954; Piexoto, 1960; Murakami, 1962; Peng, 1963). At 100 mb, 50°N the v'T' correlation decreases rapidly at the onset of the warming and stays predominately negative until 19 February. At 100 mb, 60° and 70°N the v'T' correlations are very similar to those at 50 mb with very high positive values before and during the sudden warming period.

Fig. 10 gives the u'v' correlations for the same levels and latitudes as above. In this case the computations are much more variable but there is definite indication of positive values prior to

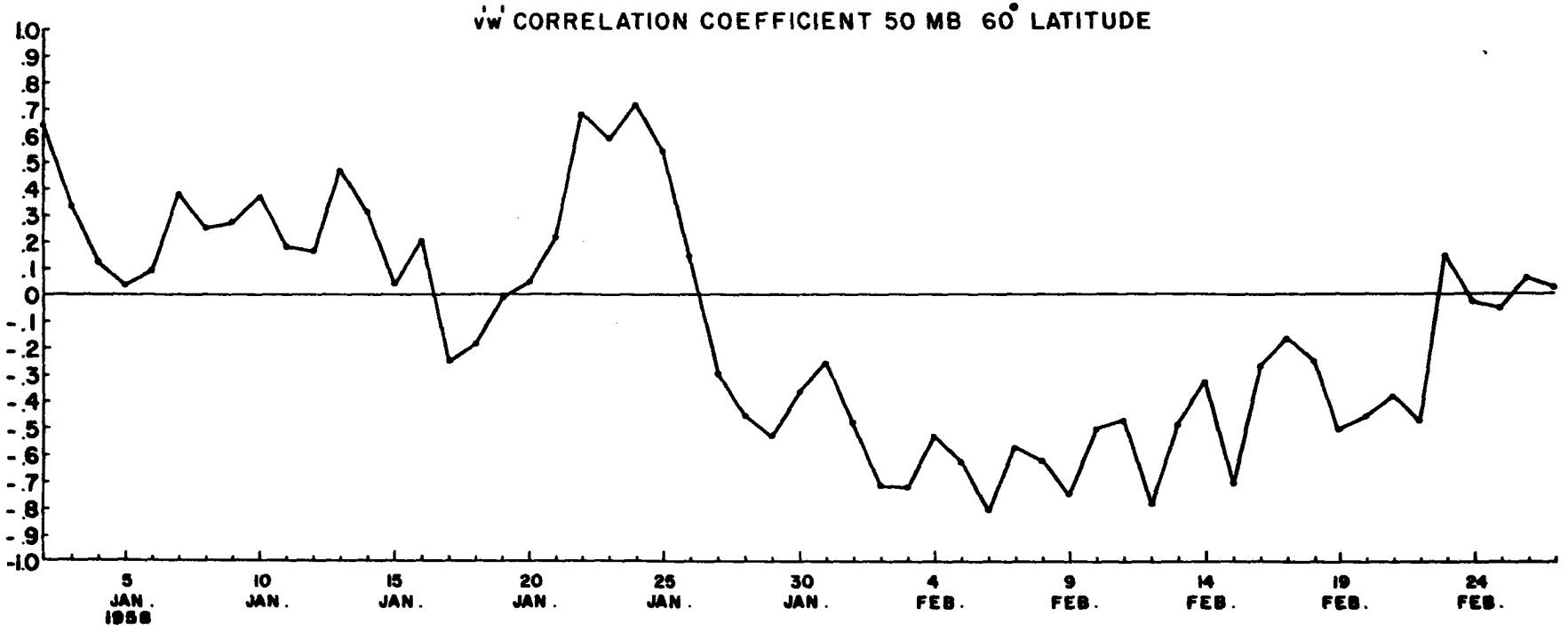

FIG. 7. v'w' correlation coefficients for 50 mb, 60° latitude from 1 January to 28 February 1958. Note presence of very large negative values after onset of the polar night vortex breakdown.

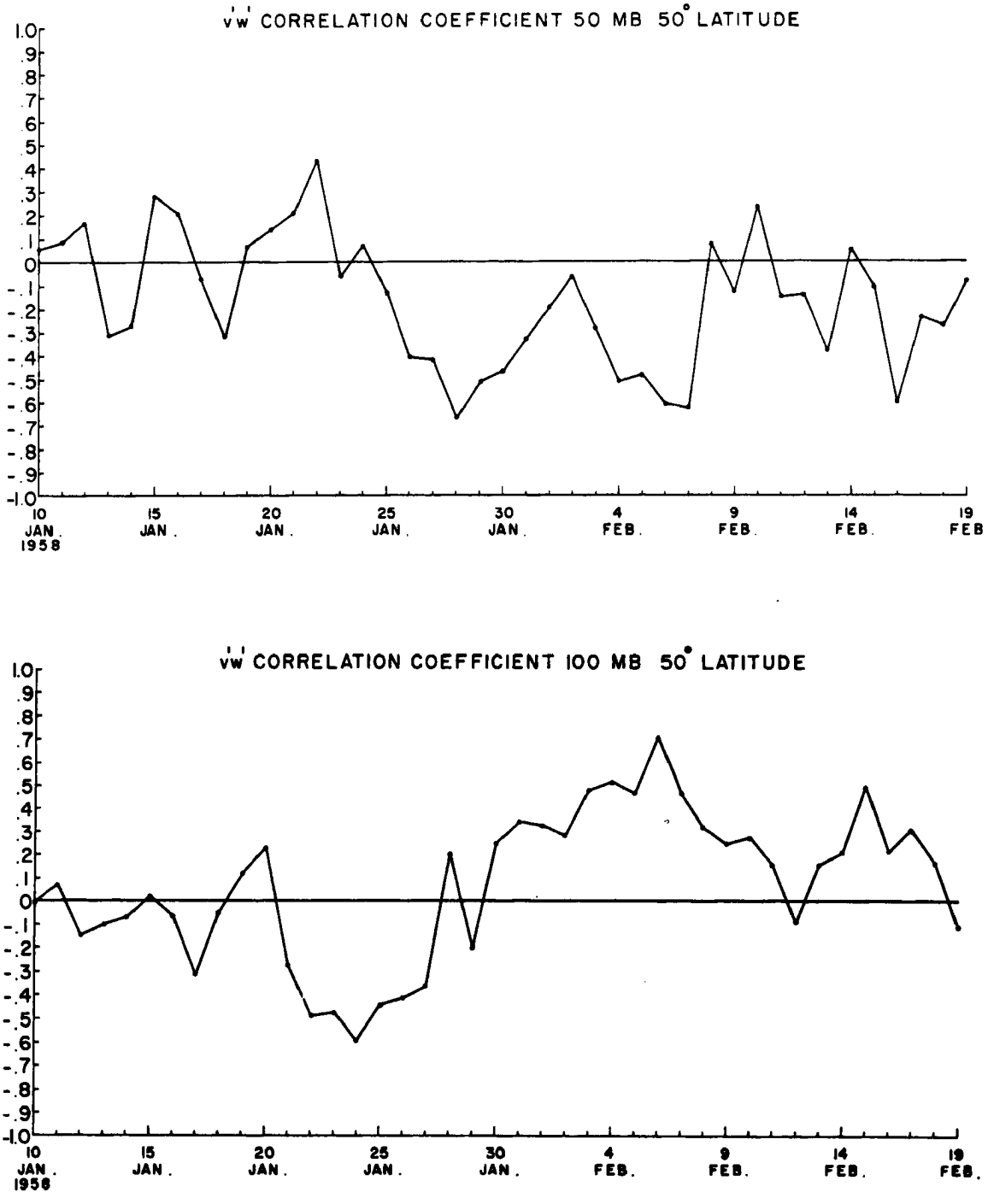

FIG. 8. $v'w'$ correlation coefficients for indicated levels and latitudes from 10 January to 19 February 1958.

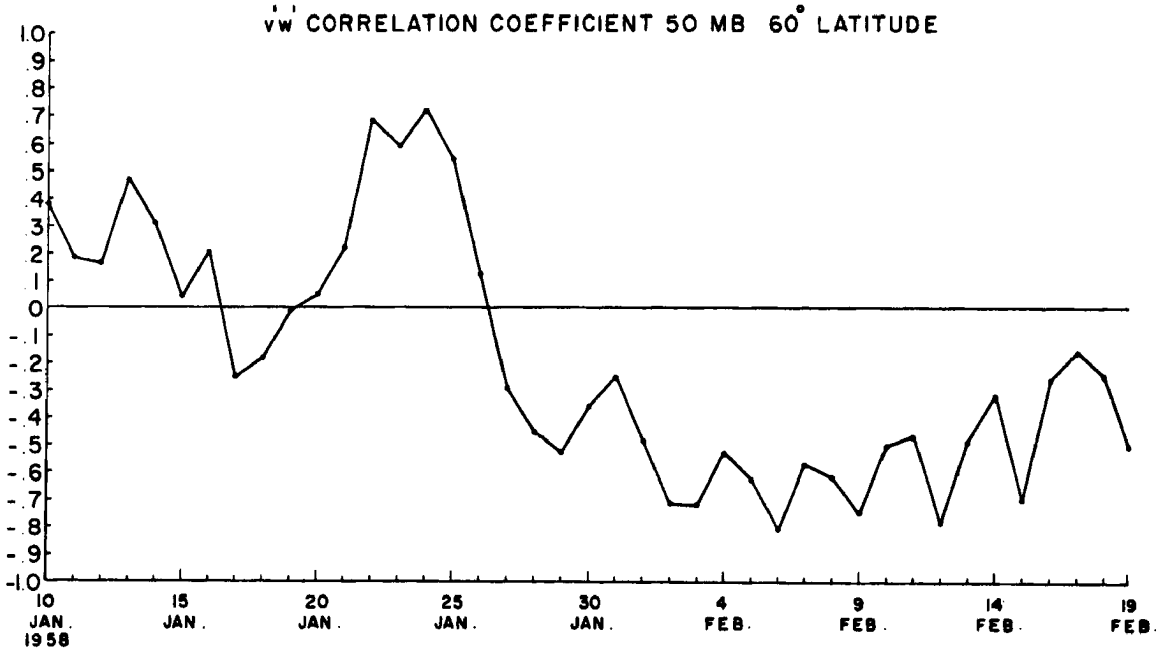

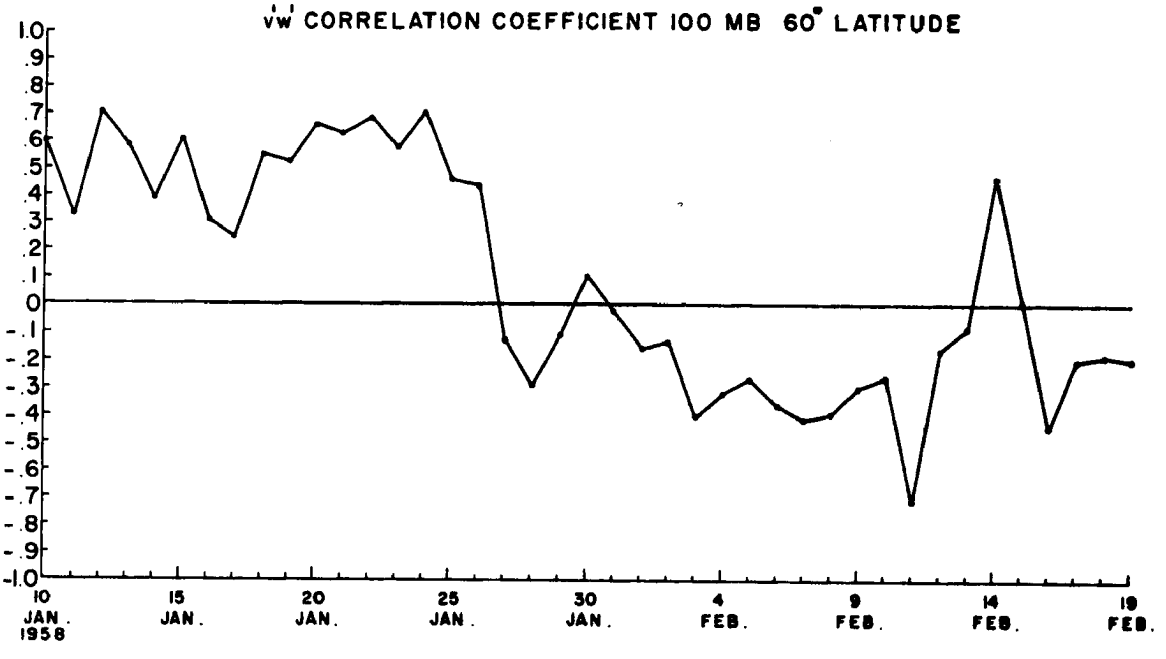

FIG. 8. Continued.

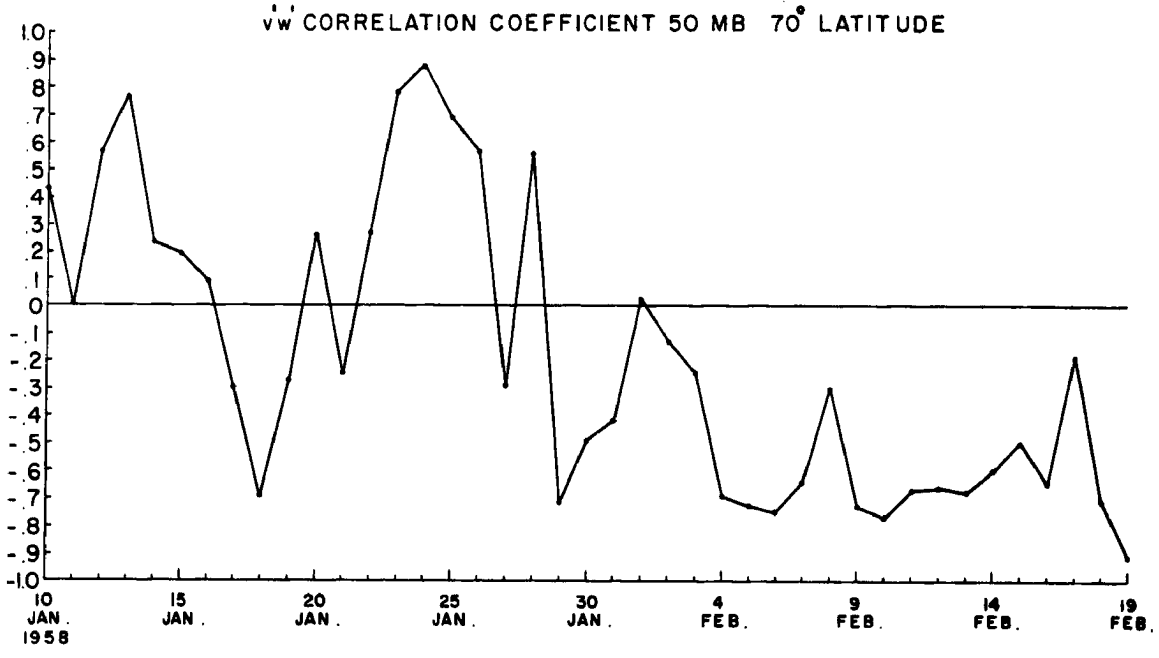

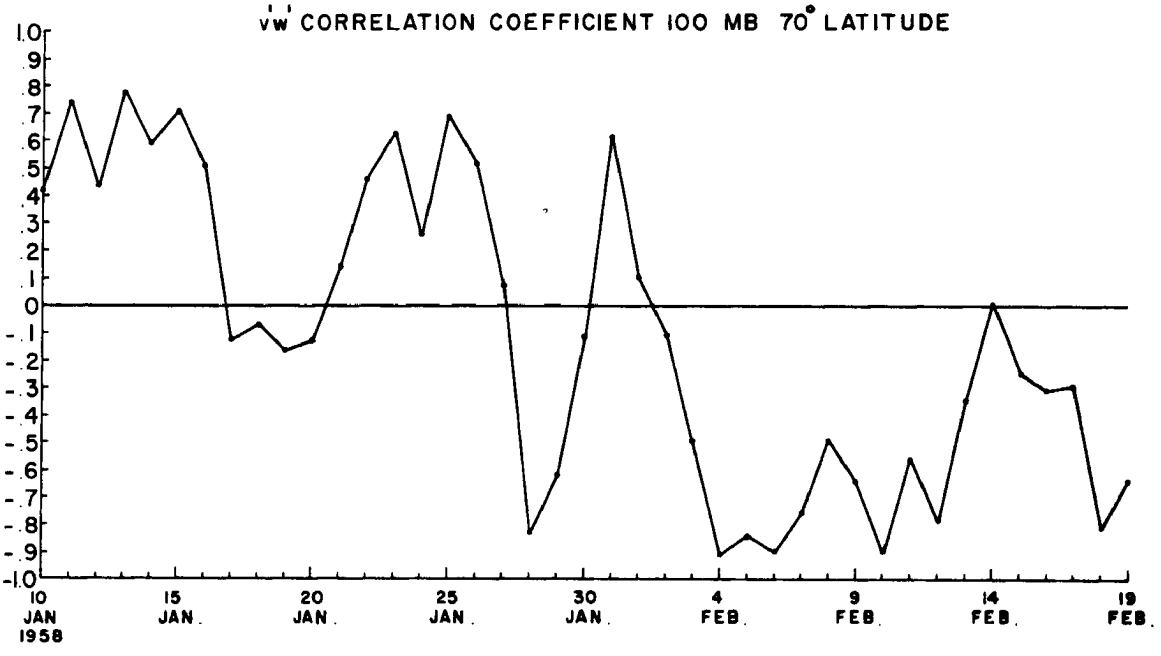

FIG. 8. Continued.

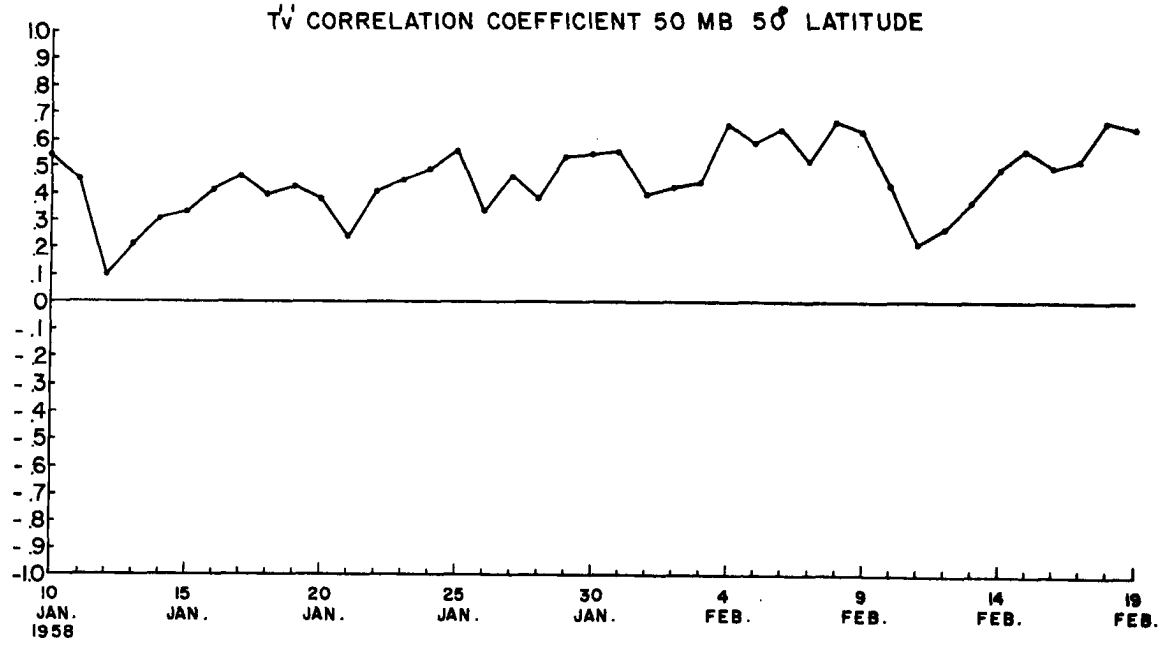

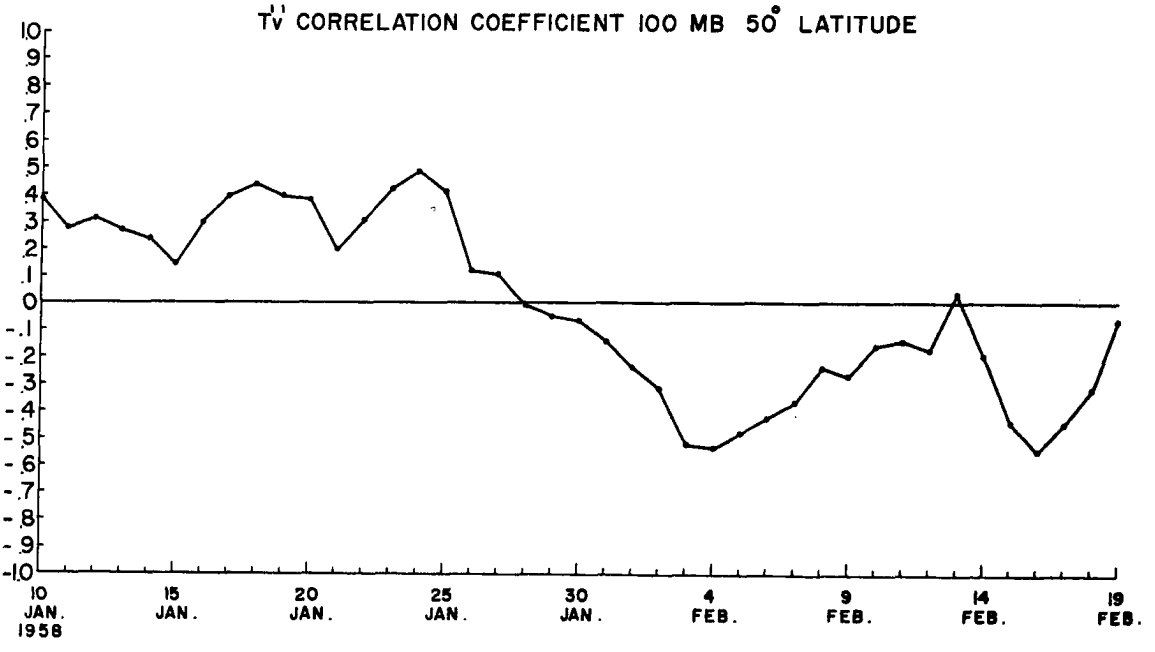

FIG. 9. T'v' correlation coefficients for indicated levels and latitudes from 10 January to 19 February 1958.

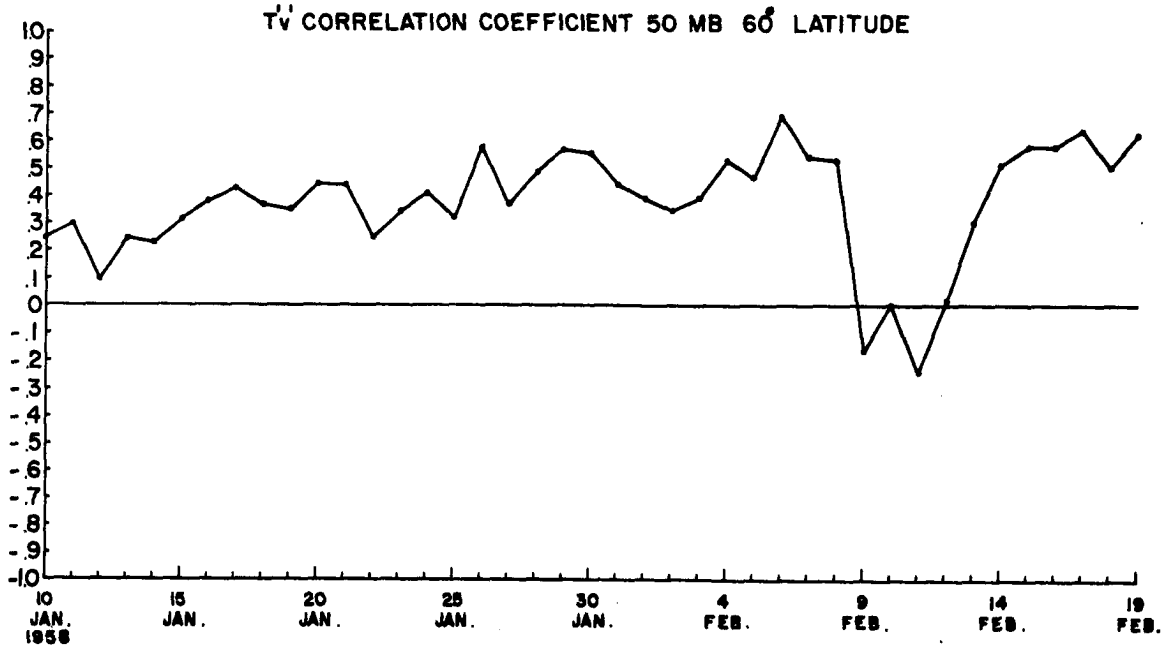

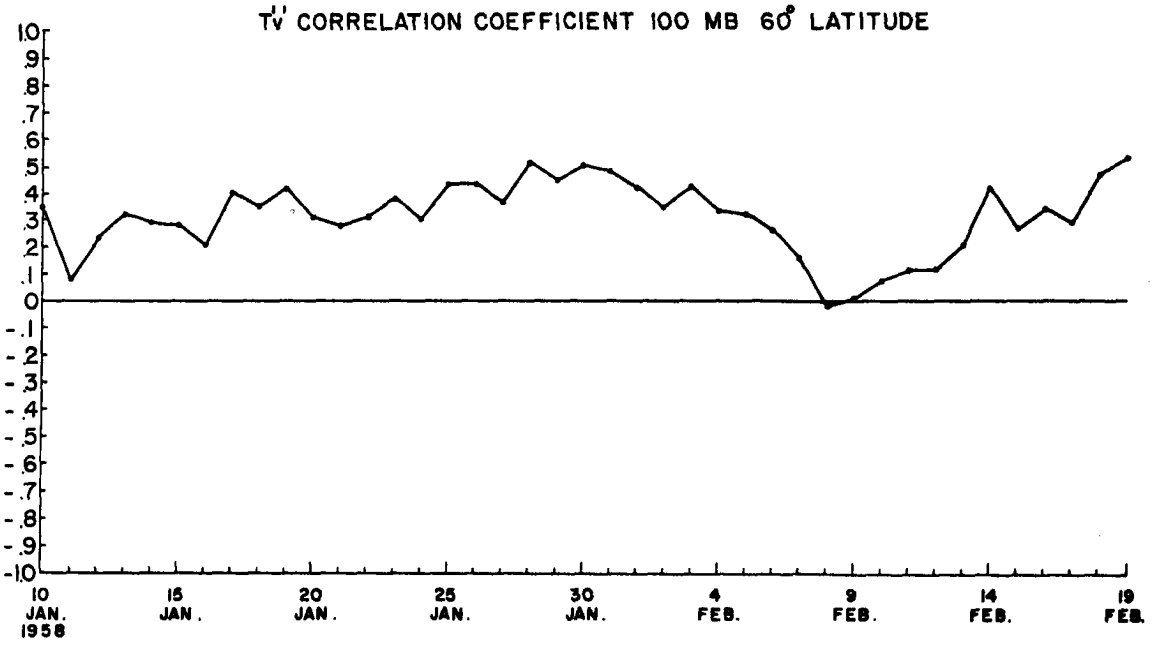

FIG. 9. Continued.

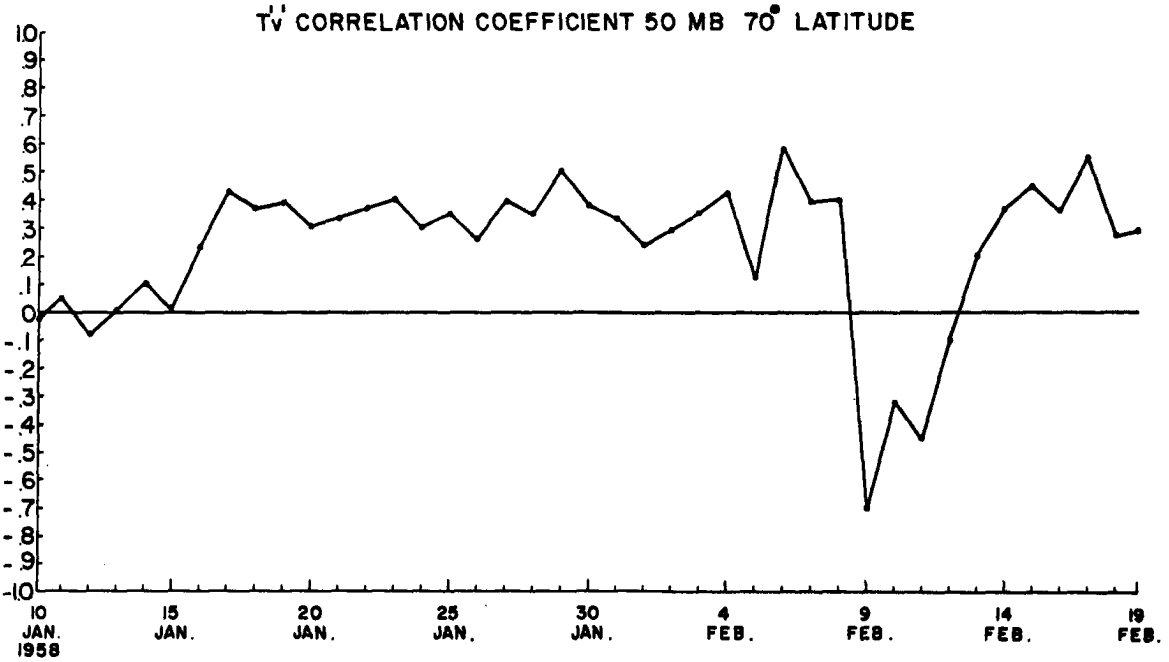

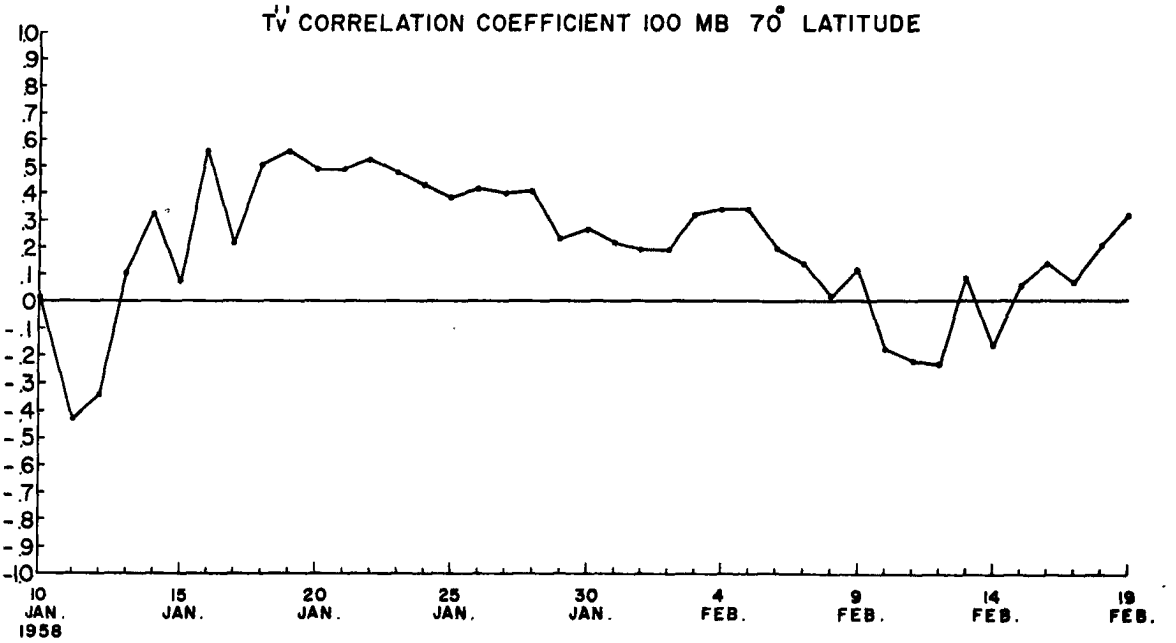

FIG. 9. Continued.

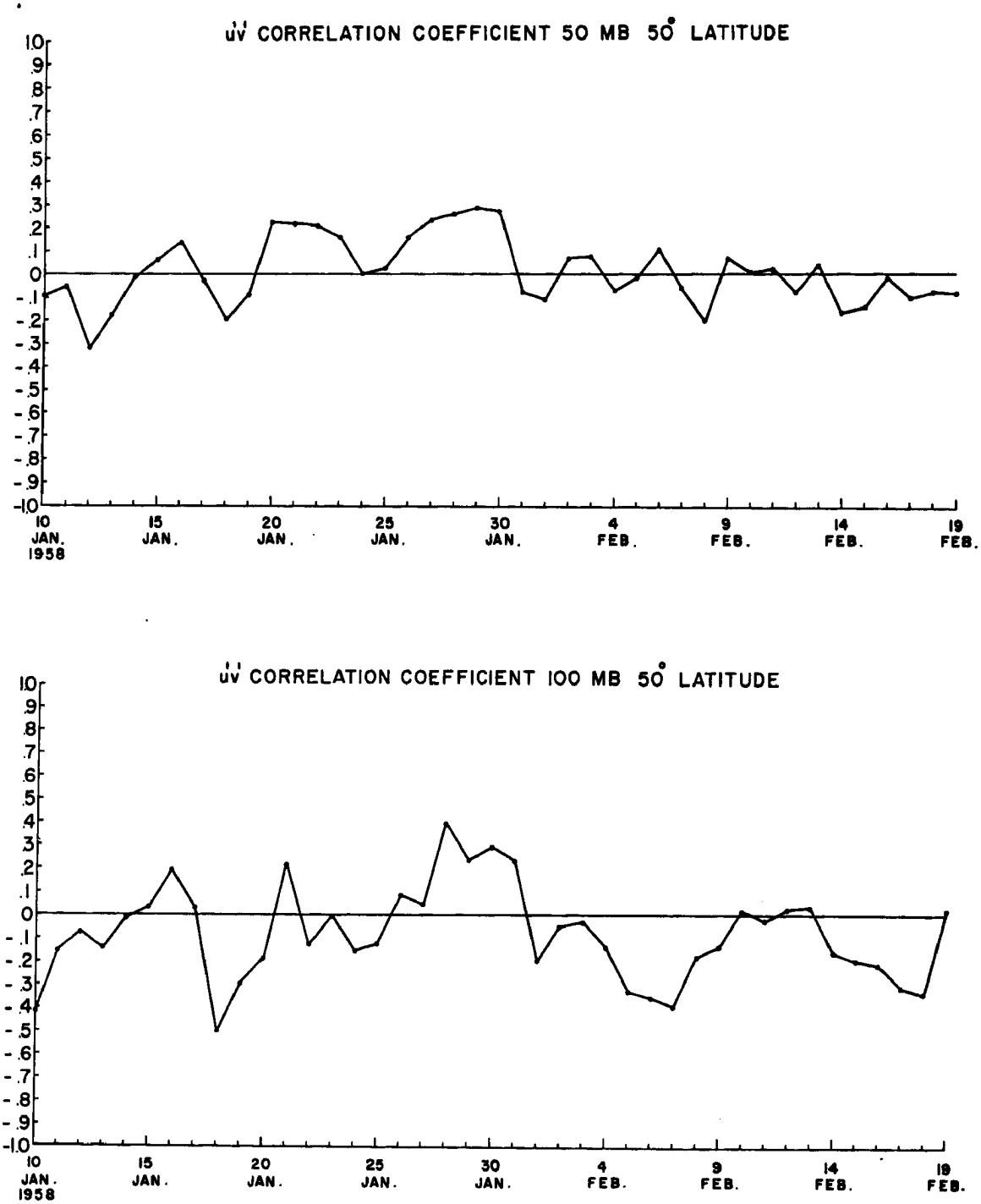

FIG. 10. $u'v'$ correlation coefficients for indicated levels and latitudes from 10 January to 19 February 1958.

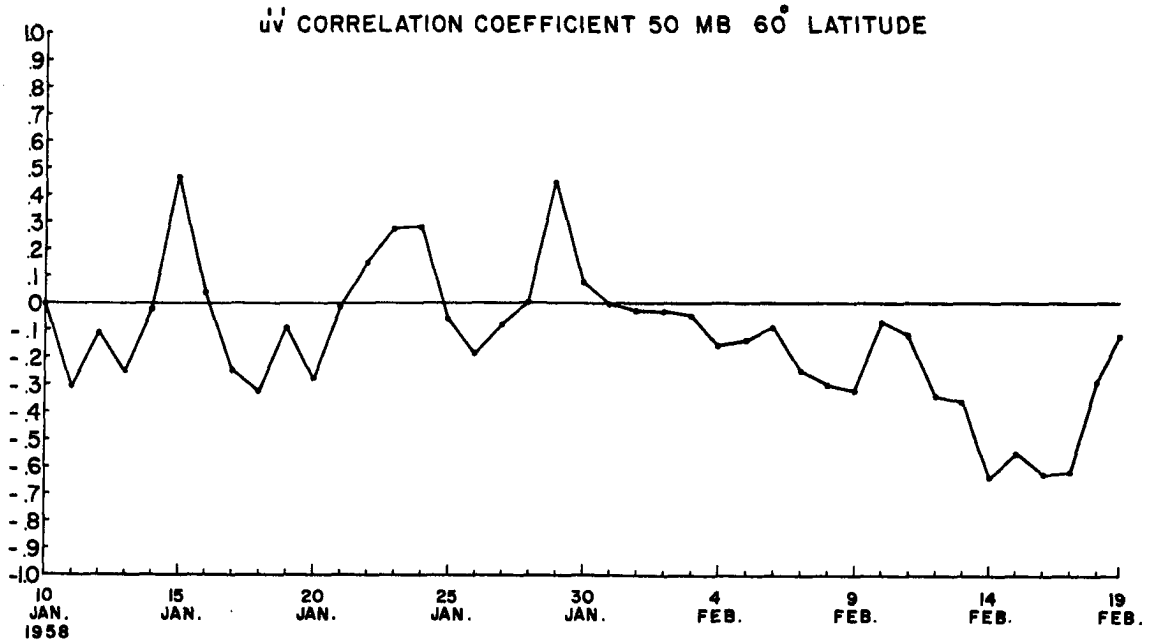

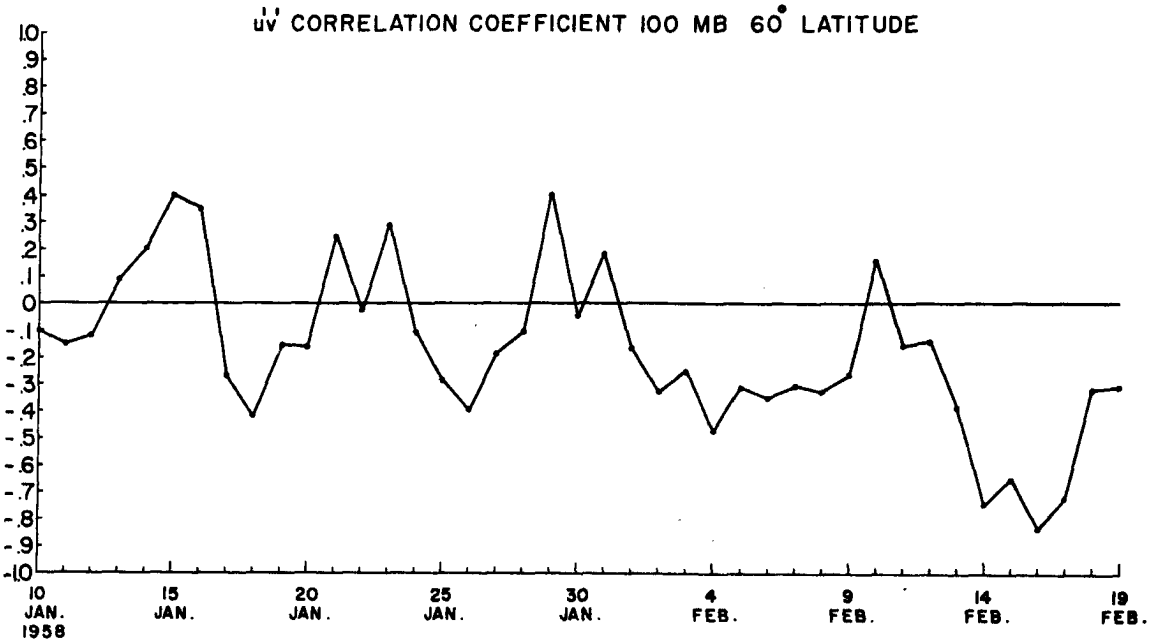

FIG. 10. Continued.

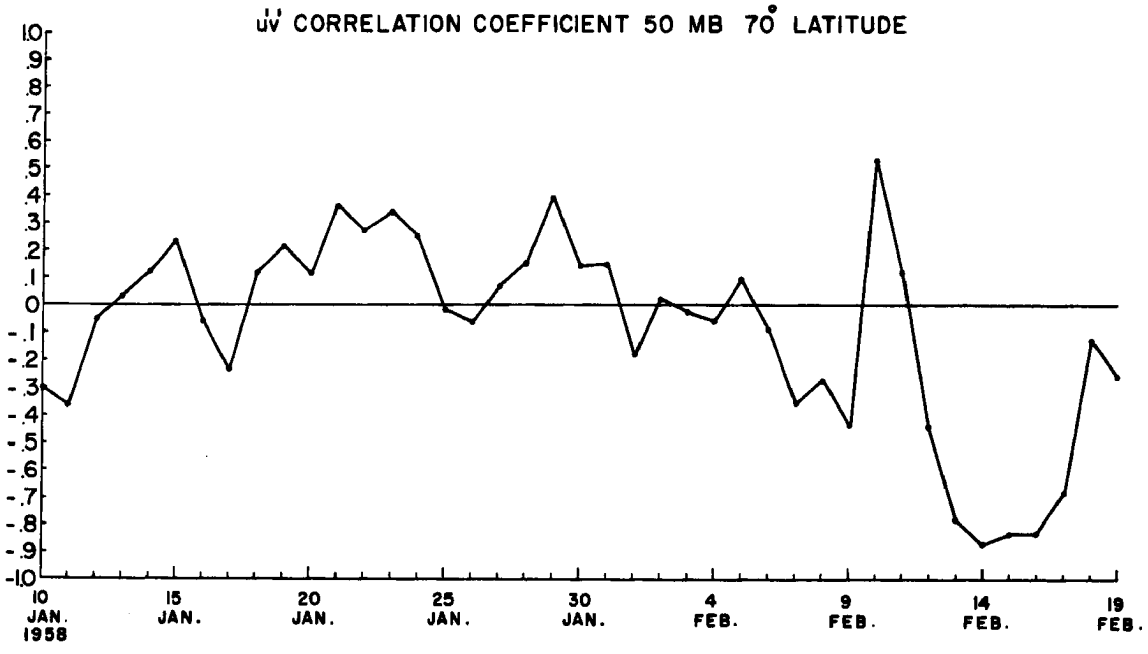

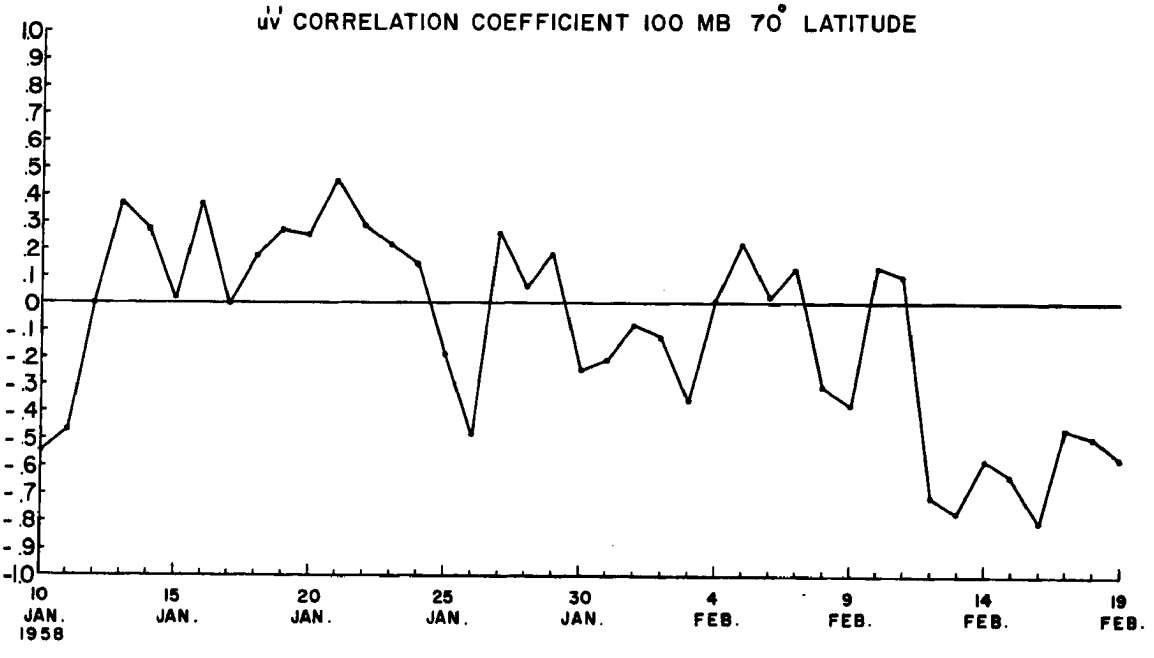

FIG. 10. Continued.

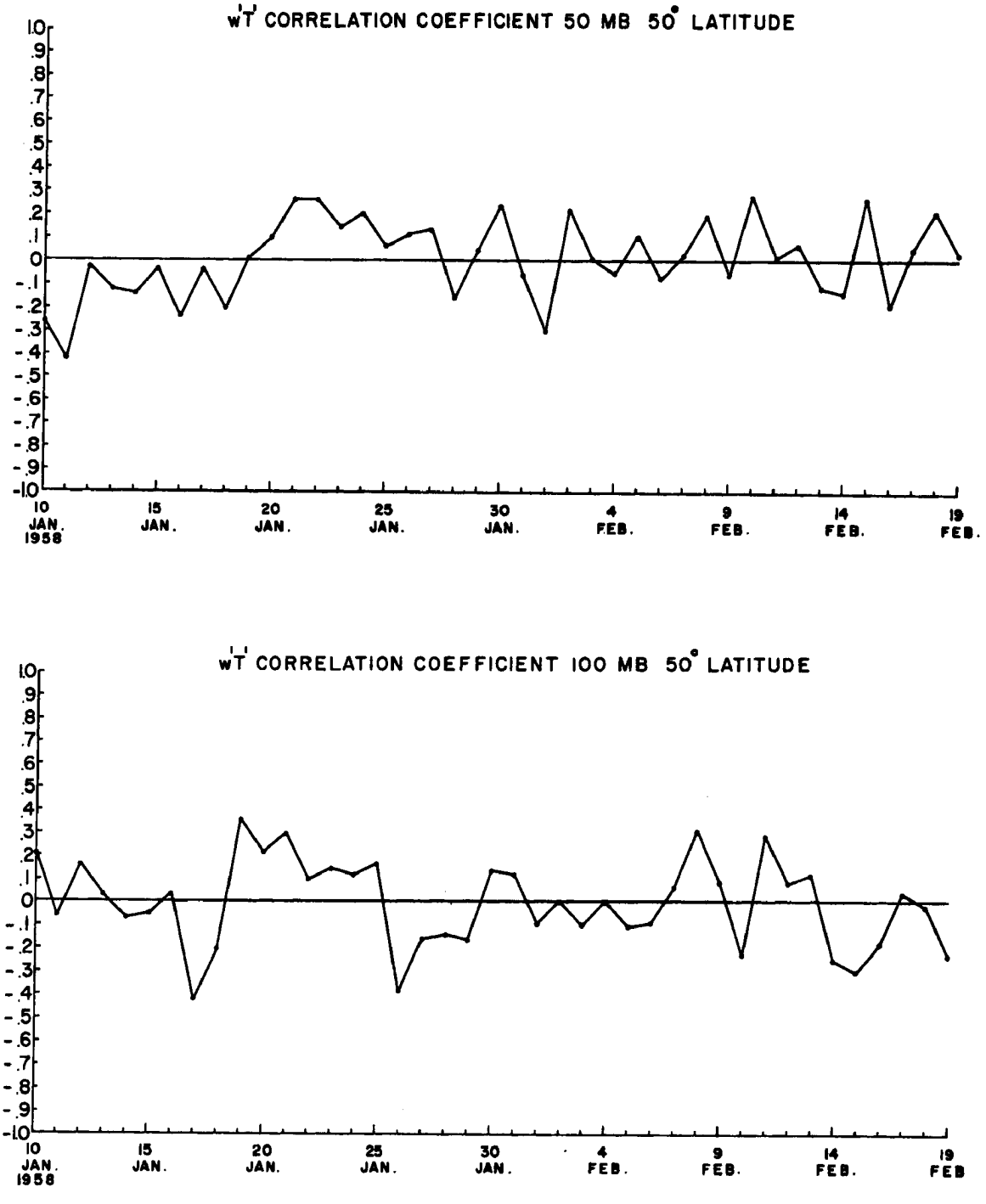

FIG. 11. w'T' correlation coefficients for indicated levels and latitudes from 10 January to 19 February 1958.

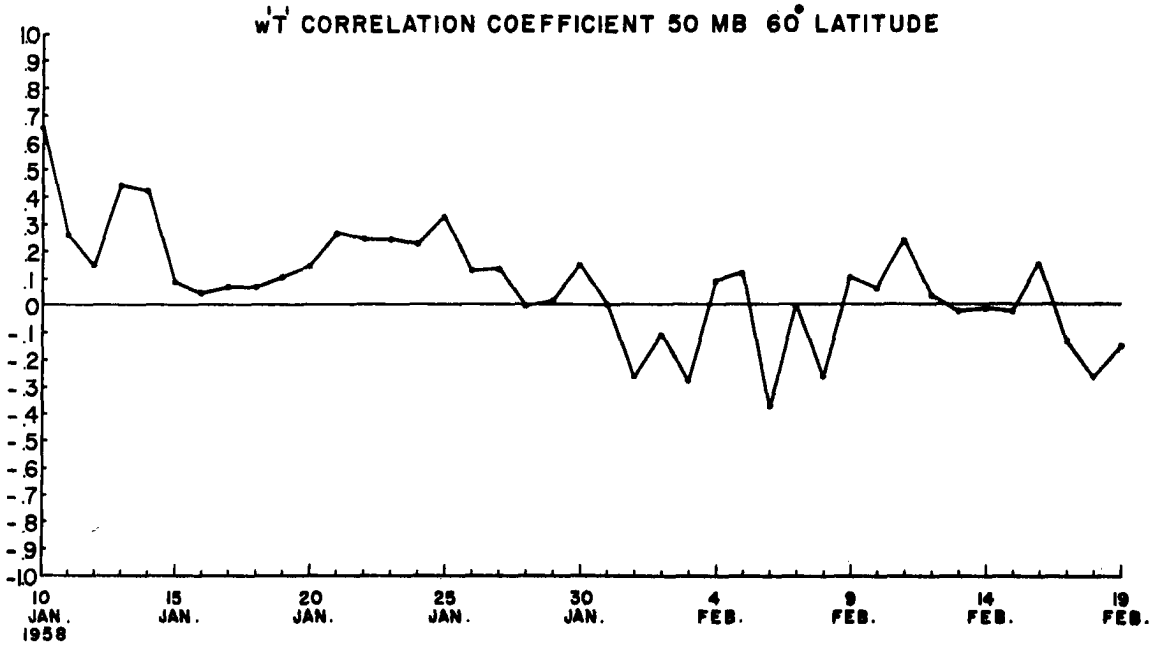

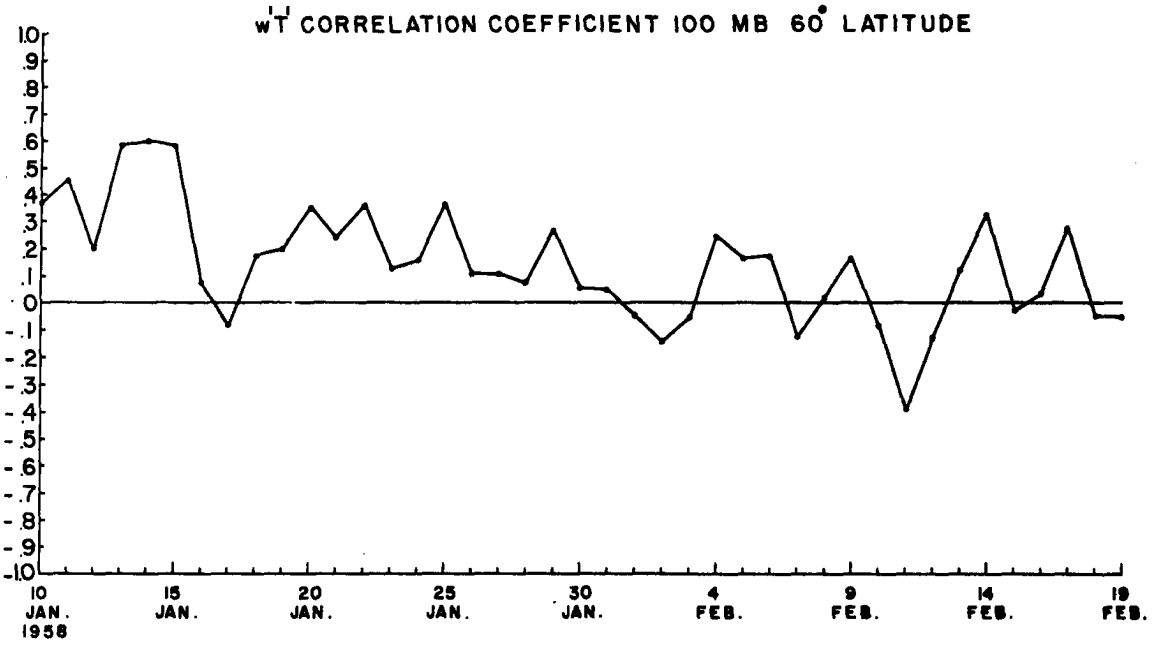

FIG. 11. Continued.

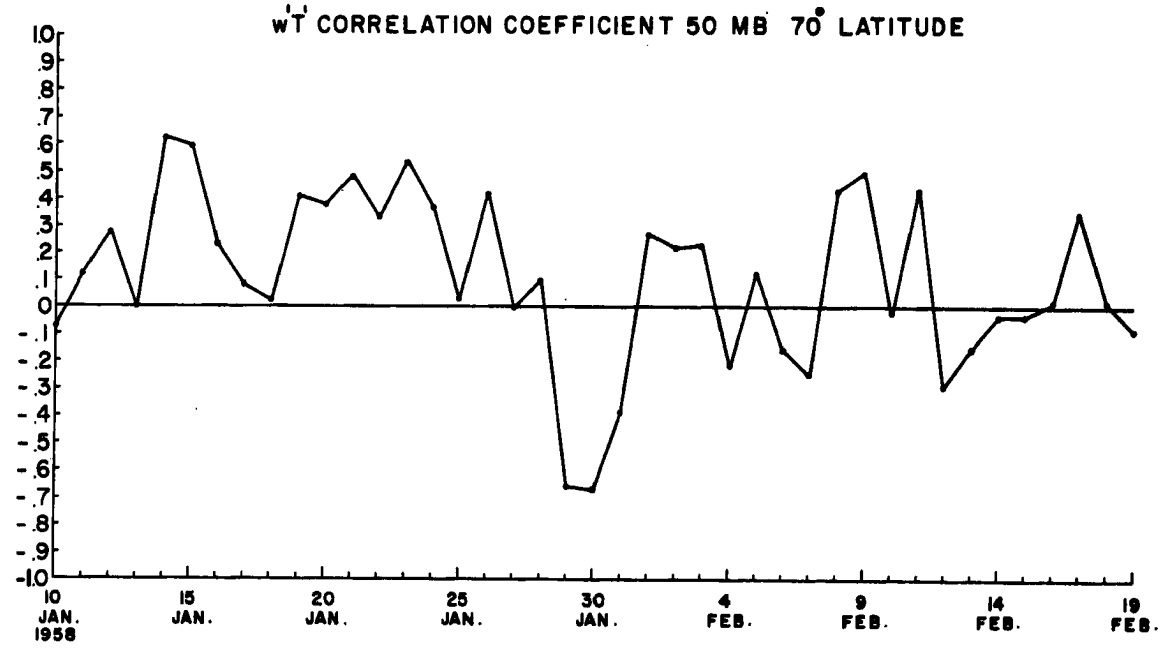

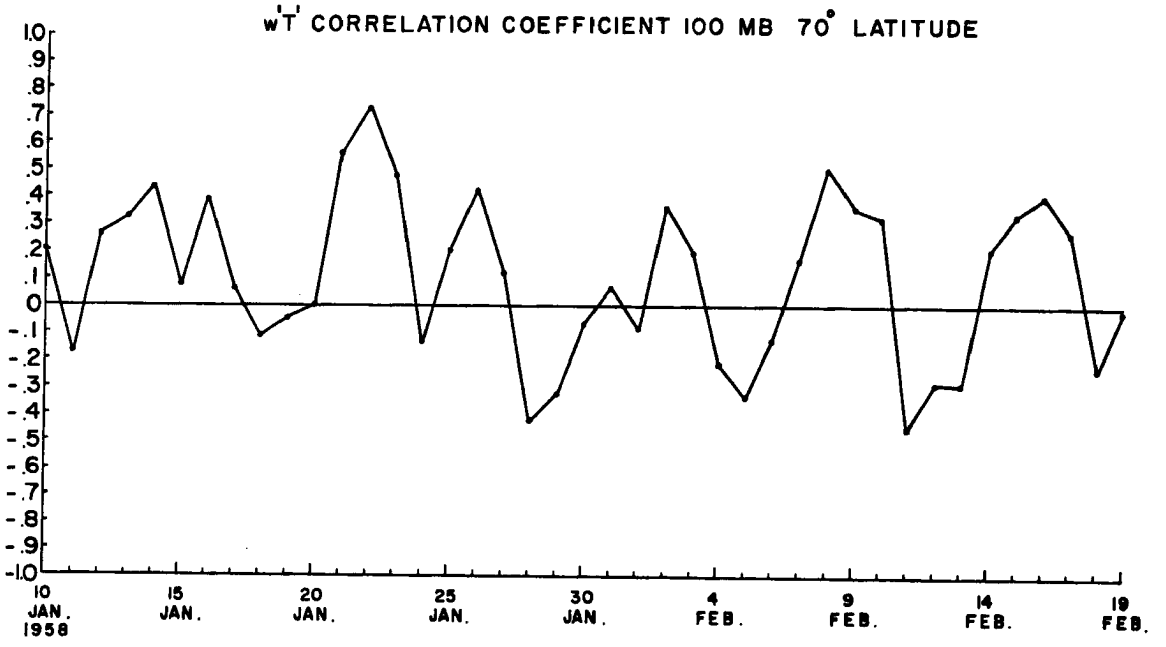

FIG. 11. Continued.

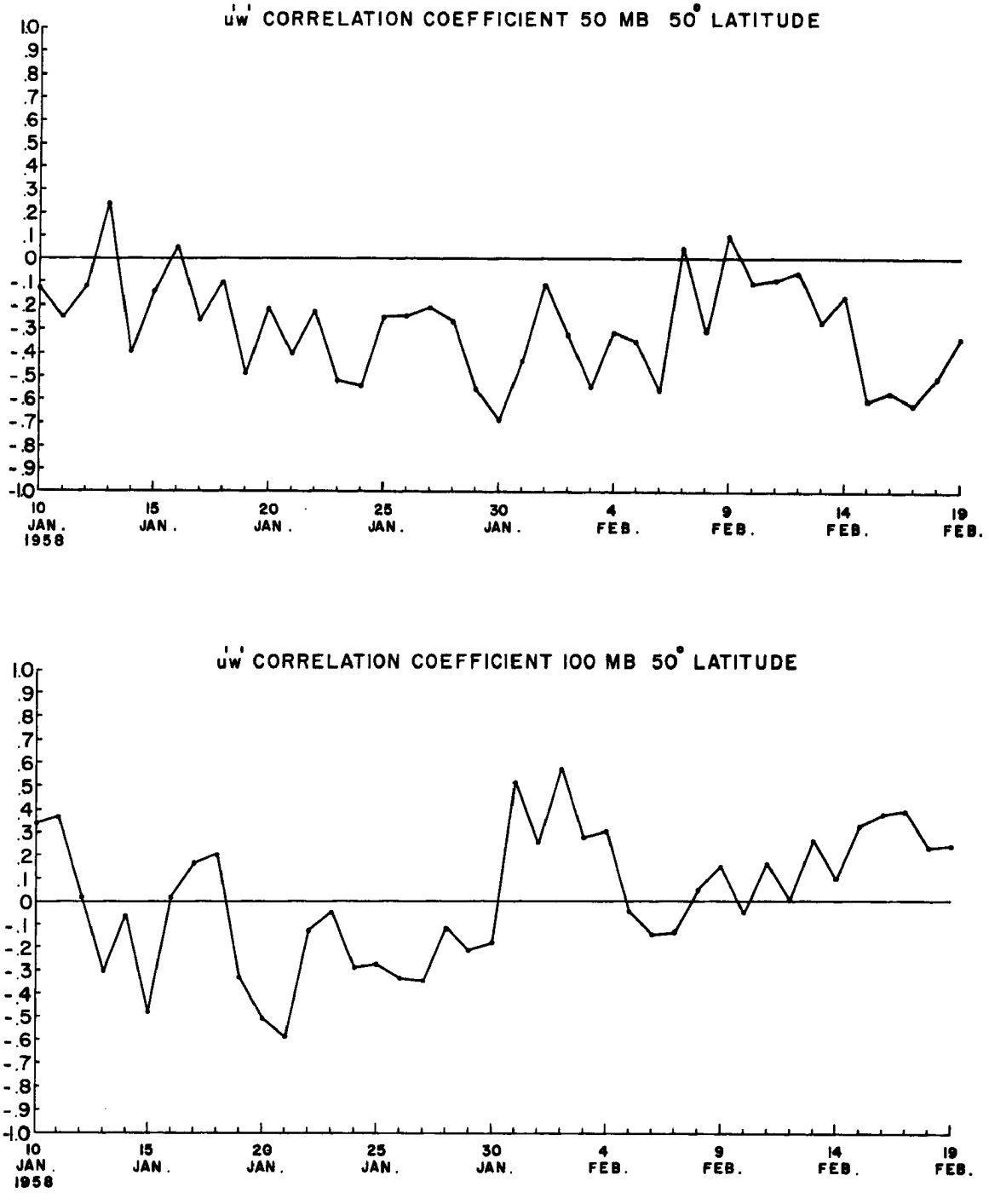

FIG. 12. u'w' correlation coefficients for indicated levels and latitudes from 10 January to 19 February 1958.

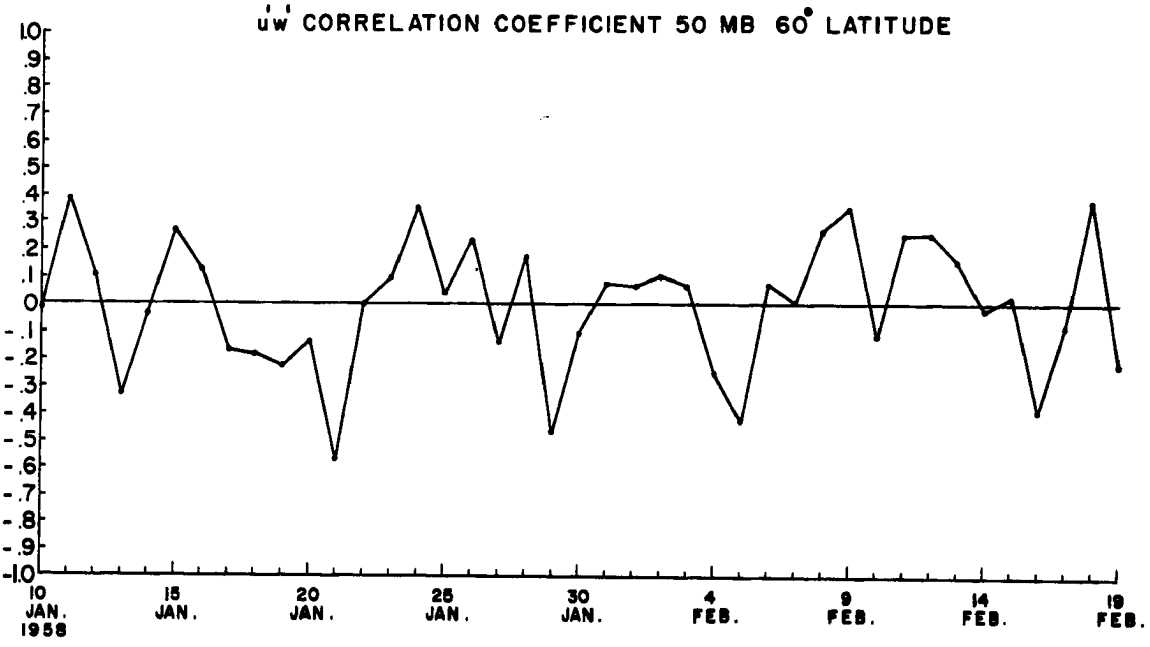

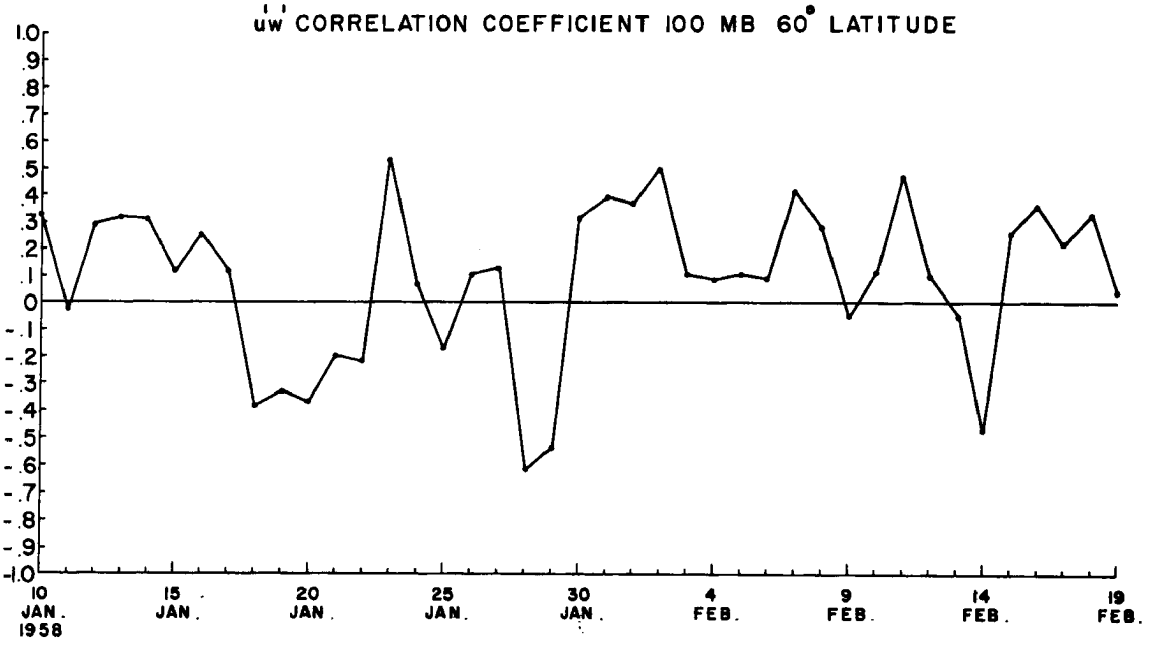

FIG. 12. Continued.

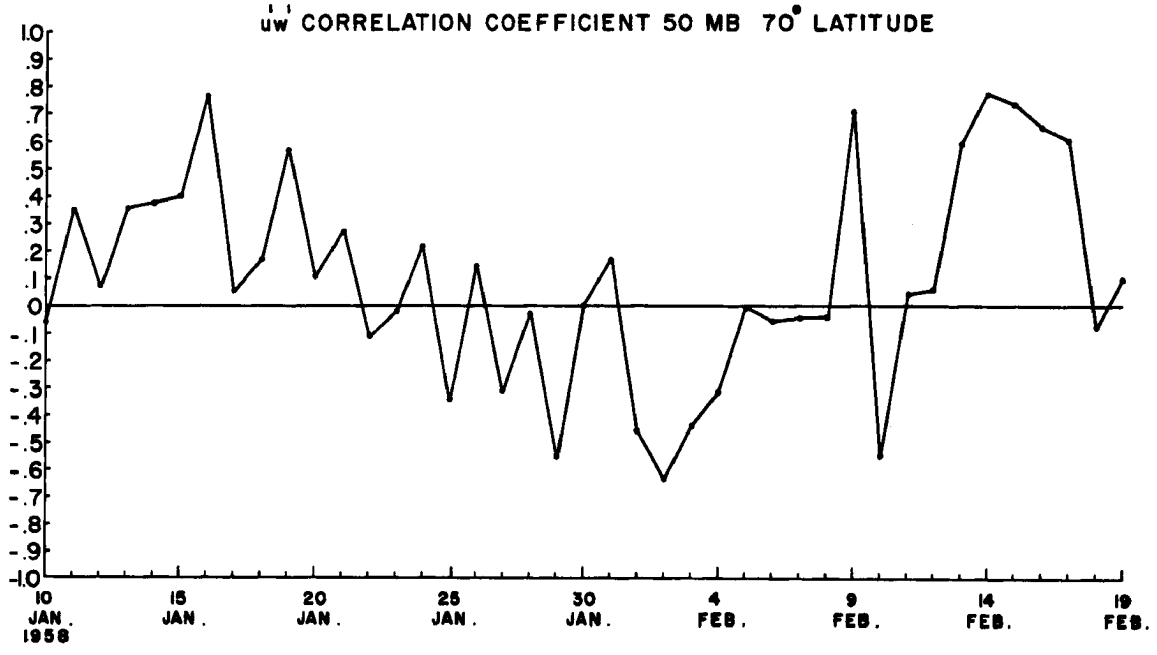

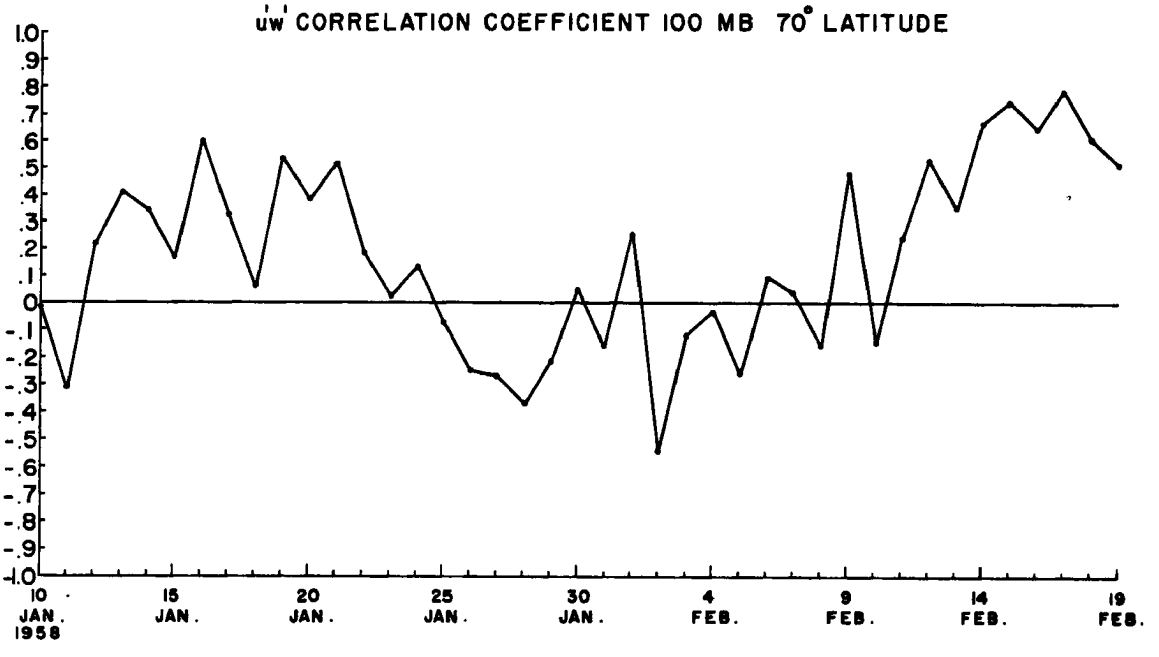

FIG. 12. Continued.

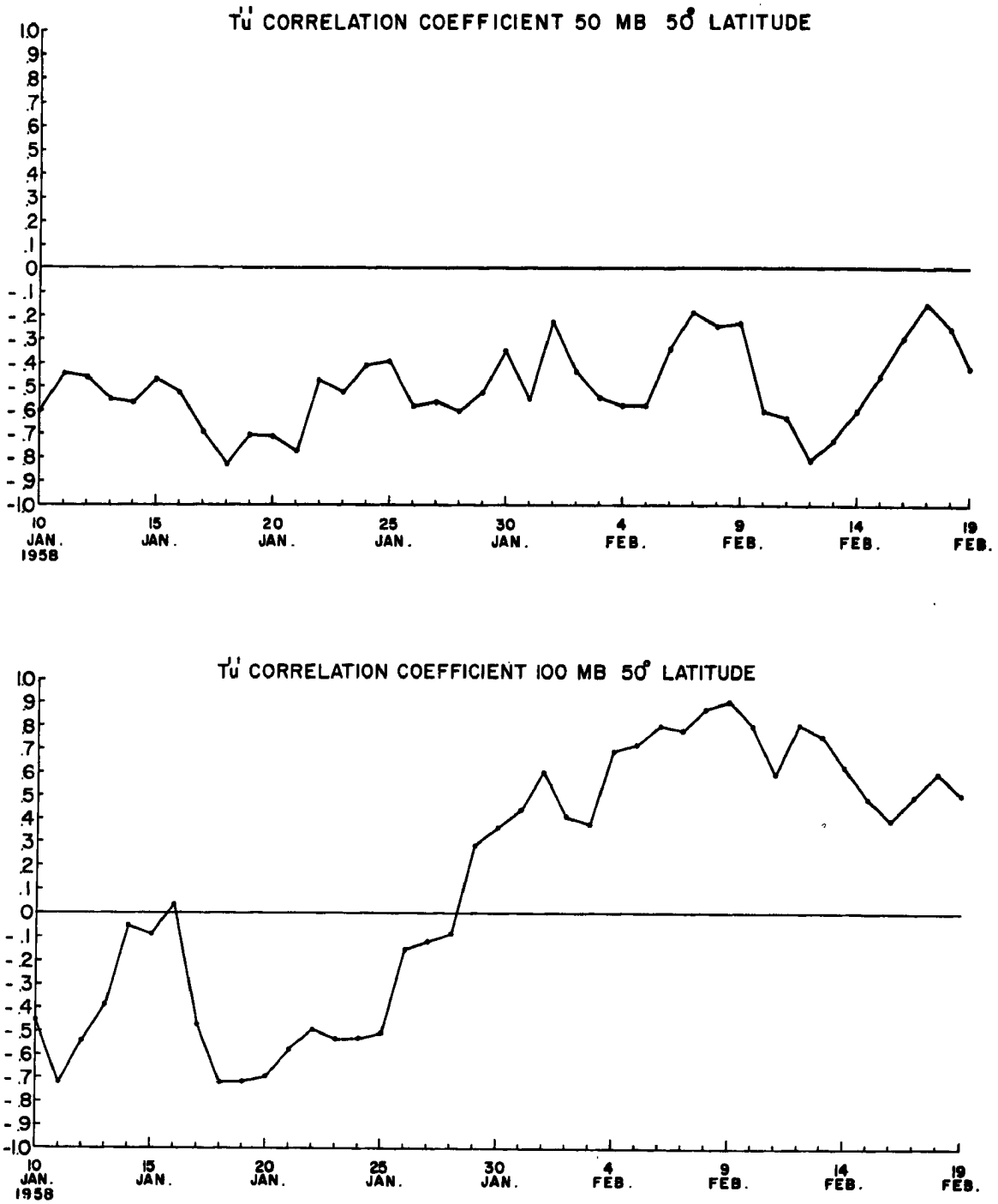

FIG. 13. T'u' correlation coefficients for indicated levels and latitudes from 10 January to 19 February 1958.

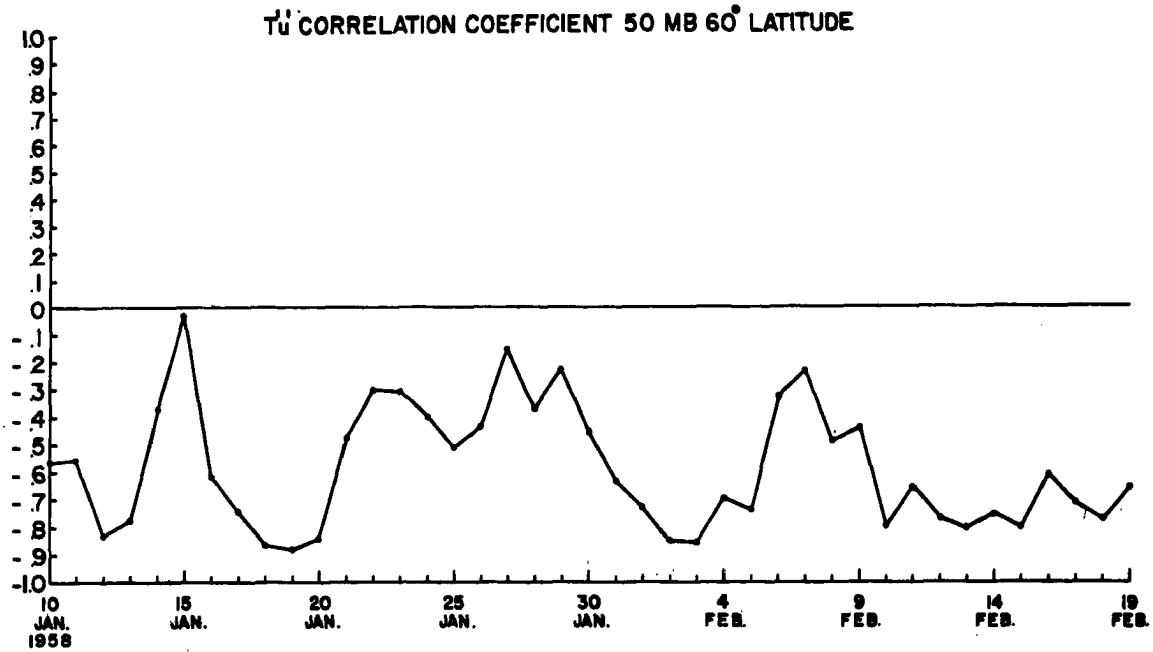

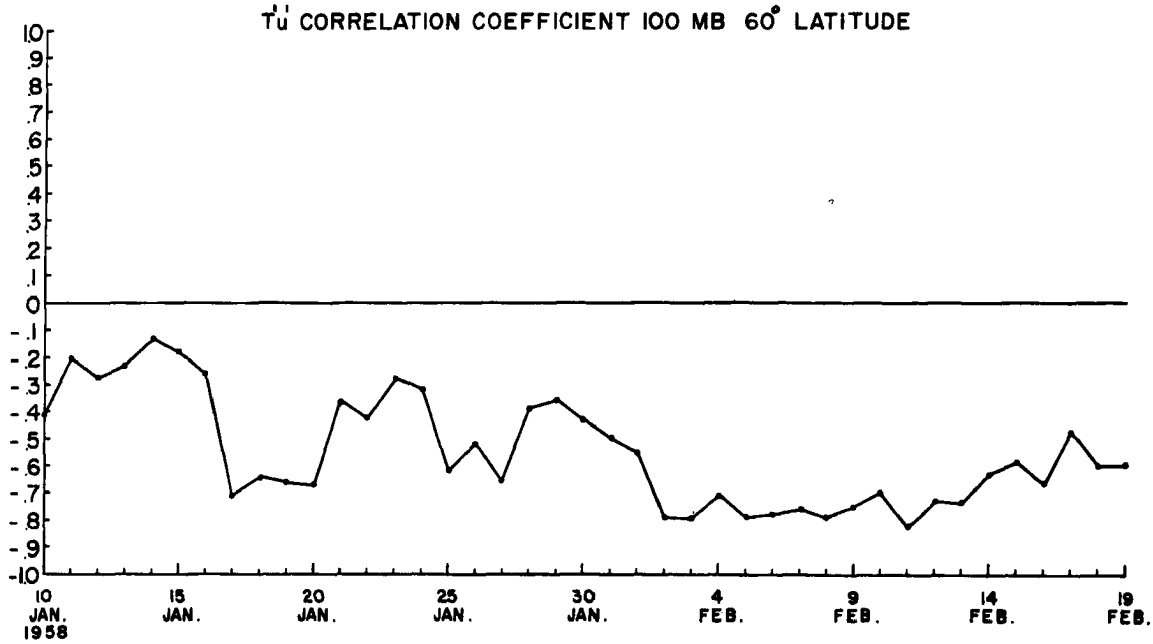

FIG. 13. Continued.

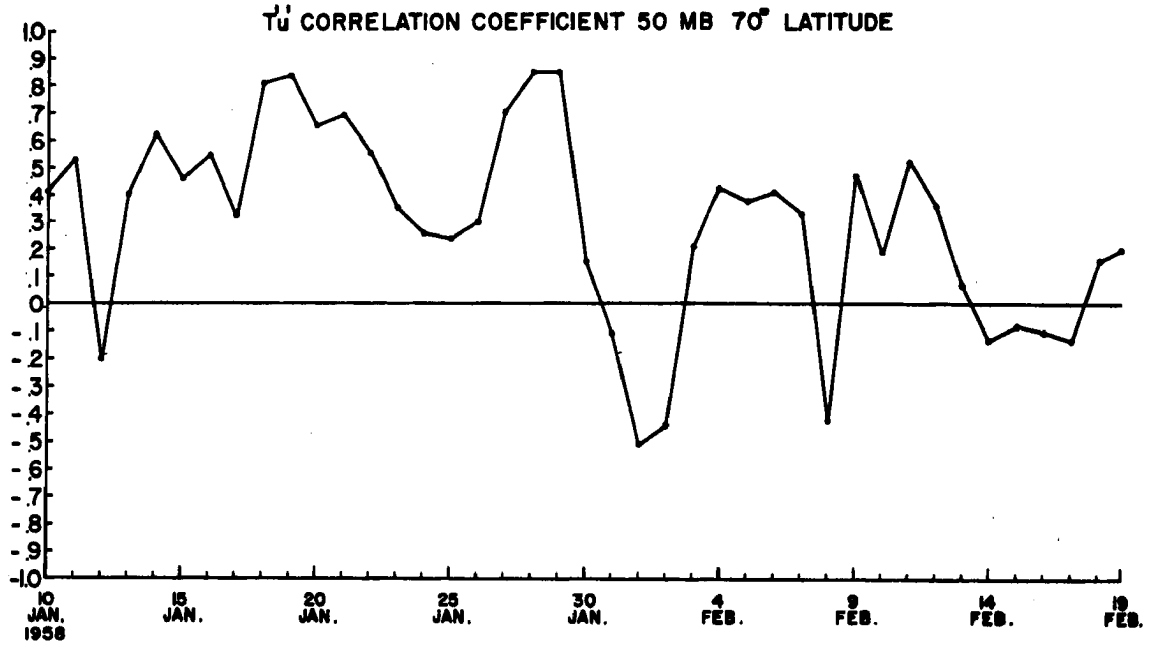

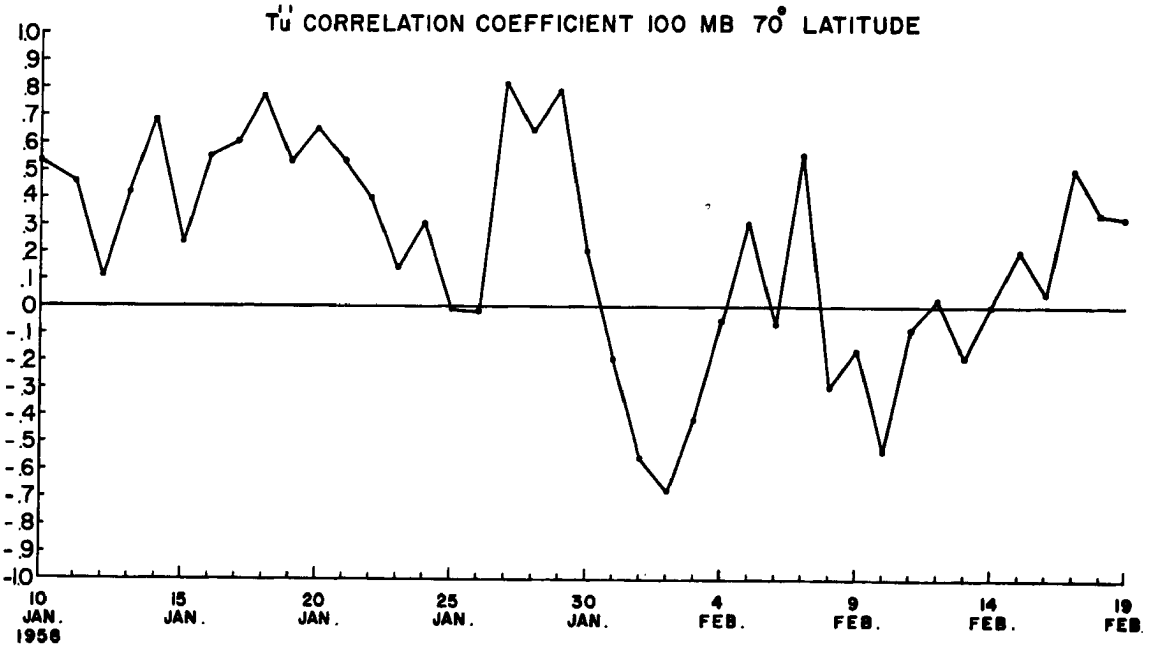

FIG. 13. Continued.

the warming and decreasing to negative values after the warming onset. This is in agreement with the decrease in mean wind after the warming period.

The correlations for w'T' may be seen in Fig. 11. In this case the pattern seems to be quite irregular with large oscillations over short periods of time. Probably the only physically significant features are the markedly negative values on 29-31 January at 50 mb, 70°N. Also the amplitude of the oscillations seem to be much higher at 70°N than at lower latitudes.

The correlations for u'w' (vertical transport of zonal momentum) are plotted in Fig. 12. At 50 mb, 50°N the values are consistently negative for the entire sequence, while at 100 mb, 50°N they become positive after the warming onset. Both 100 and 50 mb, 60°N are highly irregular with rapid fluctuations between positive and negative values. The graphs for 100 and 50 mb, 70°N exhibit a pronounced decrease from positive to negative values prior to and during the warming period. On about 3 February they begin to increase rapidly back to positive values. This indicates that a downward transport of zonal momentum operates during the warming period in high latitudes. This lends support to the contention by Miyakoda (1963) that the excess energy during the warming period is lost to the troposphere. This result is plausible in that the excess momentum does not have to be transferred to the other hemisphere to explain its large decrease during the warming period.

A particularly perplexing quantity is the u'T' correlation given in Fig. 13. At 50 mb, 50°N it is consistently negative throughout the entire time period while at 100 mb, 50°N it is initially negative and increases to very high positive values during and after the warming period. The correlations are consistently negative at 100 and 50 mb, 60°N for the entire sequence. The values are extremely large--as high as -0.8 for many successive days. Finally, at 70°N both 50

and 100 mb u'T' correlations are positive before the breakdown with a very sharp decrease to negative values with the warming onset. After the warming the correlations increase again to slightly positive values. The dynamical basis for this rather peculiar behavior is not presently evident. Perhaps with a more thorough investigation of the dynamical interrelation among all the above quantities, the significance of the u'T' correlations will become more obvious.

VII. MEAN CIRCULATION CELLS AND THE CAUSE OF THE SUDDEN WARMING IN THE STRATOSPHERE

In Chapter VI it was shown that eddy circulations in the lower stratosphere can play a very important role in transporting radioactive debris northward and downward in agreement with the sense of the observed transports. It remained to be seen what the effect would be if a mean meridional cell exists in the stratosphere. There has been considerable controversy in the literature on the subject of the existence or non-existence of mean meridional circulations in this region.

As early as 1949 (Brewer, 1949), it was hypothesized that a mean meridional cell could exist in the stratosphere. It was originally assumed that it would be a thermally driven cell of the direct Hadley type. However, in line with the discovery of an indirect meridional cell in the mid-latitude troposphere, it was realized that this cell possibly could be dynamically driven and thus operate in a thermodynamically indirect sense.

Since in the earth's atmosphere a meridional cell generally operates as a small residual on an otherwise zonal type circulation, it has been difficult if not impossible to detect even the direction of such a circulation because of the lack of data at higher levels. However, during the International Geophysical Year a concentrated effort was made to provide an adequate station network for the study of stratospheric problems. With this data a large number of studies have been undertaken on the energetic properties of this region, most notably by members of the Planetary Circulations Project at the Massachusetts Institute of Technology.

Climatically, stratospheric radioactive debris and ozone are transported northward and downward as the winter season progresses. Therefore, it is of great practical and theoretical interest to determine the direction and relative magnitude of this cell if it exists at all. Members of the Massachusetts Institute of Technology Planetary Circulations Project have attempted to solve this by two distinct approaches. Oort (1962) employed direct measurements taken from the basic wind data. His results indicate that a well-pronounced indirect cell apparently exists in the polar night stratosphere. Other investigators (Palmén, 1955; Kuo, 1956; Palmén, Riehl, and Vuorela, 1958; Haurwitz, 1961; Dickinson, 1962; Miyakoda, 1963; Gilman, 1963, 1964; Newell and Miller, 1964) have performed meridional cell computations based upon momentum budget calculations. This approach suggests that an indirect cell is operative in the polar night winter stratosphere.

Still others have used an approach invoking thermal properties (Jensen, 1961; Murgatroyd and Singleton, 1961; Teweles, 1963). Jensen (1961) and Teweles (1963) computed adiabatic vertical velocities and then averaged the resultant point measurements with respect to longitude. These studies also gave indications of an indirect cell at higher latitudes. Murgatroyd and Singleton (1961) employed a heat flux model similar to the one to be performed here, but the effect of the eddy transport terms were neglected. Their results indicated that a direct cell is present in the stratosphere.

Earlier investigators on the problem of trace substance transport concluded rather firmly that a strong direct meridional cell is necessary to make the circulation compatible with the observed sense of these transports (Brewer, 1949; Dobson, 1956; Goldie, 1958; Stewart et al., 1957; Palmer, 1959b; Libby and Palmer, 1960). The considerable controversy in the literature on this subject suggests that as a physical problem, the case is far from being closed.

Since any indirect computation of a mean meridional cell must necessarily be a relatively small residual of other larger terms, and in view of the opposite statements presented above, there is always legitimate reason to doubt computational results. As a further check on the conflicting statements given above, a meridional cell computation will be performed here through a careful inventory of the heat budget. This will be attempted for periods before, during, and after the polar night vortex breakdown of January 1958. By selecting these periods it is hoped that several questions will be answered: the sense of the meridional cell; the thermodynamic explanation for the warming process itself; and the dynamic effect of the vortex breakdown upon the meridional cell. For the above reasons a calculation of this type is essential for a thorough understanding of the breakdown process and its relation to the fallout transport problem.

Derivation of the Mean Vertical Motion Equation

An analytical expression for the mean vertical motion (resulting from a meridional cell) will now be derived in terms of measurable quantities. Consider the equation for adiabatic temperature change

$$\left(\frac{dT}{dt}\right)_{ad} = \left(\frac{dT}{dz}\right)_{ad} \frac{dz}{dt} = \Gamma w \, . \tag{16}$$

In the following development subscripts are defined as:

ad = an adiabatic process

rad = a radiative process

mea = measured directly from synoptic data assuming negligible measurement error.

Also, by definition,

$$\left(\frac{dT}{dt}\right)_{ad} = \left(\frac{dT}{dt}\right)_{mea} - \left(\frac{dT}{dt}\right)_{rad} \tag{17}$$

$$\left(\frac{dT}{dt}\right)_{rad} = \frac{1}{c_p}\frac{dh}{dt} \quad , \tag{18}$$

where h is heat per unit mass. Furthermore, assume that the radiative heat loss is independent of the motion in a region north of an arbitrary latitude circle so that $dh/dt = \partial h/\partial t$.

Combining Eqs. (16), (17), and (18) and performing an Eulerian expansion on the term $\left(\frac{dT}{dt}\right)_{mea}$ gives

$$\begin{aligned} \Gamma w &= \left(\frac{\partial T}{\partial t}\right)_{mea} - \frac{1}{c_p}\frac{\partial h}{\partial t} + \vec{V}_2 \cdot \nabla T + w\frac{\partial T}{\partial z} \quad , \\ w &= \frac{1}{\frac{\partial T}{\partial z} - \Gamma}\left[\frac{1}{c_p}\frac{\partial h}{\partial t} - \left(\frac{\partial T}{\partial t}\right)_{mea} - \vec{V}_2 \cdot \nabla T\right] . \end{aligned} \tag{19}$$

where $\vec{V}_2$ is the two-dimensional wind vector. Now by expanding $\vec{V}_2 \cdot \nabla T$ and averaging over the region north of the arbitrarily selected latitude (indicated by $\sim$) one obtains

$$\tilde{w} = \frac{1}{\frac{\partial T}{\partial z} - \Gamma}\left[\widetilde{\frac{1}{c_p}\frac{\partial h}{\partial t}} - \widetilde{\left(\frac{\partial T}{\partial t}\right)_{mea}} - \widetilde{\nabla \cdot \vec{V}T} + \widetilde{T\nabla \cdot \vec{V}}\right] \quad , \tag{20}$$

where the third term is the divergence of the temperature flux and the fourth term represents the contribution due to horizontal mass divergence. Now it is convenient to introduce the averaging procedure used in Chapter VI, e. g. ,

$$\left.\begin{aligned} h &= \bar{h} + h' \\ T &= \bar{T} + T' \\ u &= \bar{u} + u' \\ v &= \bar{v} + v' \end{aligned}\right\} \text{ or } \vec{V} = \bar{\vec{V}} + \vec{V}'$$

where a bar represents a longitudinal average and a prime represents

the point deviation from this average. However, since the third and fourth terms of Eq. (20) only depend on the properties at the boundary of the given region (in this case, the southernmost latitude circle), one can write

$$\widetilde{-\nabla \cdot \vec{V}T} + \widetilde{T\nabla \cdot \vec{V}} \equiv \overline{-\nabla \cdot \vec{V}T} + \overline{T\nabla \cdot \vec{V}} \quad . \tag{21}$$

Expanding Eq. (21) in terms of mean and eddy components gives

$$\overline{-\nabla \cdot \vec{V}T} + \overline{T\nabla \cdot \vec{V}} = -\nabla \cdot \bar{\vec{V}}\bar{T} - \overline{\nabla \cdot \vec{V}'T'} + \bar{T}\nabla \cdot \bar{\vec{V}} + \overline{T'\nabla \cdot \vec{V}'} \quad . \tag{22a}$$

By expressing the mean terms in scaler form and transforming the eddy terms to line integral form, one obtains for the right-hand side of Eq. (22a)

$$-\frac{\partial}{\partial x}(\bar{u}\bar{T}) - \frac{\partial}{\partial y}(\bar{v}\bar{T}) + \overline{\frac{1}{A}\oint_{\phi} v'T' \cdot dx} + \bar{T}\frac{\partial \bar{u}}{\partial x}$$

$$+ \bar{T}\frac{\partial \bar{v}}{\partial y} - \overline{\frac{T'}{A}\oint_{\phi} v' \cdot dx} \quad .$$

The subscript ϕ indicates that the integration is along a latitude circle. However,

$$\frac{\partial}{\partial x}(\bar{u}\bar{T}) = \bar{T}\frac{\partial \bar{u}}{\partial x} \equiv 0$$

because T and u are averaged with respect to the x coordinate and, thus, can have no variation in that direction. Also,

$$-\overline{\frac{T'}{A}\oint_{\phi} v' \cdot dx} = 0 \quad .$$

since v' is integrated over its averaging interval. Consequently, one

can write the following identity for Eq. (22a)

$$-\overline{\nabla \cdot \vec{V}T} + \overline{T\nabla \cdot \vec{V}} \equiv -\bar{v}\frac{\partial \bar{T}}{\partial y} + \overline{\frac{1}{A}\oint_{\phi} v'T' \cdot dx} \,. \qquad (22b)$$

Now, substituting Eq. (22b) into Eq. (20) gives an expression for the mean vertical velocity

$$\tilde{w} = \frac{1}{\frac{\partial T}{\partial z} - \Gamma}\left[\frac{1}{c_p}\widetilde{\frac{\partial h}{\partial t}} - \widetilde{\frac{\partial \bar{T}}{\partial t_{mea}}} - \bar{v}\frac{\partial \bar{T}}{\partial y} + \frac{1}{A}\oint_{\phi} v'T' \cdot dx\right] \qquad (23)$$

since $\widetilde{\frac{\partial h'}{\partial t}} = \widetilde{\frac{\partial T'}{\partial t}} = 0$ and $\overline{\frac{1}{A}\oint_{\phi} v'T' \cdot dx} = \frac{1}{A}\oint_{\phi} v'T' \cdot dx$.

Eq. (23) is in a form which can be evaluated from the basic meteorological data.

Computation of the Mean Meridional Cell

The first and third terms in Eq. (23) are somewhat difficult to evaluate. Calculation of the first term demands an adequate knowledge of the mean radiational cooling in the polar night stratosphere. Works by Ohring (1958), Davis (1963), and Kennedy (1964) all suggest that a net radiational cooling of 1°C per day is a reasonable value for the lower polar stratosphere during the winter season. Thus, for convenience this value will be used to calculate the first term in Eq. (23). It must be cautioned, however, that this term has a probable uncertainty of $\pm 0.5^{\circ}$C per day.

The second term $(-\widetilde{\partial \bar{T}/\partial t_{mea}})$ was evaluated by plotting successive charts of mean temperature ($\bar{T}$) with respect to latitude (see Figs. 14a, b, c) and by graphically determining the mean temperature change from these charts over the area of interest for five-day increments.

It was assumed that the third term $(-\bar{v}\partial \bar{T}/\partial y)$ was negligibly small relative to the other terms. By using Teweles' (1963) largest

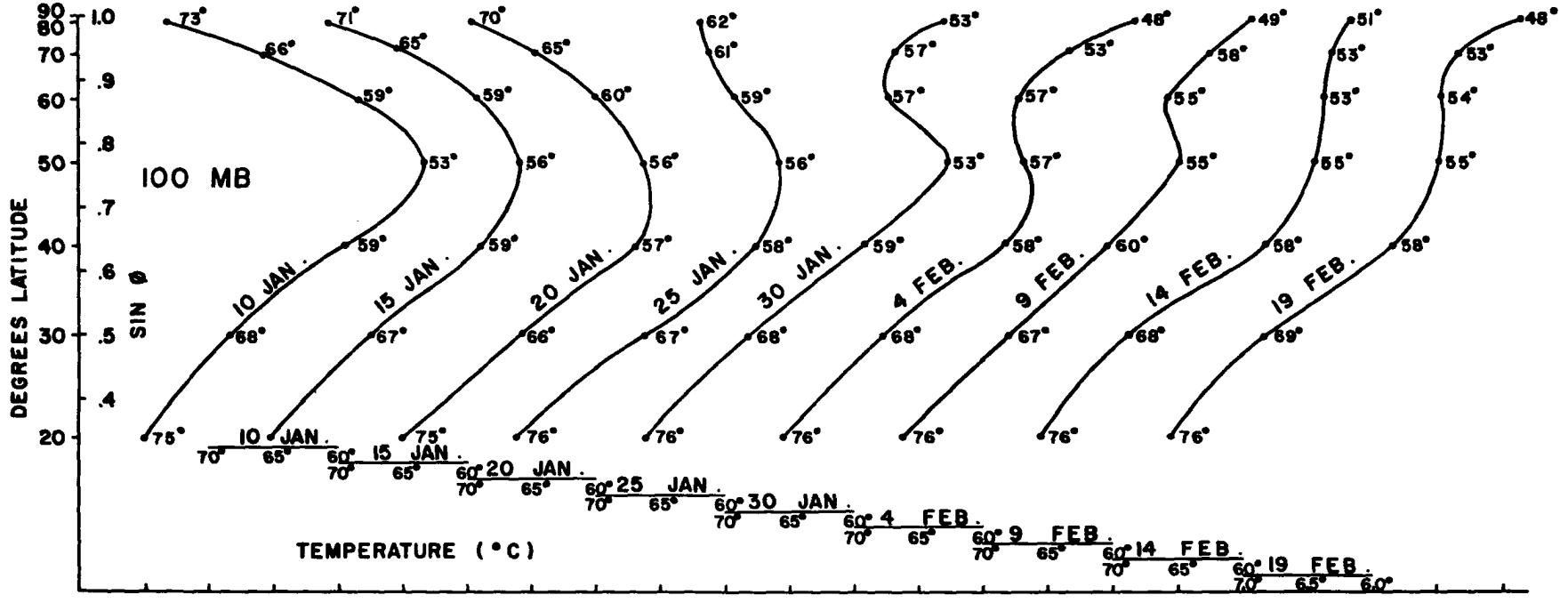

FIG. 14a. Zonal mean temperatures plotted as a function of sin latitude (ϕ) for 100 mb. Abscissa scale is shifted 10 degrees to the right for each five-day interval. Numerical values of zonal mean temperatures are given at each point to the right of the curve.

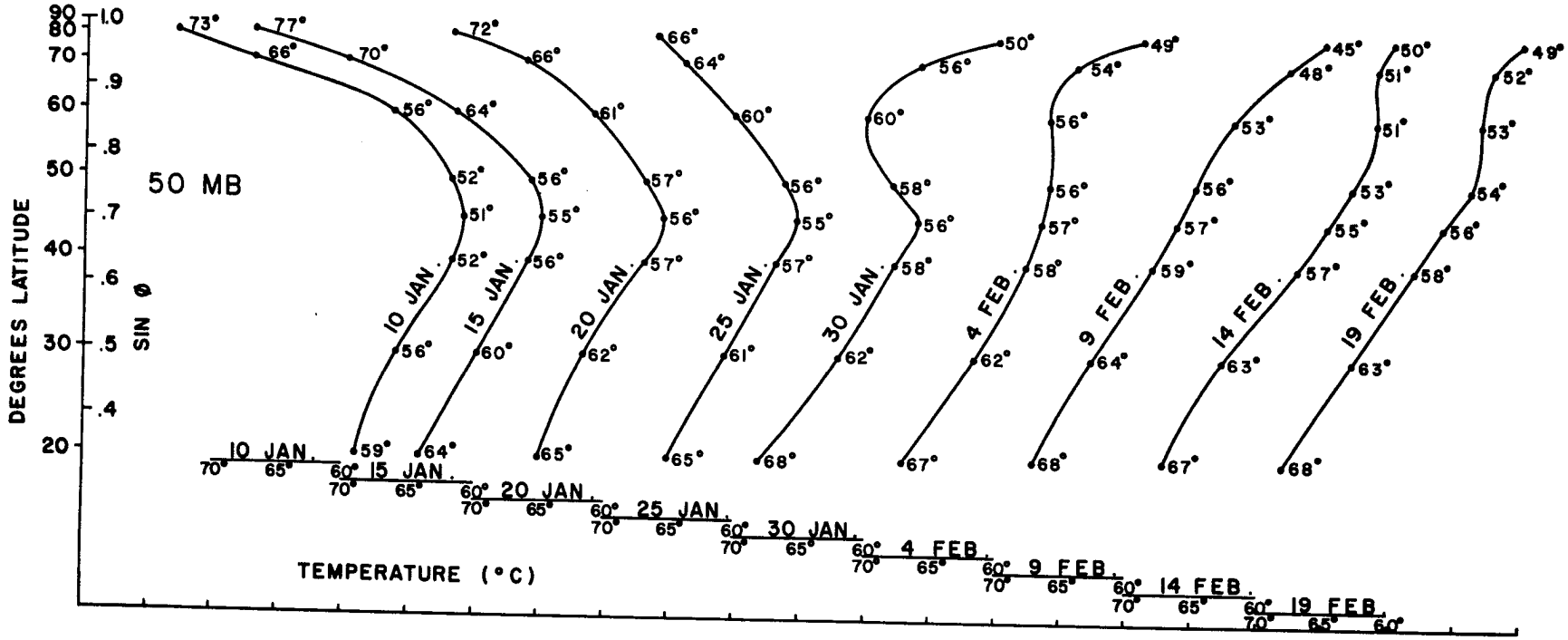

FIG. 14b. Same as 14a except at 50 mb.

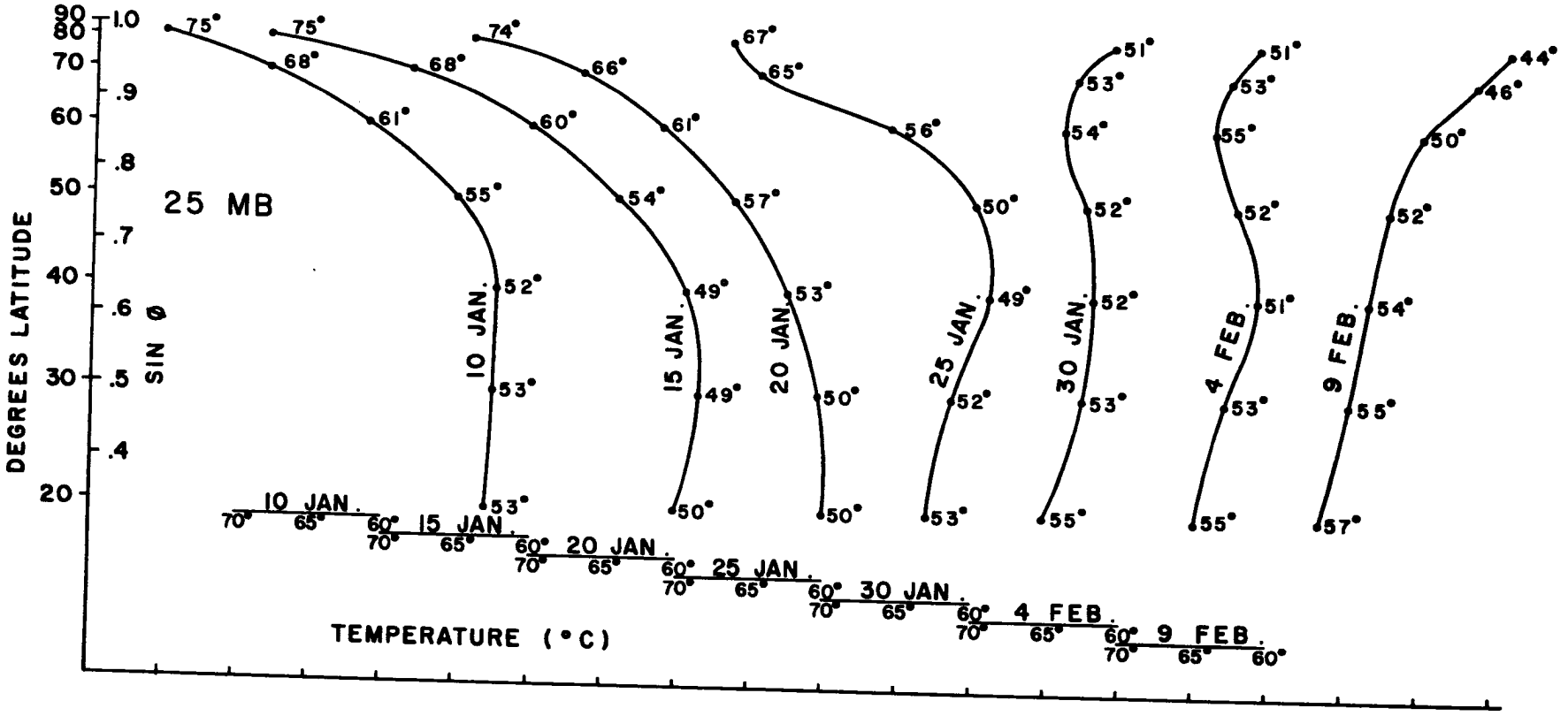

FIG. 14c. Same as 14a except at 25 mb.

value for $\bar{v}$ in this region (0.26 knot) and the highest value of $\partial\bar{T}/\partial y$ from Fig. 14, it is seen that $\bar{v}\ \partial\bar{T}/\partial y_{max} \approx 0.1$ deg day^{-1}. This is considerably smaller than the other terms in Eq. (23) and is even well within the uncertainty limits of the radiational cooling term. Consequently, the omission of this term in the calculation is justified.

The evaluation of the fourth term (eddy temperature flux) was accomplished by a careful tabulation of v and T every ten degrees of longitude at 100 and 50 mb, and at latitudes 50°N, 60°N, and 70°N. Thus, Eq. (23) gives the mean vertical motion at these two levels for the entire region north of 50°N, 60°N, and 70°N, respectively. In other words, the mean vertical motions north of a given latitude circle ($\tilde{w}_{50^\circ-90^\circ}$, $\tilde{w}_{60^\circ-90^\circ}$, and $\tilde{w}_{70^\circ-90^\circ}$) are obtained explicitly from Eq. (23). Furthermore, one can obtain values for the intermediate regions, 50° → 60°N and 60° → 70°N, by evaluating the expressions

$$\frac{A^*_{50^\circ-60^\circ}}{A^*_{50^\circ-90^\circ}}\ \tilde{w}_{50^\circ-60^\circ} + \frac{A^*_{60^\circ-90^\circ}}{A^*_{50^\circ-90^\circ}}\ \tilde{w}_{60^\circ-90^\circ} = \tilde{w}_{50^\circ-90^\circ} \tag{24a}$$

$$\frac{A^*_{60^\circ-70^\circ}}{A^*_{60^\circ-90^\circ}}\ \tilde{w}_{60^\circ-70^\circ} + \frac{A^*_{70^\circ-90^\circ}}{A^*_{60^\circ-90^\circ}}\ \tilde{w}_{70^\circ-90^\circ} = \tilde{w}_{60^\circ-90^\circ}, \tag{24b}$$

where A^* represents the area enclosed between the latitudes indicated by the respective subscripts.

Fig. 15 gives the results of these computations obtained from Eqs. (23), (24a), and (24b) for the periods before, during, and after the polar night vortex breakdown. This figure shows that a well-pronounced <u>indirect</u> cell is operating in this region during all three calculation periods. Furthermore, the cell configuration is virtually identical in all three diagrams. However, the apparent intensity of this indirect cell is greater during the period of breakdown.

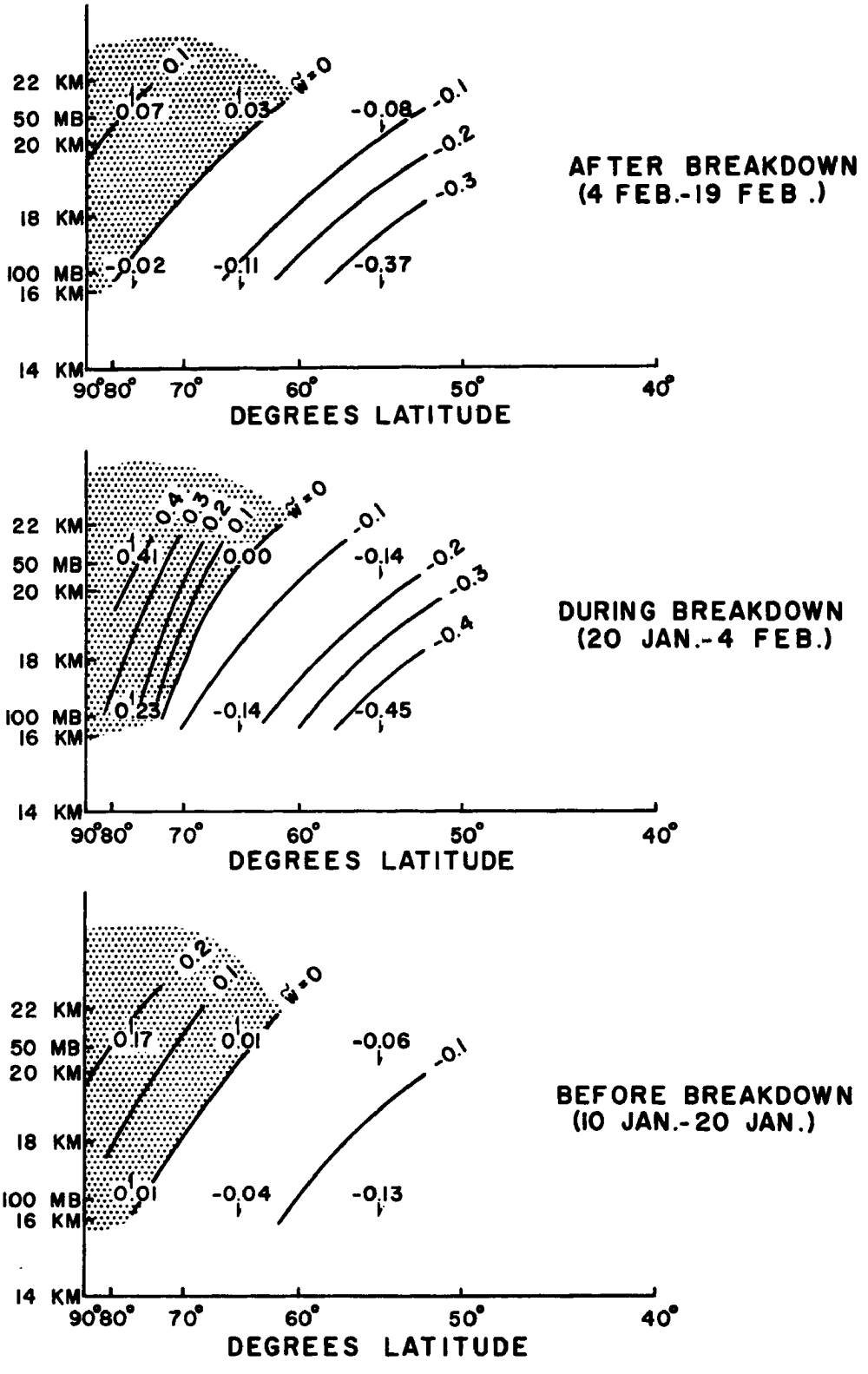

FIG. 15. Area averaged vertical motion ($\tilde{w}$) in km day^{-1} computed from Eqs. (23), (24a), and (24b) for indicated periods before, during, and after polar night vortex breakdown of January-February 1958. Hatching denotes area of rising motion.

This result agrees with the dynamic calculations of w by previous investigators, but disagrees with the values deduced from measured transports of trace substances in the stratosphere. It also disagrees with Murgatroyd and Singleton's (1961) results which neglected the contribution due to eddy heat transport. One thus can infer that the eddies play a powerful role in the mechanism of debris transport in this region. In fact, since the meridional cell acts to carry debris and ozone upward and away from the pole, this and the eddy transports of Figs. 7 and 8 must ultimately be reconciled with the climatically observed distribution of downward and northward transport of these quantities.

Cause of the Sudden Warming

There has been some controversy concerning the physical mechanism which acts to produce the temperature increase during the sudden warming period. With the data used in the computation of $\tilde{w}$, it is possible to evaluate various contributing mechanisms. Because of the relatively small energies available, heating by sudden corpuscular emissions must be discarded, although a possibility remains that this phenomenon could play a role in initiating the breakdown. The most popular theory has been that the warming is produced by rapid adiabatic descent over the pole during the breakdown period. However, Fig. 15 shows that the meridional cell operates even stronger in the <u>indirect</u> sense during the warming period. Thus, according to this, the adiabatic descent mechanism must be abandoned as a tenable explanation of the sudden warming phenomenon. On the other hand, this process is probably quite important in explaining very large temperature increases occurring in limited areas.

Consequently, it must be hypothesized that the horizontal eddy flux of temperature ($\overline{v'T'}$) is capable of producing this mean increase.

Table 3 contains tabulated values of all terms acting in Eq. (23) at five-day intervals at 100 and 50 mb, for the regions north of 50°N, 60°N, and 70°N, respectively. It is readily seen from this table that the eddy flux term ($\frac{1}{A}\oint_{\phi} v'T'\,dx$) during the warming period 20 January-4 February is transporting much more heat northward at higher latitudes than needed to account for the observed warming in these regions. It also may be seen from Figs. 16 and 17 that the warming process depends directly upon the magnitude of eddy temperature transport at this time. Fig. 17 also shows that in virtually all cases at 60° and 70°N the computed eddy temperature transport ($\frac{1}{A}\oint_{\phi} v'T'\,dx$) into the region is greater than the observed warming north of a given latitude. Consequently, it may be rather firmly concluded on the basis of these computations that a pronounced increase in the horizontal heat flux during this period is primarily responsible for the observed temperature increases associated with the polar night vortex breakdown. It should be noted that this only pinpoints the physical process producing the warming, but says nothing about the initial mechanism that produces the breakdown.

To arrive at a better estimate of the significance of the above noted relationship between observed warming and eddy temperature transport, correlation coefficients were computed from the data given in Fig. 17. For 50 mb, 60° and 70°N, over the time interval 10 January to 20 February the correlation coefficient between these two quantities was + 0.81. For 100 mb, 60° and 70°N, the correlation was + 0.86. In view of the almost complete independence of successive comparisons between eddy temperature flux and observed warming, these correlation coefficients are extremely high. In fact, they leave little or no doubt that eddy temperature fluxes are primarily responsible for the temperature increases during the sudden warming period.

TABLE 3. Contribution of various terms in Eq. (23) as possible heating mechanisms for the "sudden warming" phenomenon (all units are expressed in degrees/day).

	Warming Term $\partial\tilde{\bar{T}}/\partial t$	Radiation Term $\frac{1}{c_p}\frac{\partial\tilde{\bar{q}}}{\partial t}$ (est)	Mean Cell Terms $-(\frac{\partial T}{\partial z} - \Gamma)\tilde{w}$	$\bar{v}\frac{\partial\bar{T}}{\partial y}$	Eddy Flux Term $\frac{1}{A}\oint_\phi v't'\,dx$
10-15 January					
100 mb					
N of 50°	-0.1	-1°/day	+0.6°	±0.1°max	+0.6°
N of 60°	+0.1	-1°	+0.1°	±0.1°max	+1.0°
N of 70°	+0.3	-1°	+1.3°	±0.1°max	+0.0°
50 mb					
N of 50°	-0.8°	-1°	-0.5°	±0.1°max	+0.7°
N of 60°	-0.8°	-1°	-1.0°	±0.1°max	+1.2°
N of 70°	-1.1°	-1°	-0.3°	±0.1°max	+0.2°
15-20 January					
100 mb					
N of 50°	0.0	-1°	+0.2°	±0.1°max	+0.8°
N of 60°	+0.1°	-1°	-0.6°	±0.1°max	+1.7°
N of 70°	+0.2°	-1°	-1.3°	±0.1°max	+2.5°
50 mb					
N of 50°	+0.1°	-1°	-0.2°	±0.1°max	+1.3°
N of 60°	+0.4°	-1°	-1.1°	±0.1°max	+2.5°
N of 70°	+0.5°	-1°	-2.8°	±0.1°max	+4.3°
20-25 January					
100 mb					
N of 50°	+0.6°	-1°	+0.5°	±0.1°max	+1.1°
N of 60°	+0.8°	-1°	-0.9°	±0.1°max	+2.7°
N of 70°	+1.1°	-1°	-3.0°	±0.1°max	+5.1°

TABLE 3. Continued.

	Warming Term $\widetilde{\partial\overline{T}/\partial t}$	Radiation Term $\widetilde{\frac{1}{c_p}\frac{\partial\overline{q}}{\partial t}}$ (est)	Mean Cell Terms $-\left(\frac{\partial T}{\partial z}-\Gamma\right)\widetilde{w}$	$\overline{v}\frac{\partial\overline{T}}{\partial y}$	Eddy Flux Term $\frac{1}{A}\oint_{\phi} v't'\,dx$
20-25 January Continued					
50 mb					
N of 50°	+0.5°	-1°/day	-0.4°	±0.1°max	+1.9°
N of 60°	+0.6°	-1°	-1.4°	±0.1°max	+3.0°
N of 70°	+0.8°	-1°	-4.3°	±0.1°max	+6.1°
25-30 January					
100 mb					
N of 50°	+0.6°	-1°	+1.4°	±0.1°max	+0.2°
N of 60°	+1.0°	-1°	-1.7°	±0.1°max	+3.7°
N of 70°	+1.4°	-1°	-2.4°	±0.1°max	+4.8°
50 mb					
N of 50°	+1.0°	-1°	-0.0°	±0.1°max	+2.0°
N of 60°	+2.0°	-1°	-1.6°	±0.1°max	+4.6°
N of 70°	+2.8°	-1°	-3.0°	±0.1°max	+6.8°
30 January-4 February					
100 mb					
N of 50°	-0.1°	-1°	+1.7°	±0.1°max	-0.8°
N of 60°	+0.4°	-1°	-0.8°	±0.1°max	+2.2°
N of 70°	+0.8°	-1°	-1.1°	±0.1°max	+2.9°
50 mb					
N of 50°	+0.6°	-1°	0.0°	±0.1°max	+1.6°
N of 60°	+0.4°	-1°	-2.2°	±0.1°max	+3.6°
N of 70°	+0.3°	-1°	-4.5°	±0.1°max	+5.8°

TABLE 3. Continued.

	Warming Term	Radiation Term	Mean Cell Terms		Eddy Flux Term
	$\partial\overline{T}/\partial t$	$\frac{1}{c_p}\frac{\partial\overline{q}}{\partial t}_{(est)}$	$-(\frac{\partial T}{\partial z}-\Gamma)\widetilde{w}$	$\overline{v}\frac{\partial\overline{T}}{\partial y}$	$\frac{1}{A}\oint_{\phi} v't'\,dx$
4-9 February					
100 mb					
N of 50°	+0.2°	-1°/day	+2.1°	±0.1°max	-0.9°
N of 60°	+0.1°	-1°	+0.2°	±0.1°max	+0.9°
N of 70°	-0.0°	-1°	-0.7°	±0.1°max	+1.7°
50 mb					
N of 50°	+0.6°	-1°	+0.3°	±0.1°max	+1.3°
N of 60°	+0.8°	-1°	-0.4°	±0.1°max	+2.2°
N of 70°	+0.6°	-1°	-0.8°	±0.1°max	+2.4°
9-14 February					
100 mb					
N of 50°	+0.1°	-1°	+1.3°	±0.1°max	-0.2°
N of 60°	0.0°	-1°	+0.6°	±0.1°max	+0.4°
N of 70°	-0.4°	-1°	+1.0°	±0.1°max	-0.6°
50 mb					
N of 50°	-0.0°	-1°	+0.6°	±0.1°max	+0.4°
N of 60°	-0.7°	-1°	+0.3°	±0.1°max	+0.1°
N of 70°	-0.9°	-1°	+0.6°	±0.1°max	-0.5°
14-19 February					
100 mb					
N of 50°	0.0°	-1°	+1.5°	±0.1°max	-0.5°
N of 60°	+0.1°	-1°	+0.3°	±0.1°max	+0.8°
N of 70°	+0.4°	-1°	+0.9°	±0.1°max	+0.5°
50 mb					
N of 50°	-0.3°	-1°	0.0°	±0.1°max	+0.7°
N of 60°	-0.2°	-1°	-0.6°	±0.1°max	+1.4°
N of 70°	-0.2°	-1°	-0.9°	±0.1°max	+1.7°

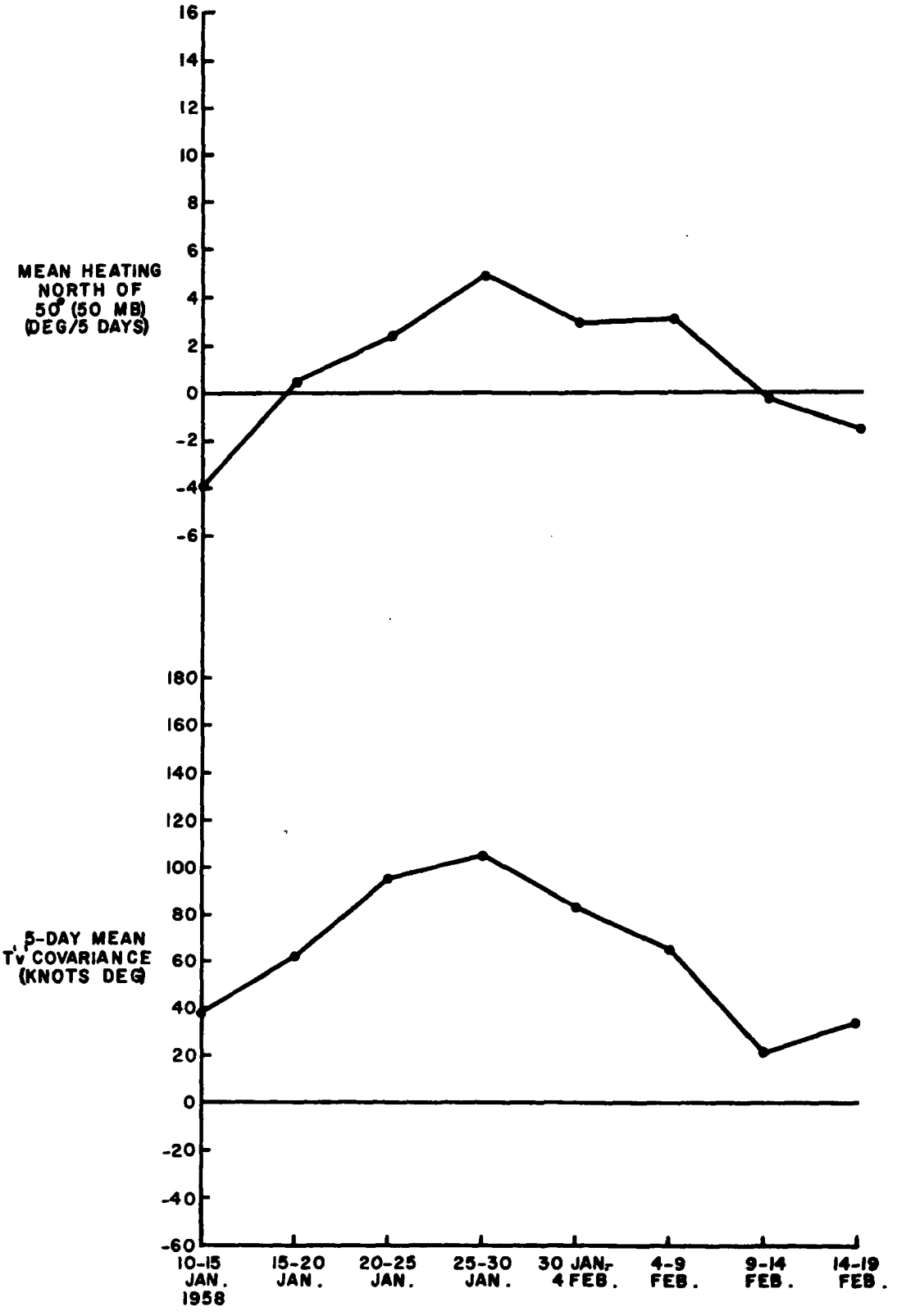

FIG. 16. Comparison between mean heating north of a given latitude and five-day mean $T'v'$ covariance at the given latitude for indicated levels and latitudes.

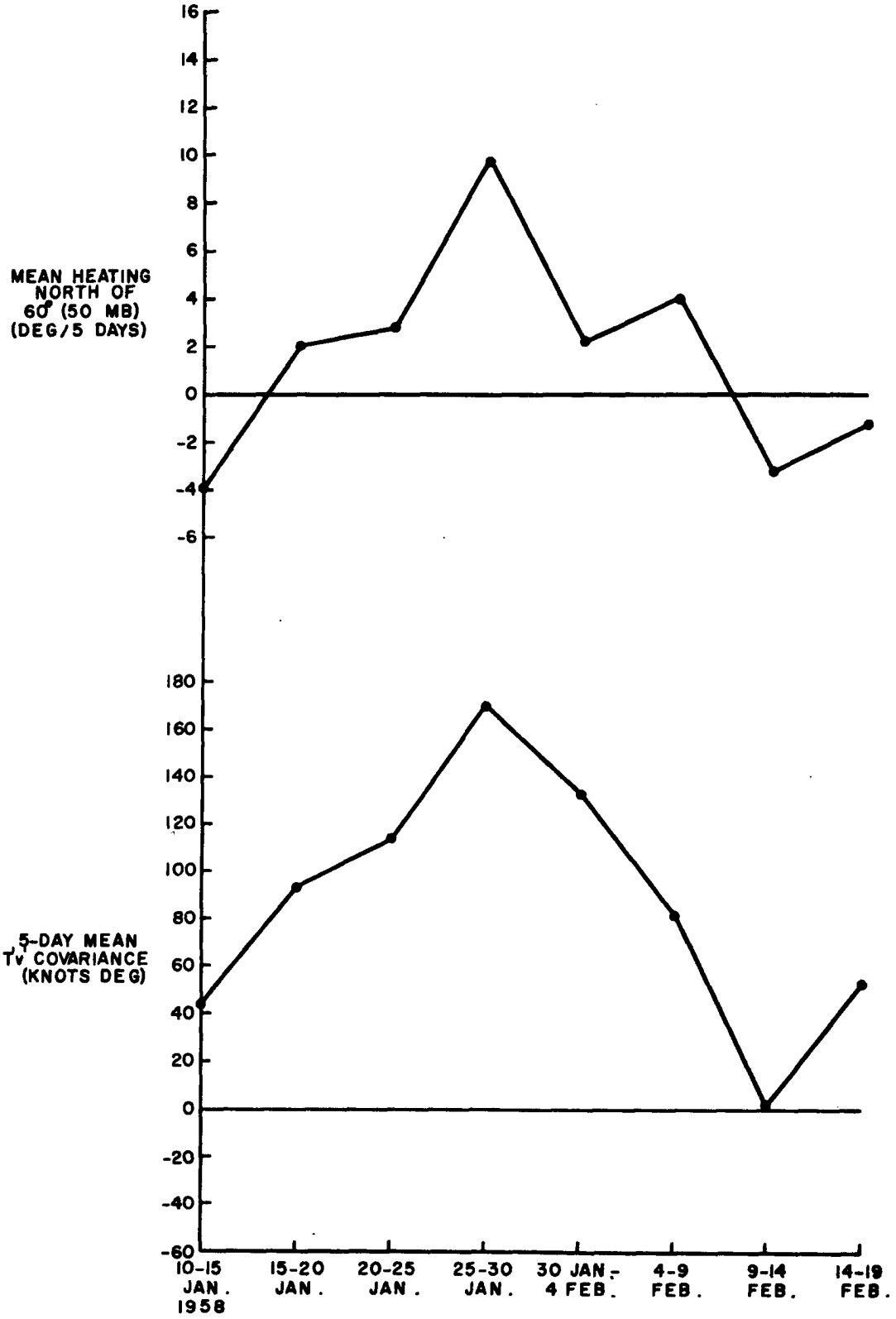

FIG. 16. Continued.

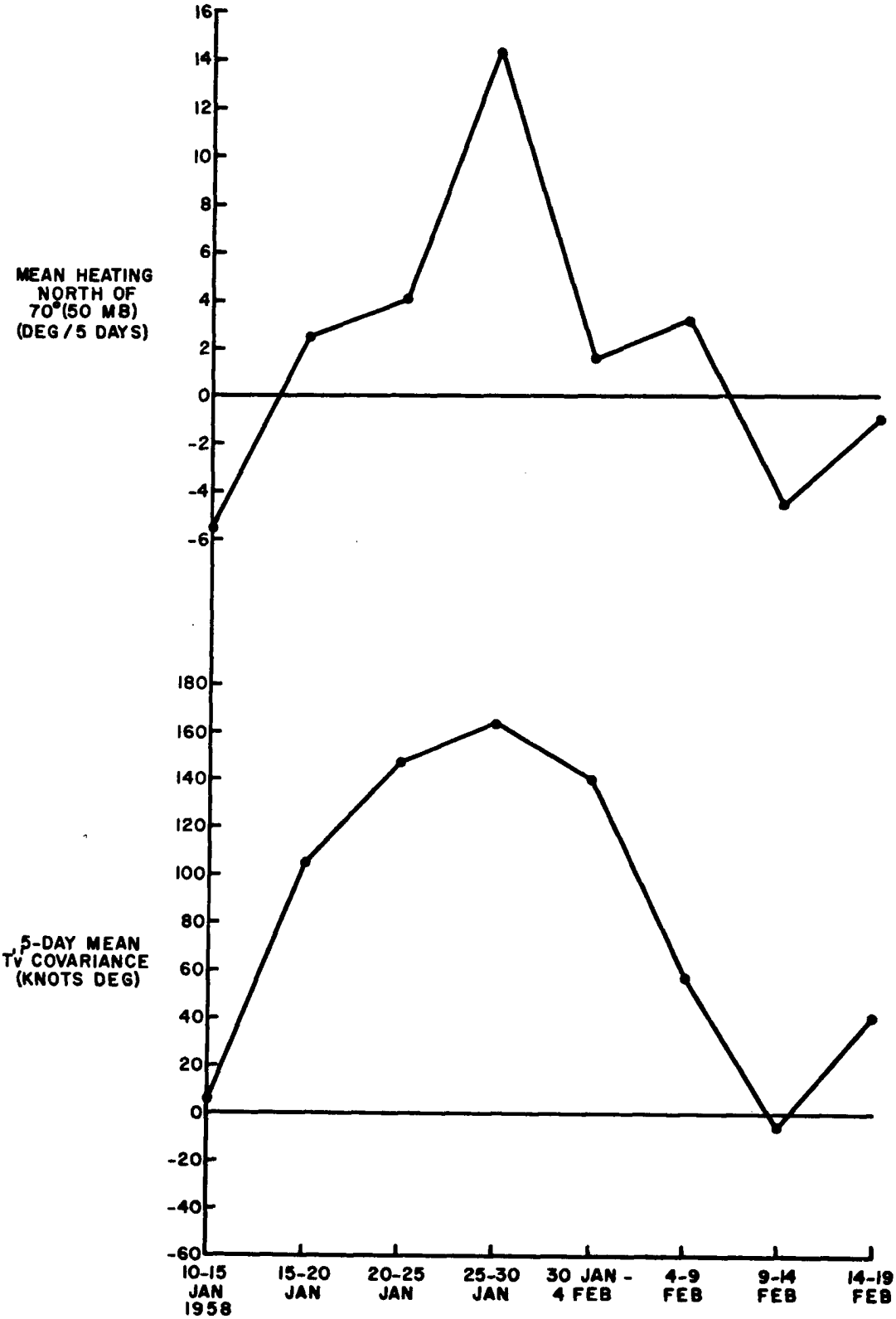

FIG. 16. Continued.

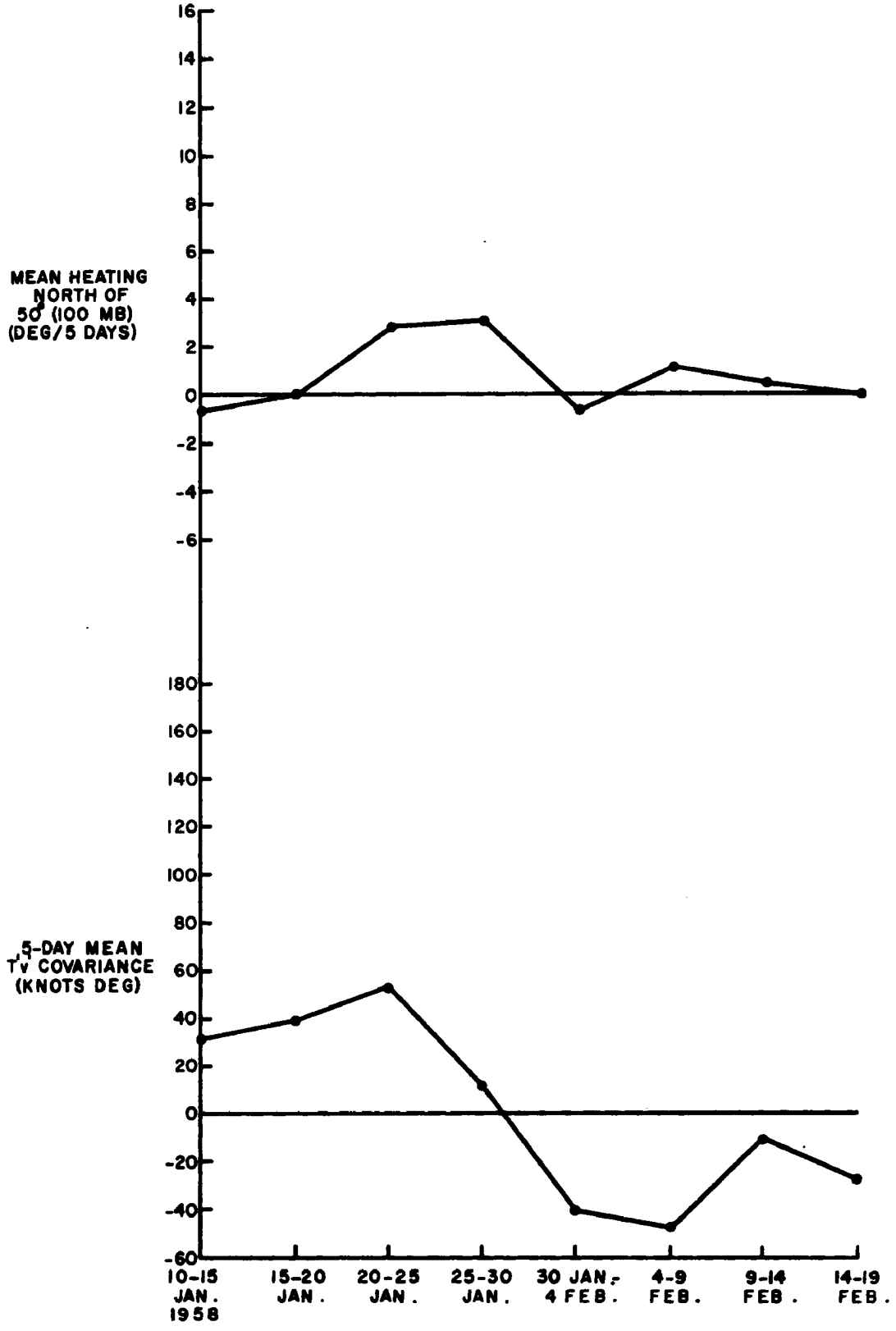

FIG. 16. Continued.

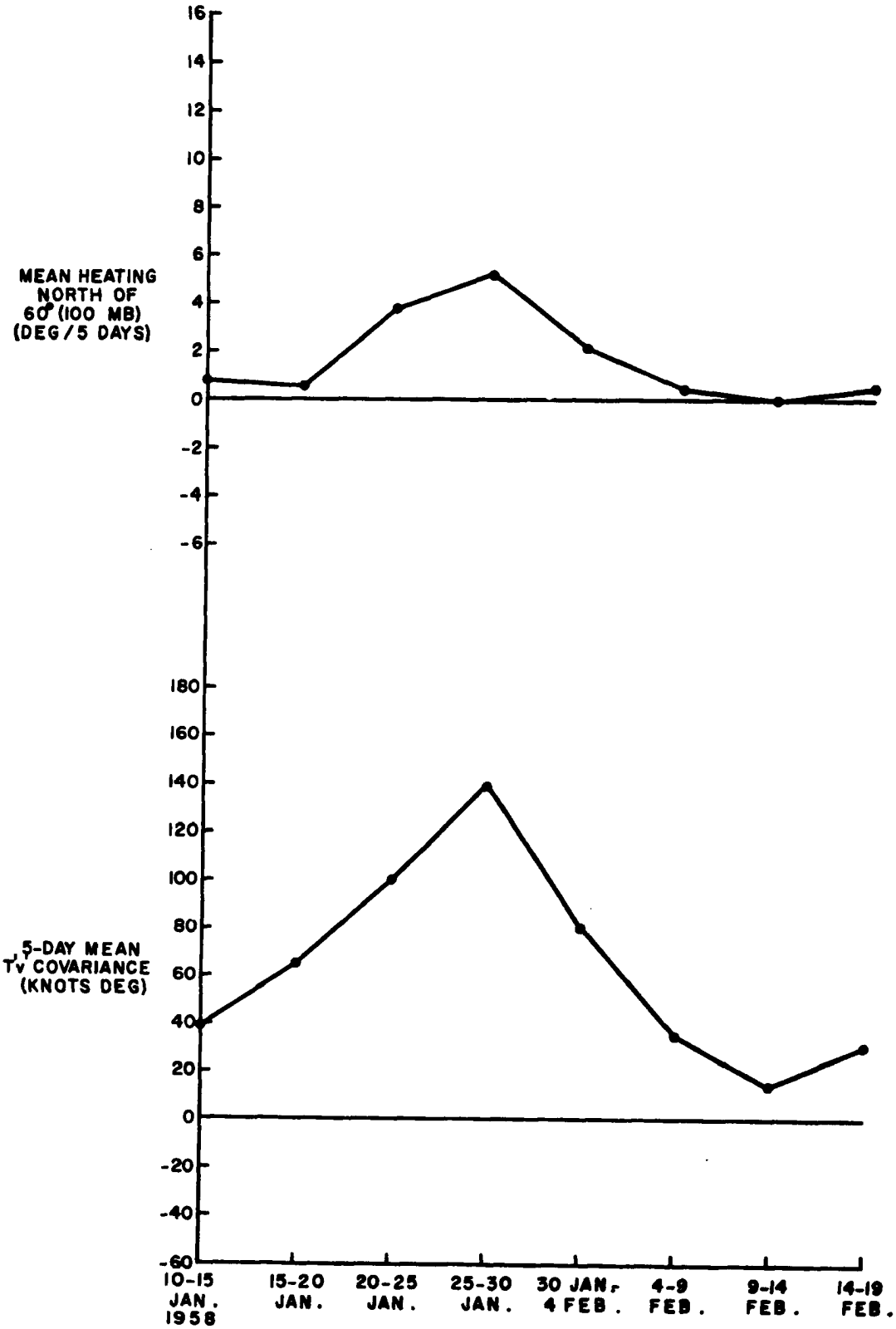

FIG. 16. Continued.

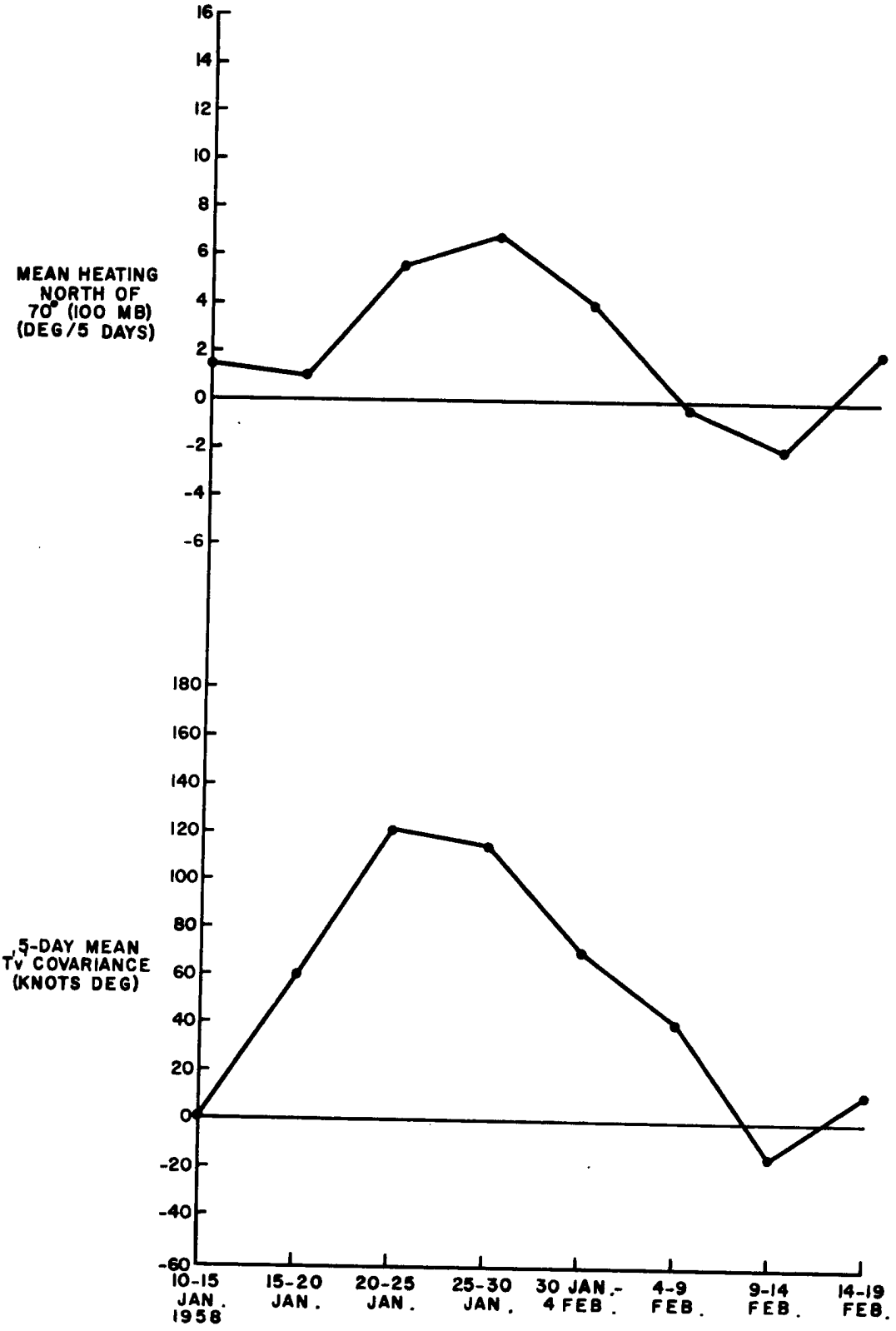

FIG. 16. Continued.

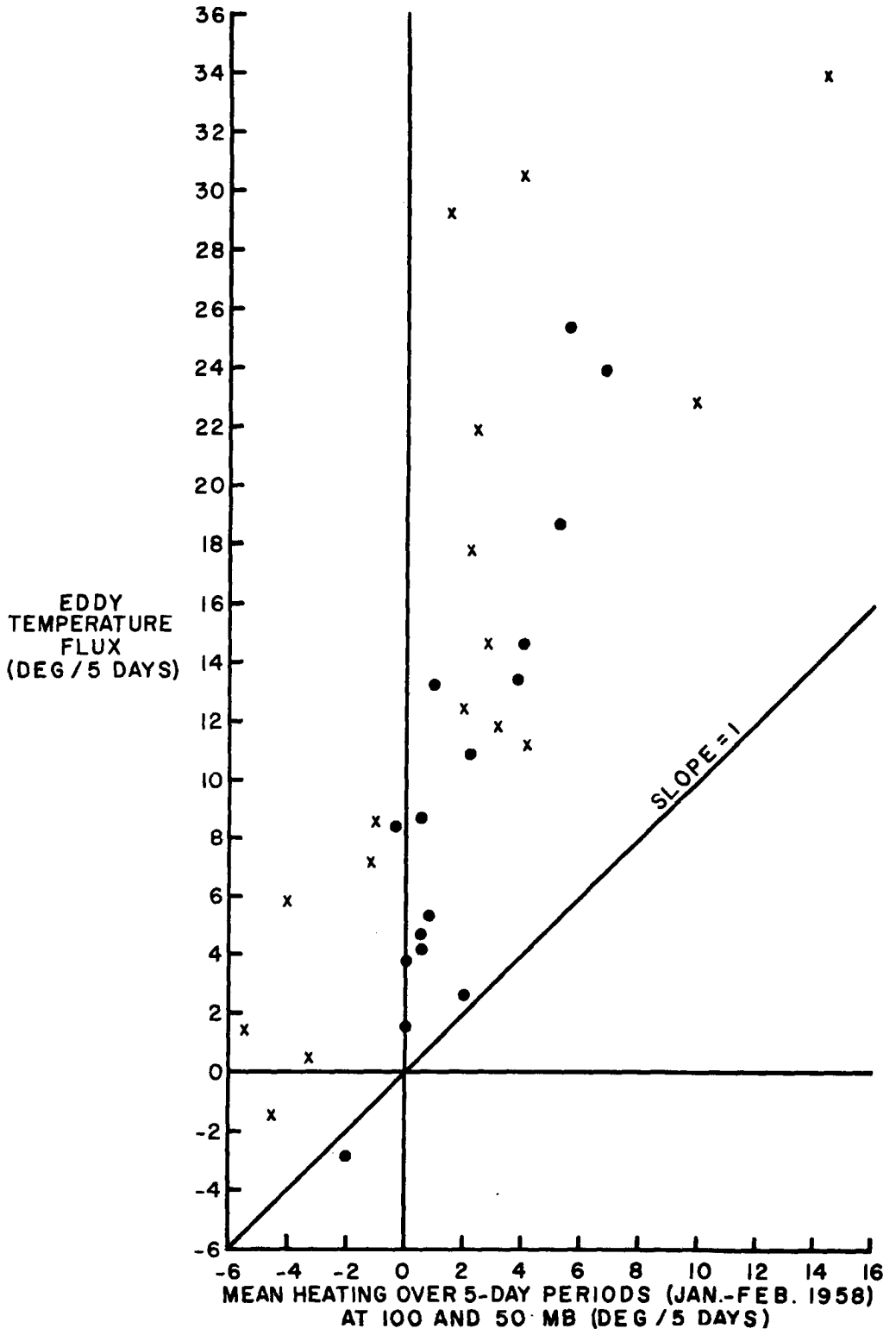

FIG. 17. Scatter diagram of eddy temperature flux and observed heating. Values computed over five-day periods during January-February 1958 at 100 mb and 50 mb, and at 60°N and 70°N. x's denote 50 mb data and •'s are 100 mb values.

If the 100 and 50 mb data are combined, the value of the correlation coefficient drops to +0.50. This is still statistically significant but strongly suggests that the nature of the warming response resulting from eddy temperature flux is somewhat different between the two levels.

Mean Cell with Respect to a Curvilinear Coordinate System

It has been demonstrated above that an indirect mean meridional cell is operative in the stratosphere during the winter months. This type of mean cell has the characteristic of transporting air (also ozone and radioactivity) upward and away from the polar regions. Consequently, one might conclude that the mean ageostrophic component acts in a sense opposite to the observed debris transports. This may not strictly be the case, however, when one considers the results obtained from geophysical model experiments at the University of Chicago Hydrodynamics Laboratory (Riehl and Fultz, 1957). These experiments demonstrated that if one averages the mean meridional component with respect to latitude, an indirect meridional cell is present in the vicinity of the jet stream. On the other hand, if one averages with respect to the jet stream itself, a well-pronounced direct cell results. Although this seemingly contradictory phenomenon has never been explicitly documented in the actual atmosphere, there remains a definite possibility of its existence. Krishnamurti (1961) performed a computation of this nature on the circulation around the subtropical jet stream. His results indicated that this cell was in the same sense as the Hadley cell present in that region.

In order to examine this possibility, the height contour of maximum circulation intensity was noted on the 50 mb surface. Then by interpolating from the analyses given in Appendix B, w values were noted at distances of $+10^{\circ}$, $+5^{\circ}$, 0°, -5°, and -10° latitude in a line normal to this chosen height contour. This process was repeated at

intervals along this contour (approximately 15 equally spaced grid points) for the period 10-27 January 1958. No attempt was made to extend the calculation past 27 January because the polar night jet stream ceased to exist after this date. The process was repeated at 100 mb utilizing the same contour employed at 50 mb. By using the same contour at both levels, continuity with height was assured. The mean w was then calculated for each day at the given distances $+10^{\circ}$, $+5^{\circ}$, 0°, -5°, -10° latitude from the maximum contour or jet axis. These values were then composited separately at each level over the entire period 10-27 January. Fig. 18 shows that according to these measurements, the circulation is direct with respect to this curvilinear coordinate (circulation latitude) system, a result precisely opposite to that obtained by averaging with respect to geographical latitude. There is an indication that the orientation of mean w field in Fig. 18 is slanted similarly to the latitudinally averaged cell in Fig. 14, but of opposite sign.

One might logically ask how such an apparent paradox can physically occur. In order to demonstrate how this can take place, the computed w fields at 50 mb were averaged from 22-27 January 1958 in the vicinity of a quasi-stationary long-wave trough in the north Atlantic. The results are given in Fig. 19 and show the probable reason for the apparent contradiction in the two types of meridional cells. This figure reveals that the strongest sinking occurs in the trough and that rising motion tends to be associated with more anti-cyclonic flow. Thus, it can be seen that relative to the curvilinear axis, the strongest sinking motion is to the north, while in a latitudinal frame the predominate descent is to the south, in agreement with the results obtained from geophysical model experiments.

It should be noted, however, that extreme caution should be exercised before extrapolating this result to periods either before or after the chosen period 10-27 January. In the period before this the

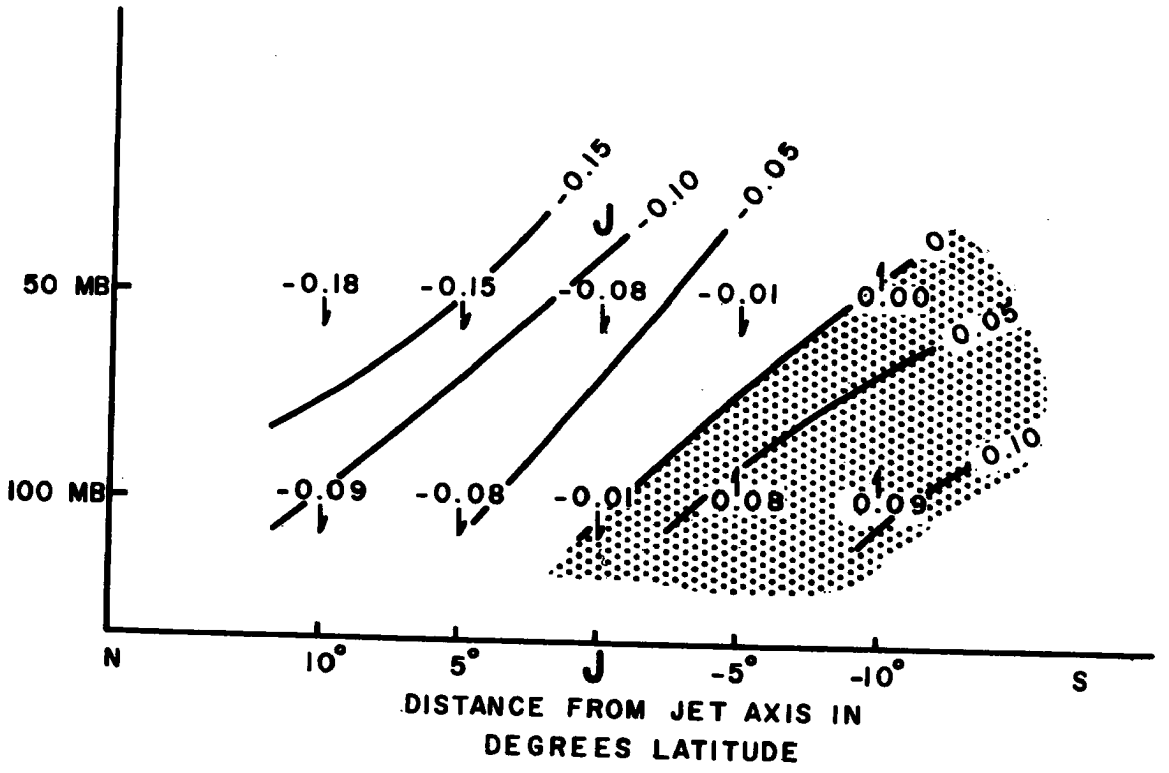

FIG. 18. Time composite of adiabatically computed mean vertical motion (km day^{-1}) with respect to coordinate system oriented along line of maximum circulation intensity at 50 mb. Composite is for the period 10-27 January 1958. Hatching denotes area of rising motion ($\widetilde{w} = +$).

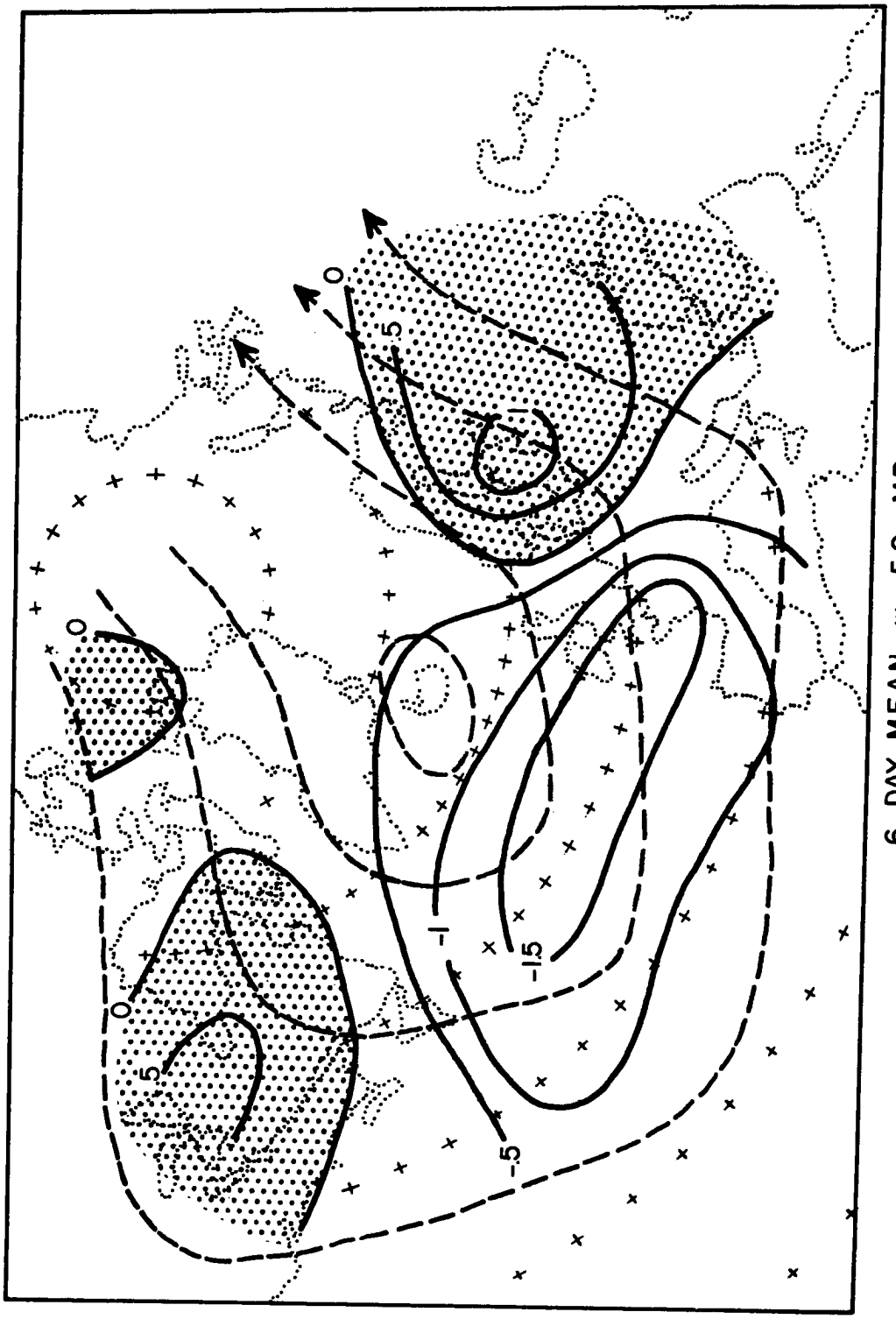

FIG. 19. Mean vertical motions (solid lines, km day^{-1}) computed at 50 mb for period 22-28 January 1958. Dashed lines are streamlines and dark hatching gives areas of rising motion (w = +).

asymmetry of the vortex may not have been sufficient to produce such a pronounced difference between the two types of coordinates. After 27 January the polar night jet stream ceases to exist as a continuous, circumpolar phenomenon and the intensity of the w fields are considerably weakened. Consequently, after the warming it is extremely difficult, if not impossible, to construct a well-defined curvilinear coordinate system. The concept thus may become meaningless in this case. From the point of view of radioactivity and ozone transport in the stratosphere, the above results suggest that the mean circulation can act to transport debris up and away from higher geographic latitudes while at the same time transporting debris downward toward higher circulation latitudes. It thus appears that the total transport during this time is an extremely complicated interaction between the above mean transport and all scales of eddy circulation.

VIII. VERTICAL MOTION AT 100 MB AND FLOW PROPERTIES AT TROPOPAUSE LEVEL

In previous sections it was demonstrated that cyclogenetic processes at tropopause level are responsible for large exchanges of air between the stratosphere and troposphere (Chapters III and IV). It was furthermore shown that both eddy and mean processes act to redistribute radioactive debris within the stratosphere with eddy processes probably predominating (Chapters VI and VII). The problem of how debris is eventually transported downward to tropopause level is still not explained adequately. As a supplement to previous chapters and as an introduction to this aspect of the problem, it is of interest to examine possible relationships between circulation types at tropopause level and the response by the vertical motion fields in the lower stratosphere.

As a first approach to this problem, the cyclone index derived in Chapter VI was calculated at 50°N, 300 mb with grid points at every five degrees longitude from 55°W to 140°W. Vertical motion values were then calculated at 100 mb over the United States and southern Canada for 39 days from 10 January to 19 February 1958. The time series of the summation of w absolute values was then compared to the index time series. Fig. 20 gives the two time series and suggests that there is some direct relationship between them. That is, high cyclone index at 300 mb is correlated with high mean absolute value of vertical motion at 100 mb. Cross correlations were computed between the two time series in Fig. 20 for time lags of -4, -3, -2, -1, 0, 1, 2, 3, and 4 days, respectively. Table 4 gives the results of these computations and shows that there is quite a high positive correlation when the $\overline{|w|}$ curve is one day later than the index curve. It may also be seen from

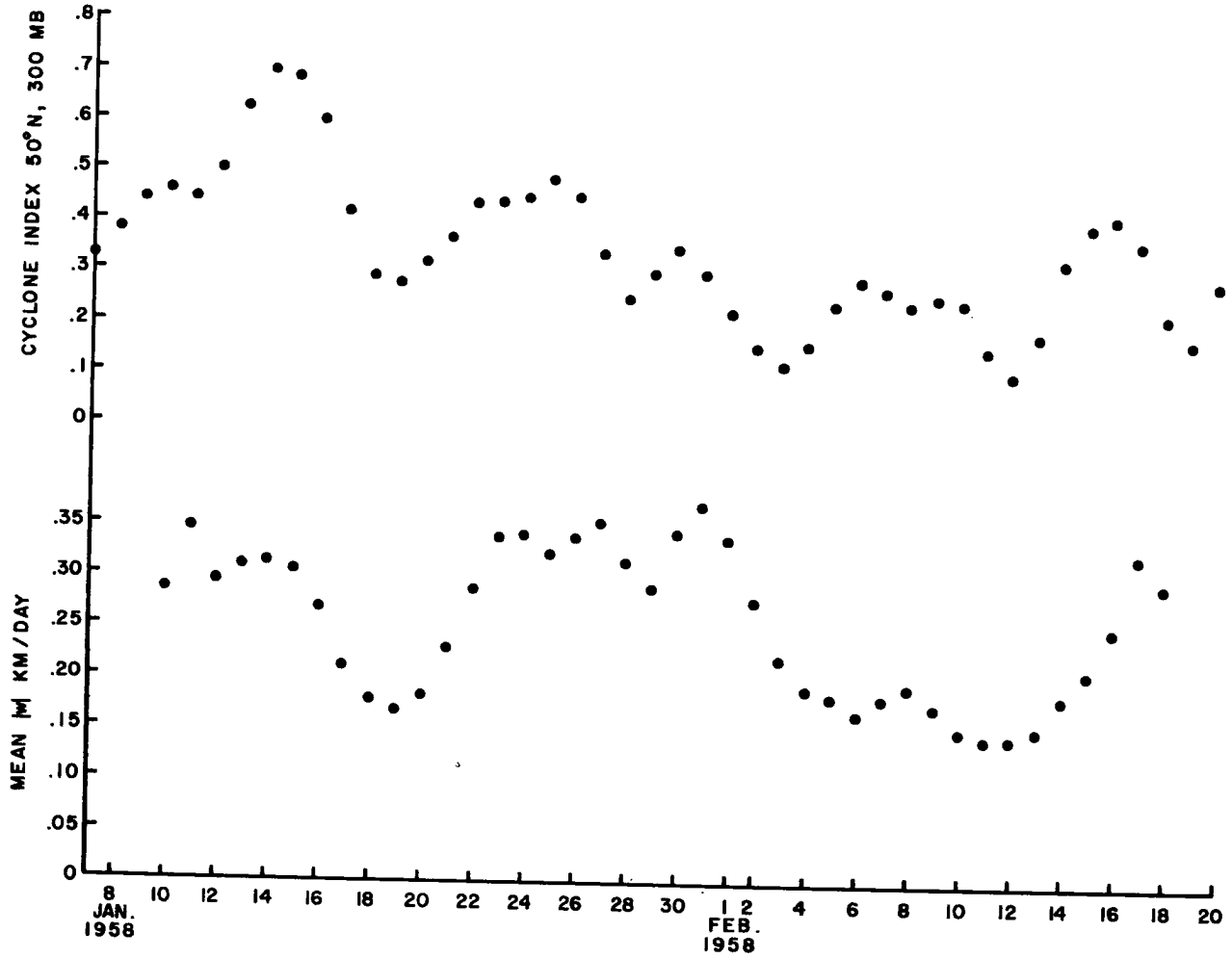

FIG. 20. Comparison between time series of cyclone index at 50°N, 300 mb (55°W - 140°W) and mean absolute value of vertical motion over United States and southern Canada.

Table 4 that the positive cross correlation decreases rapidly when the time lag becomes greater. As a means of interpreting the results in Table 4, for the 38 degrees of freedom used here, the critical correlation coefficient at the 1 per cent significance level is 0.408.

TABLE 4. Lag correlation coefficients (r) between cyclone index (C) at 300 mb (50°N, 55°-140°W) and mean absolute value of vertical motion field $\overline{|w|}$ at 100 mb over United States and southern Canada.

$$r(C_i, \overline{|w|}_{i-4}) = +0.074$$
$$r(C_i, \overline{|w|}_{i-3}) = +0.119$$
$$r(C_i, \overline{|w|}_{i-2}) = +0.224$$
$$r(C_i, \overline{|w|}_{i-1}) = +0.361$$
$$r(C_i, \overline{|w|}_{i}) = +0.507$$
$$r(C_i, \overline{|w|}_{i+1}) = +0.537$$
$$r(C_i, \overline{|w|}_{i+2}) = +0.454$$
$$r(C_i, \overline{|w|}_{i+3}) = +0.067$$
$$r(C_i, \overline{|w|}_{i+4}) = +0.126$$

This is a quite surprising result, particularly if computations made at other times yield similar positive correlations. The positive correlation suggests that the greatest mean vertical motion amplitude at 100 mb occurs when the 300 mb flow is most zonal and that lowest $\overline{|w|}$'s occur when eddies at 300 mb are most pronounced. This result furthermore suggests in terms of the results from Chapters III and IV that transport processes in the lower stratosphere would not necessarily be enhanced during periods of maximum stratospheric-tropospheric mass exchange. Consequently, it appears that a great deal more effort needs to be expended in this particular aspect of the transport problem, especially from this point of view and that of smaller scale mechanisms.

IX. SOME ASPECTS OF TRAJECTORY BEHAVIOR DURING PERIODS OF MAXIMUM INDICATED TRANSPORT IN THE STRATOSPHERE

In the previous chapters it has been shown that both mean and eddy circulations can have a significant dynamic effect on the transport and redistribution of ozone and radioactive debris in the stratosphere. Since the concept of eddy transport includes all scales of motion from micro-turbulence to planetary waves, it is still not clear as to which eddy scales are accomplishing the bulk of this transport. With the present meteorological network it appears to be difficult, if not impossible, to investigate the relative effect of small-scale motions and turbulence on the observed transports.

It does appear possible, however, that considerable insight can be gained by a more thorough investigation of the role played by the cyclone- and planetary-scale eddies. As a first approach to this problem, it is of interest to determine trajectories in the lower stratosphere during the periods of maximum transports indicated in Chapter VI.

It was first attempted to calculate the trajectories at 50 mb by using the energy method of Danielsen (1961), re-derived for pressure coordinates. However, it was soon discovered that the results from this type of trajectory computation are completely obscured by uncertainties in the geo-potential height field at these levels. Consequently, it was found that a graphical streamline method yielded the best results. This is particularly reasonable in that the waves at these heights are quasi-stationary.

In view of the large negative $\overline{v'w'}$ correlations given in Fig. 8, the period beginning on 5 February was chosen for the trajectory

computation. Because of the interest in northward transport of radioactivity and ozone, the trajectory was begun at Hong Kong (22.5°N) on 5 February at 50 mb. An estimate of the vertical motion along the trajectory was obtained by interpolating w's from the analyses in Appendix B for each successive map time along the computed trajectory. The results of this trajectory are given in Fig. 21 and show a marked northward displacement. Furthermore, the trajectory demonstrates that a rather consistent descending motion occurs during this northward displacement. By 15 February this air has descended to approximately 70 mb. After crossing the polar cap, it appears to begin rising again, although one must note that the reliability of the computed trajectory begins to deteriorate rather seriously after about ten days. The relation between v and w is thus in the same sense as the statistical transport computations. It thus can be concluded that this mechanism plus the combined effect of small-scale turbulent diffusion constitutes a quite powerful mechanism for transporting stratospheric ozone and radioactive debris northward and downward in the late winter. Computations given by Molla and Loisel (1962) show that the v'w' covariances are also negative in the 100-50 mb layer for April 1958. It appears that this mechanism operates more or less continuously after the breakdown of the polar night vortex. Before the vortex breakdown the eddy circulations act to build up concentrations in northern regions but do not favor large amounts of downward transport. This is in agreement with the observation that the total ozone builds up somewhat gradually during the entire winter with a sharper increase around the time of the vortex breakdown (Dutsch, 1961; London and Prabhakara, 1962). Also, this mechanism does not appear to conflict with the observed occurrence of the spring fallout peak given a suitable lag time of several months.

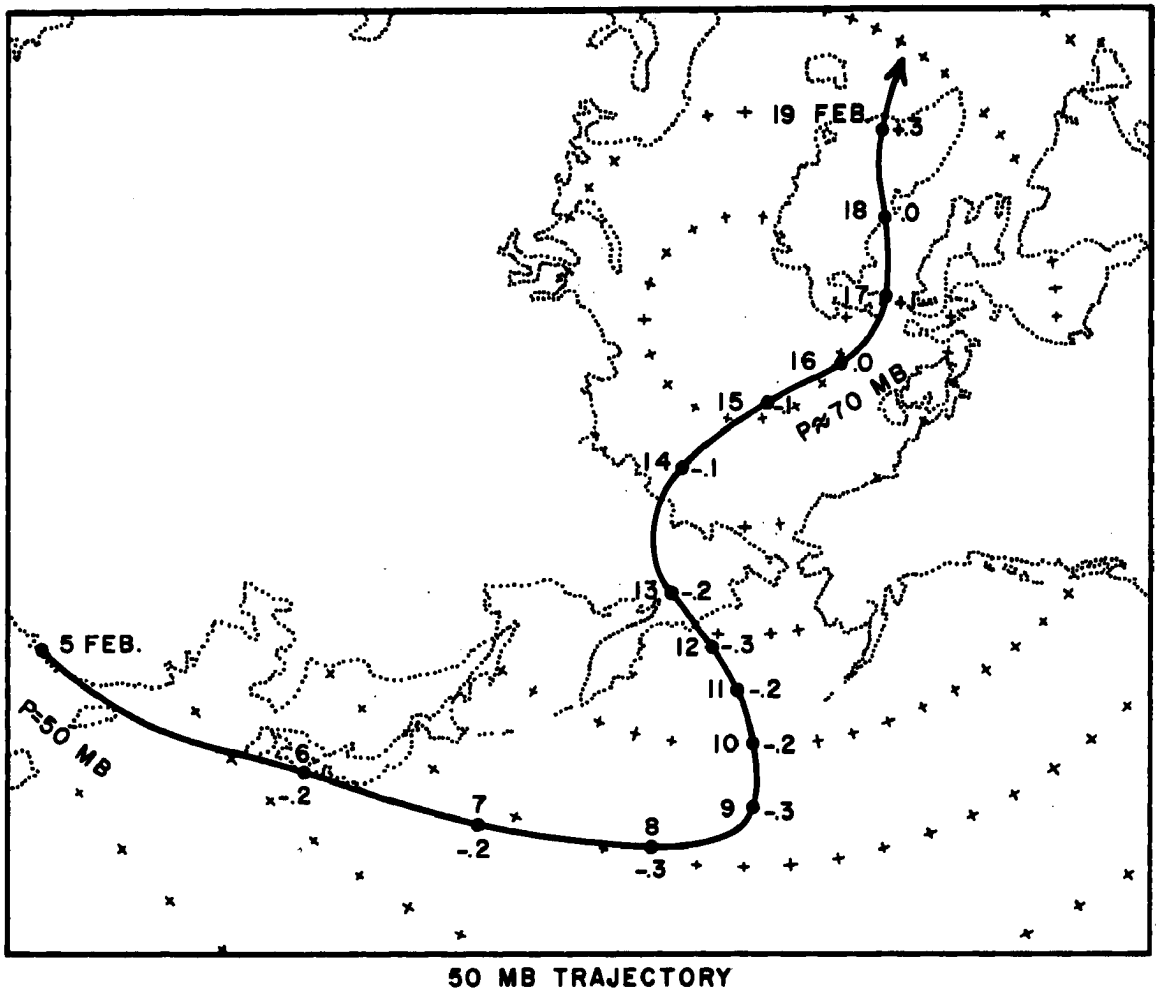

FIG. 21. Trajectory calculation during period of large indicated debris transport (5-19 February) beginning at 50 mb. Note pronounced descending motion during northward displacement.

Trajectories and Ozone Variations

Another type of study which is particularly valuable is to compare the above type of trajectory calculation with measurements taken of the ozone distribution in the middle stratosphere. Unfortunately, even during the IGY the ozone network was inadequate for obtaining reasonable area distributions. However, the limited results from this network do suggest that there is a tendency for highest values of total ozone to occur in association with pressure troughs (London, 1962). Because daily ozone soundings were taken at Arosa, Switzerland, during the IGY, it is of interest to examine trajectories in this region when there is also a trough present. On 24 January 1958 a pressure trough existed over Arosa and at the same time a quite pronounced increase in total ozone over the station was noted (Fig. 22). To check the possible reason for the large increase, trajectories were calculated forward and backward from Arosa on 24 January at 100, 50, and 25 mb. The 25 mb data was taken from the maps prepared by the Institute for Meteorology and Geophysics, The Free University of Berlin (1960).

The results of these computations are given in Fig. 23 and show that there exists a rather remarkable confluence of trajectories with height into this region and a diffluence again as they leave the trough area. The base of the trough is in a region of tremendous quasi-stationary cold-air advection. The intensity of this advection is reflected in the vertical motion fields at 100 and 50 mb given in Appendix B. Through thermal wind considerations this cross isotherm flow produces a turning of the wind with height, thus giving the results of Fig. 23. This result suggests a possible dynamic explanation for the apparent increase of ozone at the base of long-wave troughs in the stratosphere.

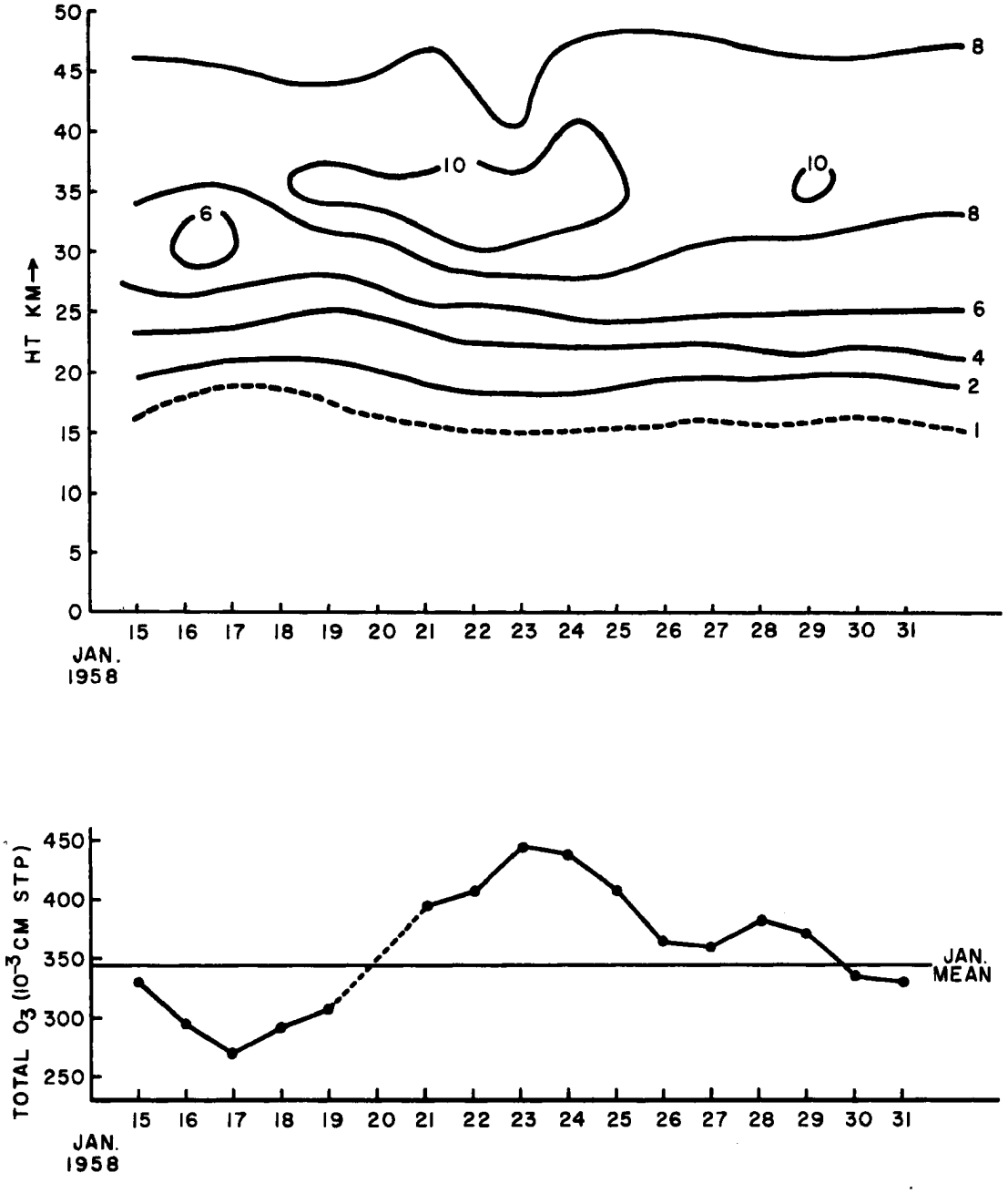

FIG. 22. Upper diagram: vertical time section of ozone mixing ratio (10^{-6} g/g) over Arosa, Switzerland, for January 1958. Lower diagram: total ozone (10^{-3} cm STP) over Arosa for January 1958 (London, 1962).

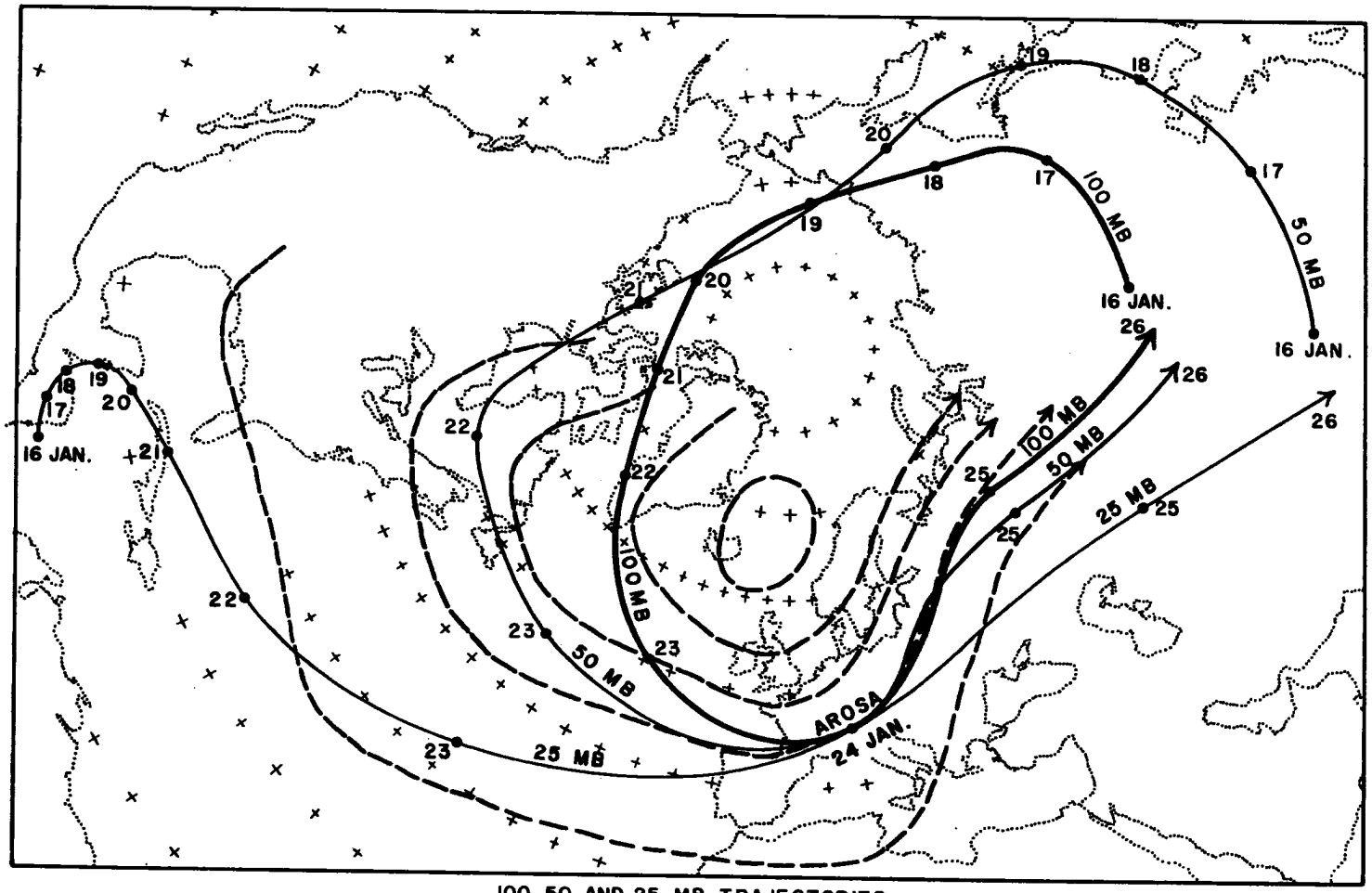

FIG. 23. Forward and backward trajectories from Arosa on 24 January at 100, 50, and 25 mb. Dashed lines are streamlines at 50 mb. 100, 50, and 25 mb trajectories are denoted by progressively thinner solid lines.

It is commonly observed that at low latitudes the ozone peak is very pronounced and located at about 20 mb (Hering, 1964). At higher latitudes the mean ozone peak is much more diffuse and is located at approximately 50 mb, with an even greater broadening and lowering of the peak at highest latitudes. As a result of this, it is quite possible that the mean total ozone maximum in trough regions directly results from a differential in the trajectory directions with increasing altitude. Since trajectories from the lower and middle latitudes tend to originate from areas which would superimpose relative ozone maxima, the final effect would be to produce a maximum in total ozone measured at the base of the trough even though the air parcels constituting the trough are continually being replaced.

If this hypothesis is correct, then it suggests that this may also serve as a mechanism for continual transport of ozone out of the maximum production region. If no smaller scale processes were acting then no net transport takes place. On the other hand, if the parcels transported out of low latitudes are subject to vertical turbulent diffusion processes, then a continuous northward transport would take place due to the more northward movement in the layers below the original layer.

Although this hypothesis appears plausible from a dynamic viewpoint, a proof of its validity awaits more detailed analyses over a period in which both ozone and meteorological data are more complete.

X. A DYNAMICAL THEORY FOR THE POLAR NIGHT VORTEX BREAKDOWN

In previous sections it has been argued that physical processes acting in the stratosphere during the period of the polar night vortex breakdown are highly significant in terms of the problem of atmospheric transport of radioactive debris and ozone. Because of the dependence of transport properties upon the dynamical behavior of the polar night circulation, it presently appears that a satisfactory dynamic explanation of the vortex breakdown must be achieved before a complete understanding of the fallout problem can be claimed.

Since the circulation is altered from a nearly symmetric vortex to large-scale eddies when the breakdown occurs, it appears reasonable to assume that the phenomenon results from a release of flow instability at the time of breakdown. This inference is substantiated by the discussion of energetics given in Chapter V. Because the pre-breakdown flow of the polar night vortex is nearly zonal, the problem might profitably be investigated through a linearized system of equations which assume small perturbations on a basic zonal current. The linearizing approach has proved to be particularly fruitful in stability investigations because it is initially only necessary to seek fulfillment of the conditions for instability. After the instability has occurred, of course, the waves in the system begin to grow to the point where the linear approximations are no longer valid. Thus, in this analysis no attempt will be made to solve for the form of the stable or unstable waves; only the conditions for instability and exponential wave growth will be sought.

Generally, it has been found that two distinct types of instability can occur in the atmosphere. The first of these is <u>barotropic instability</u>

which arises from lateral velocity variations in a barotropic fluid. It was first shown by Rayleigh (1916) and later by Kuo (1949) and Fjørtoft (1951) that this type of flow can become unstable if there are zeros in the latitudinal gradient of the absolute vorticity field. An analysis by Murray (1960) suggested that barotropic instability is probably responsible for the polar night vortex breakdown.

The second type is that of baroclinic instability which results from a super critical build-up of the available potential energy in the atmosphere. This has been thought to be particularly relevant to atmospheric flow and has been extensively investigated in the past (Charney, 1947; Berson, 1949; Eady, 1949; Fjørtoft, 1951; Kuo, 1952, 1953; Thompson, 1953, 1956; Phillips, 1954; Fleagle, 1955, 1958; Green, 1960). Although the physical assumptions utilized in these models are highly varied, the general result is that for certain values of lateral temperature gradient (or vertical wind shear) the flow will be unstable. Synoptically, it usually is found that the flow is almost always baroclinically unstable in the mid-latitude troposphere according to the above theories. However, it is not immediately evident as to how these results apply to the winter stratosphere. The wintertime stratospheric vortex is characterized by strong horizontal wind speeds and shears, generally called the polar night jet stream. Furthermore, the horizontal temperature gradients (and thus vertical wind shears) are notably strong in this region. It thus appears reasonable that any meaningful approach to the instability problem in this region must simultaneously incorporate considerations of barotropic and baroclinic instability. This general problem has usually been avoided because the analysis yields a non-separable partial differential equation. In this case, however, only the conditions for unstable wave growth will be sought and no attempt will be made to solve the derived equation for all classes of waves.

Because of the lower density the effects of compressibility are often thought to be of significant importance in these regions. The

model presented here will include the effects of compressibility through the theorem of conservation of potential vorticity. The derived condition for instability will then be calculated from the actual data for a period encompassing the polar night vortex breakdown as a check on the validity of the resulting criterion.

Models such as the one proposed here can be made considerably more tractable if some mechanism is introduced to decrease the complicating effects of vertical motion upon the system. Since, at this altitude and season diabatic effects are relatively small, a quite reasonable assumption is that the flow is dry adiabatic in character. If the relevant dynamical equations are formally transformed to an isentropic surface, there will be no vertical motion relative to this surface and consequently it can be eliminated as a direct consideration altogether. If this approach is followed, a much simpler system results.

Some objections might be legitimately raised, however, that this procedure will lead to greater complexities in other portions of the system. For example, due to the slope of the potential temperature surface, the axes are no longer orthogonal in this system of coordinates. If the non-orthogonality is appreciable, other previously non-important terms may begin to be important, e.g., the gravitation term will not have a component in this new non-horizontal plane. However, the slopes of the isentropic surfaces in this region are less than 10^{-3} and can be safely neglected with sufficient accuracy.

A more formidable difficulty is that created by the boundary conditions in this problem. It becomes difficult, if not impossible, to define a reasonable surface boundary condition because the earth's surface is generally characterized by many different values of potential temperature. Charney and Stern (1962) circumvented this difficulty by considering the hypothetical case of zero lateral potential temperature gradient at the ground, i.e., for an internal system. In this model the

problem will be circumvented by assuming that the perturbation motion vanishes at rigid upper and lower boundaries. The lateral boundaries will be assumed to be rigid vertical walls so that the disturbance also vanishes at these points. The system is thus completely internal, a justifiable procedure as long as the boundaries are sufficiently far from the disturbance. This is seen to be a reasonable approximation for the onset of the polar night vortex breakdown. Also, for reasons of mathematical simplicity the analysis will be performed in Cartesian coordinates even though the actual process takes place on a rotating sphere. This is valid because the curvature effects are small in the polar regions.

Development of the Model

In addition to the above restrictions the flow will be assumed to be inviscid and hydrostatic. In this simplified isentropic system a complete set of equations in the dependent variables u, v, M, T, p is given by

$$\frac{\partial u}{\partial t_\theta} + u \frac{\partial u}{\partial x_\theta} + v \frac{\partial u}{\partial y_\theta} + \frac{\partial M}{\partial x_\theta} - fv = 0 \tag{25}$$

$$\frac{\partial v}{\partial t_\theta} + u \frac{\partial v}{\partial x_\theta} + v \frac{\partial v}{\partial y_\theta} + \frac{\partial M}{\partial y_\theta} + fu = 0 \tag{26}$$

$$\frac{\partial u}{\partial x_\theta} + \frac{\partial v}{\partial y_\theta} + \frac{\frac{d}{dt}\left(\frac{\partial p}{\partial \theta}\right)}{\frac{\partial p}{\partial \theta}} = 0 \tag{27}$$

$$\frac{\partial M}{\partial \ln \theta} - c_p T = 0 \tag{28}$$

$$c_p \frac{\partial T}{\partial t_\theta} - \frac{RT}{p} \frac{\partial p}{\partial t_\theta} = 0 \tag{29}$$

where $M = c_p T + gz$ and the independent variables are x, y, t, $\ln\theta$.

Eqs. (25) and (26) are the momentum equations and Eq. (27) is the continuity equation in isentropic coordinates. Eq. (28) is obtained by differentiating M with respect to θ and substituting in the hydrostatic equation, the equation of state, and the definition of potential temperature. Eq. (29) is obtained by partial differentiation of $\theta = T\left(\frac{1000}{p}\right)^{\kappa}$ with respect to time on an isentropic surface.

In the linearizing procedure to be employed here, the perturbations are presumed to be superimposed upon a time-independent circulation. By applying a longitudinal averaging operator to Eqs. (25) - (29), one obtains the following set for the steady state

$$\bar{u} = -\frac{1}{f}\frac{\partial \overline{M}}{\partial y_\theta} \tag{30}$$

$$\frac{\partial \overline{M}}{\partial \ln\theta} = c_p \overline{T}, \tag{31}$$

since $\frac{\partial \overline{M}}{\partial x} = \frac{\partial \bar{u}}{\partial x} = 0$ by definition. By differentiation of Eq. (30) with respect to $\ln\theta$ and substitution of Eq. (31) into the resulting expression, one obtains the ground state dependence of $\bar{u}$ upon the vertical coordinate $\ln\theta$,

$$\frac{\partial \overline{u}}{\partial \ln\theta} = -\frac{c_p}{f}\frac{\partial \overline{T}}{\partial y_\theta} . \tag{32}$$

Since the ground state is geostrophic, the system is considerably simplified if the well-known quasi-geostrophic approximation is employed, e. g., the velocity components are expressed by their geostrophic values after the horizontal divergence has been eliminated from the equation set. This is accomplished by differentiating Eq. (26) with respect to x and Eq. (25) with respect to y and subtracting to get the vorticity equation for isentropic coordinates

$$\frac{d\zeta_a}{dt_\theta} + \zeta_a\left(\frac{\partial u}{\partial x_\theta} + \frac{\partial v}{\partial y_\theta}\right) = 0 . \tag{33}$$

The horizontal divergence is then eliminated between Eq. (27) and Eq. (33) to obtain the well-known potential vorticity equation $\frac{dP}{dt_\theta} = 0$. With the quasi-geostrophic approximation the new set of equations becomes

$$\frac{dP}{dt_\theta} = \frac{\partial P}{\partial t_\theta} + u_g \frac{\partial P}{\partial x_\theta} + v_g \frac{\partial P}{\partial y_\theta} = 0 \tag{34}$$

$$P = \frac{-\left(\frac{\partial v_g}{\partial x_\theta} - \frac{\partial u_g}{\partial y_\theta} + f\right)}{\frac{\partial p}{\partial \ln\theta}} \tag{35}$$

$$u_g = -\frac{1}{f}\frac{\partial M}{\partial y_\theta} \; ; \; v_g = \frac{1}{f}\frac{\partial M}{\partial x_\theta} \tag{36}$$

$$\frac{\partial M}{\partial \ln\theta} - c_p T = 0 \tag{28}$$

$$c_p \frac{\partial T}{\partial t_\theta} - \frac{RT}{p}\frac{\partial p}{\partial t_\theta} = 0 \, , \tag{29}$$

where Eq. (34) is the theorem of conservation of potential vorticity and Eq. (35) is the definition of potential vorticity.

Upon substitution of the geostrophic values of u and v from Eq. (36) into Eqs. (34) and (35) and linearizing, the perturbation equations become

$$\frac{\partial P'}{\partial t} - \bar{u}\frac{\partial P'}{\partial x} + \frac{1}{f}\frac{\partial \bar{P}}{\partial y}\frac{\partial M'}{\partial x} = 0 \tag{37}$$

($\frac{\partial \bar{P}}{\partial x}$ and $\frac{\partial \overline{M}}{\partial x}$ are identically zero due to the averaging procedure)

$$\overline{P}\frac{\partial p'}{\partial \ln\theta} + P'\frac{\partial \bar{p}}{\partial \ln\theta} + \frac{1}{f}\left(\frac{\partial^2 M'}{\partial x^2} + \frac{\partial^2 M'}{\partial y^2}\right) = 0 \tag{38}$$

$$\frac{\partial M'}{\partial \ln\theta} - c_p T' = 0 \tag{39}$$

$$c_p \frac{\partial T'}{\partial t} - \bar{\alpha} \frac{\partial p'}{\partial t} = 0 \tag{40}$$

by use of the definitions: $M = \overline{M} + M'$, $P = \overline{P} + P'$, $p = \overline{p} + p'$, $T = \overline{T} + T'$, where $M' \ll \overline{M}$, $P' \ll \overline{P}$, $p' \ll \overline{p}$, and $T' \ll \overline{T}$. Because the analysis is for the polar cap, the term in Eq. (38) involving the variation of f with y in the quasi-geostrophic approximation has been neglected.

This is now a complete set in terms of the dependent variables M', P', p', T'. The θ subscripts have been dropped, but all differentiations are still understood to be measured on the isentropic surface. By differentiation of Eq. (39) with respect to t and substitution into Eq. (40) one obtains

$$\frac{\partial}{\partial \ln\theta}\left(\frac{\partial M'}{\partial t}\right) - \bar{\alpha} \frac{\partial p'}{\partial t} = 0 \tag{41}$$

so that the complete equation set is now (37), (38), and (41).

Since the above set is linear one may assume exponential solutions of the form

$$\begin{aligned} P' &= A(y, \ln\theta)\, e^{i\mu(x-ct)} \\ M' &= B(y, \ln\theta)\, e^{i\mu(x-ct)} \\ p' &= C(y, \ln\theta)\, e^{i\mu(x-ct)} \end{aligned} \tag{42}$$

Substitution of these solutions into Eqs. (37), (38), and (41) gives

$$A(\bar{u}-c) + \frac{1}{f} \frac{\partial \overline{P}}{\partial y} B = 0 \tag{43}$$

$$\overline{P} \frac{\partial C}{\partial \ln\theta} + A \frac{\partial \overline{p}}{\partial \ln\theta} + \frac{1}{f}\left(\frac{\partial^2 B}{\partial y^2} - \mu^2 B\right) = 0 \tag{44}$$

$$\frac{\partial B}{\partial \ln\theta} - \bar{\alpha} C = 0 \tag{45}$$

By algebraic reduction and differentiation this set reduces to

$$\bar{\rho}\, f \bar{P}\, \frac{\partial^2 B}{\partial (\ln\theta)^2} - \bar{\rho}\, f \bar{P} \left(1 + \frac{1}{\bar{p}}\, \frac{\partial \bar{p}}{\partial \ln\theta}\right) \frac{\partial B}{\partial \ln\theta} - \frac{\frac{\partial \bar{p}}{\partial \ln\theta}\, \frac{\partial \bar{P}}{\partial y}}{\bar{u} - c}\, B$$

$$+ \frac{\partial^2 B}{\partial y^2} - \mu^2 B = 0 \ . \qquad (46)$$

This is a non-separable equation which thus reflects the coupling between the two mechanisms of barotropic and baroclinic energy exchange. To avoid this non-separability, only the conditions for initial onset of instability will be sought without directly solving Eq. (46). This will be done by assuming that B = 0 at all horizontal and vertical boundaries.

In a linear system such as the one developed here, the wave speed must have a positive complex component ($c_i > 0$) in order for exponential growth to occur. However, the B's may also become complex ($B = B_r + i B_i$).

The form of Eq. (46) under the conditions $c_i \neq 0$ and the given boundary conditions will now be investigated by a technique similar to that given by Rayleigh (1880). Eq. (46) in its present form is awkward because the phase speed $c = c_r + i c_i$ appears in the denominator of the B term, thus creating possible singularities at the point $\bar{u} = c_r$ when c is real. Also, it is difficult to separate real and imaginary parts in this term with the $\bar{u} - c$ term in the denominator. To circumvent this difficulty consider the following form of $(\bar{u} - c)^{-1}$ obtained by multiplying numerator and denominator by $\bar{u} - c_r + i c_i$:

$$\frac{1}{\bar{u} - c} = \frac{\bar{u} - c_r + i c_i}{(\bar{u} - c_r)^2 + c_i^2} \ . \qquad (47)$$

Now let $(\bar{u} - c)^{-1} = \xi_1 + i \xi_2$ where

$$\xi_1 = \frac{\bar{u} - c_r}{(\bar{u} - c_r)^2 + c_i^2} \quad \text{and} \quad \xi_2 = \frac{c_i}{(\bar{u} - c_r)^2 + c_i^2} \ . \qquad (48)$$

Now by substituting $(\bar{u} - c)^{-1} = \xi_1 + i\xi_2$ and $B = B_r + iB_i$ into Eq. (46) and dividing by $\bar{\rho} f \bar{P}$, upon separating real and imaginary parts, one obtains

$$\frac{\partial^2 B_r}{\partial (\ln\theta)^2} - \left(1 + \frac{1}{\bar{p}} \frac{\partial \bar{p}}{\partial \ln\theta}\right) \frac{\partial B_r}{\partial \ln\theta} - \frac{\frac{\partial \bar{p}}{\partial \ln\theta} \frac{\partial \bar{P}}{\partial y}}{\bar{\rho} f \bar{P}} \xi_1 B_r + \frac{1}{\bar{\rho} f \bar{P}} \frac{\partial^2 B_r}{\partial y^2} - \frac{\mu^2}{\bar{\rho} f \bar{P}} B_r + \frac{\frac{\partial \bar{p}}{\partial \ln\theta} \frac{\partial \bar{P}}{\partial y}}{\bar{\rho} f \bar{P}} \xi_2 B_i = 0 \qquad (49)$$

$$\frac{\partial^2 B_i}{\partial (\ln\theta)^2} - \left(1 + \frac{1}{\bar{p}} \frac{\partial \bar{p}}{\partial \ln\theta}\right) \frac{\partial B_i}{\partial \ln\theta} - \frac{\frac{\partial \bar{p}}{\partial \ln\theta} \frac{\partial \bar{P}}{\partial y}}{\bar{\rho} f \bar{P}} \xi_1 B_i + \frac{1}{\bar{\rho} f \bar{P}} \frac{\partial^2 B_i}{\partial y^2} - \frac{\mu^2}{\bar{\rho} f \bar{P}} B_i - \frac{\frac{\partial \bar{p}}{\partial \ln\theta} \frac{\partial \bar{P}}{\partial y}}{\bar{\rho} f \bar{P}} \xi_2 B_r = 0 . \qquad (50)$$

Now multiply Eq. (49) by B_i and Eq. (50) by B_r and subtract to get

$$\left[B_i \frac{\partial^2 B_r}{\partial (\ln\theta)^2} - B_r \frac{\partial^2 B_i}{\partial (\ln\theta)^2}\right] + \left(1 + \frac{1}{\bar{p}} \frac{\partial \bar{p}}{\partial \ln\theta}\right)\left[B_r \frac{\partial B_i}{\partial \ln\theta} - B_i \frac{\partial B_r}{\partial \ln\theta}\right] + \frac{1}{\bar{\rho} f \bar{P}}\left[B_i \frac{\partial^2 B_r}{\partial y^2} - B_r \frac{\partial^2 B_i}{\partial y^2}\right] + \frac{\frac{\partial \bar{p}}{\partial \ln\theta} \frac{\partial \bar{P}}{\partial y}}{\bar{\rho} f \bar{P}} \xi_2 (B_r^2 + B_i^2) = 0. \qquad (51)$$

By changing the form of the derivatives in the first and third terms in Eq. (51) and integrating with respect to y and $\ln\theta$ one obtains

$$\iint \frac{\partial}{\partial \ln\theta}\left[B_i \frac{\partial B_r}{\partial \ln\theta} - B_r \frac{\partial B_i}{\partial \ln\theta}\right] dy\, d\ln\theta + \iint \left(1 + \frac{1}{\bar{p}} \frac{\partial \bar{p}}{\partial \ln\theta}\right)\left[B_r \frac{\partial B_i}{\partial \ln\theta} - B_i \frac{\partial B_r}{\partial \ln\theta}\right] dy\, d\ln\theta + \iint \frac{1}{\bar{\rho} f \bar{P}} \frac{\partial}{\partial y}\left[B_i \frac{\partial B_r}{\partial y} - B_r \frac{\partial B_i}{\partial y}\right] dy\, d\ln\theta + \iint \frac{\frac{\partial \bar{p}}{\partial \ln\theta} \frac{\partial \bar{P}}{\partial y}}{\bar{\rho} f \bar{P}} \xi_2 (B_r^2 + B_i^2)\, dy\, d\ln\theta = 0 . \qquad (52)$$

Under the boundary conditions B = 0 at the lateral boundaries and B = 0 at the upper and lower boundaries, Eq. (52) can be simplified. The first integral vanishes identically under the second of the above boundary conditions. By noting that the function $(\bar{\rho}\, f\, \bar{P})^{-1}$ in the third integral of Eq. (52) is only weakly y dependent in the lower stratosphere (total variation less than 10%), it becomes negligibly small upon integrating with respect to the y coordinate. Thus, Eq. (52) reduces to

$$\iint \left[\left(1 + \frac{1}{\bar{p}} \frac{\partial \bar{p}}{\partial \ln\theta}\right)\left(B_r \frac{\partial B_i}{\partial \ln\theta} - B_i \frac{\partial B_r}{\partial \ln\theta}\right) + \frac{\frac{\partial \bar{p}}{\partial \ln\theta}\frac{\partial \bar{P}}{\partial y}}{\bar{\rho}\, f\, \bar{P}} \xi_2 \left(B_r^2 + B_i^2\right) \right] dy\, d\ln\theta = 0 \tag{53}$$

as the condition that $c_i \neq 0$. The above equation cannot be evaluated from the data because little can be inferred about the B terms in their present form. Also in its present form Eq. (52) is difficult to interpret physically. As a consequence of this, it is of interest to determine whether or not a slight simplification of the perturbation Eqs. (37) - (40) will yield a more tractable stability criterion.

One approximation which could be invoked is that

$$\frac{\frac{\partial p'}{\partial \ln\theta}}{\frac{\partial \bar{p}}{\partial \ln\theta}} \ll \frac{P'}{\bar{P}} . \tag{54}$$

This is a reasonable assumption because P is conserved with the flow in the perturbation motion while the pressure perturbations are very strongly damped due to the high static stability in the stratosphere. Also, it is synoptically observed that perturbations of the pressure field in the atmosphere are from 2 to 3 orders of magnitude smaller than the mean pressure. Again, since potential vorticity is conserved with the flow, one would expect its perturbations to be

much larger relative to $\overline{P}$. Through use of Eq. (54) the perturbation Eqs. (37) - (40) reduce to the complete set

$$\frac{\partial P'}{\partial t} + \bar{u}\frac{\partial P'}{\partial x} + \frac{1}{f}\frac{\partial \bar{P}}{\partial y}\frac{\partial M'}{\partial x} = 0 \tag{37}$$

$$P'\frac{\partial \bar{p}}{\partial \ln\theta} + \frac{1}{f}\left(\frac{\partial^2 M'}{\partial x^2} + \frac{\partial^2 M'}{\partial y^2}\right) = 0 . \tag{55}$$

Now assume solutions for P' and M' as in Eq. (42), substitute back into Eqs. (37) and (55), and eliminate A to obtain

$$\frac{\partial^2 B}{\partial y^2} - \mu^2 B - \frac{\dfrac{\partial \bar{p}}{\partial \ln\theta}\dfrac{\partial \bar{P}}{\partial y}}{\bar{u} - c} B = 0 . \tag{56}$$

It may be seen that use of the assumption (54) acts to eliminate an explicit dependence of B upon the vertical coordinate $\ln\theta$. As before let $B = B_r + iB_i$ and $(\bar{u} - c)^{-1} = \xi_1 + i\xi_2$ where ξ_1 and ξ_2 are defined in (48). Then separate Eq. (56) into real and imaginary parts, multiply the real part by B_i, the imaginary part by B_r, and subtract one from the other to yield

$$\left[B_i \frac{\partial^2 B_r}{\partial y^2} - B_r \frac{\partial^2 B_i}{\partial y^2}\right] + \frac{\partial \bar{p}}{\partial \ln\theta}\frac{\partial \bar{P}}{\partial y}\xi_2 (B_r^2 + B_i^2) = 0 . \tag{57}$$

By writing the bracketed term in different form and integrating with respect to y, Eq. (57) becomes

$$\int \frac{\partial}{\partial y}\left[B_i \frac{\partial B_r}{\partial y} - B_r \frac{\partial B_i}{\partial y}\right] dy + \int \frac{\partial \bar{p}}{\partial \ln\theta}\frac{\partial \bar{P}}{\partial y}\xi_2 (B_r^2 + B_i^2)\, dy = 0 . \tag{58}$$

The first integral vanishes identically under the lateral boundary conditions. This leaves the stability condition that

$$\int \frac{\dfrac{\partial \bar{p}}{\partial \ln\theta}\dfrac{\partial \bar{P}}{\partial y_\theta}}{(\bar{u} - c_r)^2 + c_i^2} c_i (B_r^2 + B_i^2)\, dy = 0 \tag{59}$$

where ξ_2 has been replaced by its equivalent in Eq. (48). In Eq. (59) $\partial\bar{p}/\partial \ln\theta$ is always negative, $(B_r^2 + B_i^2)$ is always positive, and $(\bar{u} - c_r)^2 + c_i^2$ is always positive. Thus, if $\partial\bar{P}/\partial y_\theta$ has the same sign everywhere on the isentropic surface, $c_i = 0$ and the motion is absolutely stable. This is a sufficient condition for stability. In order that c_i be greater than zero (unstable waves), for the integral in Eq. (59) to vanish it is necessary that

$$\frac{\partial\bar{P}}{\partial y_\theta} = 0 \qquad (60)$$

somewhere on the chosen isentropic surface. However, this is only a necessary condition and does not guarantee that instability will actually occur. The condition given in Eq. (60) is conceptually similar to that derived by Kuo (1949) $\left(\frac{\partial \xi_a}{\partial y} = 0\right)$ for quasi-geostrophic, two-dimensional, non-divergent flow in a barotropic atmosphere. It should be noted that Eq. (60) is the same necessary condition for instability as that obtained by Charney and Stern (1962). Their model also included lateral and vertical shear simultaneously, but the analysis was performed using non-dimensional equations and utilizing approximations for the transformation to isentropic coordinates. Also, Charney and Stern's basic equation set employed approximate forms of the divergence, vorticity, continuity, and thermodynamic equations. Because of the difference in the treatment of the physical equations, it is not apparent how to directly compare the results of the models. It is encouraging, however, that this independent analysis of the identical basic physical problem should yield the same instability condition. An analysis by Pedlosky (1964a, b) showed the same result, and furthermore, for a large class of flows, the product of the zonal mean wind and potential vorticity must vanish as a necessary condition for instability.

Comparison of the Model with Observation

An attractive way to check the above developed criterion (Eq. (60)) would be to formally transform it back to an x, y, p system (for compatibility with available stratosphere data) and compute it with respect to latitude before, during, and after the polar night vortex breakdown. This is difficult, however, because the formal transformations become very complicated. The most straightforward method is to construct meridional cross sections and measure the derivatives appearing in Eq. (54) directly with respect to the sloping surfaces.

An analysis by Murray (1960) suggested that the polar night vortex breaks down as a result of barotropic instability. As a means of comparing this contention with that of Eq. (60), the criterion $\left(\frac{\partial \xi_a}{\partial y} = 0\right)$ derived by Kuo (1949) was evaluated at increments of 10^{o} longitude along 120^{o}W on the 15th of each month from July 1957 to February 1958 at 100 mb. Fig. 24 shows these profiles and that the sufficient condition for stability is always fulfilled. This suggests that either the circulation does not break down as a result of instability or that the purely barotropic model does not fully describe the relevant characteristics of the breakdown.

Fig. 25 gives the distribution of $P^{*} = \theta P = -\frac{\partial \theta}{\partial p} \xi_a$ with latitude at θ = 400K ($\approx$100 mb) for the same months as in Fig. 24 and shows that the necessary condition for instability in this more general model is fulfilled as early as October and November. (P^{*} is a more common form for potential vorticity; hereafter all references to "potential vorticity" will imply P^{*}.)

This result is not unreasonable because as the winter intensifies, there usually are many instances of minor "warmings" or perturbations upon the vortex. This may be seen from Figs. 26 and 27, which show the cyclone index for 50 mb, 60^{o}N and the mean temperatures for each day at 70^{o}N from 1 September 1957 to 28 February 1958.

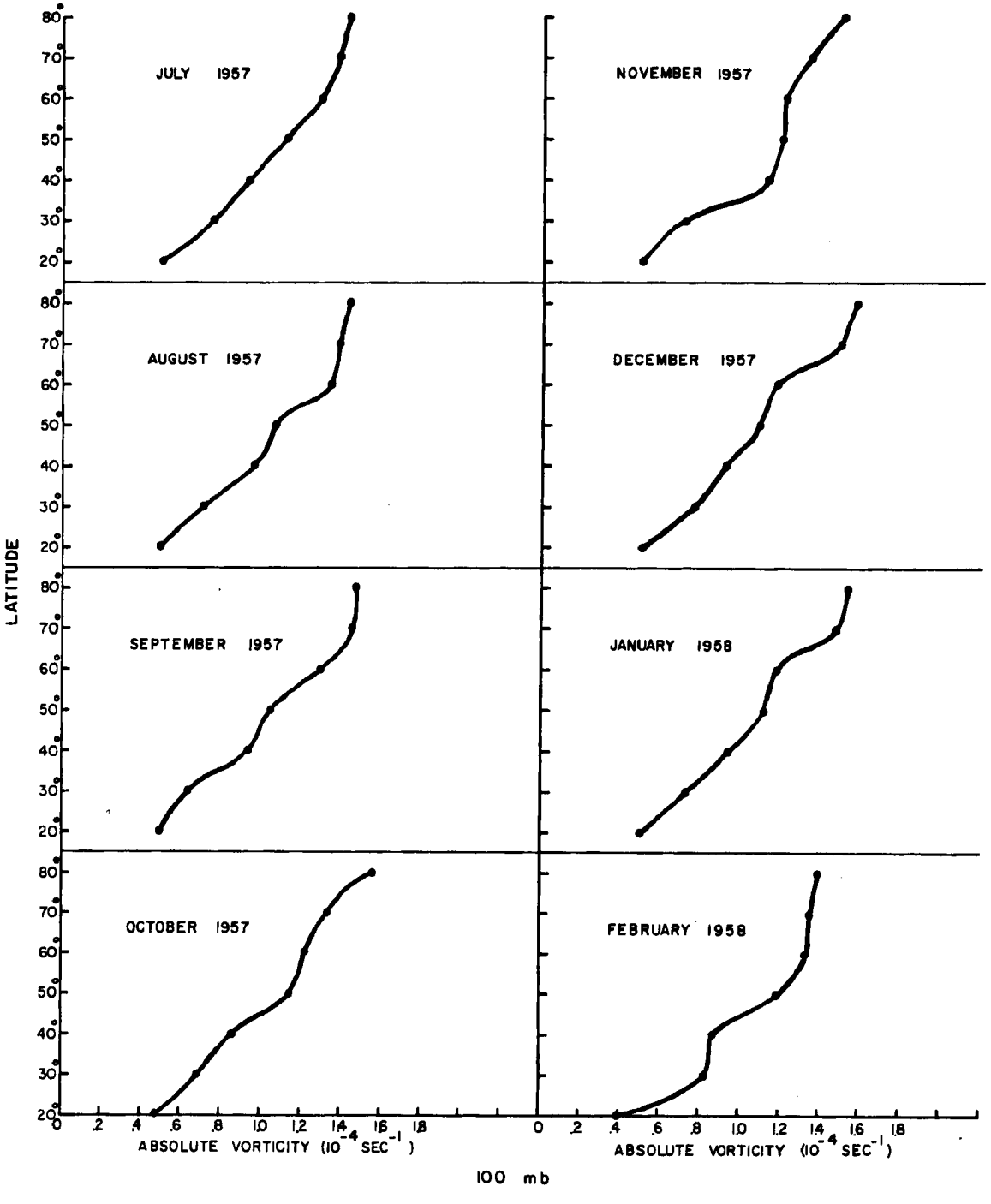

FIG. 24. Absolute vorticity at 100 mb plotted as a function of latitude along 120°W meridian.

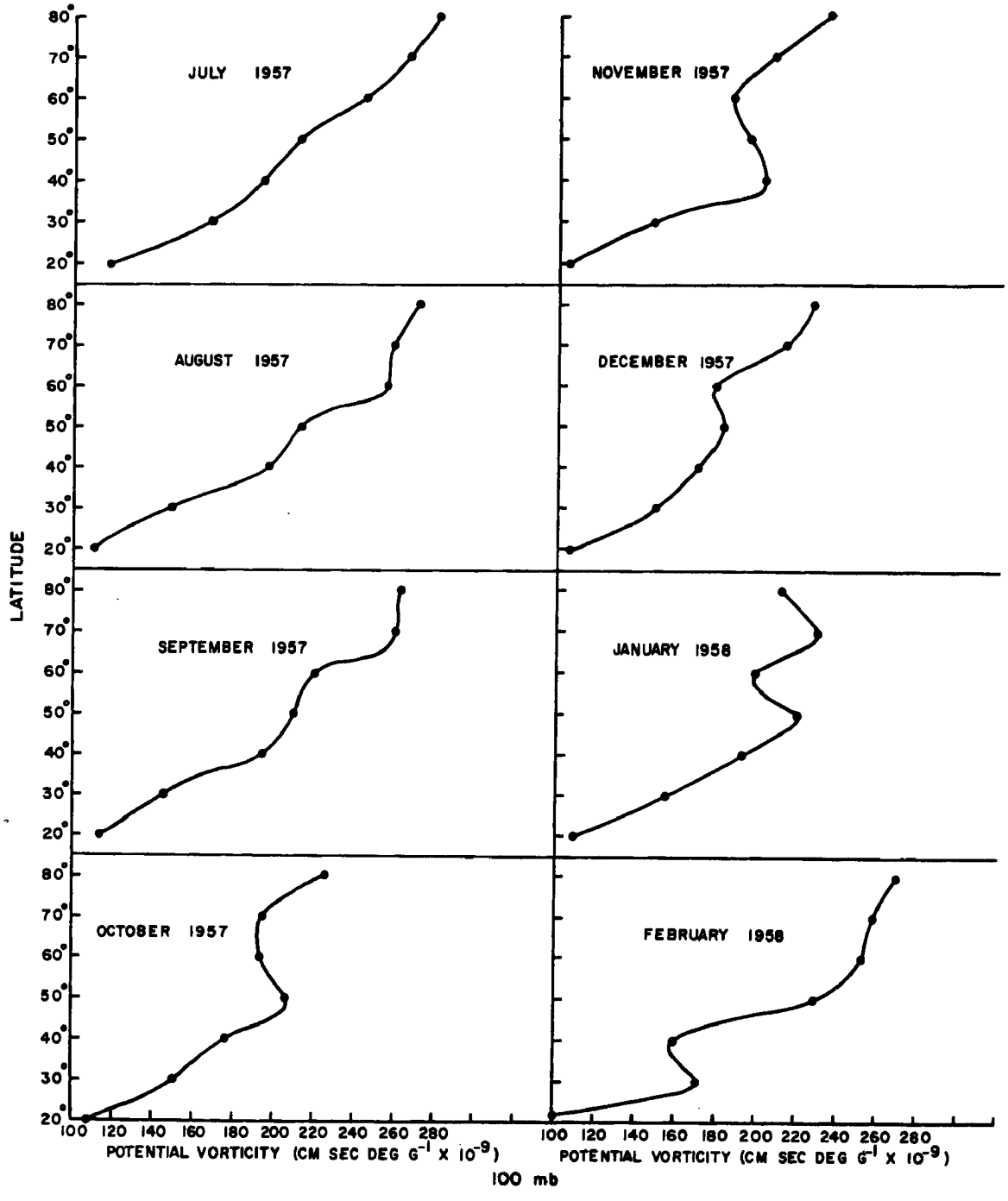

FIG. 25. Potential vorticity at θ = 400 K ($\approx$ 100 mb) plotted as a function of latitude along 120°W meridian.

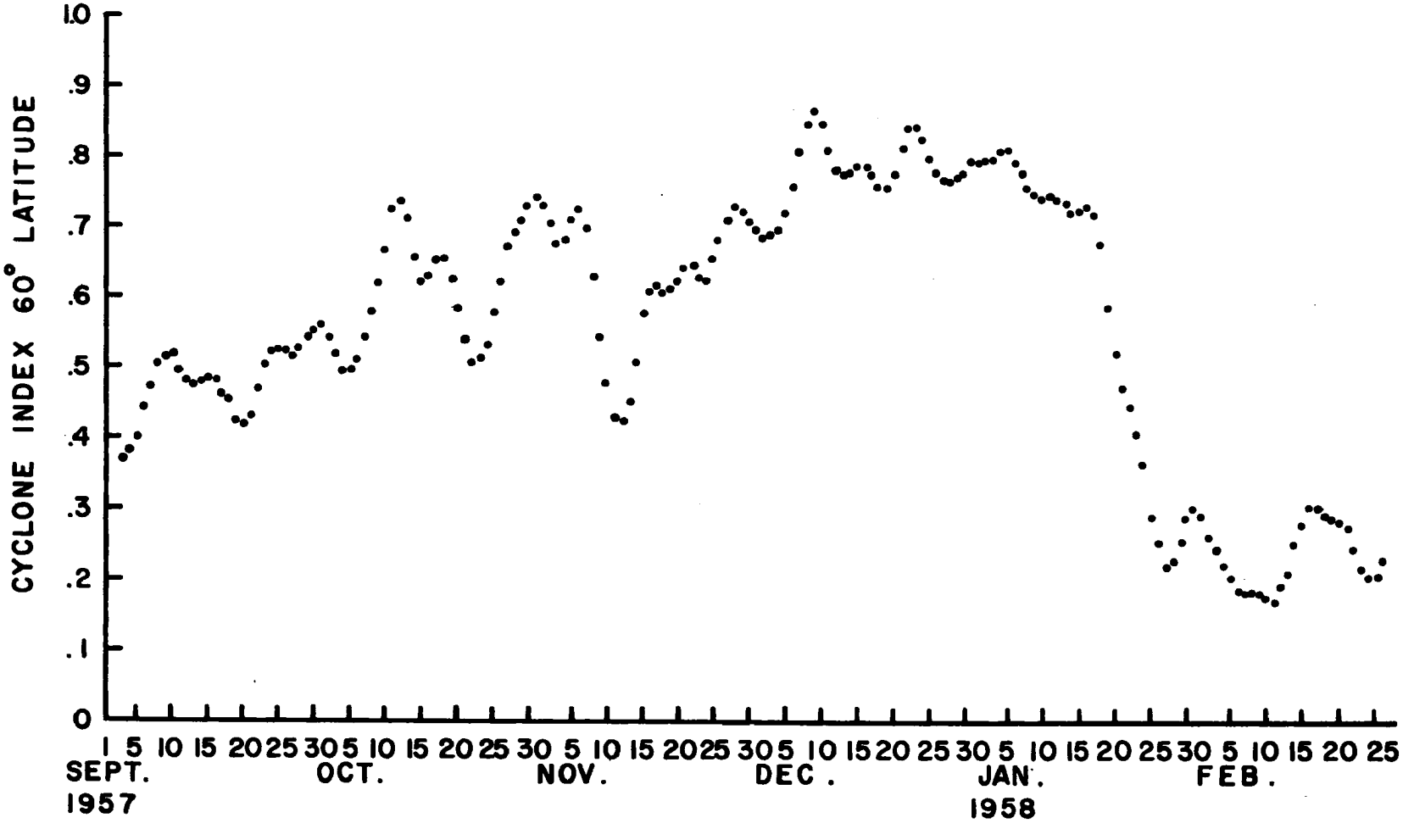

FIG. 26. Cyclone index at 50 mb, 60°N from September 1957 through February 1958.

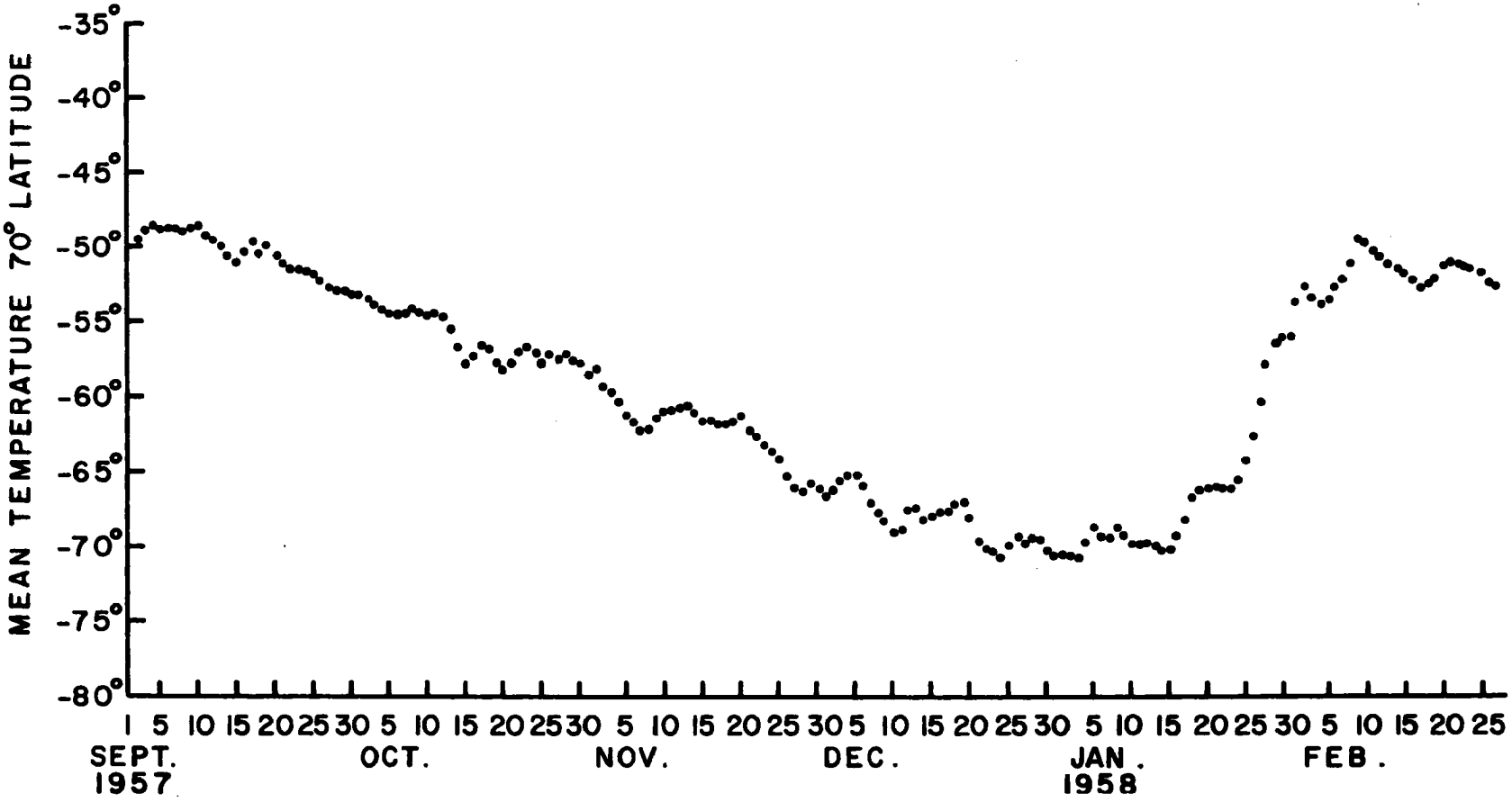

FIG. 27. Daily mean temperatures at 50 mb, 70°N from September 1957 to March 1958.

It should be noted, however, that linear theory is incapable of explaining the stabilizing processes which take place during these minor warmings since they involve non-linear effects not taken into account in the perturbation equations.

It was evident from the calculation of P^* that the influence of variations in $-\frac{\partial \theta}{\partial p}$ was much more significant than the contribution of the shearing terms.

In the polar night stratosphere of the Northern Hemisphere, it is always observed that cooling of the polar cap causes the temperature to decrease more with height in higher latitudes as the winter season progresses. This decrease is especially pronounced during the mid-winter months and results in $-\frac{\partial \theta}{\partial p}$ becoming smaller with increasing latitude. If this gradient of $-\frac{\partial \theta}{\partial p}$ is strong enough, it will offset the increase in f and the shearing effect and act to produce zeros in the $\frac{\partial P^*}{\partial y_\theta}$ field.

Thus, according to this theory, a breakdown (or instability, at least) of the polar night stratospheric vortex can occur by progressively stronger cooling with increasing height and latitude in these regions. This suggests that the warming phenomenon is a manifestation of a complicated barotropic-baroclinic energy release due to this continued cooling of the polar night stratospheric vortex. If the hypothesis is correct, then the polar night vortex contains a mechanism for its own destruction.

If the above hypothesis is to explain satisfactorily the basis for the behavior of the Arctic polar night vortex, it is also necessary that it be consistent with the observed characteristics of the Antarctic stratospheric vortex. It has been generally observed (Palmer and Taylor, 1960) that the breakdown of this system does not occur until after the return of the sun in the spring. Consequently, one must look at the data in the Antarctic region to assess the differences between the two circulation regimes. By inspection of wintertime

cross sections prepared by Taylor (1961), one observes that the thermal structure of this vortex differs from that of the Arctic region. Fig. 28 is a comparison between latitudinal profiles of $-\frac{\partial\theta}{\partial p}$ for the 100-50 mb layer during the Arctic and Antarctic winters, respectively, using Taylor's Antarctic data.

Fig. 28 shows that the thermal stability ($-\frac{\partial\theta}{\partial p}$) characteristics of the Arctic and Antarctic winter circulations are significantly different. The latitudinal gradient of $-\frac{\partial\theta}{\partial p}$ is very pronounced in the Arctic but is almost zero in the Antarctic stratosphere. As noted above, the Arctic stratosphere values of $-\frac{\partial\theta}{\partial p}$ decrease very rapidly with increasing latitude and tend to offset the tendency for increasing P^* northward due to the Coriolis effect. This indicates fulfillment of the necessary condition for instability given in Eq. (54) and is demonstrated to do so in Fig. 28. Consequently, even though the Antarctic vortex is extremely cold, it is predicted from this theory to be more stable than the corresponding Arctic circulation.

Thus, a significant difference exists between the Antarctic and Arctic vortices and may provide a framework for a satisfactory theory which explains the differences in stability of the two regimes. The above conclusion needs to be much more thoroughly tested before it can be claimed to explain the relevant features of the polar night vortex breakdowns. More adequate examination of the above theory awaits better and more plentiful data in the regions of the stratosphere and also a systematic preparation of the data as was done by the U. S. Weather Bureau (1961) for the IGY period.

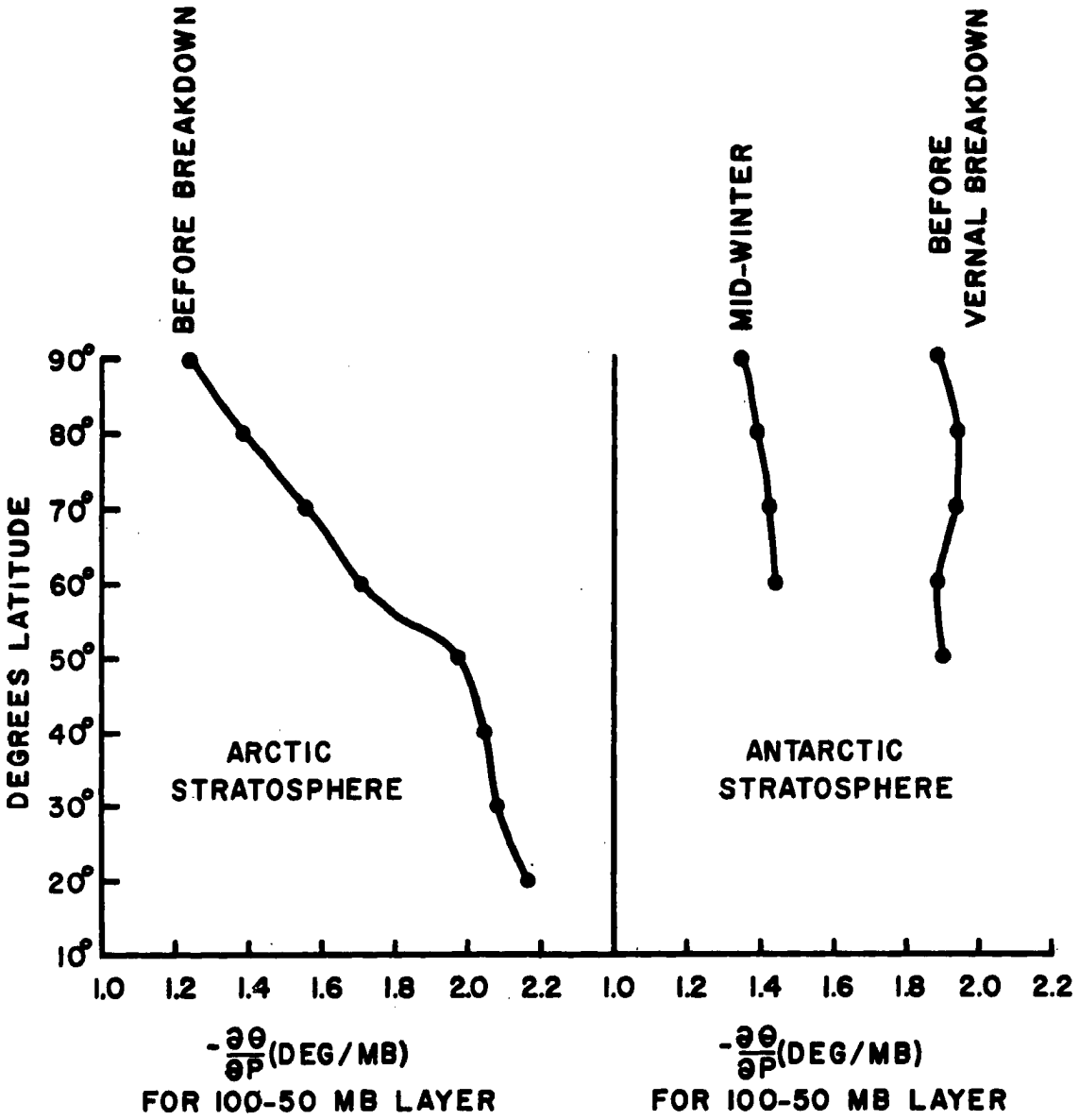

FIG. 28. Comparison between latitudinal profiles of $-\frac{\partial\theta}{\partial p}$ for Arctic and Antarctic winter stratospheres.

XI. SUMMARY, SIGNIFICANT RESULTS, AND CONCLUSIONS

The fundamental goal of this research was to investigate the possible physical mechanisms leading to seasonal, short term and latitudinal fallout variations. In Part A it was noted through reference to previous isentropic trajectory analyses that discrete intrusions of stratospheric air into the troposphere occur in association with pronounced cyclogenesis at jet stream level. This was statistically verified by investigating the relation between circulation index changes at tropopause level and surface fallout changes. The work performed in Part A demonstrated that the tropopause-level cyclogenetic process cannot be responsible for the spring fallout peaks but serves to explain adequately the short term and latitudinal fallout variations.

In an effort to isolate the physical processes leading to the spring fallout peaks, a rather comprehensive study was undertaken of the lower to middle stratosphere for the period before, during, and after the polar night vortex breakdown of January 1958. Detailed eddy transport computations were made at 50°, 60°, and 70°N latitude for this period. The most significant result was that the $\overline{v'w'}$ correlation became highly negative after the vortex breakdown occurred, thus leading to large northward and downward transport of radioactive debris in late winter.

A computation of the direction and magnitude of the mean meridional circulation was made by using a heat flux approach. The results showed that this cell operates in the indirect sense during the period, and consequently, cannot be invoked as a thermodynamic explanation of the sudden warming phenomenon. Examination of the various terms

in the mean cell computation revealed conclusively that quasi-horizontal eddy temperature flux provides the necessary warming mechanism.

As a supplement to the mean cell calculation, a computation was made of the mean abiabatic vertical motion with respect to a curvilinear coordinate system oriented along a line of maximum circulation intensity. This demonstrated that for the period before and during the vortex breakdown the circulation is direct when measured relative to such a system.

A comparison was then made of the relation between cyclone index values at tropopause level and mean vertical motion amplitude at 100 mb. This comparison showed that a direct relationship exists between the magnitude of these two quantities and suggests that it is quite possible that vertical stratospheric transport is inhibited during periods of maximum stratospheric-tropospheric mass exchange.

Detailed trajectory computations were performed and demonstrated that a pronounced descent was associated with northward trajectories after the breakdown. It was also shown that vertical directional wind shear may help to provide a dynamical explanation for the apparent maximum of total ozone at the base of long-wave stratospheric cyclones.

On the basis of the above results, it became apparent that a final solution of the stratospheric transport problem depends upon a satisfactory explanation of the behavior of the polar night vortex. In a preliminary attempt to isolate the relevant dynamical aspects of this vortex from an instability viewpoint, a linear model was constructed which simultaneously incorporated the effects of lateral and vertical wind shear. The model employed the well-known quasi-geostrophic approximation and included the effects of compressibility. This model showed that the potential vorticity gradient must vanish as a necessary condition for instability.

To compare these results with that obtained by Kuo (1949), meridional profiles of absolute vorticity and potential vorticity were plotted as a function of latitude for each month from July 1957 to February 1958. The absolute vorticity criterion is never satisfied but the potential vorticity gradient changes sign beginning in late October. This is in agreement with the observation of "minor breakdowns" beginning in the late fall months. It also suggests that the effects of compressibility are dynamically very important in the stratosphere.

The potential vorticity criterion was then used to compare the Antarctic and Arctic stratospheric vortex circulations. A striking difference between the two circulations was noted with the Antarctic vortex appearing to be much more stable than the Arctic vortex. It thus appears that this theory also contains the possibility of explaining the differences in stability between the two circulations.

On the basis of the above results it may be concluded that the mechanisms of debris transport in the stratosphere are much more complicated than previously suspected and that any successful model of stratospheric debris transport must somehow incorporate these effects. At present these effects cannot possibly be incorporated explicitly, but with successive experimentation and further research it should be possible to arrive at a completely satisfactory explanation of observed transports.

LITERATURE CITED

Allen, R. A., R. Fletcher, J. Holmboe, J. Namias, and H. C. Willett, 1940: Report on an experiment in five-day forecasting. Papers in Physical Oceanography and Meteorology, Massachusetts Institute of Technology and Woods Hole Oceanographic Institution, 8 (3), 94 pp.

Arakawa, H., 1953: Tilted-trough model as an interaction between low- and high latitude-disturbances. Journal of Meteorology, 10, 64-66.

Belmont, A., 1962: The reversal of stratospheric winds over North America during 1957, 1958, and 1959. Beiträge zur Physik der Atmosphäre, 35, 126-140.

Berson, F. A., 1949: Summary of a theoretical investigation into the factors controlling the instability of long waves in zonal currents. Tellus, 1, 44-52.

Blackman, R. B., and J. W. Tukey, 1958: Measurement of Power Spectra. Dover Publications, New York, 190 pp.

Bleichrodt, J. F., Joh. Blok, and R. H. Dekker, 1961: On the spring maximum of radioactive fallout from nuclear test explosions. Journal of Geophysical Research, 66, 135-141.

_____, Joh. Blok, and E. R. Van Abkoude, 1961: Origin of radioactive fallout in the Northern Hemisphere after the spring maximum in 1959. Journal of Geophysical Research, 66, 2183-2187.

_____, and E. R. Van Abkoude, 1963: On the deposition of cosmic ray produced beryllium-7. Journal of Geophysical Research, 68, 5283-5288.

Boville, B. W., C. W. Wilson, and F. K. Hare, 1961: Baroclinic waves of the polar night vortex. Journal of Meteorology, 18, 567-580.

Brewer, A. W., 1949: Evidence for a world circulation provided by measurements of helium and water vapor distribution in the stratosphere. Quarterly Journal of the Royal Meteorological Society, 75, 351-363.

Charney, J. G., 1947: The dynamics of long waves in a baroclinic westerly current. Journal of Meteorology, 4, 135-162.

Charney, J. G., and M. E. Stern, 1962: On the stability of internal baroclinic jets in a rotating atmosphere. Journal of the Atmospheric Sciences, 19, 159-172.

Conover, W. C., 1961: An instance of a stratospheric explosive warming. Journal of Meteorology, 18, 410-413.

Craig, R. A., and W. S. Hering, 1959: The stratospheric warming of January-February 1957. Journal of Meteorology, 16, 91-107.

_____, and M. A. Lateef, 1962: Vertical motion during the 1957 stratosphere warming. Journal of Geophysical Research, 67, 1839-1854.

Danielsen, E. F., 1959a: A determination of the mass transported from stratosphere to troposphere over North America during a thirty-six hour interval (abstract). Mitteilungen des Deutschen Wetterdienstes, 20, 10-11.

_____, 1959b: The laminar structure of the atmosphere and its relation to the concept of a tropopause. Archiv für Meteorologie, Geophysik und Bioklimatologie, A 11, 293-332.

_____, 1961: Trajectories: isobaric, isentropic, and actual. Journal of Meteorology, 18, 479-486.

_____, 1964a: Radioactivity transport from stratosphere to troposphere. Mineral Industries, 33, 1-7.

_____, 1964b: Project Springfield Report. Defense Atomic Support Agency, 97 pp.

_____, K. H. Bergman, and C. A. Paulson, 1962: Radioisotopes, potential temperature and potential vorticity--a study of stratospheric-tropospheric exchange processes. Department of Meteorology and Climatology, University of Washington, 54 pp.

Davis, P. A., 1963: An analysis of the atmospheric heat budget. Journal of the Atmospheric Sciences, 20, 5-22.

Dickenson, R. E., 1962: Momentum balance of the stratosphere during the IGY. Studies of the Stratospheric General Circulation, Final Report, Contract No. AF19(604)-5223, Massachusetts Institute of Technology, 132-167.

Dobson, G. M. B., 1956: Origin and distribution of polyatomic molecules in the atmosphere. Proceedings of the Royal Society, A236, 187-193.

Dutsch, H. U., 1962: Ozone and temperature in the stratosphere. Proceedings of the Symposium on Stratospheric and Mesospheric Circulation, Berlin, 1962, 271-290.

Eady, E. T., 1949: Long waves and cyclone waves. Tellus, 1, 33-52.

Endlich, R. M., and G. S. McLean, 1957: The structure of the jet stream core. Journal of Meteorology, 14, 543-552.

Engelmann, R. J., 1965: The calculation of precipitation scavenging. AEC Research and Development Report, Battelle-Northwest, BNWL-77, 38 pp.

Fjørtoft, R., 1951: Stability properties of large scale atmospheric disturbances. Compendium of Meteorology, 454-463.

Fleagle, R. G., 1955: Instability criteria and growth of baroclinic disturbances. Tellus, 7, 168-175.

_____, 1958: Inferences concerning the dynamics of the mesosphere. Journal of Geophysical Research, 63, 137-146.

Friend, J. P., H. W. Feely, P. W. Krey, J. Spar, and A. Walton, 1961: The High Altitude Sampling Program: Discussion of HASP Results. Final Report Contract DA-29-044-XZ-609, Isotopes, Incorporated, Vol. 3, 307 pp.

_____, H. W. Feely, E. L. Fisher, and B. Davidson, 1962: Third Quarterly Report on Project Star Dust. Contract DA-49-146-XZ-079, Isotopes, Incorporated, 65 pp.

_____, and H. W. Feely, 1962: Fifth Quarterly Report on Project Star Dust. Contract DA-49-146-XZ-079, Isotopes, Incorporated, 90 pp.

Fry, L. M., F. A. Jew, and P. K. Kuroda, 1960: On the stratospheric fallout of strontium-90; the spring peak of 1959. Journal of Geophysical Research, 65, 2061-2066.

Gilman, P. A., 1963: Indirect measurements of the mean meridional circulation in the Southern Hemisphere. Planetary Circulations Project, Report No. 3, Contract AF19(628)-2408, Massachusetts Institute of Technology, 49 pp.

_____, 1964: On the mean meridional circulations in the presence of a steady state, symmetric, circumpolar vortex. Tellus, 16, 160-167.

Goldie, A. H. R., 1958: The average planetary circulation in vertical meridian planes. Proceedings of the Royal Society, A 238, 175-180.

Green, J. S. A., 1960: A problem in baroclinic stability. Quarterly Journal of the Royal Meteorological Society, 86, 237-251.

Greenfield, S. M., 1957: Rain scavenging of radioactive particulate matter from the atmosphere. Journal of Meteorology, 14, 115-125.

Gustafson, P. F., S. S. Brar, and M. A. Kerrigan, 1961: Appearance of a spring maximum in nuclear test debris in 1960. Science, 133, 460-461.

Hare, K. R., 1960: The disturbed circulation of the Arctic stratosphere. Journal of Meteorology, 17, 36-51.

Haurwitz, B., 1961: Frictional effects and the meridional circulation in the mesosphere. Journal of Geophysical Research, 66, 2381-2392.

Hering, W. S., 1964: Ozonesonde Observations over North America, Vol. I. Air Force Cambridge Research Laboratories, 512 pp.

Holloway, J. L., Jr., 1958: Smoothing and filtering of time series and space fields. Advances in Geophysics, Academic Press, New York, 4, 351-389.

Institute fur Meteorologie und Geophysik der Freien Universität Berlin, 1960: Tägliche Höhenkarten der 25 mbar Flache für des Internationale Geophysikalische Jahr 1958. Meteorologische Abhandlungen, Band X, Heft 1.

Jensen, C. E., 1961: Energy transformation and vertical flux processes over the Northern Hemisphere. Journal of Geophysical Research, 66, 1145-1156.

Kennedy, J. S., 1964: Energy generation through radiative processes in the lower stratosphere. Planetary Circulations Project, Report No. 11, Contract No. AT(30-1)2241, Massachusetts Institute of Technology, 115 pp.

Krishnamurti, T. N., 1961: The subtropical jet stream of winter. Journal of Meteorology, 18, 172-191.

Kruger, P., and C. L. Hosler, 1963: Sr-90 concentration in precipitation from convective showers. Journal of Applied Meteorology, 2, 379-389.

Kuo, H. -L., 1949: Dynamic instability of two-dimensional nondivergent flow in a barotropic atmosphere. Journal of Meteorology, 6, 105-122.

_____, 1952: Three-dimensional disturbances in a baroclinic atmosphere. Journal of Meteorology, 9, 260-278.

_____, 1953: The stability properties and structure of disturbances in a baroclinic atmosphere. Journal of Meteorology, 10, 235-243.

_____, 1956: Forced and free meridional circulation in the atmosphere. Journal of Meteorology, 13, 561-568.

Lee, R., and W. L. Godson, 1957: The Arctic-stratospheric jet stream during the winter of 1955-1956. Journal of Meteorology, 14, 126-135.

Lettau, H. H., and K. Lettau, 1964: A meteorological study of dry fallout of radioactive debris. Archiv für Meteorologie, Geophysik und Bioklimatologie, A 14, 218-232.

Libby, W. F., 1956: Radioactive strontium fallout. Proceedings of the National Academy of Sciences, 42, 365-390.

_____, 1959: Radioactive fallout particularly from the Russian October series. Science, 45, 151-175.

_____, 1961: Tritium geophysics. Journal of Geophysical Research, 66, 3767-3782.

_____, and C. E. Palmer, 1960: Stratospheric mixing from radioactive fallout. Journal of Geophysical Research, 65, 3307-3317.

Lockhart, L. B., Jr., R. L. Patterson, Jr., A. W. Saunders, Jr., and R. W. Black, 1960: Fission product radioactivity in the air along the 80th meridian (west) during 1959. Journal of Geophysical Research, 65, 3987-3997.

London, J., 1962: Ozone variations and their relation to stratospheric warmings. Proceedings of the Symposium on Stratospheric and Mesospheric Circulation, Berlin, 1962, 299-310.

_____, and C. Prabhakara, 1962: The effect of stratospheric transport processes on the ozone distribution. Proceedings of the Symposium on Stratospheric and Mesospheric Circulation, Berlin, 1962, 291-297.

Machta, L., 1949: Dynamic characteristics of a tilted-trough model. Journal of Meteorology, 6, 261-265.

_____, 1957: Discussion of meteorological factors and fallout distribution. U. S. Department of Commerce, Weather Bureau, 11 pp.

_____, and R. J. List, 1959: Analysis of stratospheric Sr-90 measurements. Journal of Geophysical Research, 64, 1267-1276.

Mahlman, J. D., 1964a: Relation of stratospheric-tropospheric mass exchange mechanisms to surface radioactivity peaks. M. S. Thesis, Colorado State University, 54 pp.

_____, 1964b: Relation of stratospheric-tropospheric mass exchange mechanisms to surface radioactivity peaks. Atmospheric Science Paper No. 58, Colorado State University, 1-19.

_____, 1964c: On the feasibility of relating seasonal fallout oscillations to hemispheric index patterns. Atmospheric Science Paper No. 58, Colorado State University, 55-58.

_____, 1964d: Relation of upper air hemispheric patterns to seasonal fallout fluctuations. Radioactive Fallout from Nuclear Tests, U. S. Atomic Energy Commission, Division of Technical Information, 464-476.

_____, 1965a: Relation of tropopause-level index changes to radioactive fallout fluctuations. Atmospheric Science Paper No. 70, 84-109.

Mahlman, J. D., 1965b: Relation of stratospheric-tropospheric mass exchange mechanisms to surface radioactivity peaks. Archiv fur Meteorologie, Geophysik und Bioklimatologie, A15, 1-25.

Martell, E. A., 1959: Atmospheric aspects of strontium-90 fallout. Science, 129, 1197-1206.

_____, and P. J. Drevinsky, 1960: Atmospheric transport of artificial radioactivity. Science, 132, 1523-1531.

Miers, B., 1963: Zonal wind reversal between 30 and 80 km over southwestern United States. Journal of the Atmospheric Sciences, 20, 87-93.

Miller, A. J., 1966: Vertical motion atlas for the lower stratosphere during the IGY. Planetary Circulations Project, Report No. 16, Contract No. AT(30-1)2241, Massachusetts Institute of Technology, 35 pp.

Miyake, Y., K. Saruhashi, T. Katswagi, and T. Kanazawa, 1960: Radioactive fallout in Japan and its bearings on meteorological conditions. Papers in Meteorology and Geophysics, Tokyo, 9, 172-176.

_____, K. Saruhashi, Y. Katsuragi, and T. Kanazawa, 1962: Seasonal variation of radioactive fallout. Journal of Geophysical Research, 67, 189-193.

_____, K. Saruhashi, Y. Katsuragi, T. Kanazawa, and S. Tsunogai, 1963: Deposition of Sr-90 and Cs-137 in Tokyo through the end of July 1963. Journal of the Meteorological Society of Japan, 14, 58-65.

Miyakoda, K., 1963: Some characteristic features of the winter circulation in the troposphere and lower stratosphere. Technical Report No. 14 to National Science Foundation, (Grant NSF-GP-471), University of Chicago, 93 pp.

Molla, A. C., and C. J. Loisel, 1962: On the hemispheric correlations of vertical and meridional wind components. Geofisica Pura e Applicita, 51, 166-170.

Morris, J. E., and B. T. Miers, 1964: Circulation disturbances between 25 and 70 km associated with the sudden warming of 1963. Journal of Geophysical Research, 69, 201-214.

Muench, H. S., 1964: Stratospheric energy processes and associated atmospheric long-wave structure in winter. Environmental Research Paper No. 95, Air Force Cambridge Research Laboratories, 73 pp.

Murakami, T., 1962: Stratospheric wind, temperature and isobaric height conditions during the IGY period, Part I. Planetary Circulations Project, Report No. 5, Contract Nos. AT(30-1)2241 and AF19(604)5223, Massachusetts Institute of Technology, 213 pp.

_____, 1965: Energy cycle of the stratospheric warming in early 1958. Journal of the Meteorological Society of Japan, 43, 262-283.

Murgatroyd, R., and J. Singleton, 1961: Possible meridional circulations in the stratosphere and mesosphere. Quarterly Journal of the Royal Meteorological Society, 87, 125-135.

Murray, F. W., 1960: Dynamic stability in the stratosphere. Journal of Geophysical Research, 65, 3273-3305.

Namias, J., 1950: The index cycle and its role in the general circulation. Journal of Meteorology, 7, 130-139.

Newell, R. E., 1961: The transport of trace substances in the atmosphere and their implications for the general circulation of the atmosphere. Geofisica Pura e Applicita, 49, 137-158.

_____, 1963: Transfer through the tropopause and within the stratosphere. Quarterly Journal of the Royal Meteorological Society, 89, 167-205.

_____, 1964: Further ozone transport calculations and the spring maximum in ozone amount. Pure and Applied Geophysics, 59, 191-206.

_____, and A. J. Miller, 1964: Some aspects of the general circulation of the lower stratosphere. Radioactive Fallout from Nuclear Weapons Tests, U. S. Atomic Energy Commission, Division of Technical Information, 392-404.

Ohring, G., 1958: The radiation budget of the stratosphere. Journal of Meteorology, 15, 440-451.

Oort, A. H., 1962: Direct measurement of the meridional circulation in the stratosphere during the IGY. Studies of the Stratospheric General Circulation, Final Report, Contract No. AF19(604)-5223, Massachusetts Institute of Technology, 168-206.

_____, 1963: On the energy cycle in the lower stratosphere. Planetary Circulations Project, Report No. 9, Contract No. AT(30-1) 2241, Massachusetts Institute of Technology, 122 pp.

Palmén, E., 1955: On the mean meridional circulation in low latitudes of the Northern Hemisphere in winter and associated meridional flux of angular momentum. General Circulation Project, Paper No. 8, University of California at Los Angeles.

_____, H. Riehl, and L. A. Vuorela, 1958: On the meridional circulation and release of kinetic energy in the tropics. Journal of Meteorology, 15, 271-277.

Palmer, C. E., 1959a: The stratospheric polar vortex in winter. Journal of Geophysical Research, 64, 749-764.

_____, 1959b: The stratospheric polar vortex in the atmosphere. Quarterly Journal of the Royal Meteorological Society, 85, 209-224.

_____, and R. C. Taylor, 1960: The vernal breakdown of the stratospheric cyclone over the South Pole. Journal of Geophysical Research, 65, 3319-3329.

Panofsky, H. A., and G. W. Brier, 1958: Some Applications of Statistics to Meteorology. College of Mineral Industries, The Pennsylvania State University, 224 pp.

Pedlosky, J., 1964a: The stability of currents in the atmosphere and the ocean, Part I. Journal of the Atmospheric Sciences, 21, 201-219.

_____, 1964b: The stability of currents in the atmosphere and the ocean, Part II. Journal of the Atmospheric Sciences, 21, 342-353.

Peixoto, J. P., 1960: Hemispheric temperature conditions during the year 1950. Planetary Circulations Project, Scientific Report No. 4, Contract No. AF19(604)-6108, Massachusetts Institute of Technology, 211 pp.

Peng, L., 1963: Stratospheric wind, temperature, and isobaric conditions during the IGY period, Part II. Planetary Circulations Project, Report No. 10, Contract No. AT(30-1) 2241, Massachusetts Institute of Technology, 208 pp.

Phillips, N. A., 1954: Energy transformations and meridional circulations associated with simple baroclinic waves in a two-level quasi-geostrophic model. Tellus, 6, 273-286.

Pierson, D. H., 1963: Beryllium-7 in air and rain. Journal of Geophysical Research, 68, 3831-3832.

Prabhakara, C., 1963: Effects of non-photochemical processes on the meridional distribution and the total amount of ozone in the atmosphere. Monthly Weather Review, 91, 411-431.

Prawitz, J., 1964: Some quantitative properties of a fallout model. Tellus, 16, 472-480.

Priestly, C. H. B., 1949: Heat transport and zonal stresses between latitudes. Quarterly Journal of the Royal Meteorological Society, 75, 28-40.

Rayleigh, Lord, 1880: On the stability, or instability, of certain fluid motions. Proceedings of the Royal Society, A 9, 57-70.

_____, 1916: On the dynamics of revolving fluids. Proceedings of the Royal Society, A 93, 148-154.

Reed, R. J., 1955: A study of a characteristic type of upper-level frontogenesis. Journal of Meteorology, 12, 226-237.

_____, and E. F. Danielsen, 1959: Fronts in the vicinity of the tropopause. Archiv für Meteorologie, Geophysik und Bioklimatologie, A 11, 1-17.

_____, and F. Sanders, 1953: An investigation of the development of a mid-tropospheric frontal zone and its associated vorticity field. Journal of Meteorology, 10, 338-349.

Reiter, E. R., 1963a: Jet Stream Meteorology. University of Chicago Press, 513 pp.

_____, 1963b: A case study of radioactive fallout. Journal of Applied Meteorology, 2, 691-705.

Reiter, E. R., 1964: Comments on paper by S. Penn and E. A. Martell, "An analysis of the radioactive fallout over North America in late September 1961". Journal of Geophysical Research, 69, 786-788.

_____, and J. D. Mahlman, 1964: Heavy radioactive fallout over the southern United States, November 1962. Atmospheric Science Paper No. 58, Colorado State University, 21-49.

_____, and J. D. Mahlman, 1965a: Heavy iodine-131 fallout over the midwestern United States, May 1962. Atmospheric Science Paper No. 70, Colorado State University, 1-53.

_____, and J. D. Mahlman, 1965b: A case study of mass transport from stratosphere to troposphere, not associated with surface fallout. Atmospheric Science Paper No. 70, Colorado State University, 54-83.

_____, and J. D. Mahlman, 1965c: Heavy radioactive fallout over the southern United States, November 1962. Journal of Geophysical Research, 70, 4501-4520.

Riehl, H., and D. Fultz, 1957: Jet streams and long waves in a steady rotating dishpan experiment: Structure of the circulation. Quarterly Journal of the Royal Meteorological Society, 83, 215-231.

_____, T. C. Yeh, and N. E. LaSeur, 1950: A study of variations of the general circulation. Journal of Meteorology, 6, 181-194.

Rossby, C. -G. and Collaborators, 1939: Relation between variations in the intensity of the zonal circulation of the atmosphere and the displacements of the semi-permanent centers of action. Journal of Marine Research, 2, 38-55.

Scherhag, R., 1952: Die explosionsartigen Stratosphärenerwärmungen des Spätwinters 1951/1952. Berich des Deutschen Wetterdienstes in der U. S. Zone, No. 38, 51-63.

Sekiguchi, Y., 1963: Energy variation in the stratosphere during the winter season and its relation to dynamic stability of the polar vortex. University of Oklahoma Research Institute, NSF Grant 14067, University of Oklahoma, 35 pp.

Staley, D. O., 1960: Evaluation of potential vorticity changes near the tropopause and the related vertical motion, vertical advection of vorticity, and the transfer of radioactive debris from the stratosphere to the troposphere. Journal of Meteorology, 17, 591-620.

_____, 1962: On the mechanism of mass and radioactivity transport from stratosphere to troposphere. Journal of the Atmospheric Sciences, 19, 450-457.

Stewart, N. G., R. N. Crooks, and E. M. Fisher, 1955: Atomic Energy Research Establishment, Publication No. AERE HP/R 1701, Harwell.

_____, R. G. D. Osmond, R. N. Crooks, E. M. Fisher, and M. J. Owens, 1957: The world-wide deposition of long-lived fission products from nuclear explosions. Atomic Energy Research Establishment, Publication No. AERE HP/R 2790, Harwell.

Storebø, P. B., 1959: Orographical and climatological influences on deposition of nuclear-bomb debris. Journal of Meteorology, 16, 600-608.

_____, 1960: The exchange of air between stratosphere and troposphere. Journal of Meteorology, 17, 547-553.

Tauber, H., 1961: Latitudinal effect in the transfer of radiocarbon from stratosphere to troposphere. Science, 133, 461-462.

Taylor, R. C., 1961: Upper-air temperatures at U. S. Antarctic stations. IGY General Report No. 14, IGY World Data Center, 48 pp.

Teweles, S., 1958: Anomalous warming of the stratosphere over North America in early 1957. Monthly Weather Review, 86, 377-396.

_____, 1963: Spectral aspects of the stratospheric circulation during the IGY. Planetary Circulations Project, Report No. 8, Massachusetts Institute of Technology, 191 pp.

_____, and F. B. Finger, 1958: An abrupt change in stratospheric circulation beginning in mid-January 1958. Monthly Weather Review, 86, 23-28.

Thompson, P. D., 1953: On the theory of large-scale disturbances in a two-dimensional baroclinic equivalent of the atmosphere. Quarterly Journal of the Royal Meteorological Society, 79, 51-69.

_____, 1956: A theory of large-scale disturbances in non-geostrophic flow. Journal of Meteorology, 13, 251-261.

United States Weather Bureau, 1961: Daily 100-millibar and 50-millibar and three times monthly 30-millibar synoptic weather maps. U. S. Department of Commerce, Weather Bureau.

White, R. M., 1954: The counter-gradient flux of sensible heat in the lower stratosphere. Tellus, 6, 177-179.

APPENDICES

LEVEL 50 MB. LATITUDE 50 COVARIANCE

DAY	TU	TV	TW	UV	UW	VW
JAN 10	-110.646	70.514	-1.398	-34.089	-2.025	.616
JAN 11	-66.584	59.915	-1.884	-19.862	-2.939	.859
JAN 12	-79.009	11.222	-.148	-99.888	-1.842	1.804
JAN 13	-85.984	21.700	-.557	-57.731	3.485	-2.915
JAN 14	-97.375	39.352	.431	-7.898	-4.397	-2.223
JAN 15	-67.328	44.736	-.093	25.346	-1.212	2.230
JAN 16	-81.460	60.315	-.938	50.935	.541	1.915
JAN 17	-109.265	61.727	-.152	-8.178	-2.400	-.642
JAN 18	-224.649	58.190	-1.178	-97.780	-1.941	-3.401
JAN 19	-228.974	67.341	.052	-48.555	-11.546	.731
JAN 20	-289.363	80.175	.754	160.127	-5.668	1.855
JAN 21	-238.315	56.938	2.394	160.006	-11.438	4.457
JAN 22	-117.781	77.864	2.044	119.683	-5.250	8.036
JAN 23	-129.433	109.331	1.175	126.989	-13.698	-1.341
JAN 24	-105.483	124.507	1.794	1.094	-16.397	2.198
JAN 25	-99.525	136.836	.495	29.204	-7.920	-3.939
JAN 26	-170.184	74.965	.911	149.916	-8.341	-10.522
JAN 27	-177.143	116.375	1.001	277.282	-7.112	-11.109
JAN 28	-209.609	104.666	-1.377	307.464	-9.767	-19.315
JAN 29	-131.223	107.346	.316	182.605	-12.884	-9.460
JAN 30	-82.704	102.196	1.602	182.061	-16.574	-8.726
JAN 31	-68.562	92.570	-.358	-40.937	-7.552	-6.100
FEB 1	-51.093	76.106	-2.030	-68.367	-2.412	-3.741
FEB 2	-105.536	73.372	1.319	34.001	-5.741	-.756
FEB 3	-141.880	66.146	.052	44.566	-12.761	-3.684
FEB 4	-192.555	115.345	-.354	-54.147	-8.396	-7.210
FEB 5	-141.368	91.356	.533	-13.522	-9.065	-7.709
FEB 6	-54.771	72.154	-.291	80.373	-13.406	-9.992
FEB 7	-27.114	63.817	.101	-38.797	1.140	-12.713
FEB 8	-20.422	28.423	.362	-85.299	-5.836	.827
FEB 9	-21.578	29.945	-.103	29.422	1.344	-1.011
FEB 10	-55.738	27.580	.344	2.842	-1.089	1.654
FEB 11	-64.846	13.143	.019	11.400	-1.224	-1.189
FEB 12	-91.286	18.945	.064	-37.728	-.368	-.516
FEB 13	-65.780	18.273	-.138	12.593	-2.036	-1.525
FEB 14	-72.748	28.398	-.407	-42.779	-2.019	.303
FEB 15	-45.297	32.752	.404	-39.583	-4.419	-.498
FEB 16	-27.269	32.745	-.425	-4.924	-4.684	-3.607
FEB 17	-13.549	29.917	.047	-23.091	-2.435	-.632
FEB 18	-16.669	42.977	.256	-25.616	-3.139	-1.666
FEB 19	-28.361	40.989	.022	-30.200	-1.701	-.438

LEVEL 50 MB. LATITUDE 50 EDDY CORRELATION COEFFICIENTS

DAY	TU	TV	TW	UV	UW	VW
JAN 10	-.605	.541	-.262	-.091	-.132	.056
JAN 11	-.450	.451	-.425	-.057	-.250	.081
JAN 12	-.467	.096	-.026	-.320	-.122	.174
JAN 13	-.557	.216	-.125	-.177	.242	-.310
JAN 14	-.572	.311	.142	-.017	-.393	-.268
JAN 15	-.472	.335	-.035	.062	-.147	.288
JAN 16	-.529	.417	-.246	.138	.056	.210
JAN 17	-.699	.461	-.037	-.028	-.268	-.084
JAN 18	-.831	.397	-.205	-.201	-.102	-.328
JAN 19	-.712	.425	.008	-.085	-.497	.064
JAN 20	-.716	.382	.097	.223	-.212	.134
JAN 21	-.776	.238	.258	.221	-.408	.204
JAN 22	-.479	.404	.259	.209	-.224	.436
JAN 23	-.526	.449	.144	.162	-.523	-.052
JAN 24	-.411	.488	.200	.001	-.544	.073
JAN 25	-.395	.561	.063	.030	-.251	-.129
JAN 26	-.585	.329	.115	.155	-.248	-.400
JAN 27	-.564	.466	.140	.236	-.211	-.414
JAN 28	-.602	.381	-.164	.258	-.267	-.669
JAN 29	-.527	.534	.043	.288	-.559	-.508
JAN 30	-.351	.547	.239	.275	-.698	-.463
JAN 31	-.458	.556	-.067	-.077	-.444	-.323
FEB 1	-.229	.397	-.308	-.110	-.112	-.203
FEB 2	-.436	.431	.219	.068	-.327	-.061
FEB 3	-.544	.442	.009	.075	-.555	-.279
FEB 4	-.581	.652	-.059	-.070	-.320	-.515
FEB 5	-.580	.590	.103	-.018	-.356	-.476
FEB 6	-.343	.636	-.081	.108	-.574	-.602
FEB 7	-.188	.517	.022	-.062	.048	-.629
FEB 8	-.246	.661	.191	-.208	-.323	.088
FEB 9	-.231	.630	-.067	.067	.094	-.140
FEB 10	-.600	.426	.274	.006	-.110	.239
FEB 11	-.632	.211	.013	.020	-.093	-.149
FEB 12	-.814	.270	.069	-.082	-.061	-.136
FEB 13	-.734	.365	-.119	.041	-.283	-.379
FEB 14	-.608	.483	-.145	-.168	-.166	.051
FEB 15	-.456	.559	.263	-.143	-.610	-.117
FEB 16	-.301	.494	-.199	-.019	-.575	-.606
FEB 17	-.159	.519	.048	-.103	-.631	-.243
FEB 18	-.257	.663	.202	-.083	-.520	-.276
FEB 19	-.428	.649	.024	-.090	-.341	-.092

LEVEL 50 MB. LATITUDE 50 PRODUCT OF (U,V,W,T) BAR

DAY	TU	TV	TW	UV	UW	VW
JAN 10	-.605	.541	-.262	-.091	-.132	.056
JAN 11	-.450	.451	-.425	-.057	-.250	.081
JAN 12	-.467	.096	-.026	-.320	-.122	.174
JAN 13	-.557	.216	-.125	-.177	.242	-.310
JAN 14	-.572	.311	.142	-.017	-.393	-.268
JAN 15	-.472	.335	-.035	.062	-.147	.288
JAN 16	-.529	.417	-.246	.138	.056	.210
JAN 17	-.699	.461	-.037	-.028	-.268	-.084
JAN 18	-.831	.397	-.205	-.201	-.102	-.328
JAN 19	-.712	.425	.008	-.085	-.497	.064
JAN 20	-.716	.382	.097	.223	-.212	.134
JAN 21	-.776	.238	.258	.221	-.408	.204
JAN 22	-.479	.404	.259	.209	-.224	.436
JAN 23	-.526	.449	.144	.162	-.523	-.052
JAN 24	-.411	.488	.200	.001	-.544	.073
JAN 25	-.395	.561	.063	.030	-.251	-.129
JAN 26	-.585	.329	.115	.155	-.248	-.400
JAN 27	-.564	.466	.140	.236	-.211	-.414
JAN 28	-.602	.381	-.164	.258	-.267	-.669
JAN 29	-.527	.534	.043	.288	-.559	-.508
JAN 30	-.351	.547	.239	.275	-.698	-.463
JAN 31	-.458	.556	-.067	-.077	-.444	-.323
FEB 1	-.229	.397	-.308	-.110	-.112	-.203
FEB 2	-.436	.431	.219	.068	-.327	-.061
FEB 3	-.544	.442	.009	.075	-.555	-.279
FEB 4	-.581	.652	-.059	-.070	-.320	-.515
FEB 5	-.580	.590	.103	-.018	-.356	-.476
FEB 6	-.343	.636	-.081	.108	-.574	-.602
FEB 7	-.188	.517	.022	-.062	.048	-.629
FEB 8	-.246	.661	.191	-.208	-.323	.088
FEB 9	-.231	.630	-.067	.067	.094	-.140
FEB 10	-.600	.426	.274	.006	-.110	.239
FEB 11	-.632	.211	.013	.020	-.093	-.149
FEB 12	-.814	.270	.069	-.082	-.061	-.136
FEB 13	-.734	.365	-.119	.041	-.283	-.379
FEB 14	-.608	.483	-.145	-.168	-.166	.051
FEB 15	-.456	.559	.263	-.143	-.610	-.117
FEB 16	-.301	.494	-.199	-.019	-.575	-.606
FEB 17	-.159	.519	.048	-.103	-.631	-.243
FEB 18	-.257	.663	.202	-.083	-.520	-.276
FEB 19	-.428	.649	.024	-.090	-.341	-.092

LEVEL 50 MB. LATITUDE 50 MEANS OF T,U,V,AND W

DAY	TBAR	UBAR	VBAR	WBAR
JAN 10	-56.722	46.418	-1.444	-.395
JAN 11	-56.556	43.290	-.886	-.476
JAN 12	-55.889	44.571	-.781	-.254
JAN 13	-56.028	43.685	.201	-.218
JAN 14	-56.472	43.654	-1.026	-.484
JAN 15	-56.194	39.524	-.512	-.400
JAN 16	-56.333	32.465	-.092	-.192
JAN 17	-56.694	34.832	.725	-.236
JAN 18	-57.000	39.745	.988	-.322
JAN 19	-56.389	41.194	.490	-.419
JAN 20	-57.250	42.330	1.742	-.343
JAN 21	-56.278	35.240	1.604	-.368
JAN 22	-56.111	33.680	-1.031	-.172
JAN 23	-56.194	39.384	-.102	-.424
JAN 24	-55.861	35.117	-.102	-.436
JAN 25	-55.528	38.794	.408	-.480
JAN 26	-56.528	45.086	.089	-.434
JAN 27	-57.083	45.269	.758	-.348
JAN 28	-57.389	44.373	-.208	-.452
JAN 29	-57.972	27.856	1.455	-.566
JAN 30	-57.278	31.806	-.210	-.519
JAN 31	-56.278	28.377	.090	-.380
FEB 1	-57.083	24.873	-.371	-.223
FEB 2	-57.583	26.310	-1.420	-.299
FEB 3	-57.694	24.272	.407	-.453
FEB 4	-56.528	22.221	.086	-.345
FEB 5	-56.306	18.093	1.196	-.284
FEB 6	-55.528	17.556	.408	-.380
FEB 7	-54.944	17.857	-.688	-.076
FEB 8	-54.750	21.226	-.870	-.276
FEB 9	-54.750	19.602	.327	-.132
FEB 10	-54.583	16.312	-.049	-.132
FEB 11	-54.417	18.898	.824	-.030
FEB 12	-54.139	15.791	1.320	-.094
FEB 13	-54.250	16.085	.110	-.219
FEB 14	-53.056	20.738	.078	-.215
FEB 15	-53.194	16.066	-.827	-.237
FEB 16	-53.167	14.326	-.291	-.176
FEB 17	-53.722	15.056	-.571	-.184
FEB 18	-53.861	12.876	-.715	-.181
FEB 19	-54.306	14.620	.085	-.224

APPENDIX A. Covariances, eddy correlation coefficients, mean products, and means of u, v, w, and T from 10 January to 19 February 1958 for indicated levels and latitudes.

LEVEL 50 MB. LATITUDE 60 COVARIANCE

DAY	TU	TV	TW	UV	UW	VW
JAN 10	-109.495	51.136	2.914	-2.891	-.151	4.404
JAN 11	-101.907	50.809	1.379	-130.023	5.013	2.195
JAN 12	-105.085	17.756	1.073	-26.104	1.054	2.342
JAN 13	-54.334	43.343	3.233	-39.607	-2.117	6.567
JAN 14	-33.735	54.679	2.854	-8.446	-.185	6.669
JAN 15	-2.329	56.555	.519	105.118	1.511	.645
JAN 16	-86.744	86.110	.289	11.224	1.169	3.225
JAN 17	-105.844	83.790	.652	-57.136	-1.901	-3.933
JAN 18	-149.763	96.885	.647	-95.189	-2.023	-3.074
JAN 19	-141.219	103.701	1.048	-23.312	-2.020	-.213
JAN 20	-157.124	130.573	1.603	-64.997	-1.457	.848
JAN 21	-104.749	136.884	2.285	-5.536	-6.817	3.729
JAN 22	-41.948	64.397	2.033	39.964	.037	11.325
JAN 23	-69.532	130.959	1.862	205.614	1.338	14.879
JAN 24	-81.461	148.260	3.350	177.743	9.082	33.311
JAN 25	-96.653	119.970	2.736	-30.015	.434	13.268
JAN 26	-105.836	172.165	.943	-113.634	3.603	2.311
JAN 27	-48.042	138.168	.627	-84.328	-1.877	-4.732
JAN 28	-70.422	183.661	-.036	.296	2.180	-11.412
JAN 29	-39.181	214.317	.149	224.489	-6.900	-17.199
JAN 30	-78.926	149.111	1.474	35.096	-1.599	-8.733
JAN 31	-164.567	124.027	.009	-.922	1.625	-5.983
FEB 1	-178.558	99.923	-2.904	-13.918	1.346	-10.939
FEB 2	-233.338	109.656	-1.021	-191.391	1.842	-15.272
FEB 3	-212.219	108.713	-2.918	-23.377	1.175	-14.370
FEB 4	-194.184	198.076	.673	-137.280	-4.597	-13.215
FEB 5	-125.706	96.878	.459	-87.884	-5.164	-9.277
FEB 6	-41.507	114.478	-1.527	-55.236	1.072	-16.026
FEB 7	-24.393	61.321	-.172	-111.530	.035	-8.592
FEB 8	-41.700	45.772	-.818	-134.064	4.047	-9.900
FEB 9	-37.363	-14.877	.287	-145.834	5.199	-11.524
FEB 10	-85.643	.194	.175	-37.285	-1.942	-7.498
FEB 11	-57.052	-22.745	.377	-46.701	1.697	-3.410
FEB 12	-80.268	1.254	.082	-149.817	2.849	-8.776
FEB 13	-98.287	29.057	-.056	-163.781	1.558	-4.041
FEB 14	-74.799	37.047	-.030	-162.491	-.182	-1.707
FEB 15	-67.927	48.280	-.450	-129.386	1.137	-3.738
FEB 16	-50.052	53.717	.326	-140.195	-2.070	-1.625
FEB 17	-69.164	54.901	-.381	-149.000	-.634	-1.155
FEB 18	-68.628	60.748	-.473	-92.754	1.663	-1.548
FEB 19	-52.916	63.073	-.167	-48.968	-.888	-2.616

LEVEL 50 MB. LATITUDE 60 EDDY CORRELATION COEFFICIENTS

DAY	TU	TV	TW	UV	UW	VW
JAN 10	-.577	.243	.651	-.006	-.014	.379
JAN 11	-.557	.293	.260	-.310	.391	.181
JAN 12	-.835	.095	.143	-.107	.108	.160
JAN 13	-.778	.241	.444	-.256	-.338	.407
JAN 14	-.374	.224	.422	-.030	-.024	.314
JAN 15	-.029	.308	.086	.471	.207	.039
JAN 16	-.615	.377	.041	.037	.123	.210
JAN 17	-.749	.422	.067	-.250	-.171	-.252
JAN 18	-.865	.366	.066	-.328	-.187	-.185
JAN 19	-.883	.348	.104	-.090	-.229	-.013
JAN 20	-.841	.443	.144	-.228	-.135	.050
JAN 21	-.481	.433	.267	-.013	-.576	.217
JAN 22	-.309	.247	.246	.146	.004	.681
JAN 23	-.310	.336	.245	.275	.092	.588
JAN 24	-.403	.403	.225	.282	.356	.719
JAN 25	-.519	.319	.325	-.055	.036	.540
JAN 26	-.436	.574	.125	-.190	.240	.124
JAN 27	-.157	.366	.132	-.083	-.146	-.299
JAN 28	-.373	.481	-.004	.001	.176	-.455
JAN 29	-.230	.566	.013	.450	-.474	-.532
JAN 30	-.455	.550	.148	.084	-.104	-.364
JAN 31	-.635	.440	.001	-.001	.074	-.251
FEB 1	-.730	.386	-.275	-.027	.064	-.489
FEB 2	-.852	.341	-.111	-.302	.101	-.715
FEB 3	-.860	.387	-.288	-.048	.067	-.722
FEB 4	-.709	.528	.085	-.159	-.253	-.531
FEB 5	-.741	.460	.117	-.137	-.431	-.625
FEB 6	-.336	.688	-.384	-.090	.073	-.815
FEB 7	-.235	.535	-.050	-.246	.003	-.573
FEB 8	-.498	.526	-.275	-.299	.265	-.623
FEB 9	-.442	-.170	.101	-.321	.352	-.754
FEB 10	-.806	.002	.057	-.073	-.128	-.505
FEB 11	-.652	-.244	.233	-.119	.250	-.471
FEB 12	-.774	.012	.031	-.342	.256	-.791
FEB 13	-.808	.297	-.025	-.364	.152	-.490
FEB 14	-.752	.503	-.014	-.641	-.026	-.325
FEB 15	-.804	.578	-.275	-.550	.248	-.712
FEB 16	-.619	.575	.151	-.626	-.400	-.272
FEB 17	-.715	.634	-.135	-.617	-.080	-.163
FEB 18	-.777	.499	-.271	-.299	.374	-.253
FEB 19	-.655	.617	-.156	-.128	-.222	-.516

LEVEL 50 MB. LATITUDE 60 PRODUCT OF (U,V,W,T) BAR

DAY	TU	TV	TW	UV	UW	VW
JAN 10	-.577	.243	.651	-.006	-.014	.379
JAN 11	-.557	.293	.260	-.310	.391	.181
JAN 12	-.835	.095	.143	-.107	.108	.160
JAN 13	-.778	.241	.444	-.256	-.338	.407
JAN 14	-.374	.224	.422	-.030	-.024	.314
JAN 15	-.029	.308	.086	.471	.207	.039
JAN 16	-.615	.377	.041	.037	.123	.210
JAN 17	-.749	.422	.067	-.250	-.171	-.252
JAN 18	-.865	.366	.066	-.328	-.187	-.185
JAN 19	-.883	.348	.104	-.090	-.229	-.013
JAN 20	-.841	.443	.144	-.228	-.135	.050
JAN 21	-.481	.433	.267	-.013	-.576	.217
JAN 22	-.309	.247	.246	.146	.004	.681
JAN 23	-.310	.336	.245	.275	.092	.588
JAN 24	-.403	.403	.225	.282	.356	.719
JAN 25	-.519	.319	.325	-.055	.036	.540
JAN 26	-.436	.574	.125	-.190	.240	.124
JAN 27	-.157	.366	.132	-.083	-.146	-.299
JAN 28	-.373	.481	-.004	.001	.176	-.455
JAN 29	-.230	.566	.013	.450	-.474	-.532
JAN 30	-.455	.550	.148	.084	-.104	-.364
JAN 31	-.635	.440	.001	-.001	.074	-.251
FEB 1	-.730	.386	-.275	-.027	.064	-.489
FEB 2	-.852	.341	-.111	-.302	.101	-.715
FEB 3	-.860	.387	-.288	-.048	.067	-.722
FEB 4	-.709	.528	-.085	-.159	-.253	-.531
FEB 5	-.741	.460	.117	-.137	-.431	-.625
FEB 6	-.336	.688	-.384	-.090	.073	-.815
FEB 7	-.235	.535	-.050	-.246	.003	-.573
FEB 8	-.498	.526	-.275	-.299	.265	-.623
FEB 9	-.442	-.170	.101	-.321	.352	-.754
FEB 10	-.806	.002	.057	-.073	-.128	-.505
FEB 11	-.652	-.244	.233	-.119	.250	-.471
FEB 12	-.774	.012	.031	-.342	.256	-.791
FEB 13	-.808	.297	-.025	-.364	.152	-.490
FEB 14	-.752	.503	-.014	-.641	-.026	-.325
FEB 15	-.804	.578	-.275	-.550	.248	-.712
FEB 16	-.619	.575	.151	-.626	-.400	-.272
FEB 17	-.715	.634	-.135	-.617	-.080	-.163
FEB 18	-.777	.499	-.271	-.299	.374	-.253
FEB 19	-.655	.617	-.156	-.128	-.222	-.516

LEVEL 50 MB. LATITUDE 60 MEANS OF T,U,V,AND W

DAY	TBAR	UBAR	VBAR	WBAR
JAN 10	-61.667	59.620	3.319	.146
JAN 11	-61.500	59.661	-.671	.030
JAN 12	-61.806	44.541	1.850	.030
JAN 13	-61.250	45.334	.741	-.043
JAN 14	-62.333	45.210	-.600	-.086
JAN 15	-62.111	40.380	.316	.001
JAN 16	-61.028	45.380	-.718	-.172
JAN 17	-61.278	50.661	1.172	-.147
JAN 18	-60.472	45.706	.659	-.193
JAN 19	-60.556	32.088	.773	-.135
JAN 20	-61.028	29.397	-.602	-.036
JAN 21	-61.083	31.596	-3.591	-.253
JAN 22	-60.278	23.901	-1.379	-.122
JAN 23	-60.056	31.946	-3.708	-.077
JAN 24	-59.694	27.999	-3.553	.019
JAN 25	-58.944	20.660	-.879	.051
JAN 26	-60.361	21.839	-1.126	.106
JAN 27	-60.806	23.883	-4.202	-.046
JAN 28	-59.944	14.540	-1.348	.034
JAN 29	-58.694	17.530	-3.641	-.346
JAN 30	-59.222	17.806	-2.258	-.210
JAN 31	-58.306	19.533	-1.343	-.198
FEB 1	-56.444	8.780	.237	-.214
FEB 2	-56.083	9.275	.266	-.039
FEB 3	-56.972	8.412	-.095	-.178
FEB 4	-56.361	12.303	1.971	-.129
FEB 5	-54.861	11.575	-1.095	-.123
FEB 6	-53.833	6.531	1.019	-.031
FEB 7	-54.222	7.569	.659	-.140
FEB 8	-53.417	7.897	.645	-.174
FEB 9	-52.611	4.496	-.275	-.144
FEB 10	-52.750	6.587	1.589	-.006
FEB 11	-52.806	4.974	1.322	-.007
FEB 12	-52.556	5.687	-.115	-.091
FEB 13	-52.167	7.979	.609	-.169
FEB 14	-51.250	9.766	-.129	-.166
FEB 15	-51.611	5.758	.807	-.070
FEB 16	-52.528	12.865	.976	-.126
FEB 17	-52.667	13.408	2.076	-.086
FEB 18	-52.667	9.692	2.015	.082
FEB 19	-53.444	12.027	-1.360	-.074

LEVEL 50 MB. LATITUDE 70 COVARIANCE

DAY	TU	TV	TW	UV	UW	VW
JAN 10	69.263	-3.890	-.160	-201.116	-.527	3.921
JAN 11	78.334	8.596	.364	-148.390	2.832	.153
JAN 12	-12.229	-7.407	.510	-7.819	.221	2.499
JAN 13	52.190	3.197	-.042	18.150	4.585	14.754
JAN 14	113.494	23.210	2.163	93.189	4.750	3.434
JAN 15	63.988	3.246	1.763	174.050	4.488	3.084
JAN 16	90.929	40.214	.925	-36.552	11.710	1.476
JAN 17	36.594	67.771	.343	-81.687	.506	-4.065
JAN 18	195.877	144.363	.243	73.230	2.563	-16.259
JAN 19	218.900	184.954	3.567	195.681	7.872	-6.748
JAN 20	165.710	157.266	3.645	83.678	1.430	7.548
JAN 21	116.939	131.493	4.977	189.739	3.280	-8.207
JAN 22	117.777	138.365	1.722	168.522	-1.065	4.246
JAN 23	90.270	170.509	3.574	329.959	-.443	19.728
JAN 24	67.285	124.467	2.512	229.995	3.416	21.430
JAN 25	71.689	144.438	.115	-21.910	-5.098	13.855
JAN 26	83.484	117.507	1.740	-60.362	1.353	8.156
JAN 27	204.803	160.097	-.008	82.185	-3.186	-4.116
JAN 28	235.913	145.015	.718	198.925	-.811	19.486
JAN 29	181.104	230.667	-4.293	444.070	-8.856	-24.377
JAN 30	29.753	173.036	-4.188	107.635	-.016	-12.474
JAN 31	-22.953	162.474	-2.027	104.781	1.237	-6.677
FEB 1	-100.513	122.494	1.716	-113.700	-3.595	.406
FEB 2	-66.958	120.794	.965	11.448	-3.253	-2.020
FEB 3	23.273	132.516	.552	-12.968	-1.236	-2.311
FEB 4	74.745	152.321	-1.073	-42.431	-2.895	-12.570
FEB 5	38.350	36.434	.459	44.057	-.100	-13.214
FEB 6	28.855	99.653	-.370	-40.222	-.348	-9.418
FEB 7	16.470	50.790	-.408	-105.629	-.159	-6.162
FEB 8	-17.003	46.973	.442	-88.800	-.119	-2.670
FEB 9	11.227	-53.518	.306	-107.637	1.398	-4.639
FEB 10	4.201	-33.342	-.030	150.895	-1.194	-4.336
FEB 11	12.379	-47.187	.546	30.130	.123	-8.788
FEB 12	11.268	-8.317	-.429	-99.342	.277	-6.833
FEB 13	3.327	25.462	-.374	-215.661	2.825	-8.898
FEB 14	-9.832	48.118	-.056	-319.981	2.753	-3.796
FEB 15	-6.850	55.499	-.053	-294.356	2.804	-3.060
FEB 16	-6.089	40.868	.020	-247.002	2.070	-4.009
FEB 17	-7.503	51.462	.329	-171.226	1.552	-.830
FEB 18	5.464	20.553	.016	-37.828	-.372	-7.272
FEB 19	9.616	24.761	-.153	-84.894	.585	-10.801

LEVEL 50 MB. LATITUDE 70 EDDY CORRELATION COEFFICIENTS

DAY	TU	TV	TW	UV	UW	VW
JAN 10	.424	-.025	-.071	-.309	-.057	.437
JAN 11	.537	.058	.128	-.357	.354	.019
JAN 12	-.208	-.086	.288	-.054	.074	.570
JAN 13	.403	.017	-.009	.035	.359	.774
JAN 14	.627	.108	.622	.120	.379	.231
JAN 15	.455	.016	.597	.234	.409	.198
JAN 16	.548	.237	.221	-.059	.768	.095
JAN 17	.321	.440	.083	-.242	.056	-.331
JAN 18	.803	.379	.026	.122	.174	-.698
JAN 19	.835	.394	.403	.214	.574	-.275
JAN 20	.659	.313	.375	.113	.100	.264
JAN 21	.692	.343	.489	.361	.271	-.260
JAN 22	.559	.370	.320	.272	-.119	.268
JAN 23	.352	.402	.532	.341	-.029	.867
JAN 24	.266	.307	.369	.250	.221	.867
JAN 25	.246	.352	.020	-.021	-.355	.685
JAN 26	.305	.266	.425	-.063	.151	.565
JAN 27	.701	.398	-.002	.075	-.325	-.305
JAN 28	.840	.355	.097	.152	-.034	.566
JAN 29	.845	.508	-.667	.398	-.560	-.728
JAN 30	.160	.388	-.678	.142	-.001	-.493
JAN 31	-.105	.335	-.397	.155	.174	-.422
FEB 1	-.513	.245	.265	-.189	-.462	.020
FEB 2	-.444	.299	.214	.025	-.646	-.150
FEB 3	.218	.358	.219	-.033	-.459	-.248
FEB 4	.429	.431	-.237	-.061	-.327	-.699
FEB 5	.378	.123	.122	.091	-.016	-.734
FEB 6	.416	.581	-.164	-.105	-.069	-.751
FEB 7	.337	.395	-.253	-.367	-.044	-.648
FEB 8	-.438	.409	.422	-.275	-.040	-.307
FEB 9	.476	-.714	.499	-.447	.708	-.740
FEB 10	.109	-.326	-.040	.536	-.565	-.771
FEB 11	.528	-.462	.420	.129	.041	-.678
FEB 12	.366	-.106	-.301	-.447	.069	-.665
FEB 13	.071	.199	-.168	-.782	.589	-.682
FEB 14	-.132	.362	-.043	-.879	.779	-.600
FEB 15	-.090	.455	-.041	-.830	.736	-.503
FEB 16	-.105	.363	.017	-.831	.660	-.658
FEB 17	-.135	.548	.341	-.682	.601	-.191
FEB 18	.162	.276	.014	-.125	-.081	-.713
FEB 19	.199	.286	-.086	-.266	.089	-.920

LEVEL 50 MB. LATITUDE 70 PRODUCT OF (U,V,W,T) BAR

DAY	TU	TV	TW	UV	UW
JAN 10	.424	-.025	-.071	-.309	-.057
JAN 11	.537	.058	.128	-.357	.354
JAN 12	-.208	-.086	.288	-.054	.074
JAN 13	.403	.017	-.009	.035	.359
JAN 14	.627	.108	.622	.120	.379
JAN 15	.455	.016	.597	.234	.409
JAN 16	.548	.237	.221	-.059	.768
JAN 17	.321	.440	.083	-.242	.056
JAN 18	.803	.379	.026	.122	.174
JAN 19	.835	.394	.403	.214	.574
JAN 20	.659	.313	.375	.113	.100
JAN 21	.692	.343	.489	.361	.271
JAN 22	.559	.370	.320	.272	-.119
JAN 23	.352	.402	.532	.341	-.029
JAN 24	.266	.307	.369	.250	.221
JAN 25	.246	.352	.020	-.021	-.355
JAN 26	.305	.266	.425	-.063	.151
JAN 27	.701	.398	-.002	.075	-.325
JAN 28	.840	.355	.097	.152	-.034
JAN 29	.845	.508	-.667	.398	-.560
JAN 30	.160	.388	-.678	.142	-.001
JAN 31	-.105	.335	-.397	.155	.174
FEB 1	-.513	.245	.265	-.189	-.462
FEB 2	-.444	.299	.214	.025	-.646
FEB 3	.218	.358	.219	-.033	-.459
FEB 4	.429	.431	-.237	-.061	-.327
FEB 5	.378	.123	.122	.091	-.016
FEB 6	.416	.581	-.164	-.105	-.069
FEB 7	.337	.395	-.253	-.367	-.044
FEB 8	-.438	.409	.422	-.275	-.040
FEB 9	.476	-.714	.499	-.447	.708
FEB 10	.109	-.326	-.040	.536	-.565
FEB 11	.528	-.462	.420	.129	.041
FEB 12	.366	-.106	-.301	-.447	.069
FEB 13	.071	.199	-.168	-.782	.589
FEB 14	-.132	.362	-.043	-.879	.779
FEB 15	-.090	.455	-.041	-.830	.736
FEB 16	-.105	.363	.017	-.831	.660
FEB 17	-.135	.548	.341	-.682	.601
FEB 18	.162	.276	.014	-.125	-.081
FEB 19	.199	.286	-.086	-.266	.089

LEVEL 50 MB. LATITUDE 70 MEANS OF T,U,V,AND W

DAY	TBAR	UBAR	VBAR	WBAR
JAN 10	-71.000	43.329	3.282	.034
JAN 11	-69.278	39.002	.608	-.101
JAN 12	-70.333	32.813	-.676	-.062
JAN 13	-69.667	44.559	.447	.067
JAN 14	-70.444	52.391	-.650	.143
JAN 15	-70.333	55.834	.018	-.071
JAN 16	-69.278	60.028	-.174	.024
JAN 17	-68.278	61.474	-1.366	-.241
JAN 18	-66.278	50.192	-.179	.135
JAN 19	-66.333	42.310	-2.078	.184
JAN 20	-66.111	33.957	-.053	.239
JAN 21	-66.000	44.133	-1.257	.134
JAN 22	-66.111	38.307	-.592	-.101
JAN 23	-66.167	27.343	-1.458	-.048
JAN 24	-65.944	25.091	-.275	.046
JAN 25	-63.944	8.987	-1.035	.015
JAN 26	-63.556	.277	-.789	.028
JAN 27	-60.111	-23.631	-.260	-.128
JAN 28	-57.444	-23.424	.427	.067
JAN 29	-56.000	-10.856	.229	.351
JAN 30	-56.444	-10.784	-2.963	.340
JAN 31	-56.500	-3.222	-2.318	-.095
FEB 1	-52.833	-1.752	2.156	.052
FEB 2	-52.667	3.817	-1.813	-.086
FEB 3	-53.278	-6.826	-1.237	.159
FEB 4	-53.944	-6.164	-.088	.135
FEB 5	-54.111	.452	-6.085	-.113
FEB 6	-51.778	-4.326	2.108	-.025
FEB 7	-52.889	-5.459	3.709	-.037
FEB 8	-51.056	-4.343	.801	-.280
FEB 9	-48.333	-11.327	-.974	-.169
FEB 10	-49.944	-6.891	.331	.013
FEB 11	-50.444	2.421	-.252	-.236
FEB 12	-50.389	6.734	-.875	-.055
FEB 13	-51.500	12.821	-.073	.019
FEB 14	-51.389	11.188	-.013	.009
FEB 15	-51.722	10.150	.297	.095
FEB 16	-52.611	6.440	.687	.104
FEB 17	-52.722	2.814	.698	-.040
FEB 18	-52.278	2.162	-1.071	.046
FEB 19	-52.556	1.100	-.903	-.027

LEVEL 100 MB. LATITUDE 50 COVARIANCE

DAY	TU	TV	TW	UV	UW	VW
JAN 10	-60.293	46.001	.885	-173.850	5.027	-.123
JAN 11	-79.496	35.106	-.323	-53.868	4.758	1.072
JAN 12	-51.363	38.134	.607	-25.356	.351	-1.934
JAN 13	-37.904	27.114	.094	-45.561	-2.786	-.975
JAN 14	-6.424	22.507	-.125	-6.566	-.402	-.382
JAN 15	-13.119	17.446	-.207	13.868	-5.660	.244
JAN 16	3.616	33.612	.094	54.317	.100	-.468
JAN 17	-26.680	35.733	-1.112	3.998	.647	-2.017
JAN 18	-107.503	44.820	-.434	-185.280	1.503	-.256
JAN 19	-138.322	43.355	1.847	-149.325	-7.970	1.630
JAN 20	-165.707	54.719	1.649	-117.787	-16.970	4.320
JAN 21	-100.421	30.258	1.893	110.128	-12.409	-5.313
JAN 22	-77.972	53.648	.987	-63.212	-2.195	-9.402
JAN 23	-73.143	86.381	.752	-.061	-.521	-8.141
JAN 24	-74.685	76.928	.786	-70.398	-4.569	-13.460
JAN 25	-87.358	75.872	1.769	-96.428	-6.981	-12.362
JAN 26	-25.271	17.269	-2.920	48.774	-9.369	-10.746
JAN 27	-20.582	17.121	-.915	28.756	-6.788	-6.989
JAN 28	-17.054	-1.068	-1.005	249.655	-2.964	4.795
JAN 29	53.310	-7.907	-.730	106.665	-2.819	-2.198
JAN 30	43.918	-10.610	.567	94.754	-1.746	2.772
JAN 31	46.964	-18.657	.475	88.110	6.146	4.724
FEB 1	63.999	-33.134	-.455	-62.075	2.494	4.243
FEB 2	53.088	-41.845	.004	-16.160	6.442	3.139
FEB 3	53.630	-66.068	-.507	-10.895	3.449	5.341
FEB 4	118.038	-70.954	-.053	-52.168	4.670	6.113
FEB 5	122.708	-68.515	-.497	-161.123	-.675	5.959
FEB 6	143.961	-64.328	-.435	-173.636	-2.167	8.512
FEB 7	116.019	-33.011	.178	-138.379	-1.632	3.307
FEB 8	105.132	-16.650	.551	-47.223	.329	1.218
FEB 9	77.311	-17.727	.105	-57.091	1.253	1.533
FEB 10	64.895	-11.323	-.238	8.030	-.321	1.284
FEB 11	78.496	-12.367	.526	-10.718	1.435	.880
FEB 12	74.663	-13.448	.130	9.472	.009	-.631
FEB 13	68.512	2.408	.145	12.747	1.503	.693
FEB 14	56.118	-13.034	-.375	-37.902	.474	.918
FEB 15	43.501	-31.551	-.509	-42.448	1.639	2.019
FEB 16	35.402	-37.447	-.245	-46.366	1.552	.654
FEB 17	33.280	-35.183	.048	-81.806	1.946	1.784
FEB 18	38.675	-21.149	-.023	-97.940	.962	.679
FEB 19	31.959	-9.782	-.289	6.427	1.615	-.689

LEVEL 100 MB. LATITUDE 50 EDDY CORRELATION COEFFICIENTS

DAY	TU	TV	TW	UV	UW	VW
JAN 10	-.457	.387	.209	-.414	.336	-.009
JAN 11	-.721	.277	-.068	-.155	.365	.072
JAN 12	-.540	.311	.162	-.077	.035	-.151
JAN 13	-.394	.270	.032	-.144	-.302	-.101
JAN 14	-.056	.238	-.072	-.018	-.062	-.071
JAN 15	-.097	.141	-.055	.030	-.408	.019
JAN 16	.037	.292	.037	.190	.016	-.063
JAN 17	-.469	.392	-.425	.029	.164	-.318
JAN 18	-.723	.438	-.211	-.505	.204	-.050
JAN 19	-.718	.395	.354	-.295	-.333	.119
JAN 20	-.648	.382	.217	-.189	-.514	.233
JAN 21	-.587	.192	.292	.218	-.598	-.277
JAN 22	-.499	.302	.096	-.129	-.130	-.491
JAN 23	-.537	.418	.146	-.000	-.046	-.474
JAN 24	-.534	.482	.115	-.152	-.230	-.594
JAN 25	-.513	.410	.165	-.129	-.275	-.448
JAN 26	-.157	.116	-.393	.087	-.335	-.416
JAN 27	-.124	.106	-.168	.049	-.348	-.366
JAN 28	-.094	-.006	-.148	.400	-.116	.205
JAN 29	.284	-.053	-.168	.235	-.214	-.210
JAN 30	.356	-.073	.131	.295	-.182	.246
JAN 31	.437	-.150	.118	.239	.517	.343
FEB 1	.600	-.239	-.101	-.201	.246	.323
FEB 2	.405	-.316	.001	-.052	.578	.279
FEB 3	.376	-.524	-.106	-.033	.274	.479
FEB 4	.685	-.538	-.010	-.136	.301	.515
FEB 5	.716	-.483	-.111	-.328	-.044	.464
FEB 6	.792	-.430	-.097	-.356	-.148	.708
FEB 7	.776	-.371	.059	-.392	-.137	.466
FEB 8	.870	-.242	.307	-.180	.048	.312
FEB 9	.901	-.273	.083	-.134	.151	.245
FEB 10	.798	-.163	-.236	.021	-.059	.274
FEB 11	.586	-.144	.287	-.026	.164	.156
FEB 12	.802	-.177	.078	.027	.001	-.100
FEB 13	.755	.034	.116	.040	.264	.157
FEB 14	.715	-.193	-.256	-.157	.091	.204
FEB 15	.487	-.441	-.308	-.193	.322	.495
FEB 16	.392	-.548	-.189	-.210	.373	.207
FEB 17	.491	-.448	.032	-.308	.388	.307
FEB 18	.592	-.325	-.024	-.340	.230	.163
FEB 19	.501	-.170	-.238	.020	.237	-.112

LEVEL 100 MB. LATITUDE 50 PRODUCT OF (U,V,W,T) BAR

DAY	TU	TV	TW	UV	UW	VW
JAN 10	-.457	.387	.209	-.414	.336	-.009
JAN 11	-.721	.277	-.068	-.155	.365	.072
JAN 12	-.540	.311	.162	-.077	.035	-.151
JAN 13	-.394	.270	.032	-.144	-.302	-.101
JAN 14	-.056	.238	-.072	-.018	-.062	-.071
JAN 15	-.097	.141	-.055	.030	-.408	.019
JAN 16	.037	.292	.037	.190	.016	-.063
JAN 17	-.469	.392	-.425	.029	.164	-.318
JAN 18	-.723	.438	-.211	-.505	.204	-.050
JAN 19	-.718	.395	.354	-.295	-.333	.119
JAN 20	-.648	.382	.217	-.189	-.514	.233
JAN 21	-.587	.192	.292	.218	-.598	-.277
JAN 22	-.499	.302	.096	-.129	-.130	-.491
JAN 23	-.537	.418	.146	-.000	-.046	-.474
JAN 24	-.534	.482	.115	-.152	-.230	-.594
JAN 25	-.513	.410	.165	-.129	-.275	-.448
JAN 26	-.157	.116	-.393	.087	-.335	-.416
JAN 27	-.124	.106	-.168	.049	-.348	-.366
JAN 28	-.094	-.006	-.148	.400	-.116	.205
JAN 29	.284	-.053	-.168	.235	-.214	-.210
JAN 30	.356	-.073	.131	.295	-.182	.246
JAN 31	.437	-.150	.118	.239	.517	.343
FEB 1	.600	-.239	-.101	-.201	.246	.323
FEB 2	.405	-.316	.001	-.052	.578	.279
FEB 3	.376	-.524	-.106	-.033	.274	.479
FEB 4	.685	-.538	-.010	-.136	.301	.515
FEB 5	.716	-.483	-.111	-.328	-.044	.464
FEB 6	.792	-.430	-.097	-.356	-.148	.708
FEB 7	.776	-.371	.059	-.392	-.137	.466
FEB 8	.870	-.242	.307	-.180	.048	.312
FEB 9	.901	-.273	.083	-.134	.151	.245
FEB 10	.798	-.163	-.236	.021	-.059	.274
FEB 11	.586	-.144	.287	-.026	.164	.156
FEB 12	.802	-.177	.078	.027	.001	-.100
FEB 13	.755	.034	.116	.040	.264	.157
FEB 14	.715	-.193	-.256	-.157	.091	.204
FEB 15	.487	-.441	-.308	-.193	.322	.495
FEB 16	.392	-.548	-.189	-.210	.373	.207
FEB 17	.491	-.448	.032	-.308	.388	.307
FEB 18	.592	-.325	-.024	-.340	.230	.163
FEB 19	.501	-.170	-.238	.020	.237	-.112

LEVEL 100 MB. LATITUDE 50 MEANS OF T,U,V,AND W

DAY	TBAR	UBAR	VBAR	WBAR
JAN 10	-55.250	50.215	.784	-.102
JAN 11	-54.556	43.704	-1.081	-.010
JAN 12	-54.861	40.279	-.472	-.053
JAN 13	-55.944	38.591	.425	-.236
JAN 14	-55.556	35.497	1.277	-.291
JAN 15	-55.667	35.239	.229	-.334
JAN 16	-55.194	27.036	-.196	-.057
JAN 17	-56.000	30.723	.216	-.144
JAN 18	-56.056	35.362	.387	-.108
JAN 19	-55.083	41.215	-.427	-.342
JAN 20	-56.194	40.331	-.656	-.292
JAN 21	-56.417	35.987	-.122	-.301
JAN 22	-56.028	34.955	-1.261	-.204
JAN 23	-55.500	32.223	-.309	-.282
JAN 24	-55.444	34.227	.497	-.384
JAN 25	-53.917	36.923	-1.591	-.315
JAN 26	-55.278	35.355	.356	-.184
JAN 27	-56.000	38.954	-.207	-.160
JAN 28	-57.389	34.456	1.088	.040
JAN 29	-57.917	35.240	.175	-.401
JAN 30	-56.500	28.952	-.435	-.246
JAN 31	-55.611	29.401	.628	.008
FEB 1	-56.333	24.273	1.353	-.042
FEB 2	-56.806	25.530	-.137	.031
FEB 3	-57.167	22.068	-.128	-.039
FEB 4	-57.139	23.665	.077	-.037
FEB 5	-56.861	22.712	1.360	-.187
FEB 6	-56.194	22.423	1.240	-.187
FEB 7	-55.389	20.287	-.320	-.210
FEB 8	-55.361	24.602	.241	-.080
FEB 9	-55.444	23.215	.329	-.210
FEB 10	-54.500	20.211	.770	-.097
FEB 11	-54.222	22.420	.174	-.062
FEB 12	-54.111	23.093	-.721	-.141
FEB 13	-54.944	24.292	.200	-.035
FEB 14	-54.583	25.931	-.541	-.126
FEB 15	-54.194	26.980	.774	-.100
FEB 16	-54.667	24.275	.023	-.064
FEB 17	-55.139	20.483	.005	-.125
FEB 18	-54.528	19.292	-.406	-.172
FEB 19	-54.028	22.974	-.287	-.119

LEVEL 100 MB. LATITUDE 60 COVARIANCE

DAY	TU	TV	TW	UV	UW	VW
JAN 10	-75.403	50.317	1.429	-63.606	5.502	7.514
JAN 11	-32.108	10.401	1.126	-73.973	-.363	2.571
JAN 12	-43.692	32.593	.772	-63.951	4.307	9.265
JAN 13	-27.601	45.942	1.761	35.290	2.517	5.455
JAN 14	-18.336	55.482	1.995	119.577	3.319	5.548
JAN 15	-23.997	45.675	2.208	212.815	1.389	9.112
JAN 16	-36.314	30.530	.284	166.858	3.191	4.047
JAN 17	-134.849	94.706	-.481	-114.509	1.992	2.746
JAN 18	-149.588	67.067	.817	-227.163	-5.381	6.050
JAN 19	-107.600	104.865	.936	-56.351	-2.404	5.783
JAN 20	-125.225	87.007	1.938	-70.178	-3.073	8.061
JAN 21	-111.464	78.457	2.175	177.220	-4.491	12.734
JAN 22	-131.814	88.899	1.834	-30.067	-3.199	8.947
JAN 23	-76.153	129.039	1.108	261.074	12.337	16.478
JAN 24	-70.424	96.972	.816	-73.886	.614	10.502
JAN 25	-131.278	134.737	2.116	-178.434	-2.212	7.752
JAN 26	-111.498	131.244	.583	-236.427	1.121	6.597
JAN 27	-141.304	120.824	.259	-122.198	.624	-.917
JAN 28	-47.680	172.270	.326	-40.878	-2.949	-3.962
JAN 29	-63.335	139.996	1.737	233.486	-6.617	-2.564
JAN 30	-71.146	136.992	.384	-29.573	4.106	2.130
JAN 31	-109.114	-10.587	.440	95.720	5.715	-.587
FEB 1	-123.243	109.023	-.423	-80.189	5.119	-2.634
FEB 2	-161.870	82.554	-1.217	-127.331	5.910	-1.899
FEB 3	-144.434	115.338	-.247	-99.455	.537	-3.237
FEB 4	-111.182	80.197	.888	-179.241	.451	-2.863
FEB 5	-89.126	66.016	.653	-121.162	.755	-3.729
FEB 6	-81.092	46.409	.375	-137.920	.470	-3.058
FEB 7	-84.389	22.733	-.268	-139.544	2.733	-3.446
FEB 8	-103.496	-2.331	.037	-128.224	2.067	-2.642
FEB 9	-106.849	1.200	.211	-133.143	-.323	-1.339
FEB 10	-82.553	8.065	-.104	59.342	.440	-.890
FEB 11	-108.730	13.931	-.687	-65.310	2.611	-3.742
FEB 12	-98.761	12.612	-.178	-47.967	.815	-.530
FEB 13	-87.039	20.114	.160	-119.870	-.222	-.348
FEB 14	-96.891	31.708	.334	-137.728	-1.227	.992
FEB 15	-53.921	20.490	-.042	-141.201	.827	-.037
FEB 16	-71.237	30.384	.043	-240.438	1.600	-1.692
FEB 17	-39.554	22.527	.265	-207.694	.761	-.705
FEB 18	-44.097	37.784	-.052	-95.269	1.055	-.641
FEB 19	-47.247	51.566	-.053	-104.055	.135	-.780

LEVEL 100 MB. LATITUDE 60 EDDY CORRELATION COEFFICIENTS

DAY	TU	TV	TW	UV	UW	VW
JAN 10	-.403	.350	.368	-.105	.336	.599
JAN 11	-.216	.083	.452	-.159	-.039	.329
JAN 12	-.285	.238	.197	-.124	.292	.703
JAN 13	-.235	.329	.590	.097	.322	.588
JAN 14	-.134	.299	.591	.209	.319	.394
JAN 15	-.183	.283	.588	.409	.115	.613
JAN 16	-.267	.214	.075	.355	.254	.307
JAN 17	-.711	.405	-.094	-.279	.129	.249
JAN 18	-.642	.353	.171	-.422	-.396	.547
JAN 19	-.663	.427	.193	-.154	-.333	.529
JAN 20	-.675	.312	.353	-.167	-.373	.650
JAN 21	-.369	.281	.241	.259	-.203	.622
JAN 22	-.432	.314	.368	-.038	-.227	.685
JAN 23	-.287	.389	.128	.297	.536	.572
JAN 24	-.327	.305	.157	-.119	.061	.702
JAN 25	-.628	.439	.362	-.292	-.190	.453
JAN 26	-.527	.440	.107	-.402	.104	.434
JAN 27	-.663	.369	.102	-.195	.129	-.124
JAN 28	-.393	.516	.077	-.110	-.624	-.304
JAN 29	-.367	.450	.266	.401	-.543	-.117
JAN 30	-.432	.510	.057	-.057	.317	.101
JAN 31	-.508	-.041	.059	.193	.395	-.034
FEB 1	-.555	.421	-.054	-.178	.376	-.166
FEB 2	-.792	.341	-.159	-.339	.497	-.135
FEB 3	-.799	.422	-.067	-.258	.103	-.410
FEB 4	-.719	.332	.244	-.488	.082	-.331
FEB 5	-.794	.321	.166	-.318	.104	-.278
FEB 6	-.784	.263	.171	-.357	.098	-.373
FEB 7	-.763	.167	-.132	-.317	.416	-.426
FEB 8	-.798	-.020	.017	-.332	.284	-.407
FEB 9	-.755	.009	.165	-.276	-.068	-.308
FEB 10	-.702	.076	-.094	.164	.117	-.263
FEB 11	-.834	.115	-.408	-.163	.467	-.720
FEB 12	-.731	.125	-.145	-.141	.196	-.171
FEB 13	-.746	.212	.110	-.393	-.048	-.092
FEB 14	-.648	.425	.324	-.753	-.485	.461
FEB 15	-.593	.273	-.035	-.659	.242	-.013
FEB 16	-.672	.344	.031	-.850	.357	-.453
FEB 17	-.490	.297	.274	-.736	.211	-.208
FEB 18	-.608	.464	-.059	-.323	.334	-.181
FEB 19	-.606	.530	-.056	-.313	.042	-.194

LEVEL 100 MB. LATITUDE 60 PRODUCT OF (U,V,W,T) BAR

DAY	TU	TV	TW	UV	UW	VW
JAN 10	-.403	.350	.368	-.105	.336	.599
JAN 11	-.216	.083	.452	-.159	-.039	.329
JAN 12	-.285	.238	.197	-.124	.292	.703
JAN 13	-.235	.329	.590	.097	.322	.588
JAN 14	-.134	.299	.591	.209	.319	.394
JAN 15	-.183	.283	.588	.409	.115	.613
JAN 16	-.267	.214	.075	.355	.254	.307
JAN 17	-.711	.405	-.094	-.279	.129	.249
JAN 18	-.642	.353	.171	-.422	-.396	.547
JAN 19	-.663	.427	.193	-.154	-.333	.529
JAN 20	-.675	.312	.353	-.167	-.373	.650
JAN 21	-.369	.281	.241	.259	-.203	.622
JAN 22	-.432	.314	.368	-.038	-.227	.685
JAN 23	-.287	.389	.128	.297	.536	.572
JAN 24	-.327	.305	.157	-.119	.061	.702
JAN 25	-.628	.439	.362	-.292	-.190	.453
JAN 26	-.527	.440	.107	-.402	.104	.434
JAN 27	-.663	.369	.102	-.195	.129	-.124
JAN 28	-.393	.516	.077	-.110	-.624	-.304
JAN 29	-.367	.450	.266	.401	-.543	-.117
JAN 30	-.432	.510	.057	-.057	.317	.101
JAN 31	-.508	-.041	.059	.193	.395	-.034
FEB 1	-.555	.421	-.054	-.178	.376	-.166
FEB 2	-.792	.341	-.159	-.339	.497	-.135
FEB 3	-.799	.422	-.067	-.258	.103	-.410
FEB 4	-.719	.332	.244	-.488	.082	-.331
FEB 5	-.794	.321	.166	-.318	.104	-.278
FEB 6	-.784	.263	.171	-.357	.098	-.373
FEB 7	-.763	.167	-.132	-.317	.416	-.426
FEB 8	-.798	-.020	.017	-.332	.284	-.407
FEB 9	-.755	.009	.165	-.276	-.068	-.308
FEB 10	-.702	.076	-.094	.164	.117	-.263
FEB 11	-.834	.115	-.408	-.163	.467	-.720
FEB 12	-.731	.125	-.145	-.141	.196	-.171
FEB 13	-.746	.212	.110	-.393	-.048	-.092
FEB 14	-.648	.425	.324	-.753	-.485	.461
FEB 15	-.593	.273	-.035	-.659	.242	-.013
FEB 16	-.672	.344	.031	-.850	.357	-.453
FEB 17	-.490	.297	.274	-.736	.211	-.208
FEB 18	-.608	.464	-.059	-.323	.334	-.181
FEB 19	-.606	.530	-.056	-.313	.042	-.194

LEVEL 100 MB. LATITUDE 60 MEANS OF T,U,V,AND W

DAY	TBAR	UBAR	VBAR	WBAR
JAN 10	-58.778	46.289	1.520	.137
JAN 11	-59.694	46.781	.288	.134
JAN 12	-60.556	45.668	2.409	.113
JAN 13	-60.583	38.382	-.198	.004
JAN 14	-60.639	38.874	-1.212	-.207
JAN 15	-59.083	40.581	-.968	-.258
JAN 16	-59.056	47.038	-1.697	-.143
JAN 17	-59.389	49.793	.737	-.070
JAN 18	-59.111	47.045	.662	-.165
JAN 19	-58.750	33.113	-1.147	-.125
JAN 20	-60.222	24.447	1.003	.020
JAN 21	-60.556	29.585	-.289	-.318
JAN 22	-60.028	34.560	-.237	-.316
JAN 23	-59.917	30.211	-.990	-.131
JAN 24	-59.389	22.641	-1.031	-.117
JAN 25	-59.167	22.172	.546	-.023
JAN 26	-60.056	15.707	.719	-.045
JAN 27	-61.028	19.779	-1.439	-.120
JAN 28	-59.000	13.812	.239	-.114
JAN 29	-57.667	23.255	-.417	-.357
JAN 30	-57.361	26.830	.437	-.061
JAN 31	-56.806	25.049	-7.022	-.004
FEB 1	-57.361	17.430	-.403	.101
FEB 2	-57.806	19.315	-1.623	.075
FEB 3	-58.528	15.031	.039	-.069
FEB 4	-57.306	12.546	1.709	-.183
FEB 5	-56.056	9.783	-1.331	-.024
FEB 6	-55.417	11.780	.827	-.085
FEB 7	-54.833	3.907	2.194	-.078
FEB 8	-54.889	9.341	.011	-.025
FEB 9	-55.389	7.979	-.516	-.037
FEB 10	-55.250	12.793	-10.779	-.073
FEB 11	-54.389	9.525	-.172	-.025
FEB 12	-54.056	9.548	.193	-.033
FEB 13	-53.583	12.754	-.153	-.122
FEB 14	-53.389	10.776	-1.839	-.090
FEB 15	-53.500	13.142	.475	.023
FEB 16	-54.167	12.379	-.235	-.007
FEB 17	-53.889	10.094	1.219	-.053
FEB 18	-54.417	11.261	-.504	-.027
FEB 19	-54.389	10.315	-.098	-.150

LEVEL 100 MB. LATITUDE 70 COVARIANCE

DAY	TU	TV	TW	UV	UW	VW
JAN 10	43.717	1.287	.256	-242.074	-.100	2.737
JAN 11	29.676	-29.708	-.216	-125.841	-1.517	3.635
JAN 12	7.233	-24.901	.255	1.110	.919	1.934
JAN 13	18.956	16.480	.309	111.304	1.426	4.969
JAN 14	46.866	36.327	.538	122.391	1.680	4.720
JAN 15	17.785	7.491	.099	7.653	1.048	6.439
JAN 16	35.689	47.406	.520	135.734	3.411	3.741
JAN 17	45.176	16.085	.148	-1.102	2.335	-1.017
JAN 18	79.959	75.788	-.476	48.170	.437	-.847
JAN 19	64.021	122.618	-.234	85.372	3.374	-1.795
JAN 20	109.616	118.540	.012	95.375	1.537	-.792
JAN 21	71.806	109.481	1.844	123.865	2.038	.969
JAN 22	50.871	129.872	1.628	86.525	.537	2.376
JAN 23	29.009	130.913	1.322	137.522	.172	5.159
JAN 24	51.716	124.429	-.317	67.376	.490	1.542
JAN 25	-4.282	113.139	.514	-113.947	-.439	4.196
JAN 26	-5.256	110.567	1.306	-260.877	-1.561	3.522
JAN 27	139.490	112.072	.470	117.356	-1.730	.805
JAN 28	104.811	144.042	-1.583	37.933	-2.348	-11.511
JAN 29	149.748	103.209	-1.193	129.898	-1.475	-8.432
JAN 30	31.319	97.143	-.214	-122.446	.220	-1.086
JAN 31	-31.813	68.786	.296	-79.539	-.771	5.769
FEB 1	-94.702	56.334	-.372	-27.527	1.084	.748
FEB 2	-122.747	54.679	1.518	-54.514	-3.114	-1.134
FEB 3	-50.581	81.836	1.019	-119.972	-.855	-7.718
FEB 4	-4.578	80.278	-.877	3.753	-.154	-11.110
FEB 5	34.172	81.275	-1.414	89.672	-1.803	-12.198
FEB 6	-5.699	43.974	-.480	8.349	.500	-12.415
FEB 7	44.141	31.571	.346	36.756	.083	-5.064
FEB 8	-20.944	2.037	.768	-93.326	-.476	-3.140
FEB 9	-6.383	17.270	.531	-65.028	.846	-4.229
FEB 10	-28.875	-21.245	.377	37.161	-.411	-5.165
FEB 11	-3.435	-31.088	-.468	16.025	.258	-2.283
FEB 12	1.296	-28.459	-.508	-112.587	1.194	-4.202
FEB 13	-18.582	12.365	-.665	-210.817	1.413	-2.157
FEB 14	.662	-23.660	.759	-227.495	6.605	.072
FEB 15	17.567	6.613	1.020	-123.678	3.869	-1.789
FEB 16	3.811	16.331	.701	-218.644	2.898	-1.777
FEB 17	41.243	7.216	.443	-133.706	3.190	-1.621
FEB 18	28.258	21.860	-.389	-127.459	2.335	-3.989
FEB 19	30.492	42.263	-.053	-159.153	1.721	-3.131

LEVEL 100 MB. LATITUDE 70 EDDY CORRELATION COEFFICIENTS

DAY	TU	TV	TW	UV	UW	VW
JAN 10	.532	.013	.209	-.558	-.018	.424
JAN 11	.455	-.440	-.179	-.477	-.322	.745
JAN 12	.110	-.343	.263	.004	.228	.435
JAN 13	.416	.198	.321	.374	.413	.789
JAN 14	.685	.324	.446	.271	.346	.593
JAN 15	.234	.071	.063	.018	.161	.716
JAN 16	.549	.562	.395	.375	.604	.511
JAN 17	.596	.208	.066	-.004	.313	-.133
JAN 18	.769	.502	-.112	.173	.056	-.074
JAN 19	.926	.556	-.054	.275	.547	-.161
JAN 20	.650	.490	.005	.255	.383	-.137
JAN 21	.528	.487	.560	.455	.511	.147
JAN 22	.393	.525	.736	.284	.197	.456
JAN 23	.137	.476	.475	.222	.027	.635
JAN 24	.308	.429	-.141	.147	.138	.252
JAN 25	-.017	.378	.197	-.192	-.085	.697
JAN 26	-.022	.414	.422	-.493	-.254	.519
JAN 27	.814	.398	.117	.261	-.270	.076
JAN 28	.639	.406	-.436	.061	-.372	-.841
JAN 29	.789	.277	-.330	.184	-.214	-.625
JAN 30	.198	.263	-.072	-.259	.058	-.122
JAN 31	-.199	.216	.073	-.215	-.164	.617
FEB 1	-.558	.189	-.094	-.088	.260	.102
FEB 2	-.679	.188	.363	-.139	-.555	-.125
FEB 3	-.416	.315	.190	-.373	-.129	-.545
FEB 4	-.057	.336	-.223	.015	-.038	-.916
FEB 5	.308	.337	-.346	.228	-.270	-.841
FEB 6	-.069	.194	-.134	.026	.100	-.905
FEB 7	.558	.135	.175	.139	.037	-.766
FEB 8	-.302	.013	.510	-.320	-.173	-.495
FEB 9	-.163	.118	.352	-.384	.486	-.650
FEB 10	-.536	-.180	.338	.137	-.160	-.918
FEB 11	-.091	-.220	-.468	.105	.240	-.564
FEB 12	.025	-.234	-.295	-.710	.931	-.792
FEB 13	-.192	.083	-.295	-.778	.346	-.340
FEB 14	.004	-.166	.209	-.583	.664	.008
FEB 15	.214	.059	.336	-.645	.744	-.252
FEB 16	.040	.138	.354	-.814	.645	-.317
FEB 17	.501	.065	.276	-.475	.782	-.296
FEB 18	.334	.201	-.245	-.494	.619	-.824
FEB 19	.328	.314	-.032	-.572	.514	-.645

LEVEL 100 MB. LATITUDE 70 PRODUCT OF (U,V,W,T) BAR

DAY	TU	TV	TW	UV	UW	VW
JAN 10	.532	.013	.209	-.558	-.018	.424
JAN 11	.455	-.440	-.179	-.477	-.322	.745
JAN 12	.110	-.343	.263	.004	.228	.435
JAN 13	.416	.198	.321	.374	.413	.789
JAN 14	.685	.324	.446	.271	.346	.593
JAN 15	.234	.071	.063	.018	.161	.716
JAN 16	.549	.562	.395	.375	.604	.511
JAN 17	.596	.208	.066	-.004	.313	-.133
JAN 18	.769	.502	-.112	.173	.056	-.074
JAN 19	.526	.556	-.054	.275	.547	-.161
JAN 20	.650	.490	.005	.255	.383	-.137
JAN 21	.528	.487	.560	.455	.511	.147
JAN 22	.393	.525	.736	.284	.197	.456
JAN 23	.137	.476	.475	.222	.027	.635
JAN 24	.308	.429	-.141	.147	.138	.252
JAN 25	-.017	.378	.197	-.192	-.085	.697
JAN 26	-.022	.414	.422	-.493	-.254	.519
JAN 27	.814	.398	.117	.261	-.270	.076
JAN 28	.639	.406	-.436	.061	-.372	-.841
JAN 29	.789	.277	-.330	.184	-.214	-.625
JAN 30	.198	.263	-.072	-.259	.058	-.122
JAN 31	-.199	.216	.073	-.215	-.164	.617
FEB 1	-.558	.189	-.094	-.088	.260	.102
FEB 2	-.679	.188	.363	-.139	-.555	-.125
FEB 3	-.416	.315	.190	-.373	-.129	-.545
FEB 4	-.057	.336	-.223	.015	-.038	-.916
FEB 5	.308	.337	-.346	.228	-.270	-.841
FEB 6	-.069	.194	-.134	.026	.100	-.905
FEB 7	.558	.135	.175	.139	.037	-.766
FEB 8	-.302	.013	.510	-.320	-.173	-.495
FEB 9	-.163	.118	.352	-.384	.486	-.650
FEB 10	-.536	-.180	.338	.137	-.160	-.918
FEB 11	-.091	-.220	-.468	.105	.240	-.564
FEB 12	.025	-.234	-.295	-.710	.931	-.792
FEB 13	-.192	.083	-.295	-.778	.346	-.340
FEB 14	.004	-.166	.209	-.583	.664	.008
FEB 15	.214	.059	.336	-.645	.744	-.252
FEB 16	.040	.138	.354	-.814	.645	-.317
FEB 17	.501	.065	.276	-.475	.782	-.296
FEB 18	.334	.201	-.245	-.494	.619	-.824
FEB 19	.328	.314	-.032	-.572	.514	-.645

LEVEL 100 MB. LATITUDE 70 MEANS OF T,U,V,AND W

DAY	T8AR	UBAR	VBAR	WBAR
JAN 10	-65.833	20.944	-.559	.036
JAN 11	-67.444	24.253	1.896	.055
JAN 12	-68.167	23.842	-.825	-.048
JAN 13	-67.500	30.511	.475	-.125
JAN 14	-66.889	30.267	.589	-.131
JAN 15	-65.444	36.391	-1.793	-.119
JAN 16	-65.056	42.722	-1.165	.027
JAN 17	-66.667	38.966	-.672	.048
JAN 18	-65.556	30.272	.309	.053
JAN 19	-65.944	28.135	1.591	.150
JAN 20	-64.667	21.019	1.320	.048
JAN 21	-65.111	23.345	.073	-.013
JAN 22	-64.500	19.025	.843	-.111
JAN 23	-63.833	13.140	1.162	-.074
JAN 24	-62.611	5.417	-.696	-.186
JAN 25	-61.333	3.681	1.956	-.086
JAN 26	-59.611	-4.485	-.496	-.092
JAN 27	-58.278	-13.066	.138	-.186
JAN 28	-55.944	-7.182	-.056	.082
JAN 29	-56.833	-4.354	-.255	.186
JAN 30	-56.667	5.744	.040	.106
JAN 31	-56.333	2.874	.725	.062
FEB 1	-54.278	9.001	1.017	.003
FEB 2	-53.611	9.049	-1.034	-.097
FEB 3	-53.667	2.813	-.522	.126
FEB 4	-52.944	6.875	.749	-.056
FEB 5	-53.722	9.087	-.606	-.120
FEB 6	-53.333	11.517	-2.102	.037
FEB 7	-53.722	1.935	1.390	-.155
FEB 8	-52.444	4.574	.159	-.131
FEB 9	-52.778	-1.971	-1.124	-.068
FEB 10	-52.722	5.193	-1.666	-.015
FEB 11	-52.333	6.791	-1.831	-.027
FEB 12	-52.333	9.576	-1.187	-.021
FEB 13	-52.722	14.024	1.532	.042
FEB 14	-52.667	15.845	-.158	.149
FEB 15	-52.167	14.714	-.846	.046
FEB 16	-52.722	12.313	.640	.053
FEB 17	-53.000	3.483	-.179	.007
FEB 18	-53.056	5.442	.890	.006
FEB 19	-53.056	5.166	.726	-.039

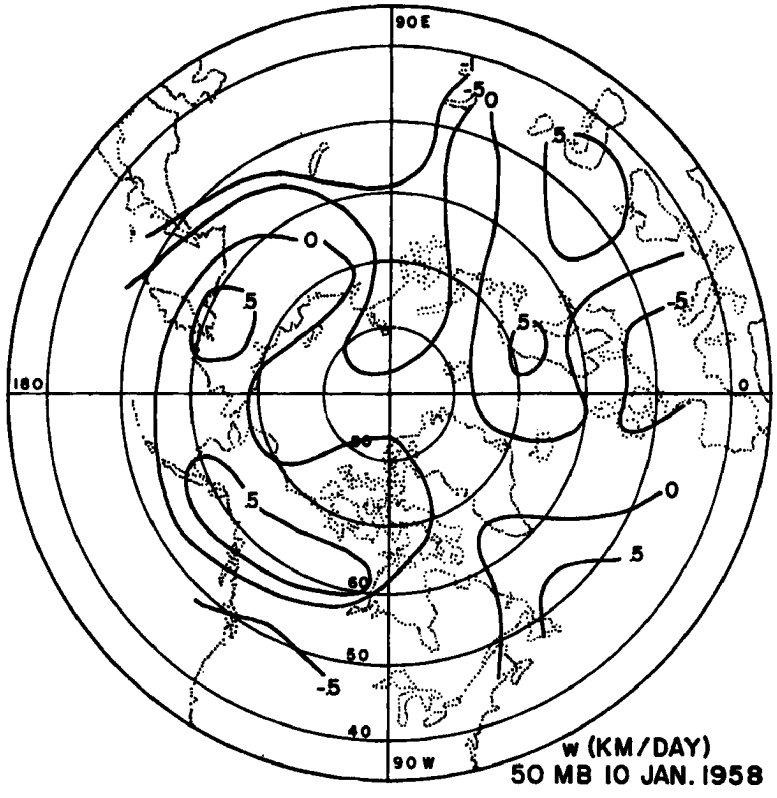

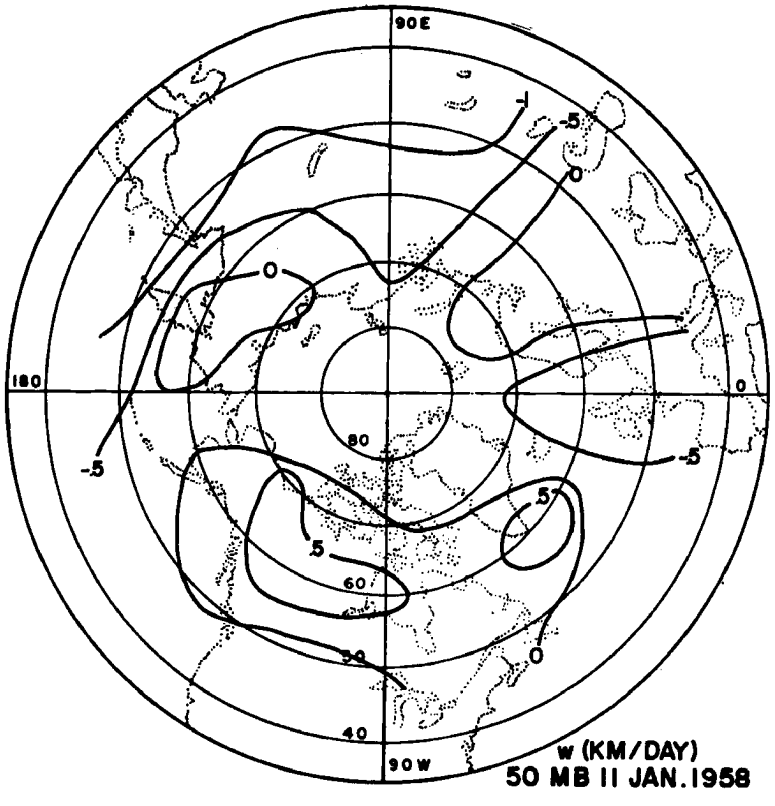

APPENDIX B. Daily vertical motion (km/day) at 50 mb for indicated dates for period before, during, and after the sudden warming of January 1958.

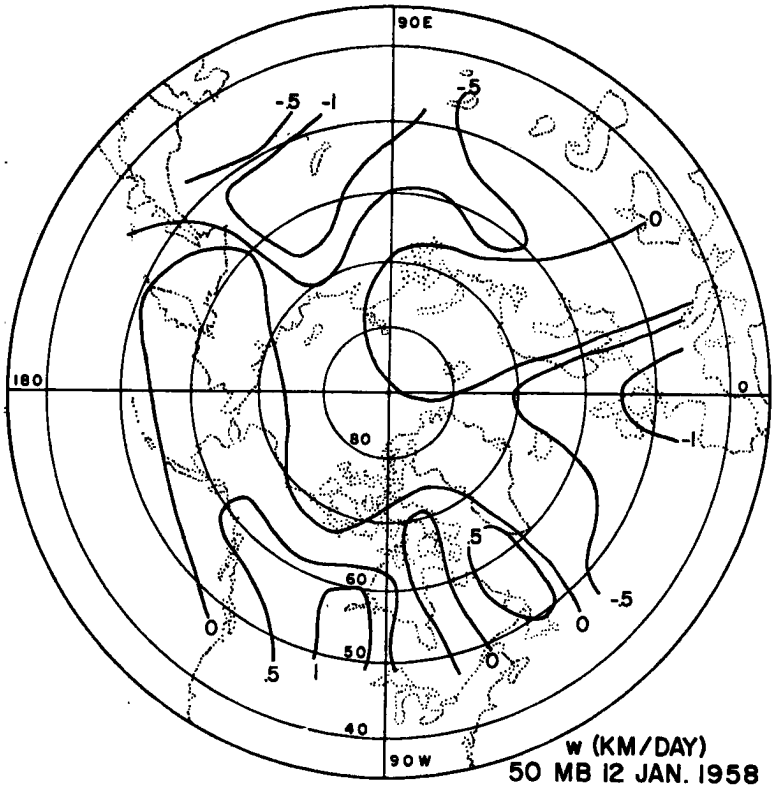
90E
180
0
80
60
50
40
90W
-5
-1
-.5
0
.5
1
w (KM/DAY)
50 MB 12 JAN. 1958

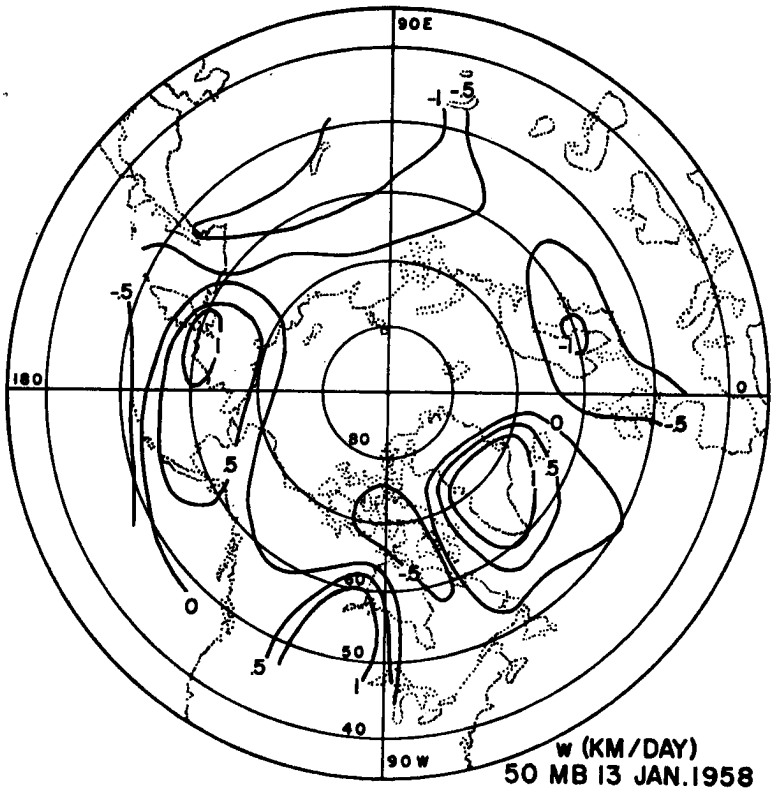
90E
180
0
80
60
50
40
90W
-1
-.5
-5
0
.5
1
w (KM/DAY)
50 MB 13 JAN. 1958

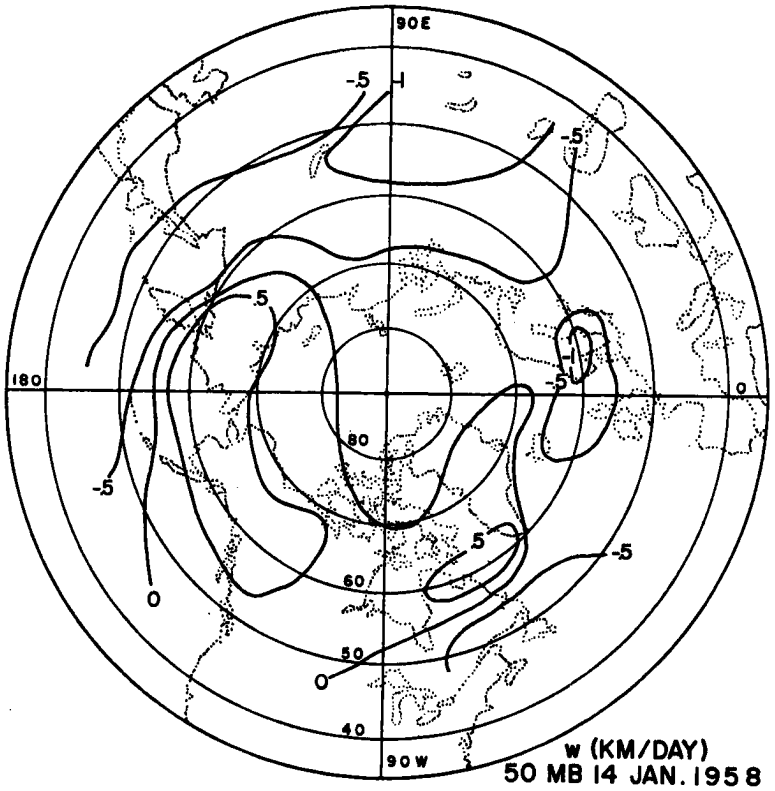

W (KM/DAY)
50 MB 14 JAN. 1958

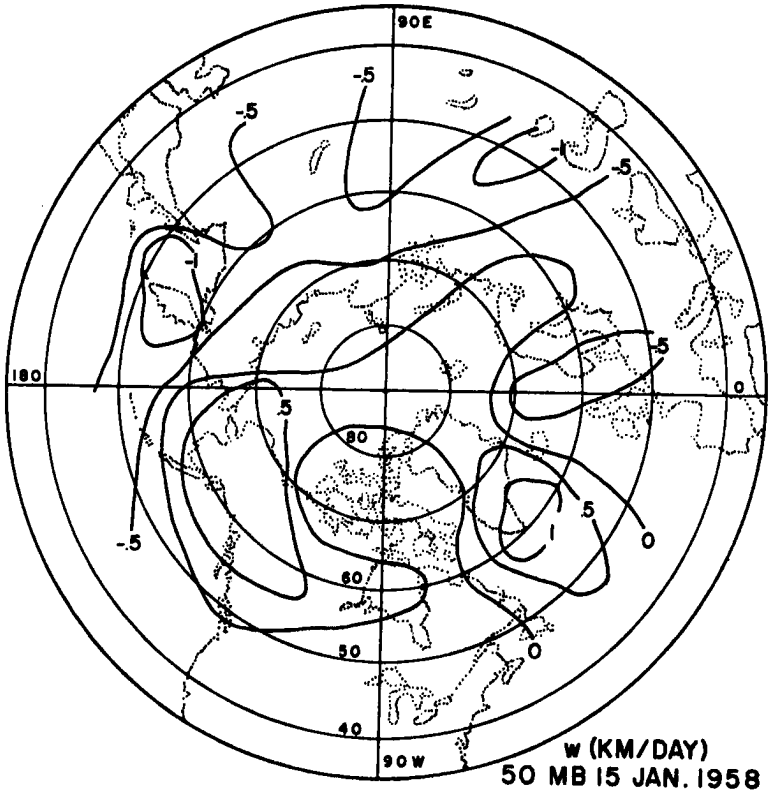

W (KM/DAY)
50 MB 15 JAN. 1958

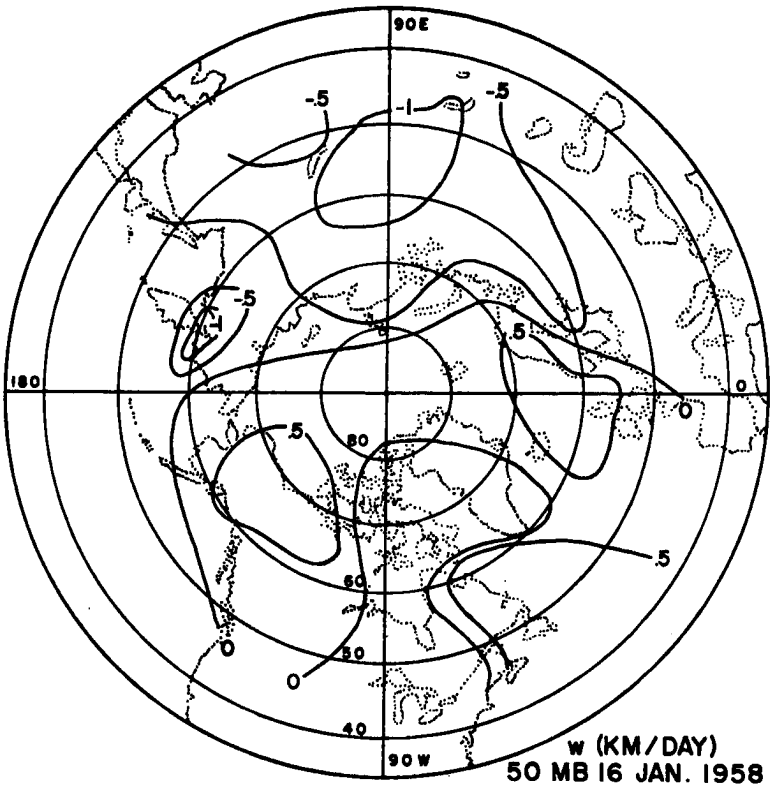

w (KM/DAY)
50 MB 16 JAN. 1958

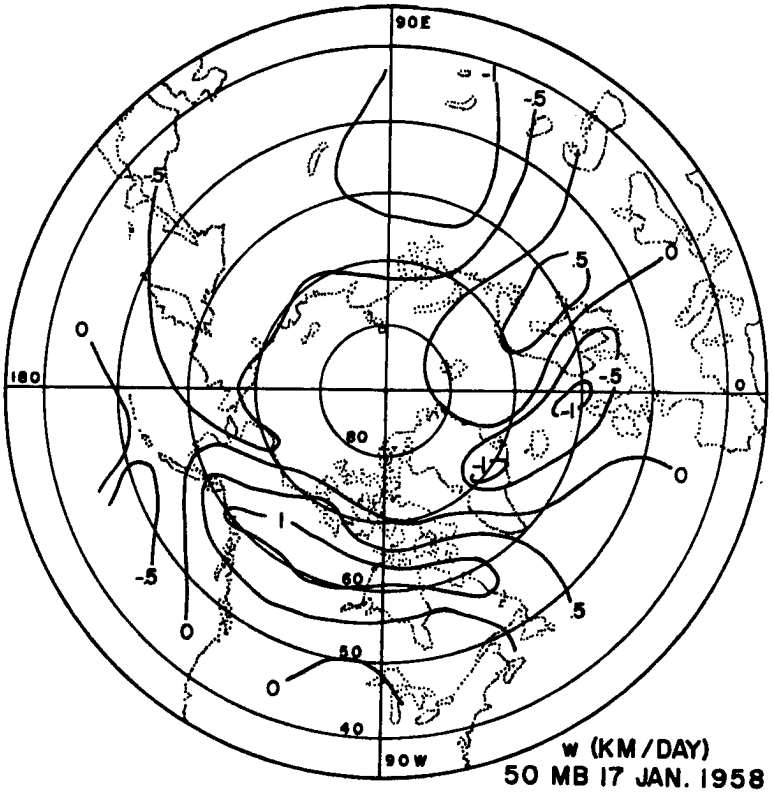

w (KM/DAY)
50 MB 17 JAN. 1958

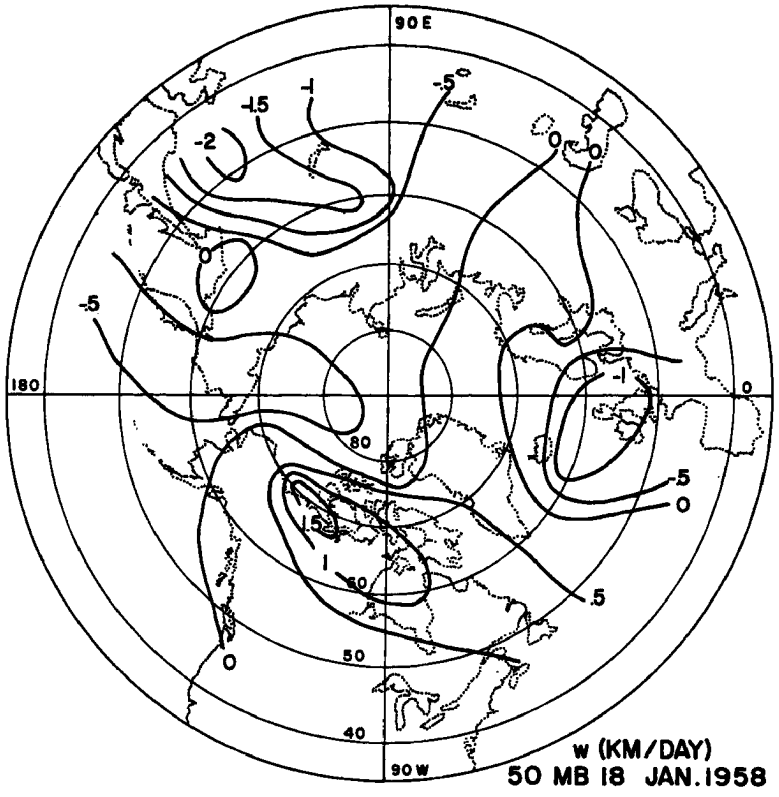

w (KM/DAY)
50 MB 18 JAN. 1958

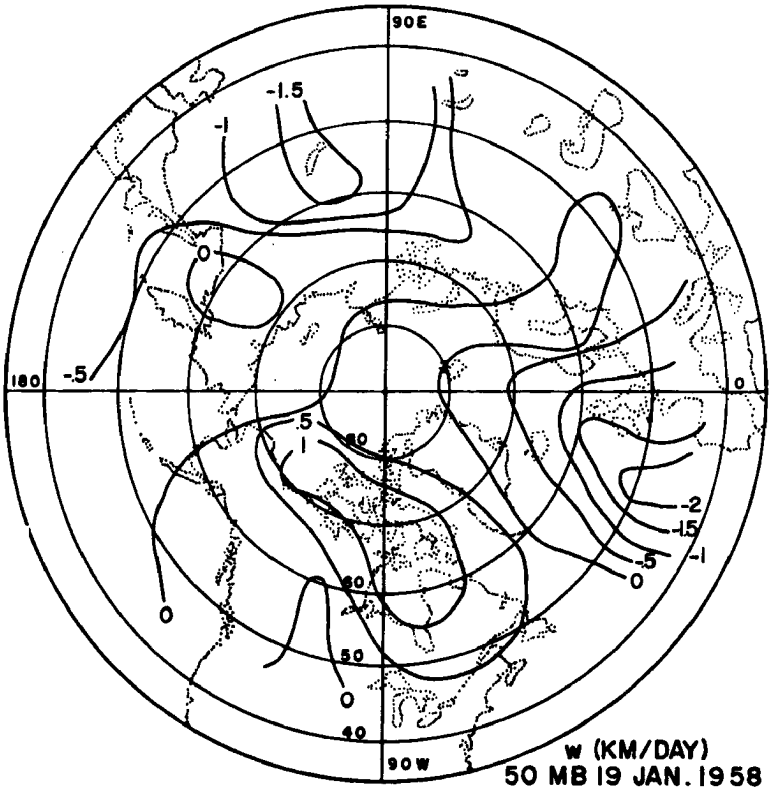

w (KM/DAY)
50 MB 19 JAN. 1958

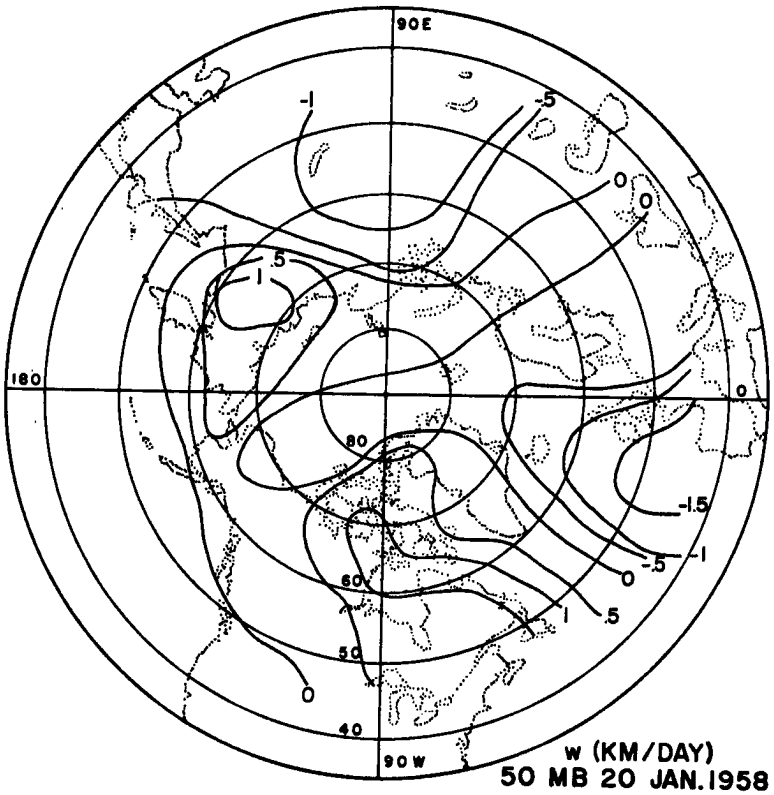

w (KM/DAY)
50 MB 20 JAN. 1958

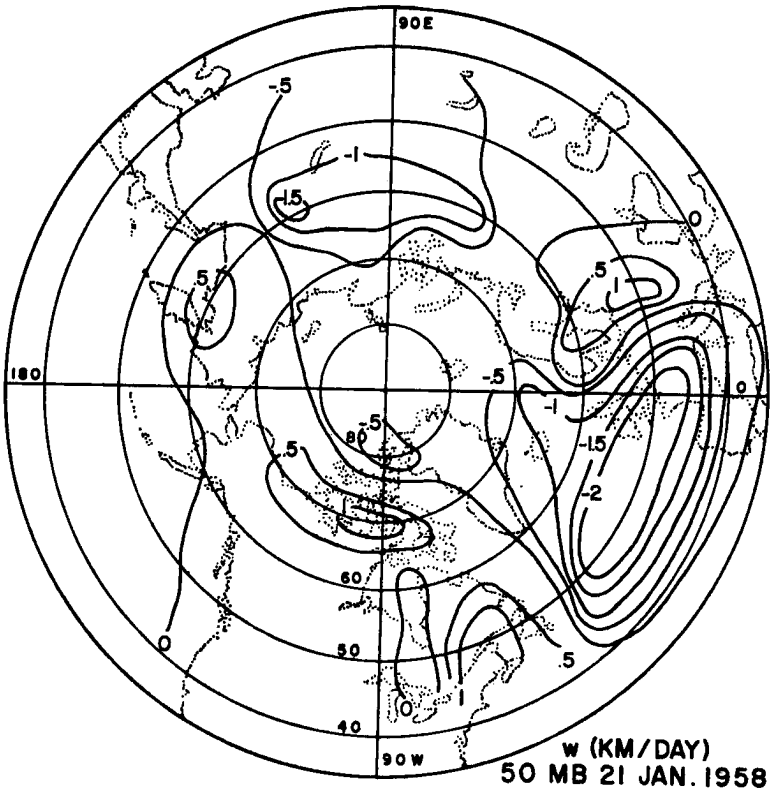

w (KM/DAY)
50 MB 21 JAN. 1958

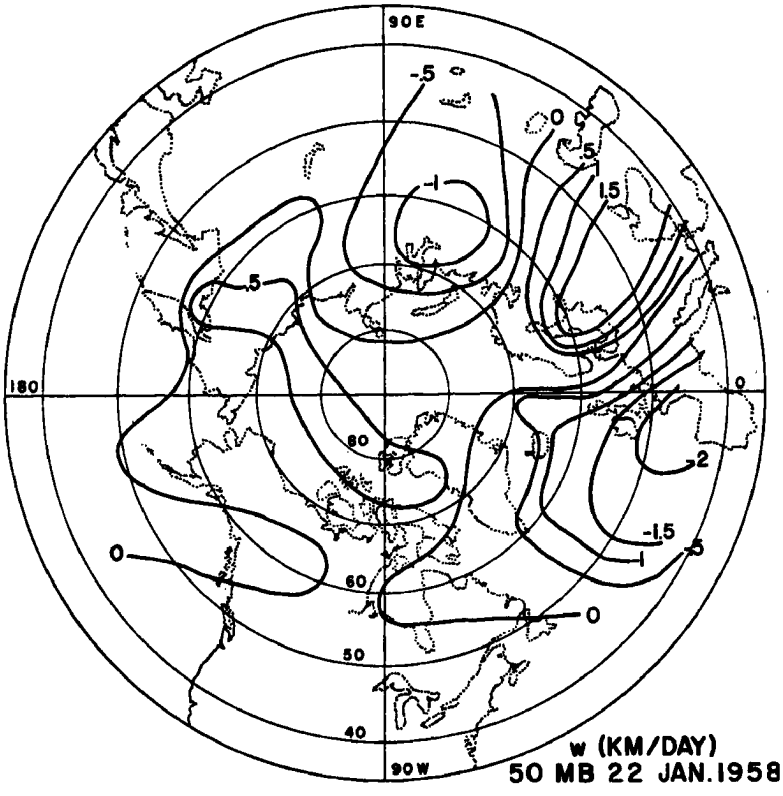

w (KM/DAY)
50 MB 22 JAN.1958

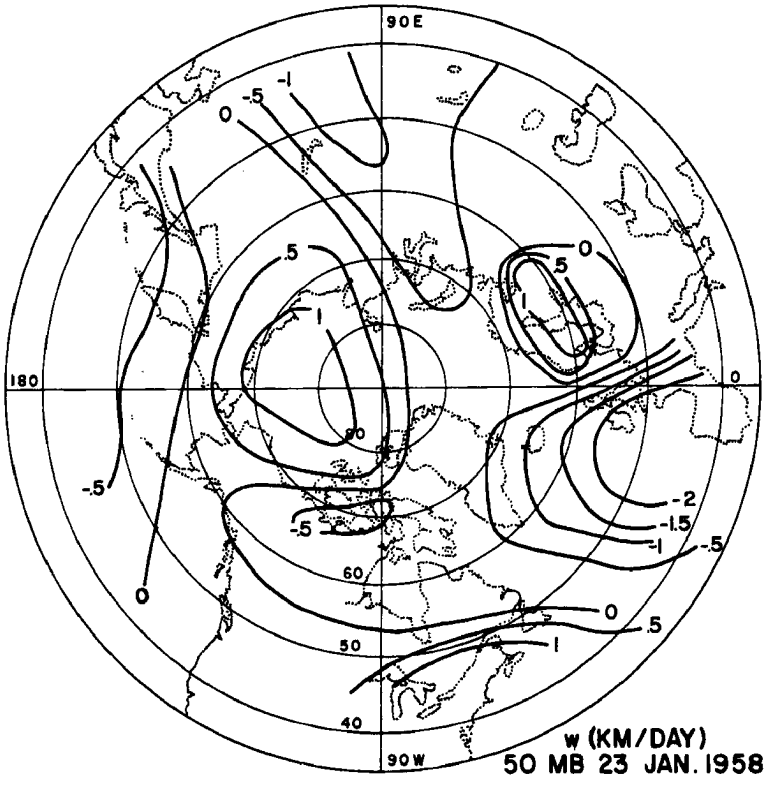

w (KM/DAY)
50 MB 23 JAN.1958

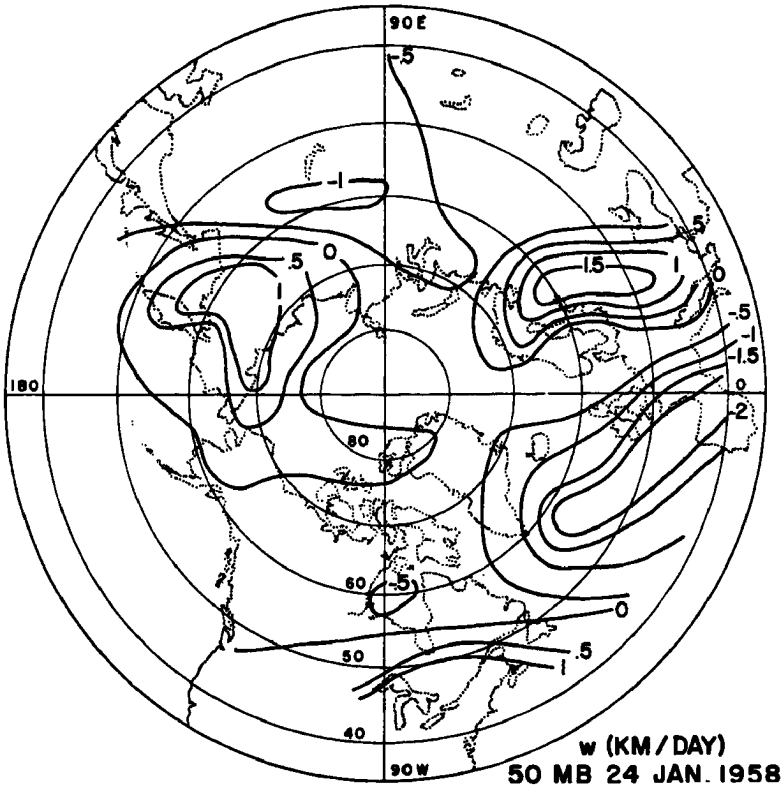

w (KM/DAY)
50 MB 24 JAN. 1958

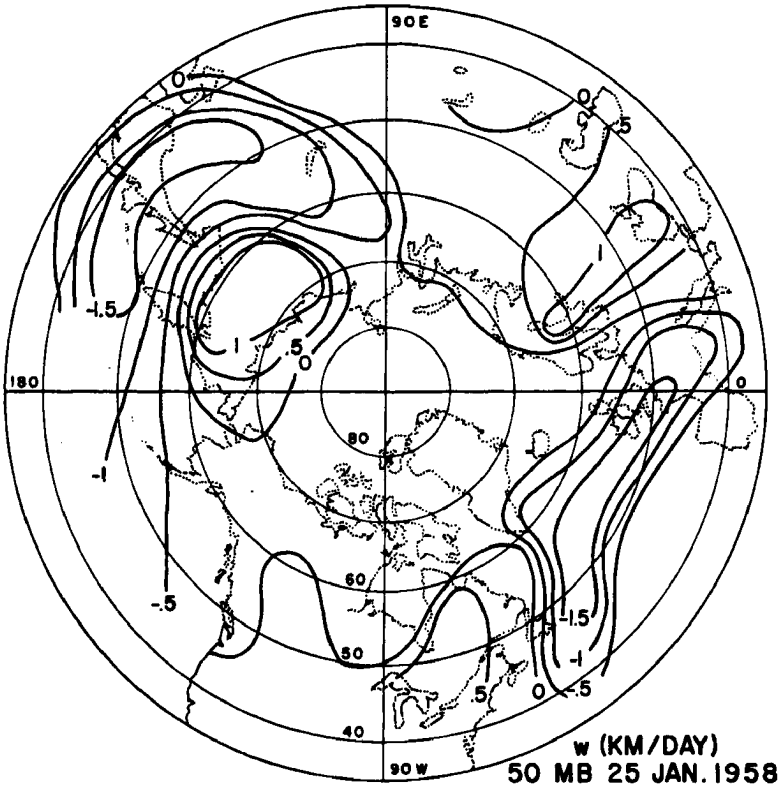

w (KM/DAY)
50 MB 25 JAN. 1958

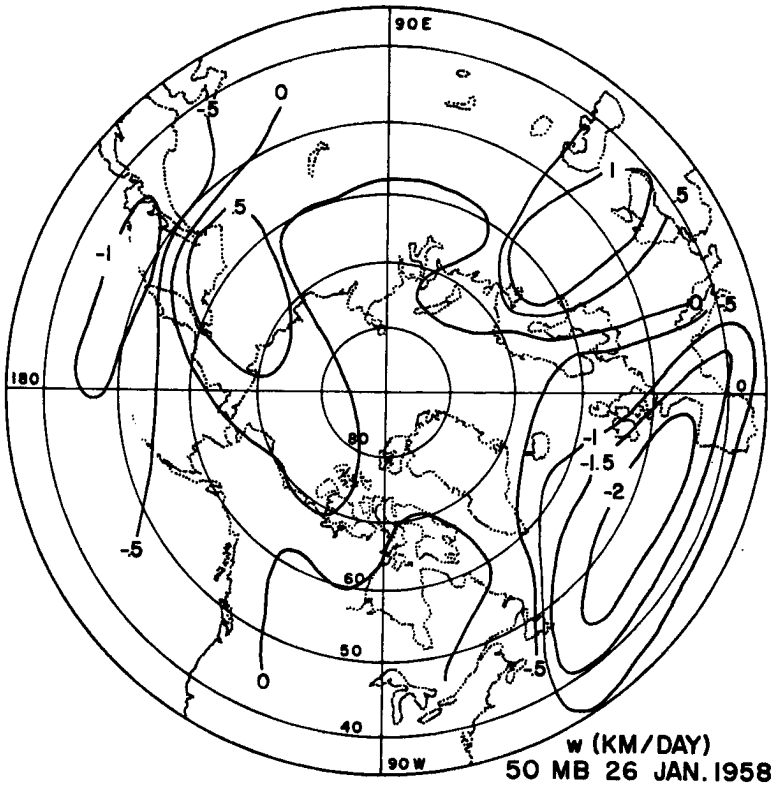

w (KM/DAY)
50 MB 26 JAN. 1958

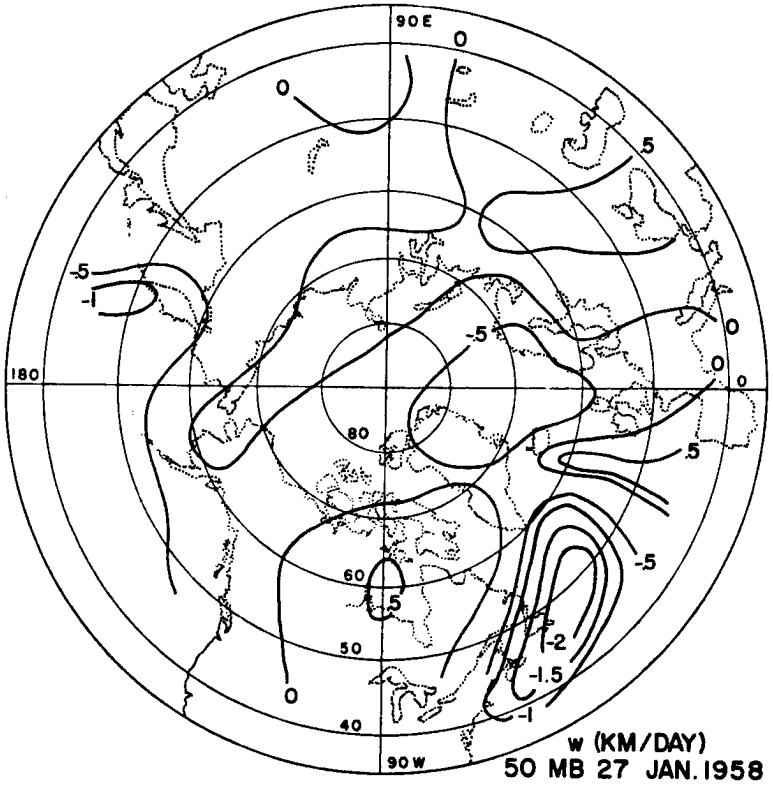

w (KM/DAY)
50 MB 27 JAN. 1958

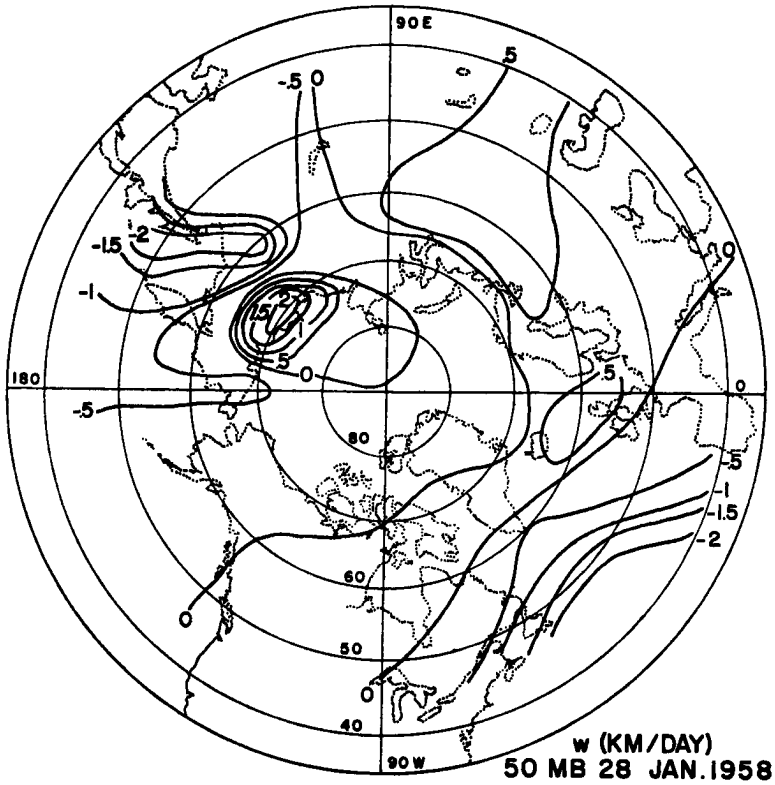

w (KM/DAY)
50 MB 28 JAN.1958

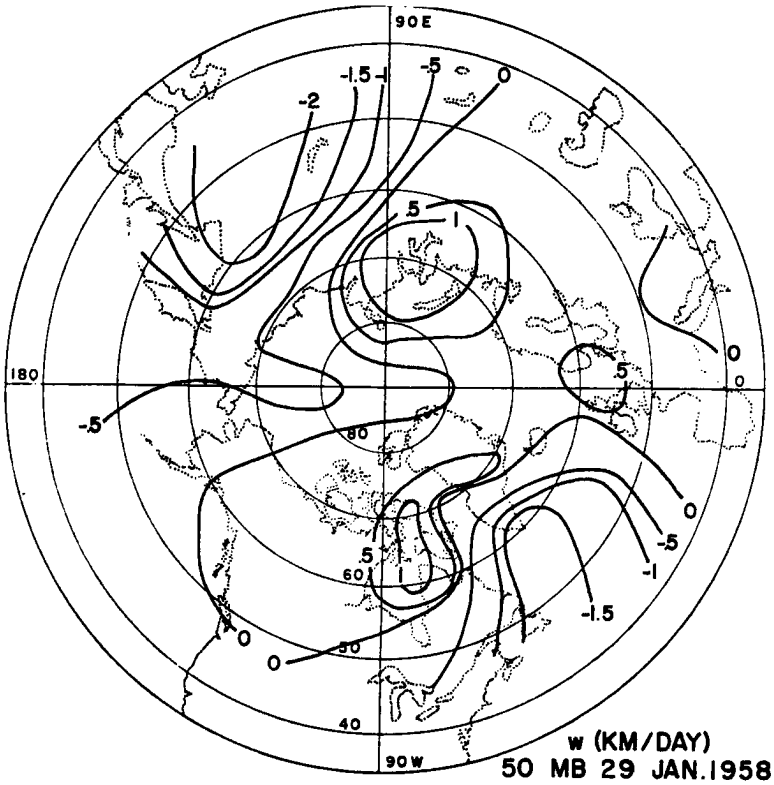

w (KM/DAY)
50 MB 29 JAN.1958

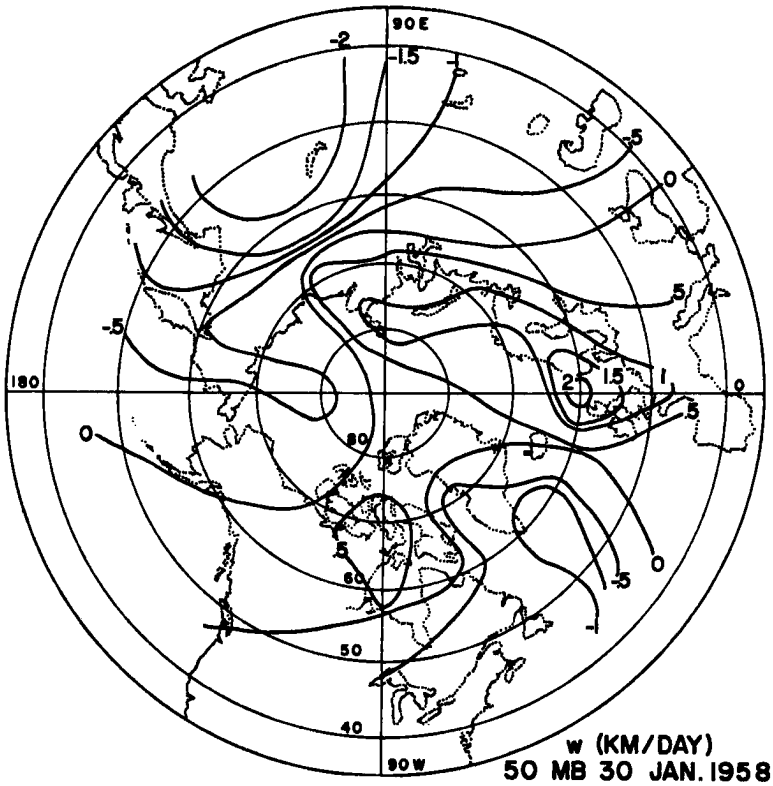

w (KM/DAY)
50 MB 30 JAN. 1958

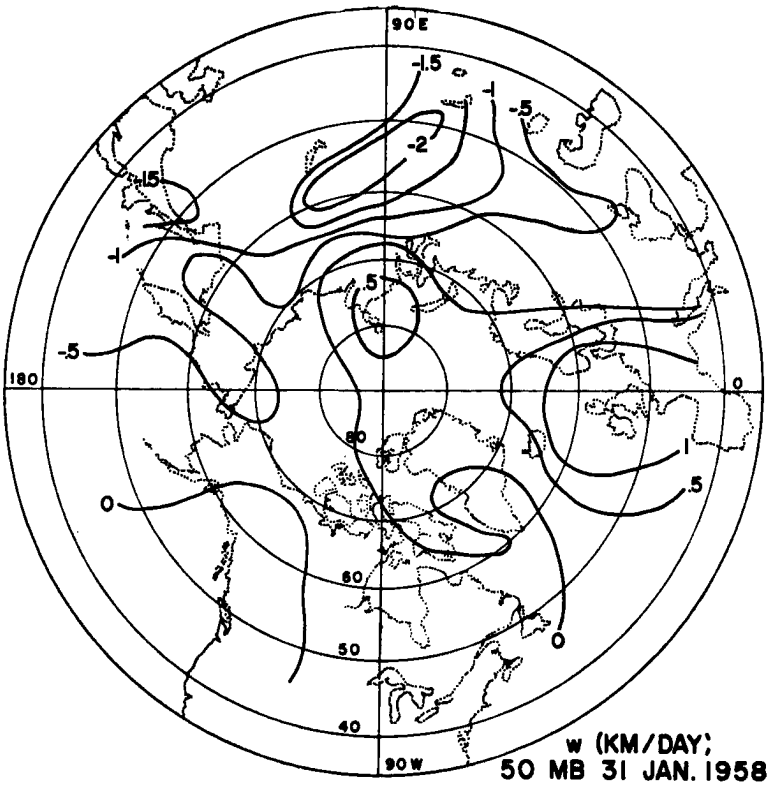

w (KM/DAY)
50 MB 31 JAN. 1958

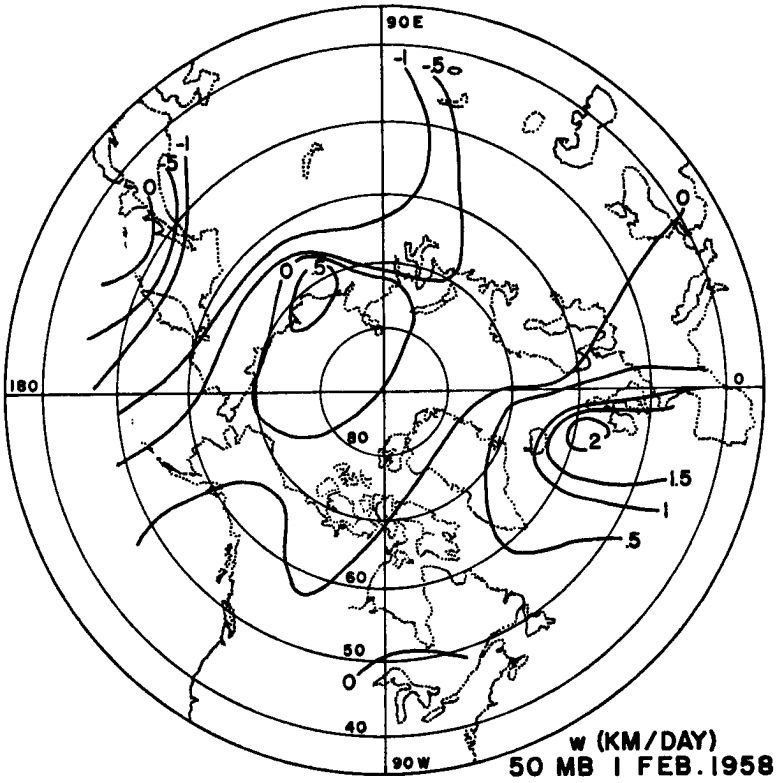

w (KM/DAY)
50 MB 1 FEB. 1958

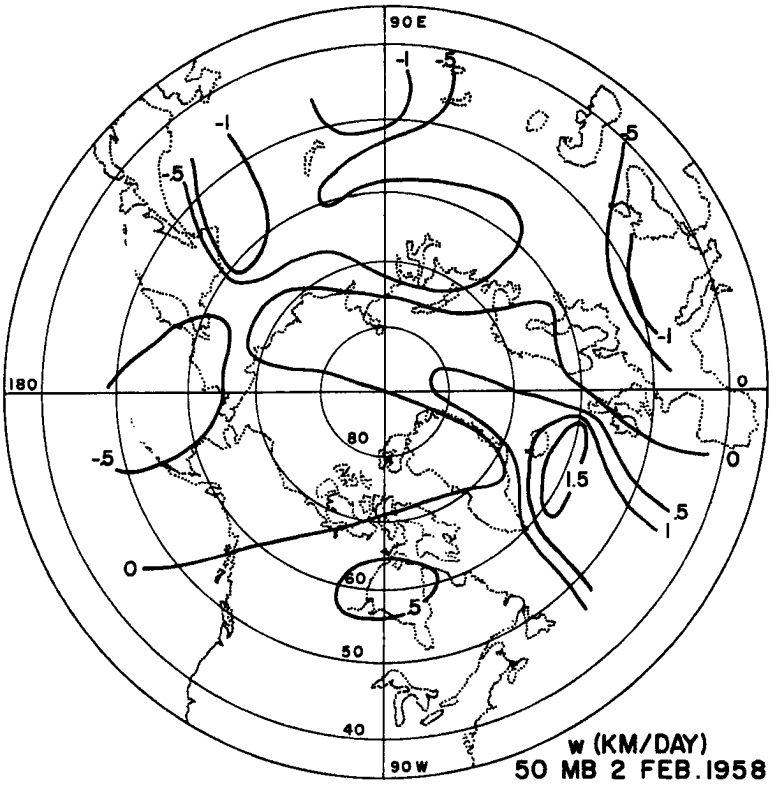

w (KM/DAY)
50 MB 2 FEB. 1958

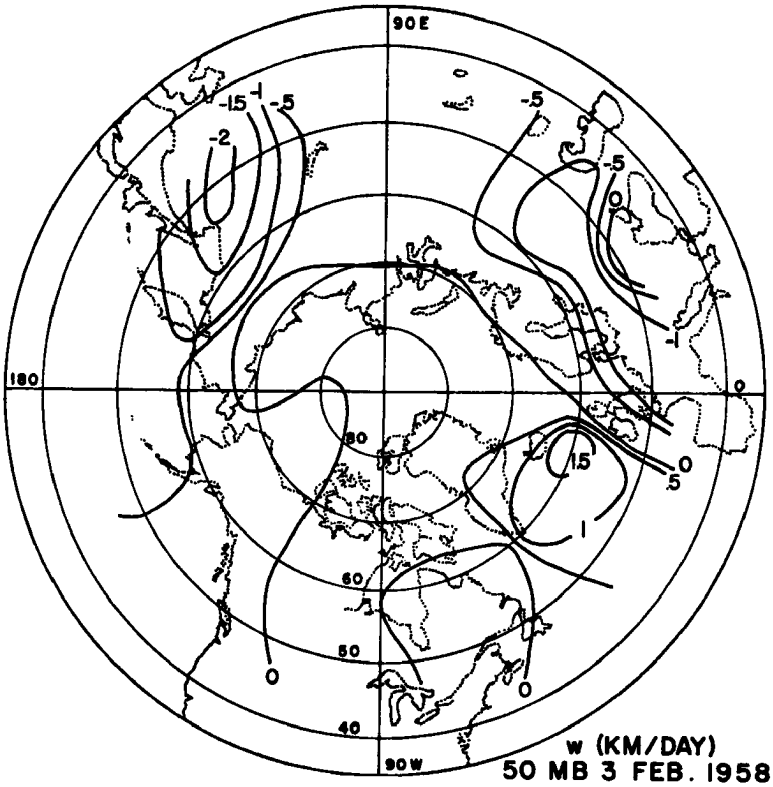

w (KM/DAY)
50 MB 3 FEB. 1958

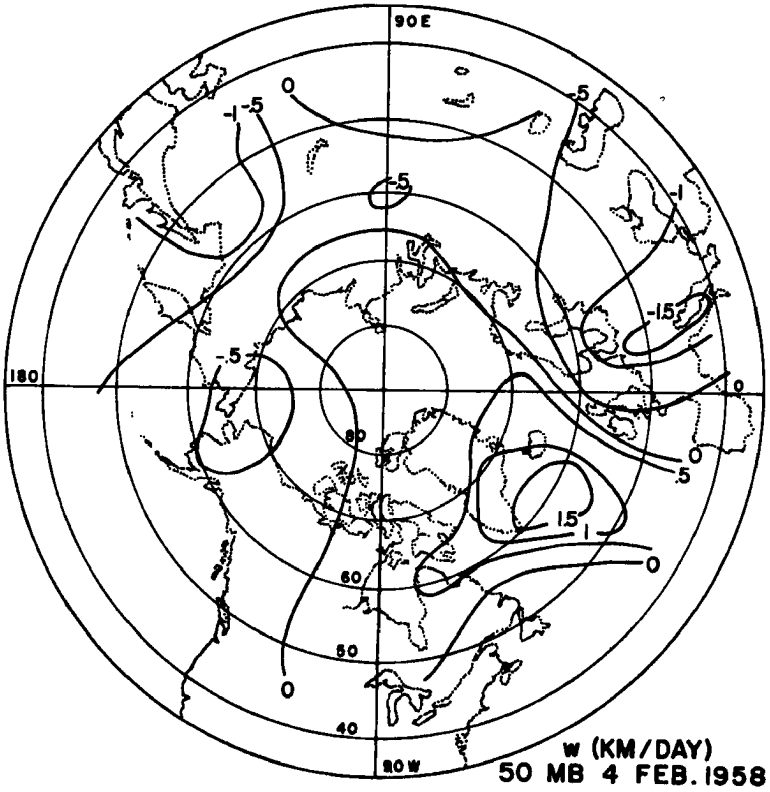

w (KM/DAY)
50 MB 4 FEB. 1958

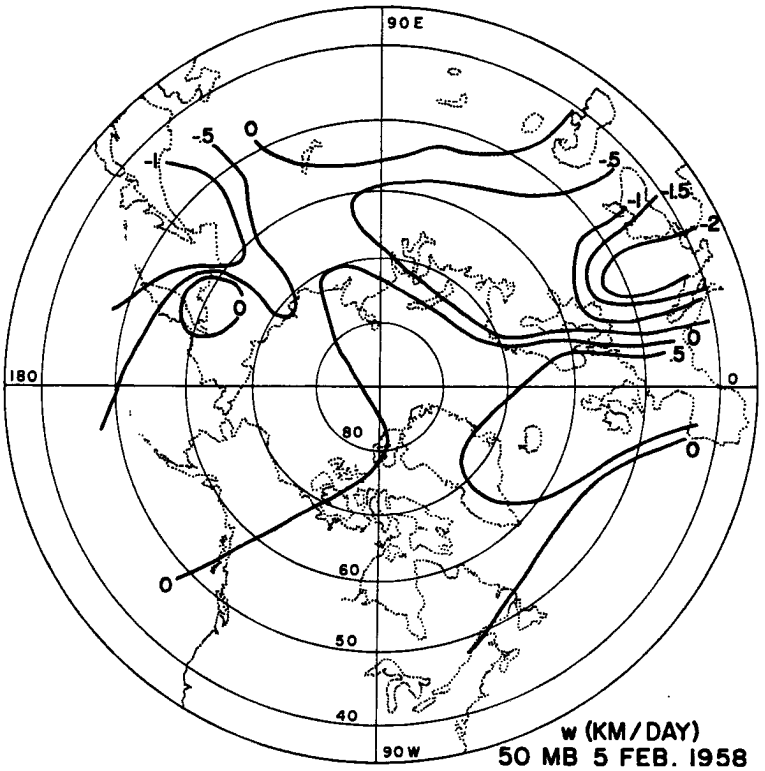

w (KM/DAY)
50 MB 5 FEB. 1958

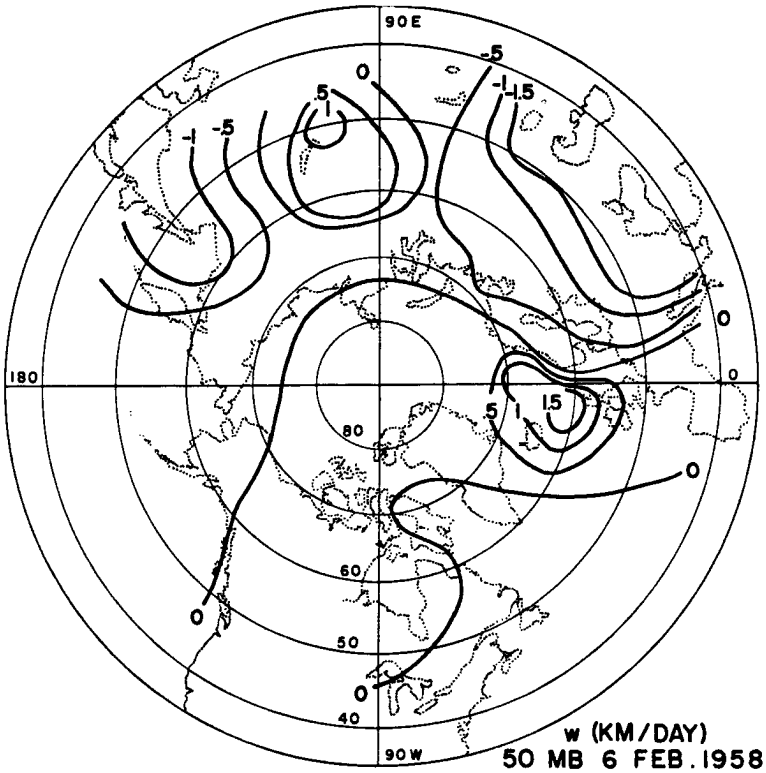

w (KM/DAY)
50 MB 6 FEB. 1958

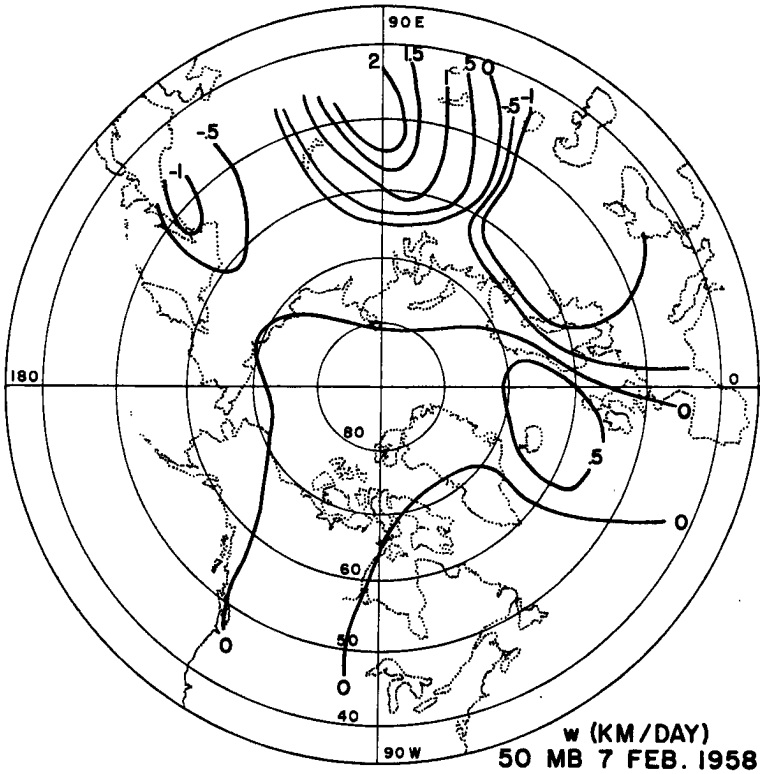

w (KM/DAY)
50 MB 7 FEB. 1958

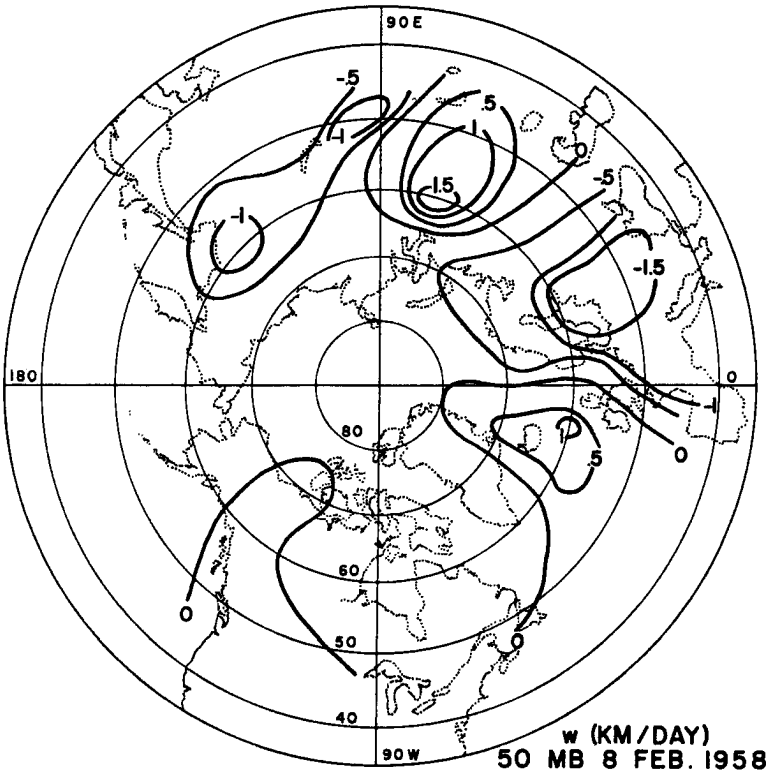

w (KM/DAY)
50 MB 8 FEB. 1958

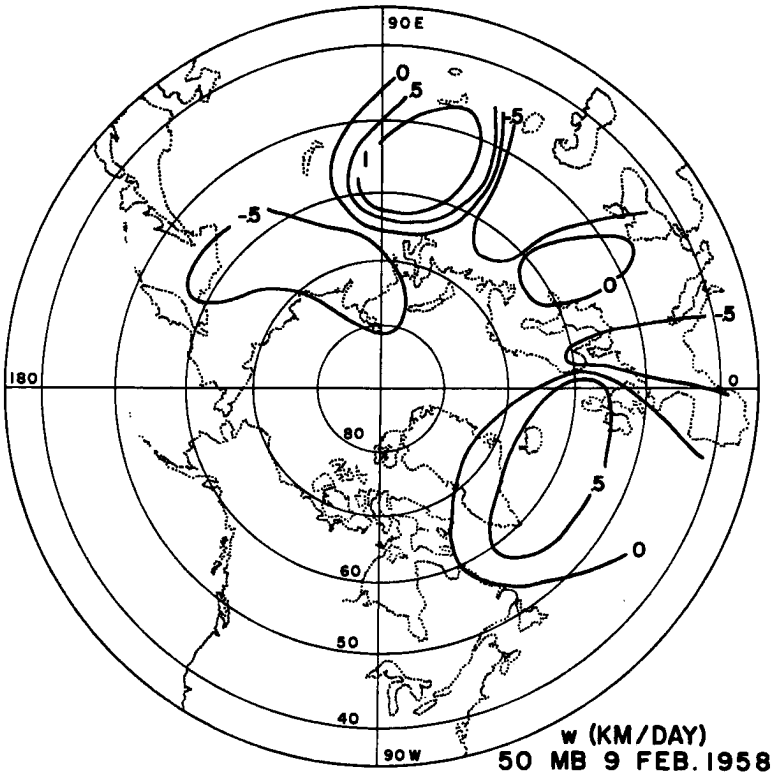

w (KM/DAY)
50 MB 9 FEB. 1958

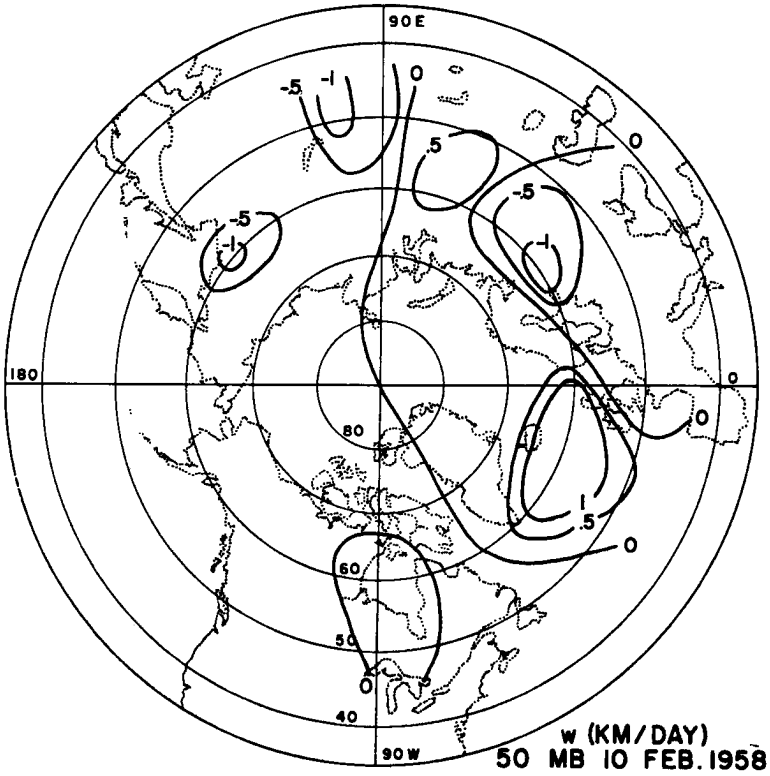

w (KM/DAY)
50 MB 10 FEB. 1958

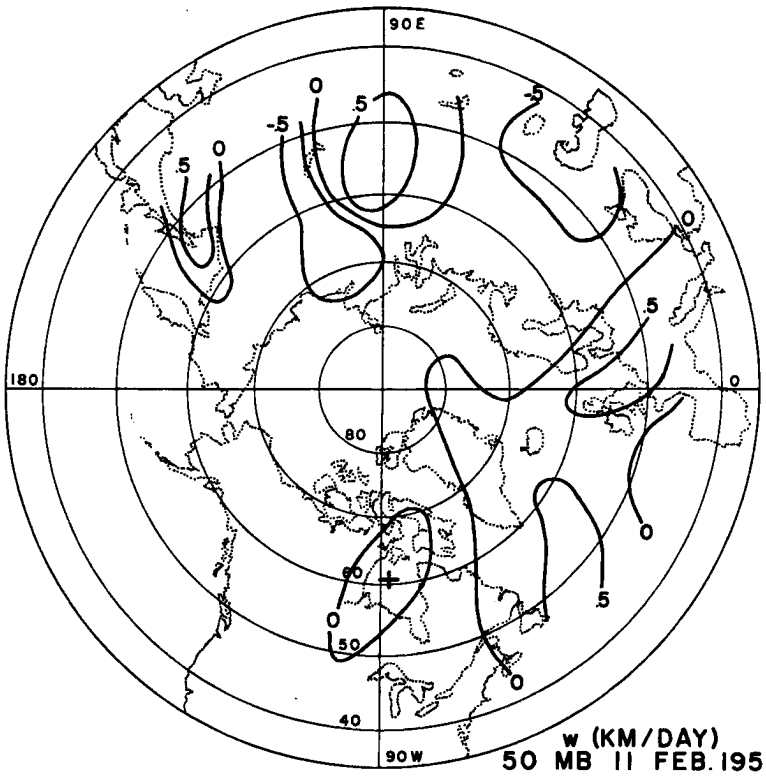
90E
180
0
80
60
50
40
90W
0
.5
-.5
-5
w (KM/DAY)
50 MB 11 FEB. 1958

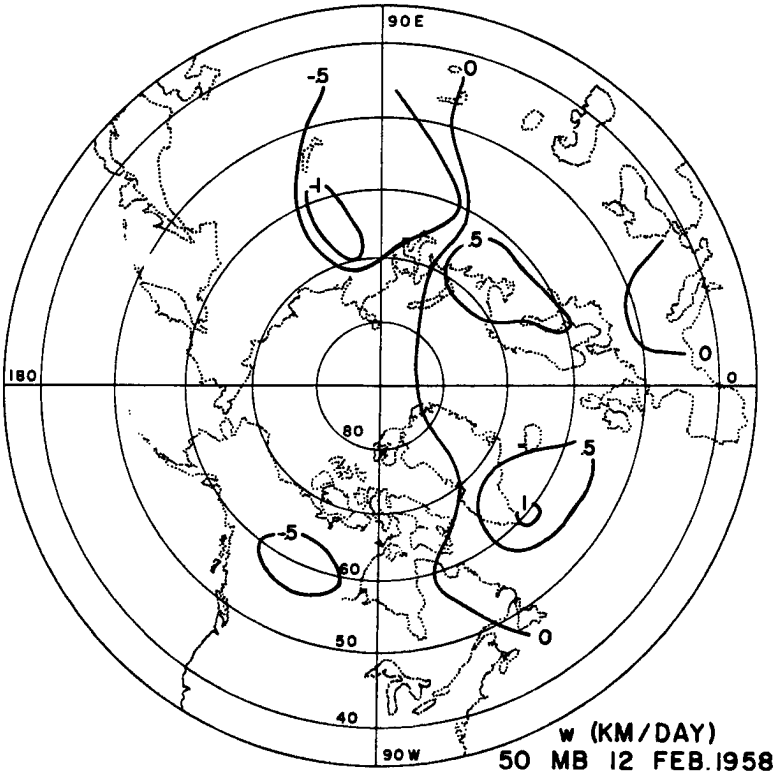
90E
180
0
80
60
50
40
90W
-5
-1
.5
-.5
w (KM/DAY)
50 MB 12 FEB. 1958

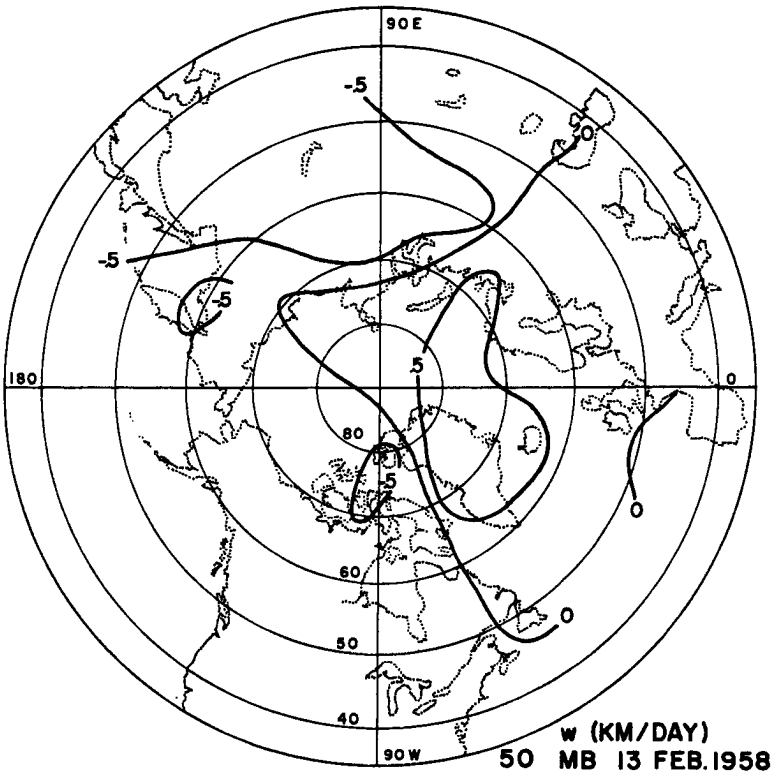

w (KM/DAY)
50 MB 13 FEB.1958

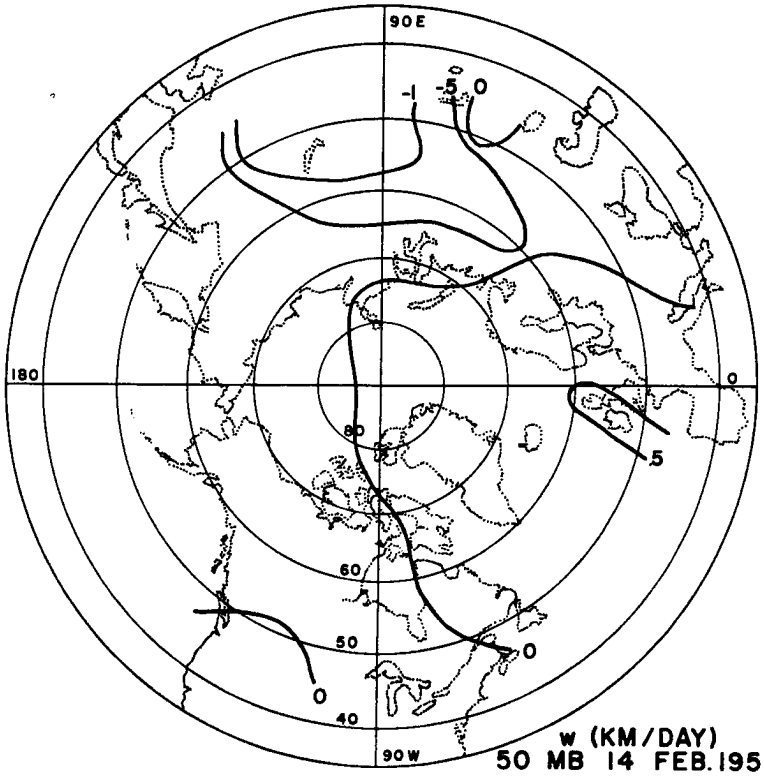

w (KM/DAY)
50 MB 14 FEB.1958

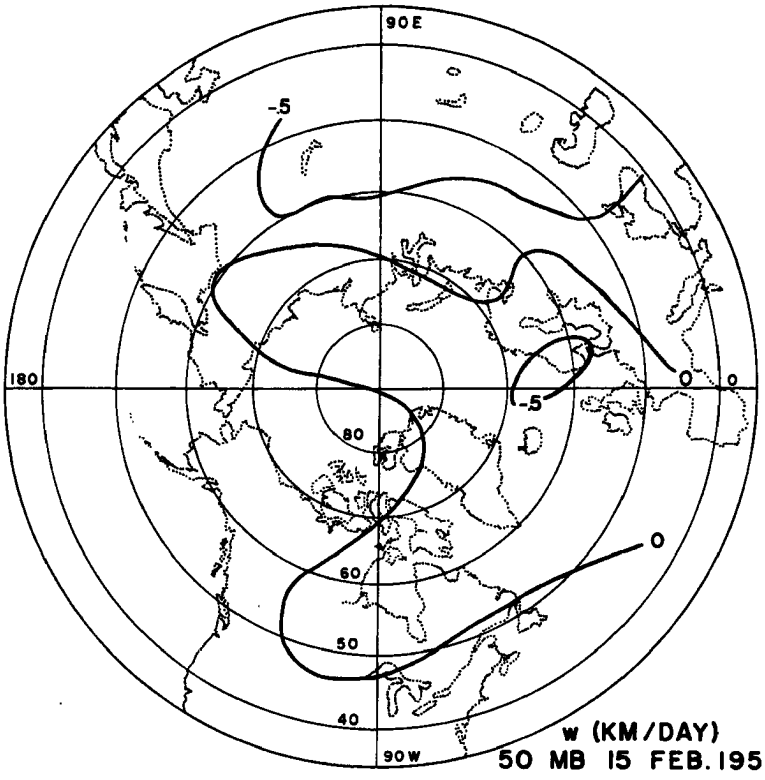

w (KM/DAY)
50 MB 15 FEB. 1958

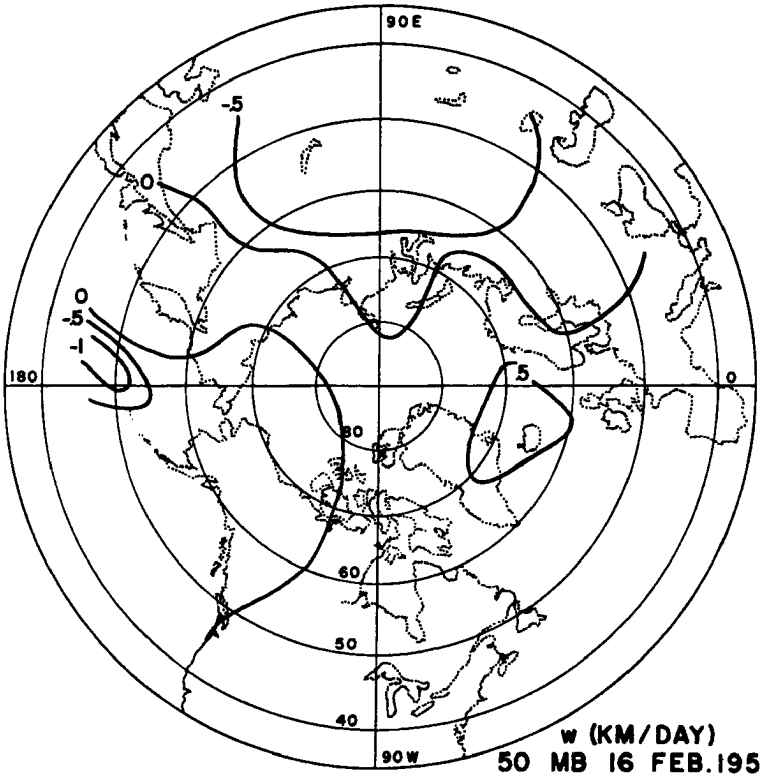

w (KM/DAY)
50 MB 16 FEB. 1958

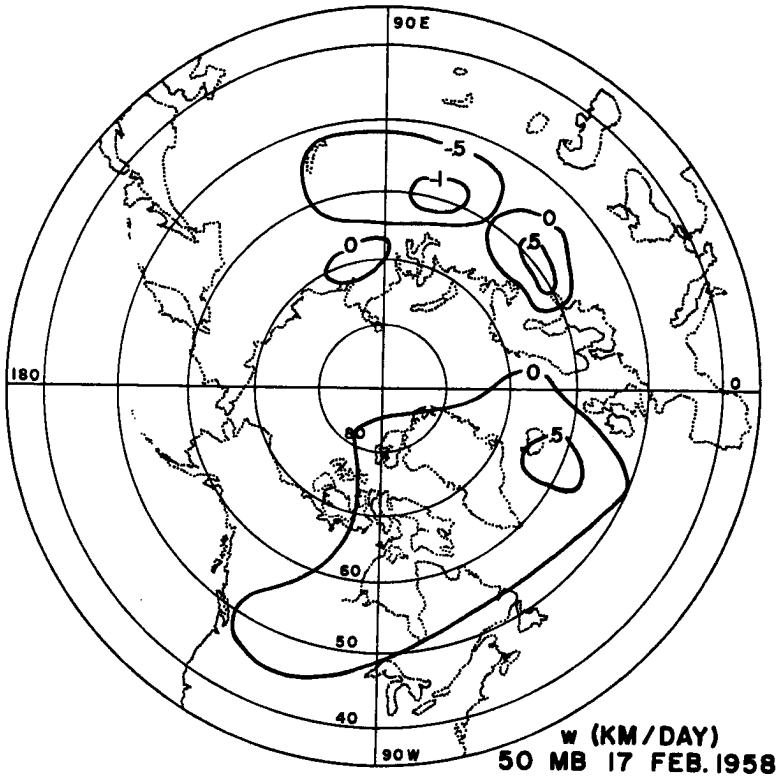

w (KM/DAY)
50 MB 17 FEB. 1958

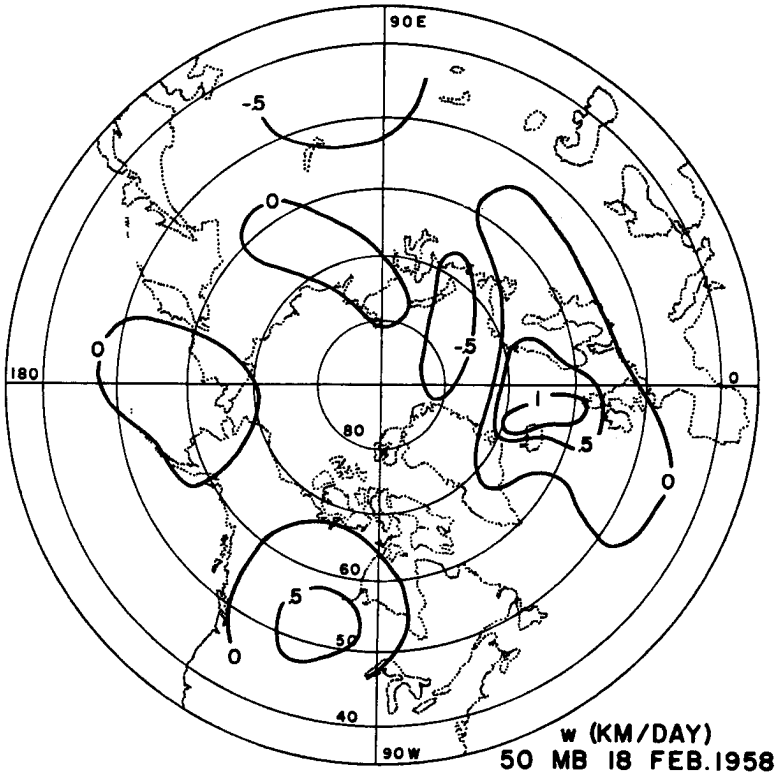

w (KM/DAY)
50 MB 18 FEB. 1958

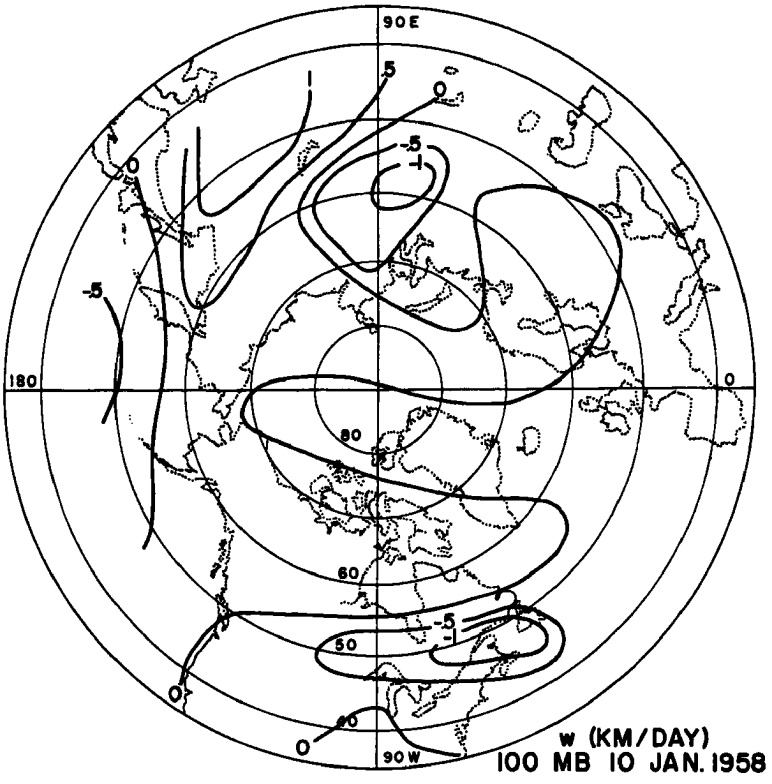

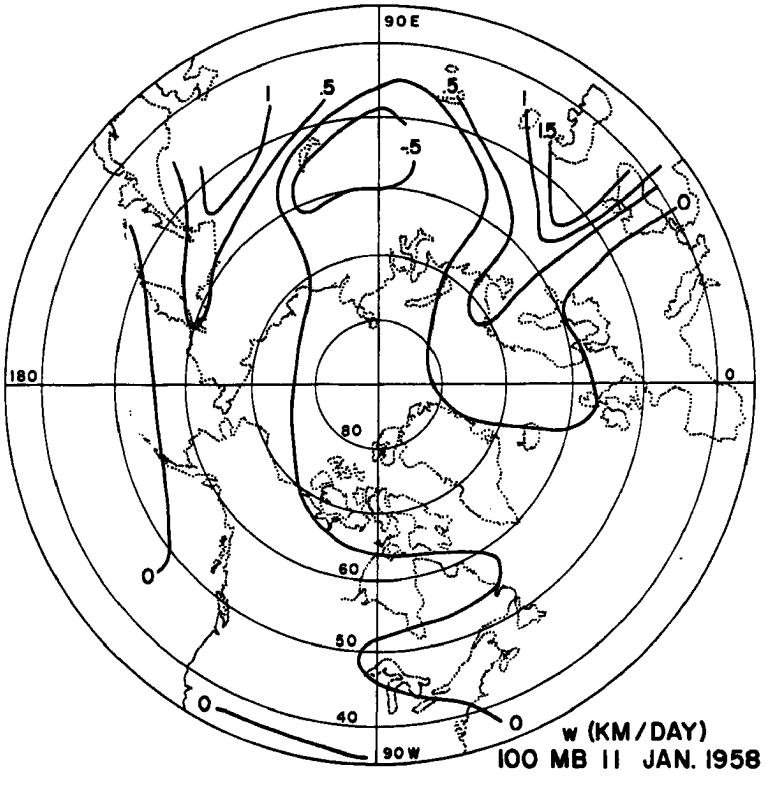

APPENDIX C. Daily vertical motion (km/day) at 100 mb for indicated dates for period before, during, and after the sudden warming of January 1958.

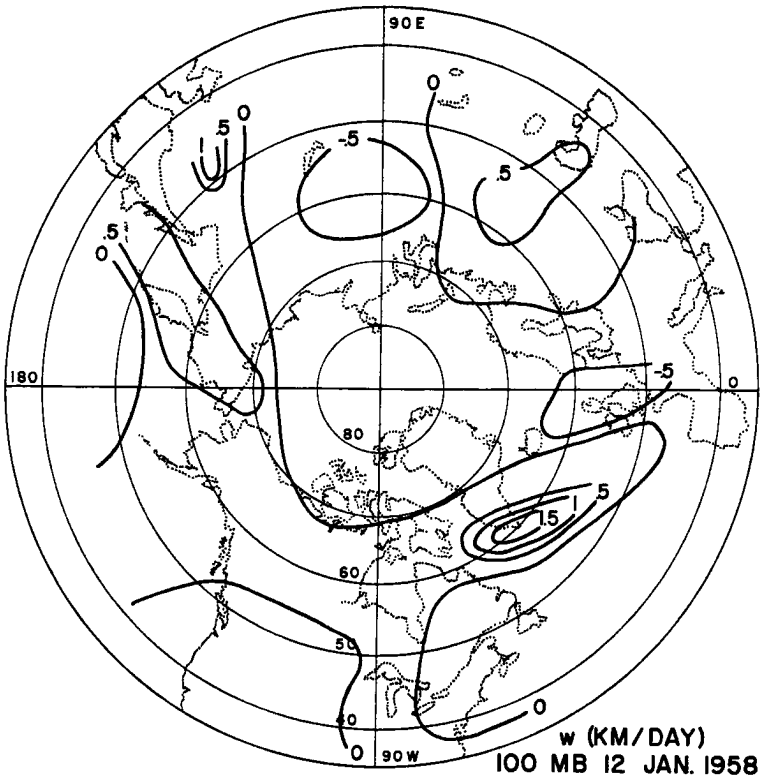
90E
180
0
80
60
40
90W
.5
0
-5
.5
0
-5
.5
1
1.5
0
0
0
w (KM/DAY)
100 MB 12 JAN. 1958

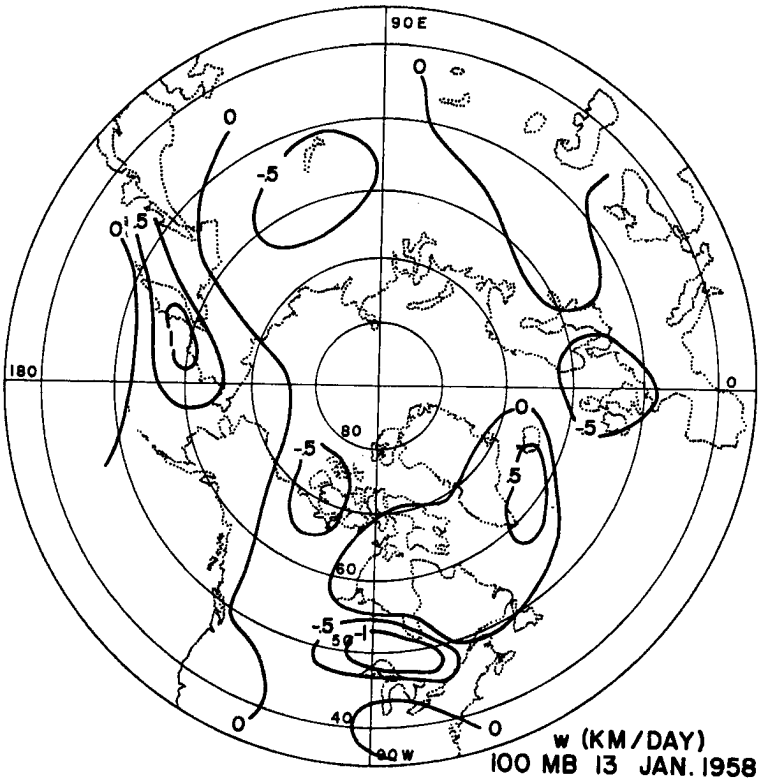
90E
180
0
80
60
40
90W
0
0
-5
0
.5
-5
0
-5
.5
-5
-1
0
0
w (KM/DAY)
100 MB 13 JAN. 1958

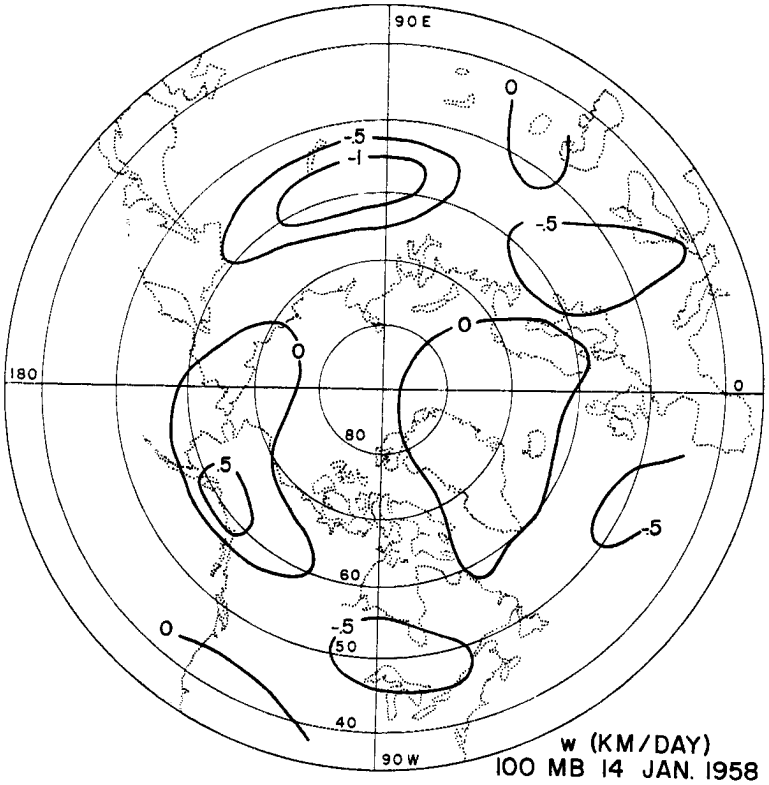

w (KM/DAY)
100 MB 14 JAN. 1958

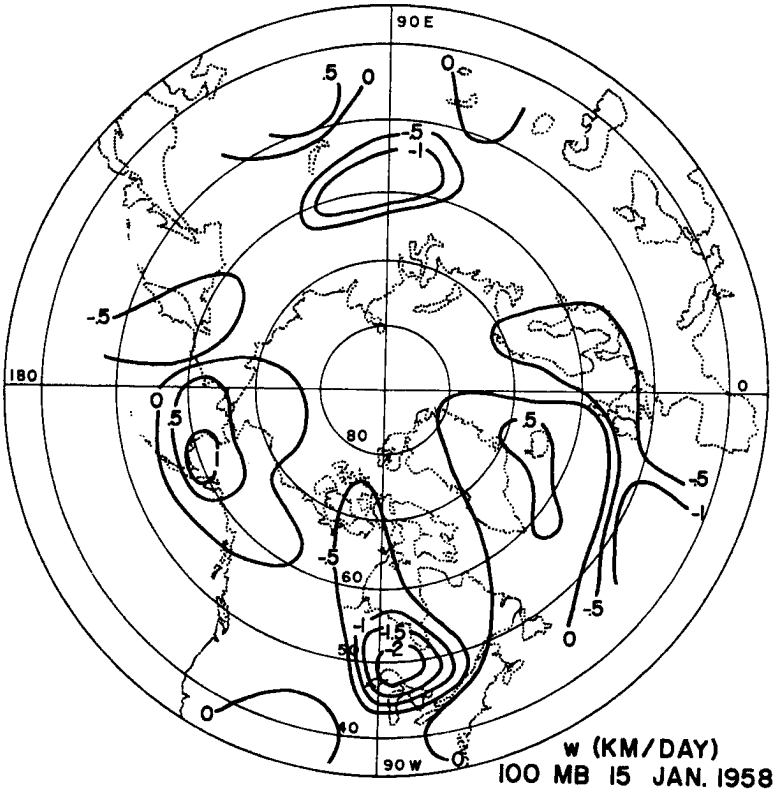

w (KM/DAY)
100 MB 15 JAN. 1958

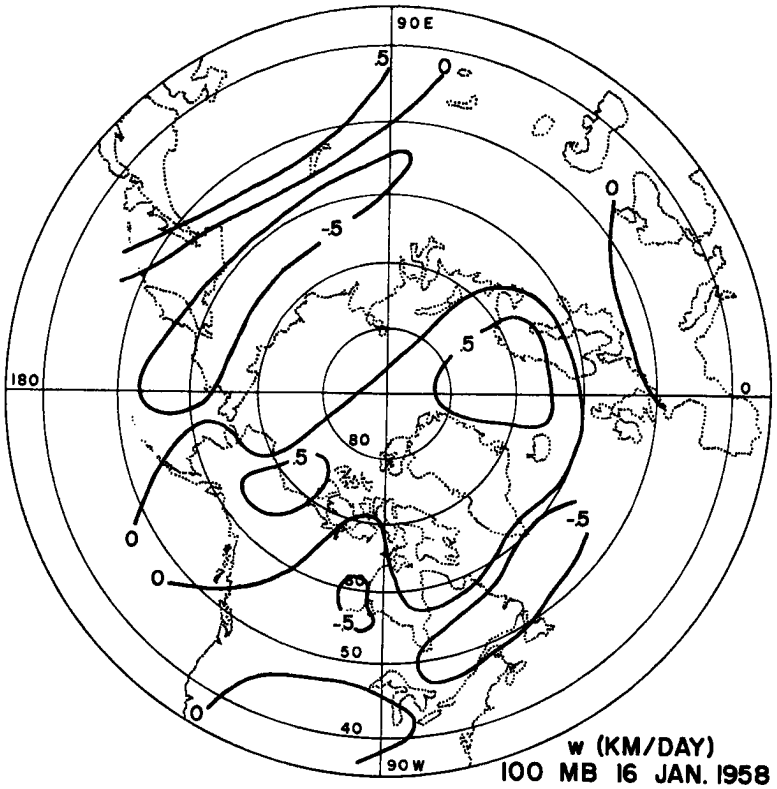
90E
180
0
80
60
50
40
90W
.5
0
-.5
w (KM/DAY)
100 MB 16 JAN. 1958

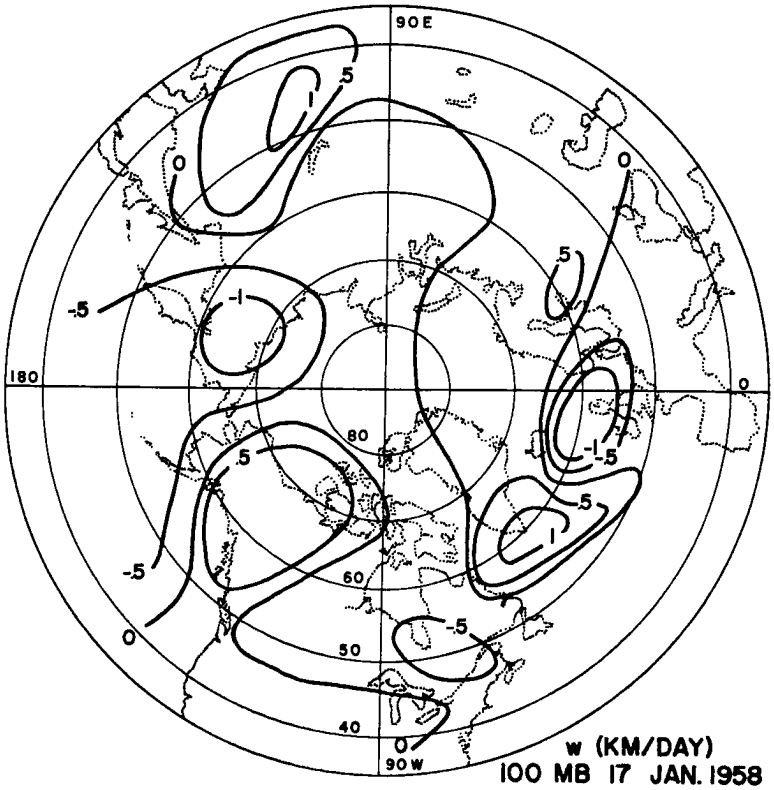
90E
180
0
80
60
50
40
90W
.5
1
0
-.5
-1
w (KM/DAY)
100 MB 17 JAN. 1958

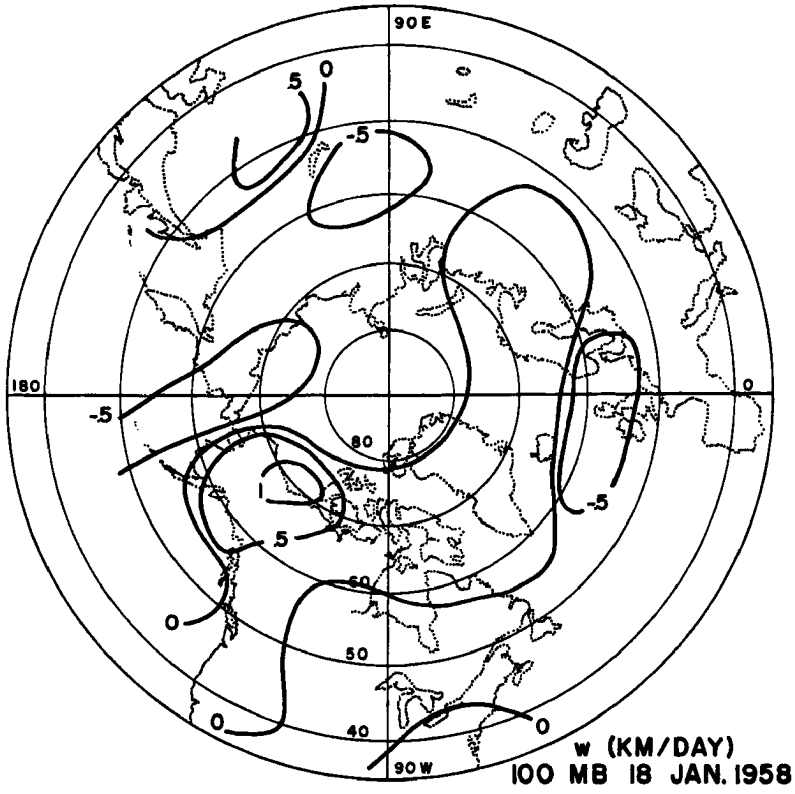
90E
180
0
80
60
50
40
90W
.5
0
-5
1
-5
.5
0
0
0
w (KM/DAY)
100 MB 18 JAN. 1958

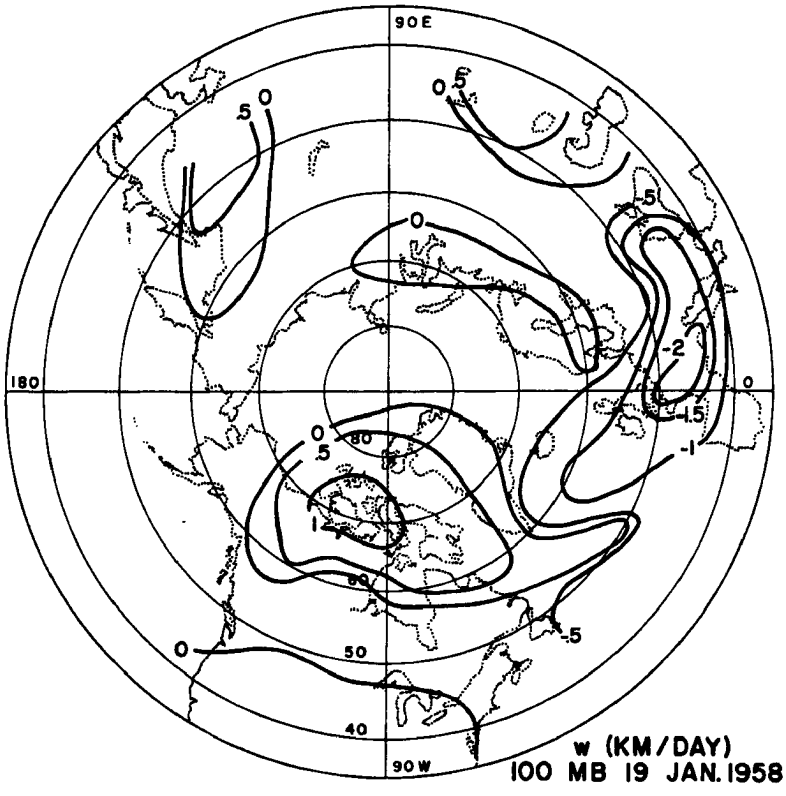
90E
180
0
80
60
50
40
90W
.5
0
0
.5
-5
0
-2
-1.5
-1
0
.5
1
-.5
0
w (KM/DAY)
100 MB 19 JAN. 1958

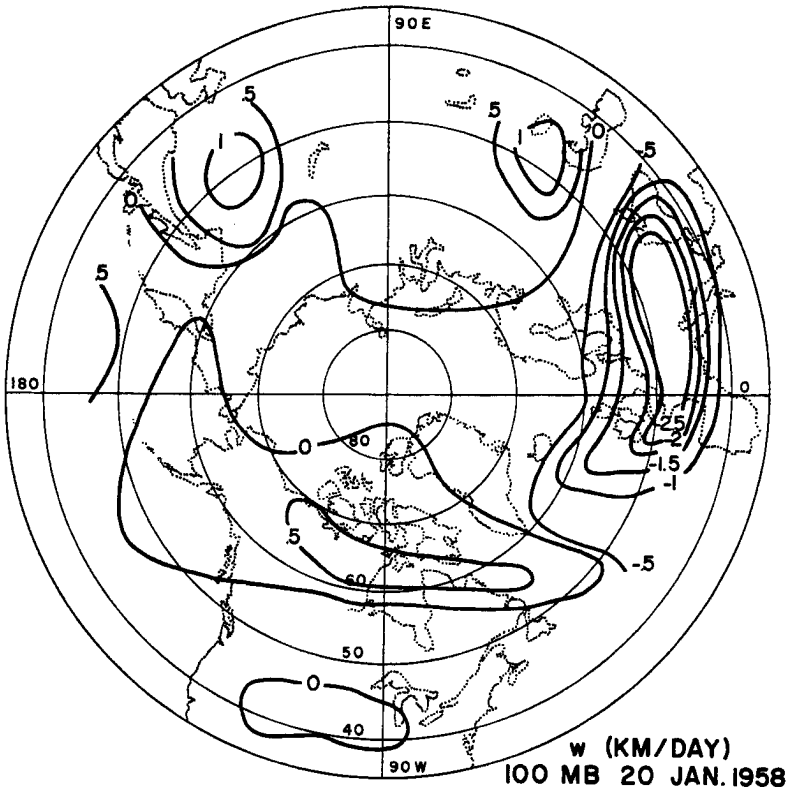

w (KM/DAY)
100 MB 20 JAN. 1958

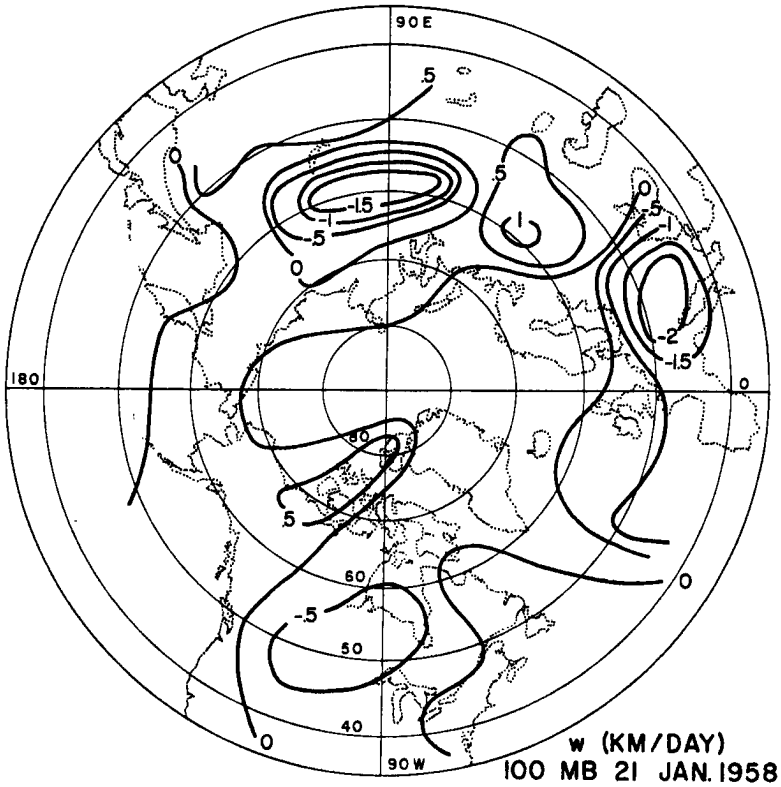

w (KM/DAY)
100 MB 21 JAN. 1958

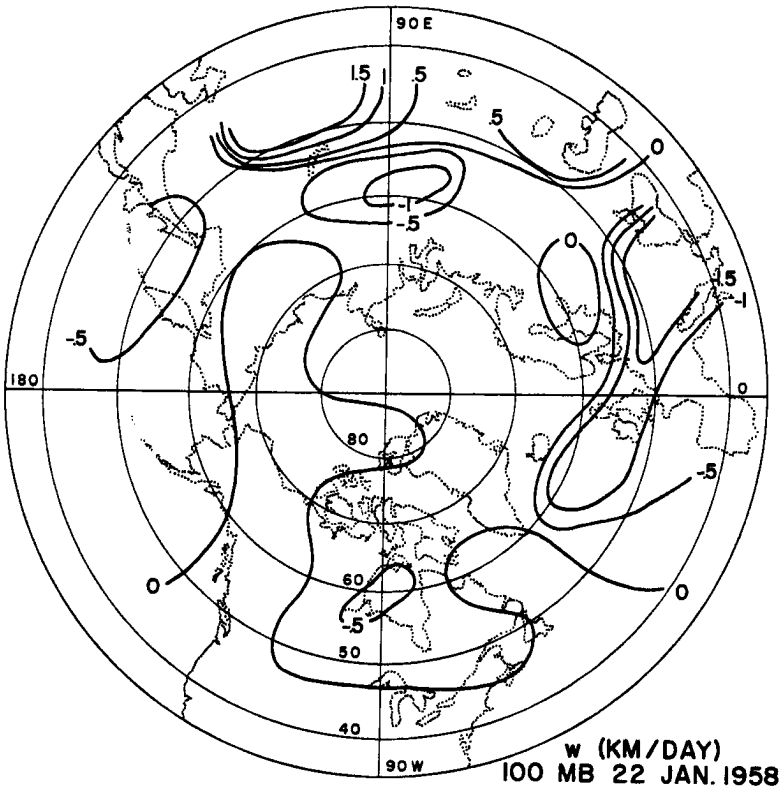

w (KM/DAY)
100 MB 22 JAN. 1958

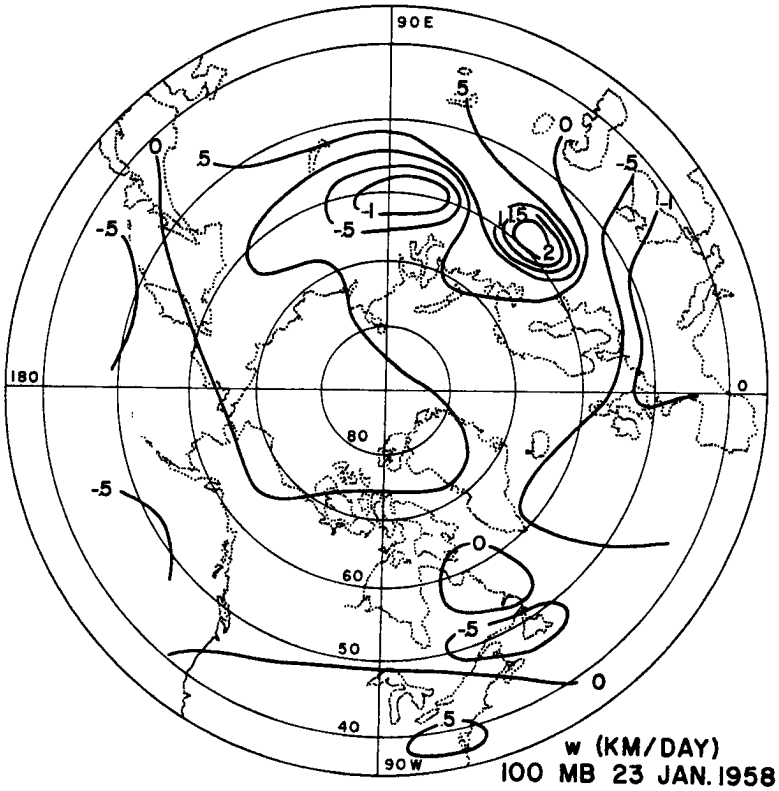

w (KM/DAY)
100 MB 23 JAN. 1958

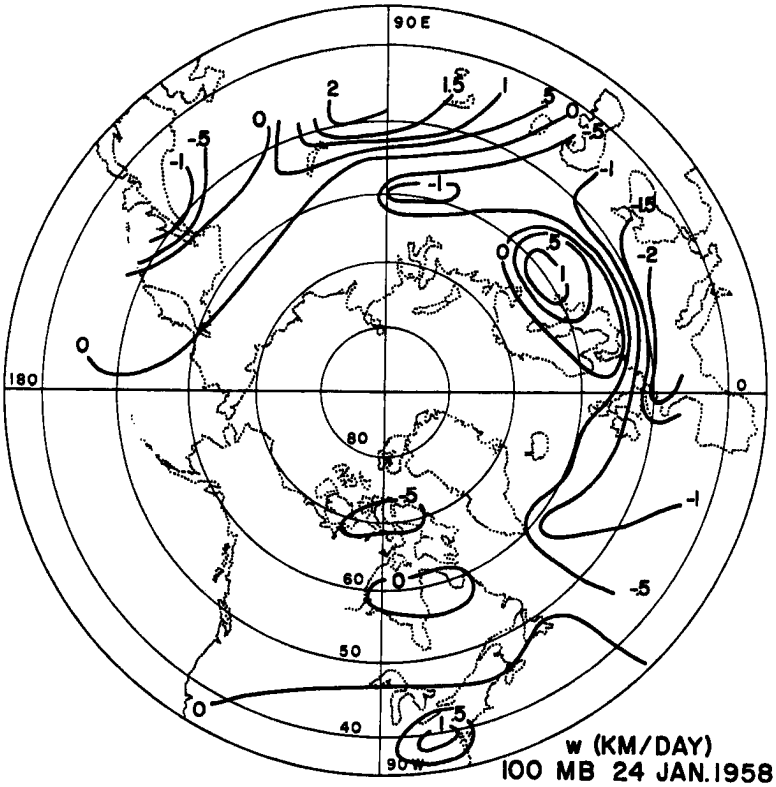

w (KM/DAY)
100 MB 24 JAN. 1958

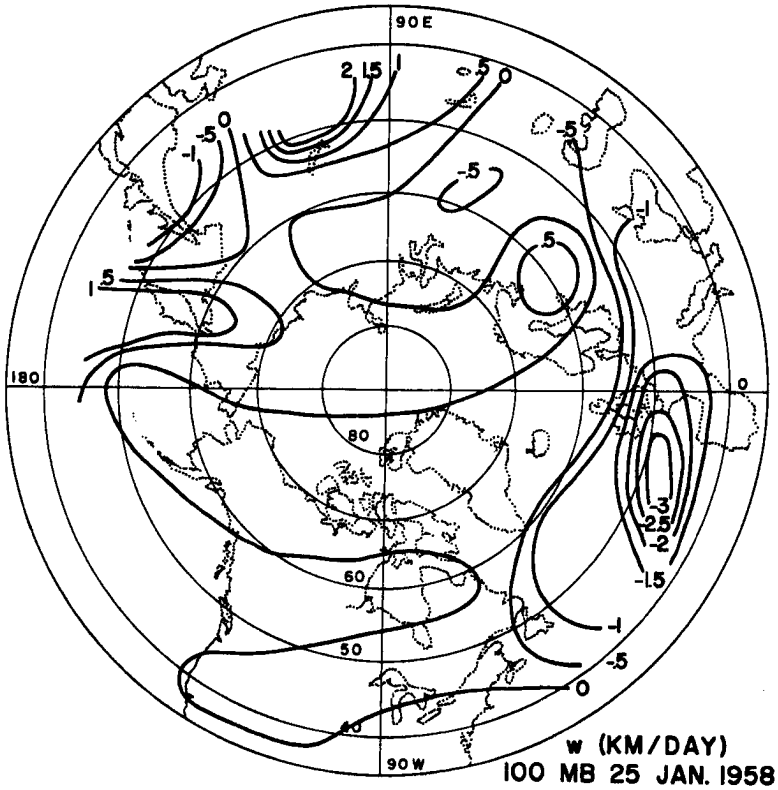

w (KM/DAY)
100 MB 25 JAN. 1958

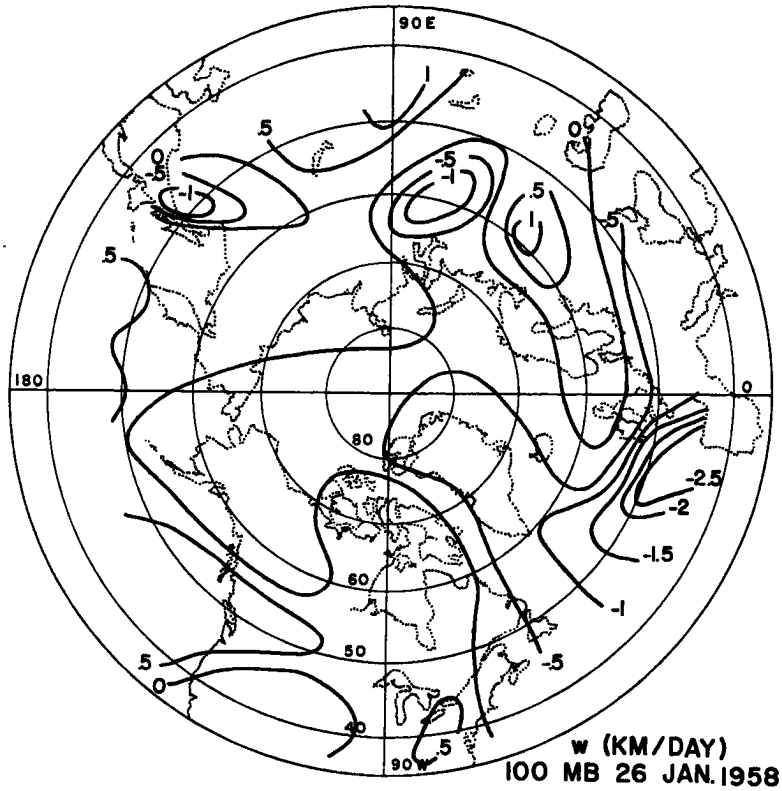

w (KM/DAY)
100 MB 26 JAN. 1958

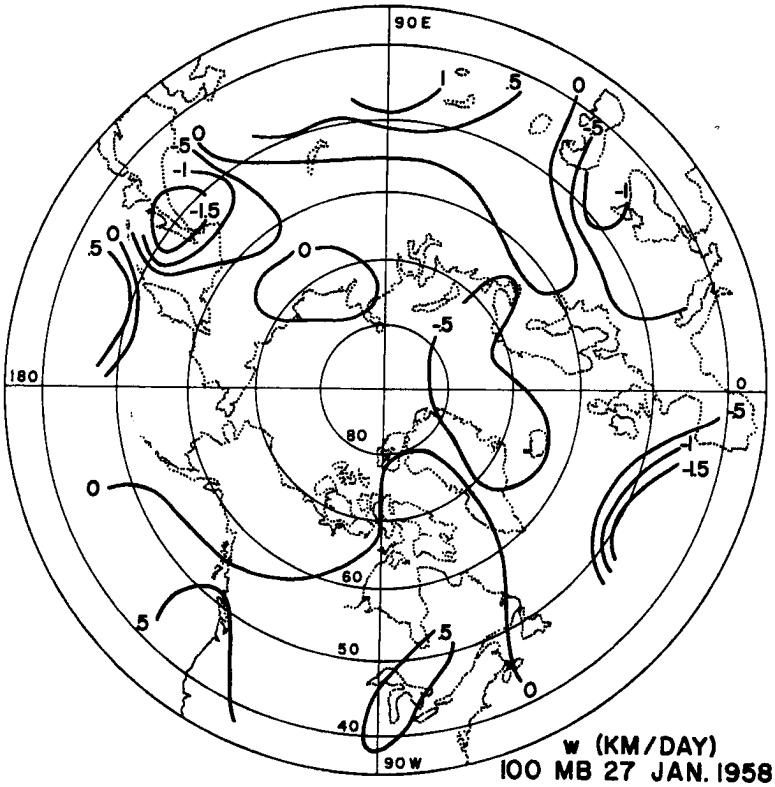

w (KM/DAY)
100 MB 27 JAN. 1958

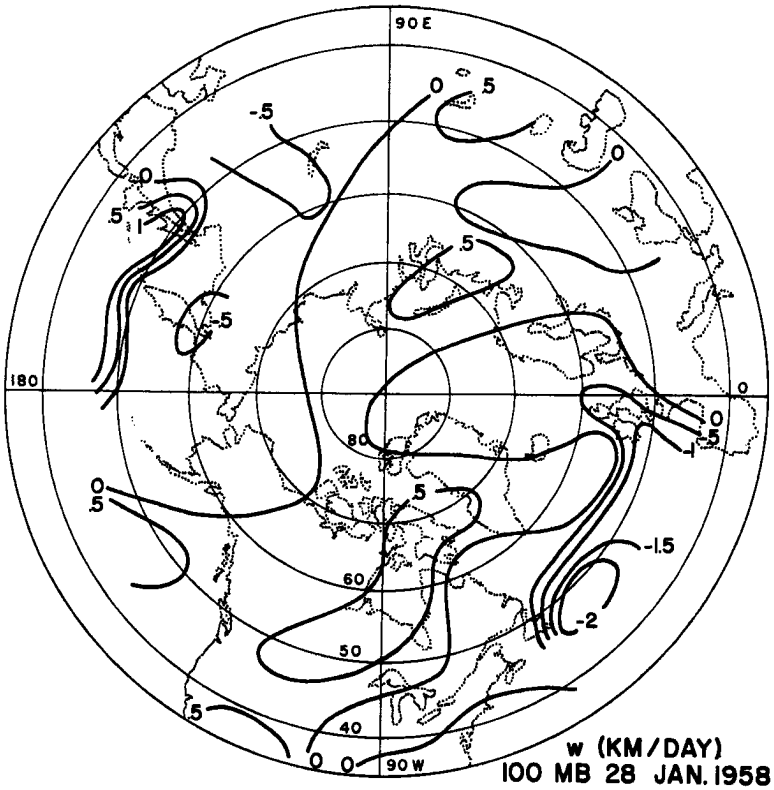

w (KM/DAY)
100 MB 28 JAN. 1958

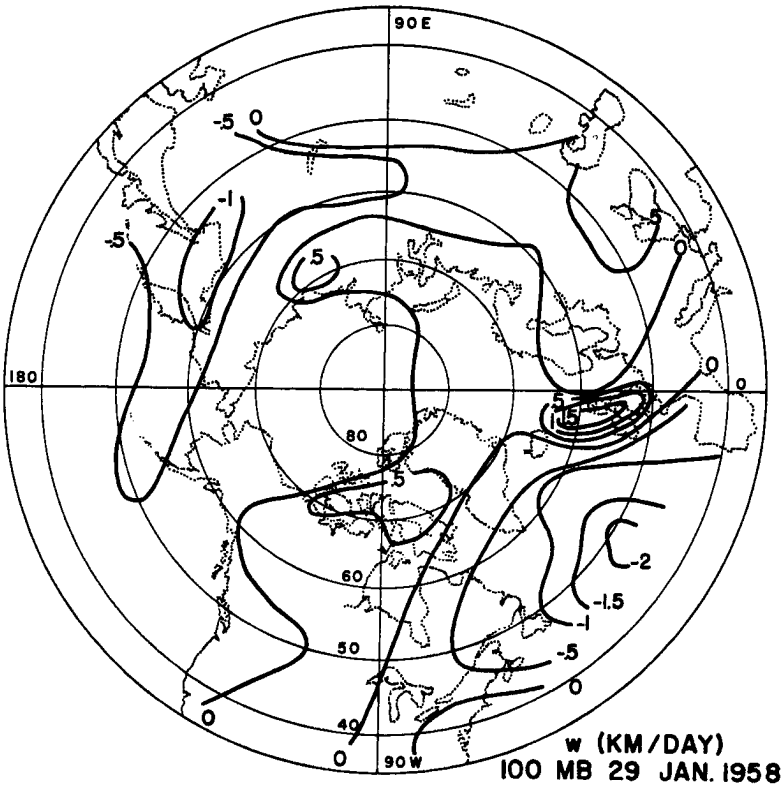

w (KM/DAY)
100 MB 29 JAN. 1958

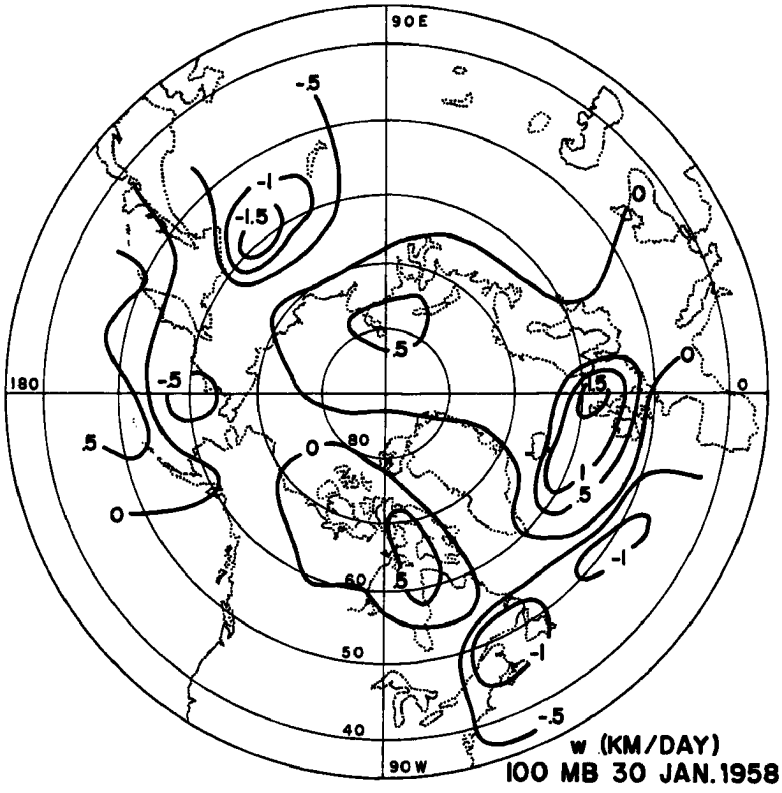

w (KM/DAY)
100 MB 30 JAN. 1958

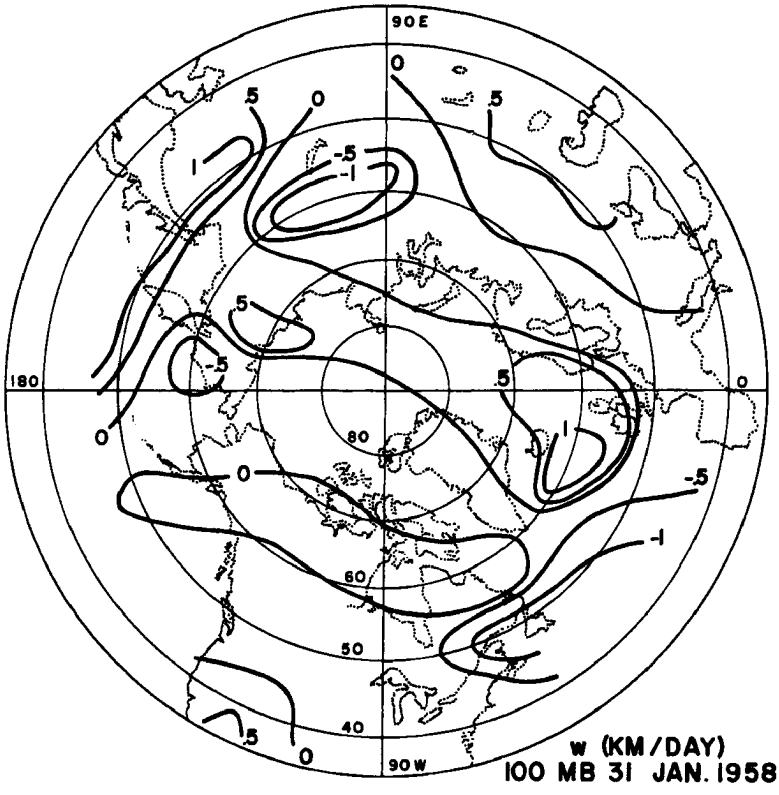

w (KM/DAY)
100 MB 31 JAN. 1958

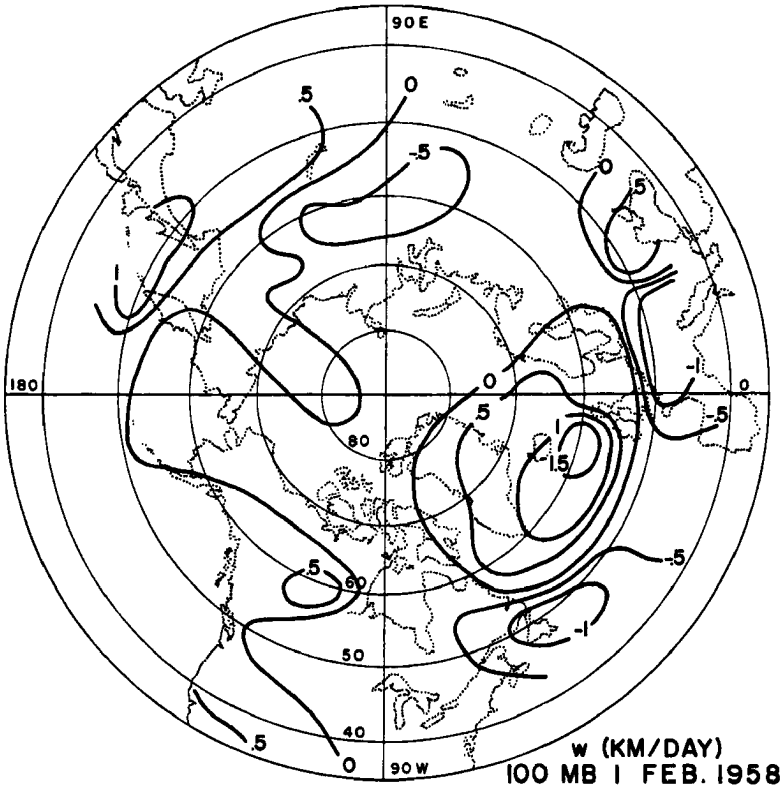

w (KM/DAY)
100 MB 1 FEB. 1958

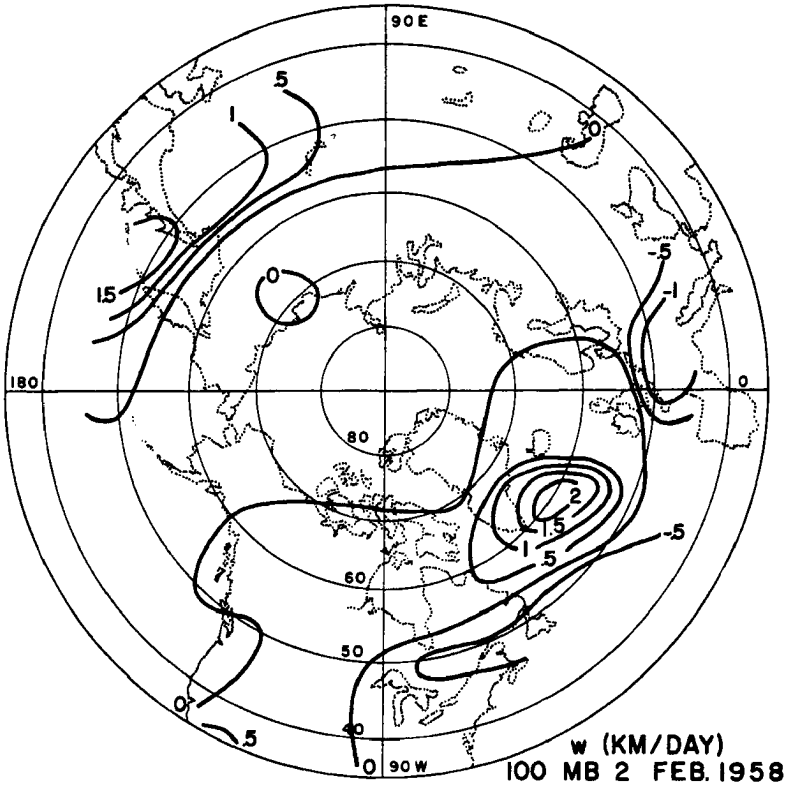

w (KM/DAY)
100 MB 2 FEB. 1958

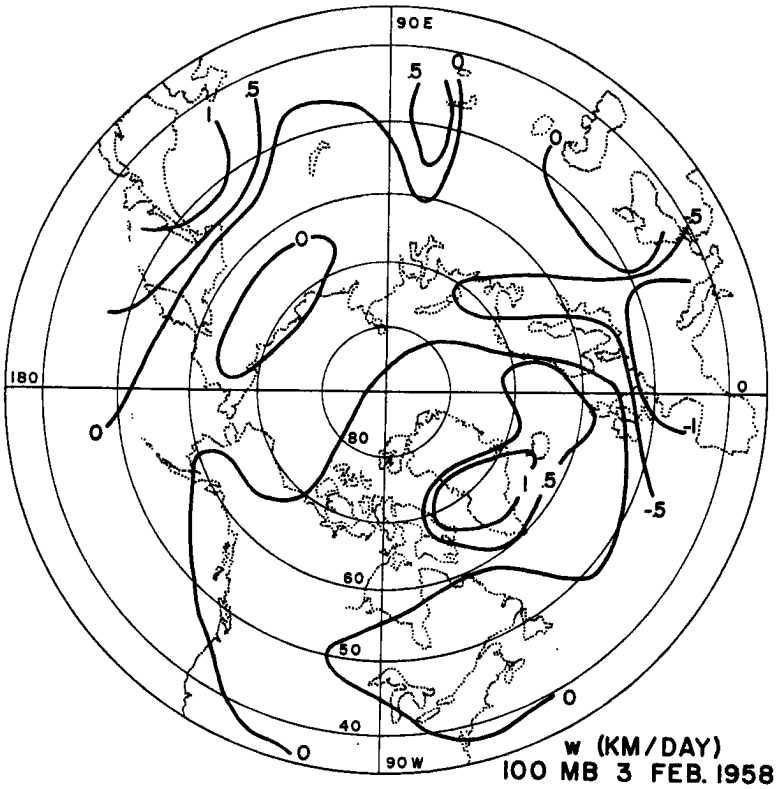

w (KM/DAY)
100 MB 3 FEB. 1958

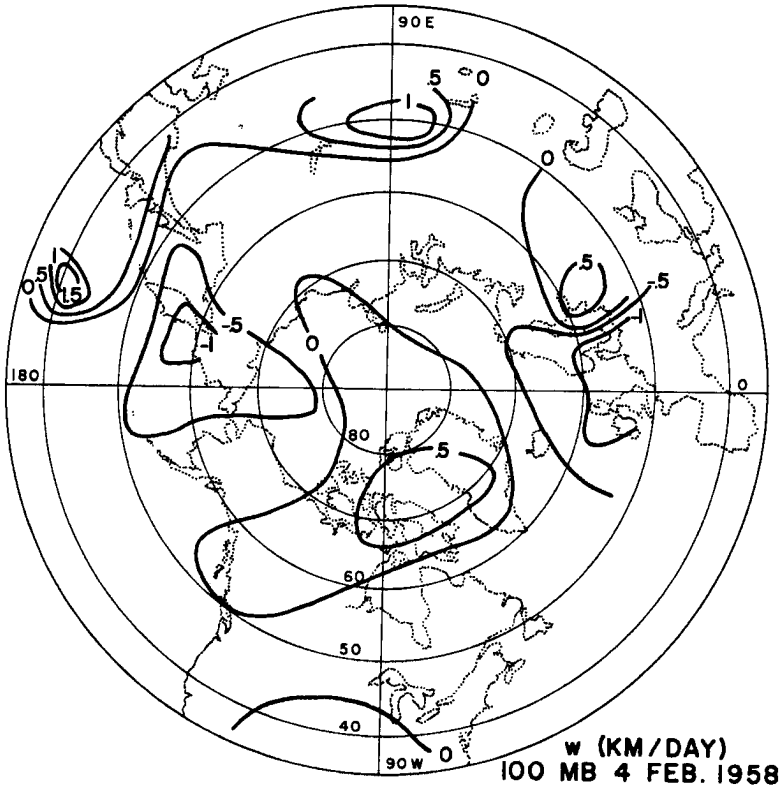

w (KM/DAY)
100 MB 4 FEB. 1958

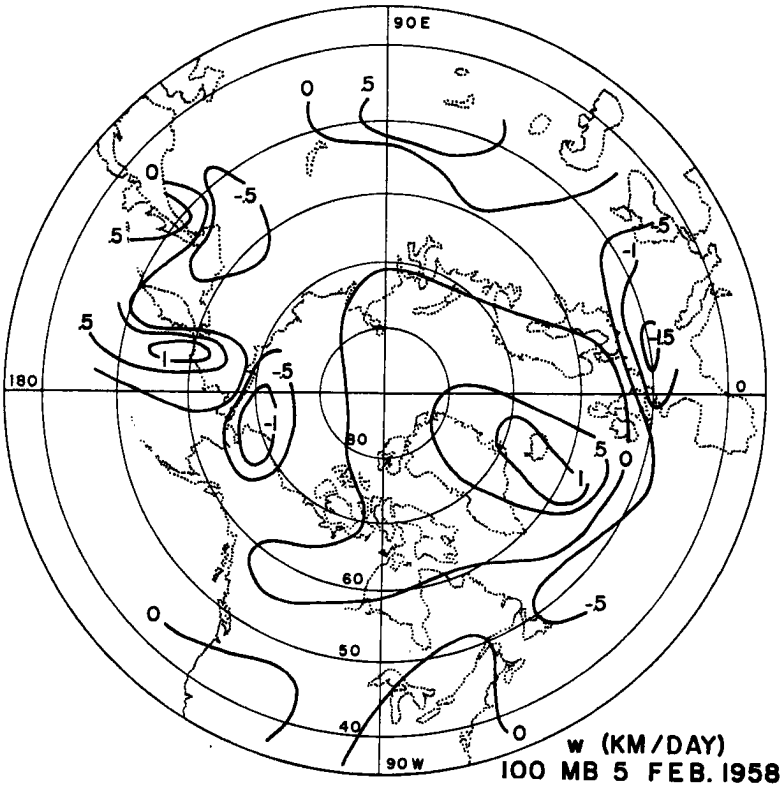
90E
180
0
80
60
50
40
90W
0
.5
-.5
-1
-1.5
1
w (KM/DAY)
100 MB 5 FEB. 1958

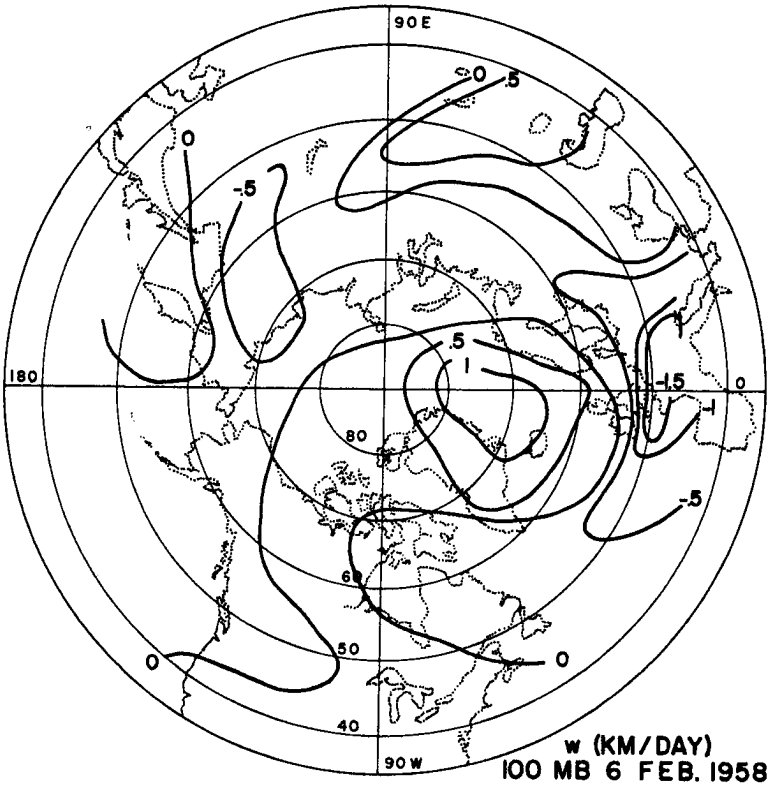
90E
180
0
80
60
50
40
90W
0
.5
-.5
-1
-1.5
1
w (KM/DAY)
100 MB 6 FEB. 1958

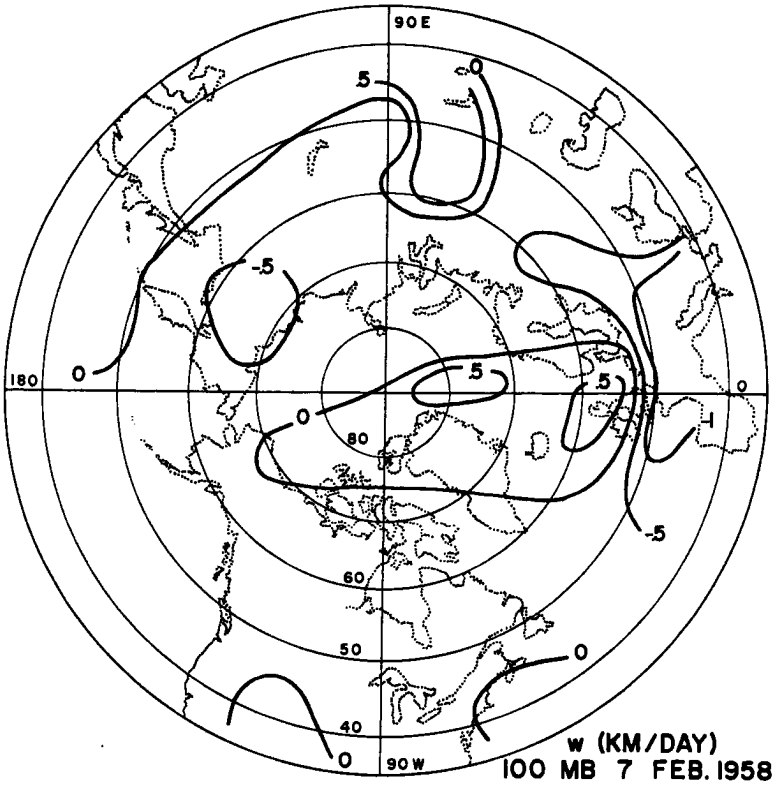
90E
180
0
80
60
50
40
90W
5
-5
0
w (KM/DAY)
100 MB 7 FEB. 1958

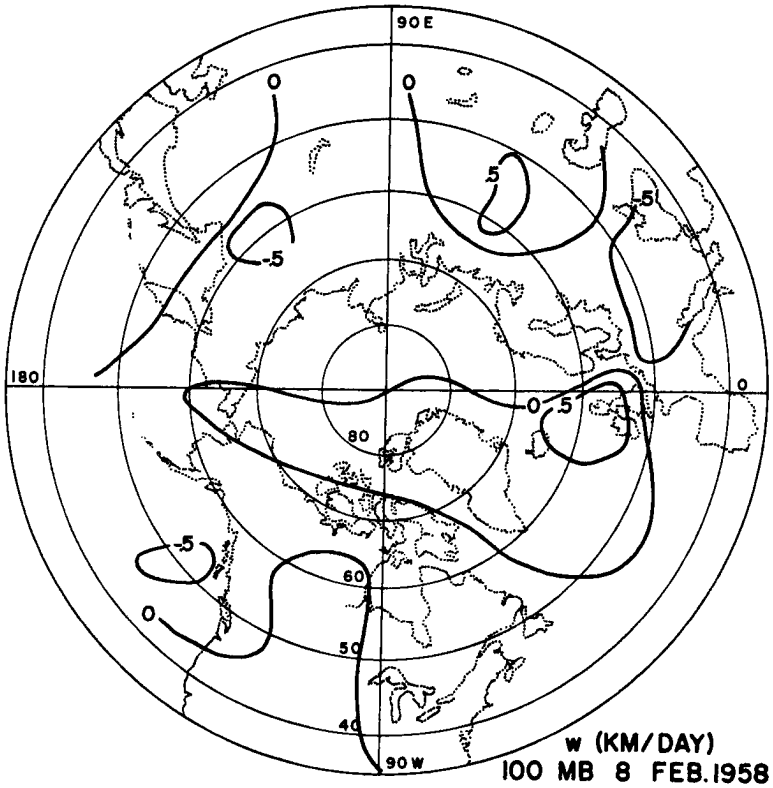
90E
180
0
80
60
50
40
90W
5
-5
0
w (KM/DAY)
100 MB 8 FEB. 1958

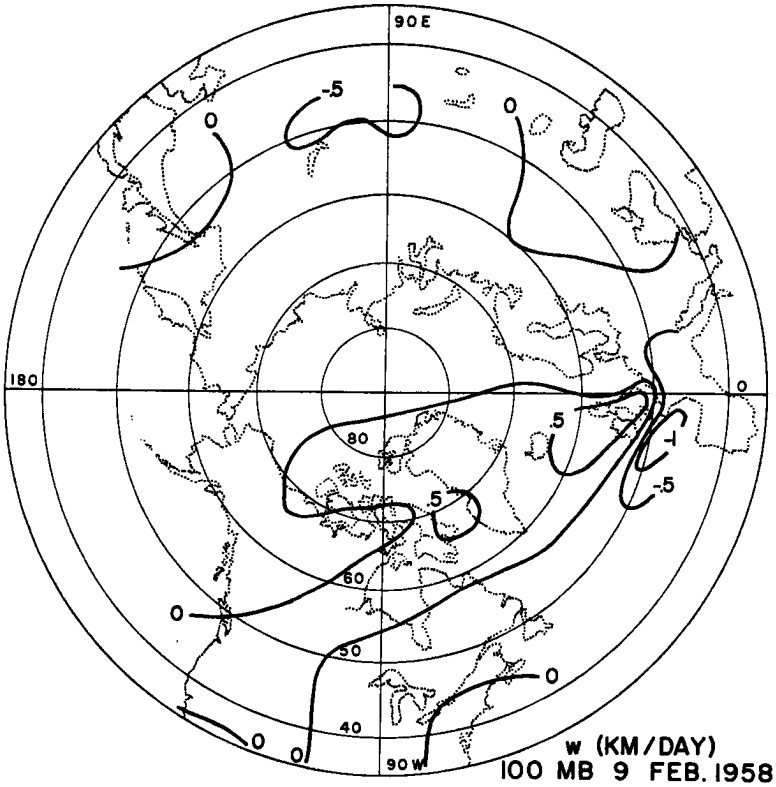

w (KM/DAY)
100 MB 9 FEB. 1958

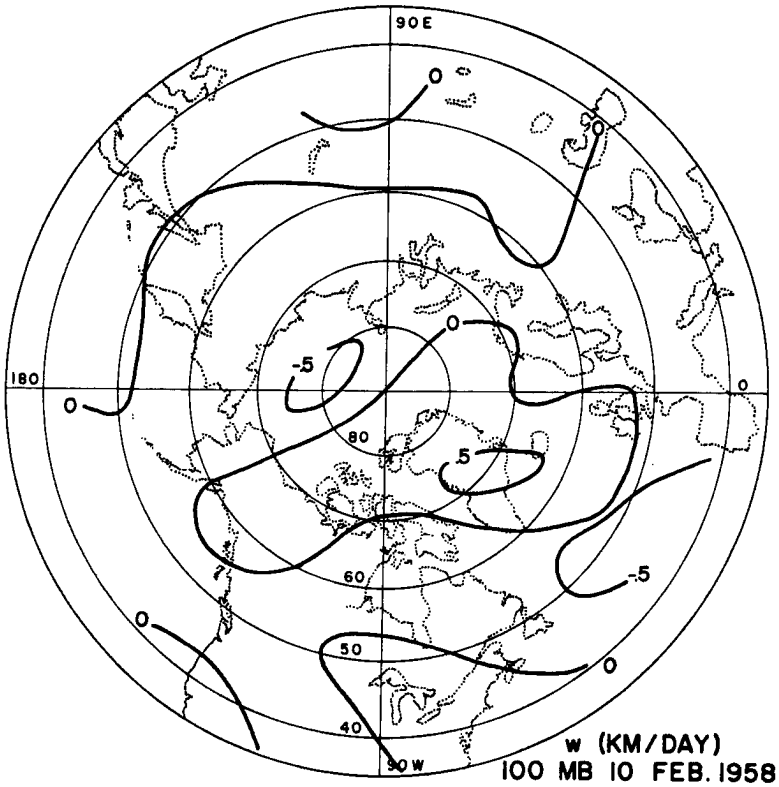

w (KM/DAY)
100 MB 10 FEB. 1958

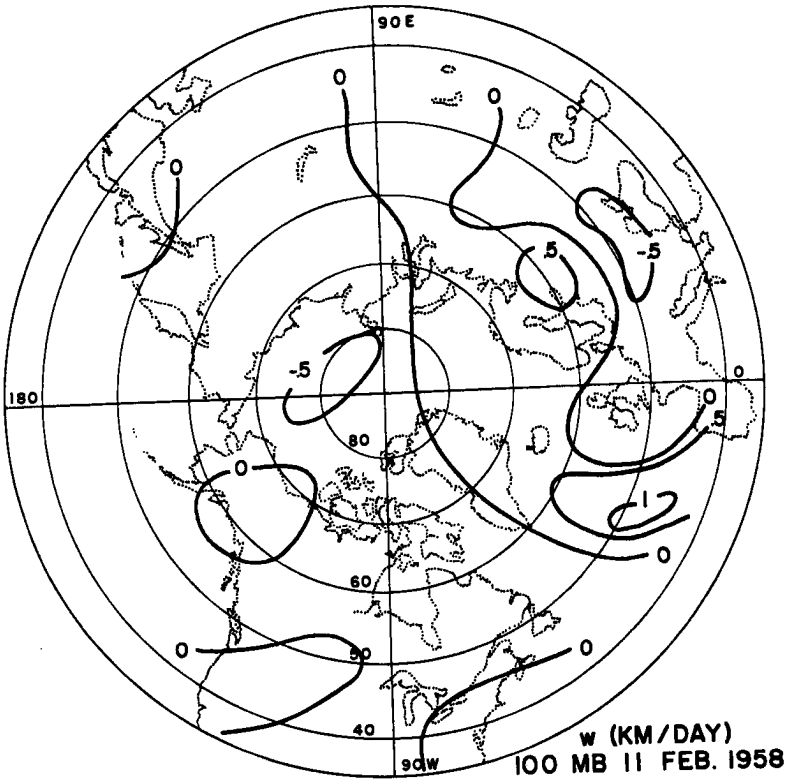

w (KM/DAY)
100 MB 11 FEB. 1958

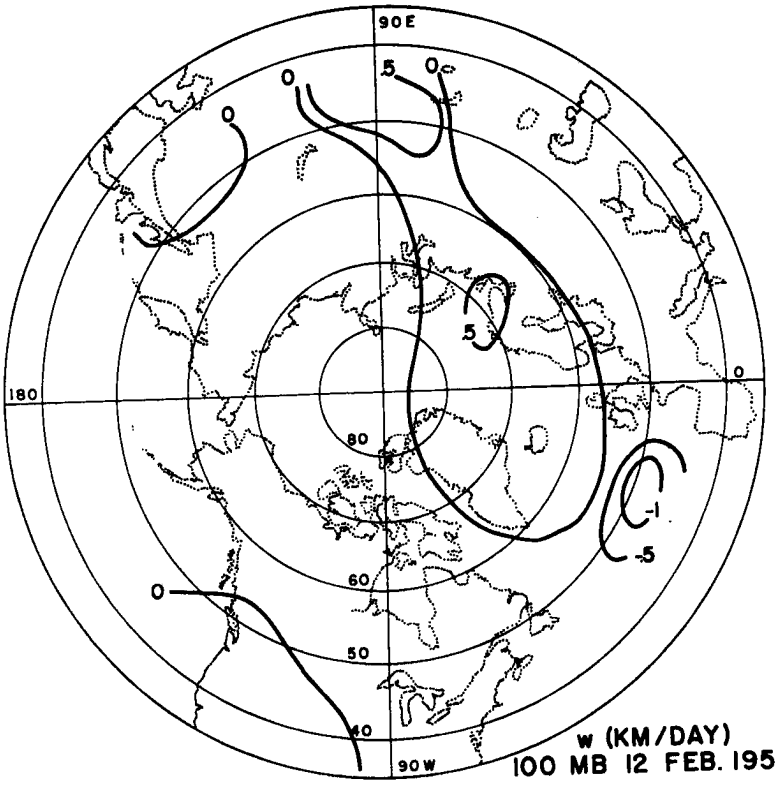

w (KM/DAY)
100 MB 12 FEB. 1958

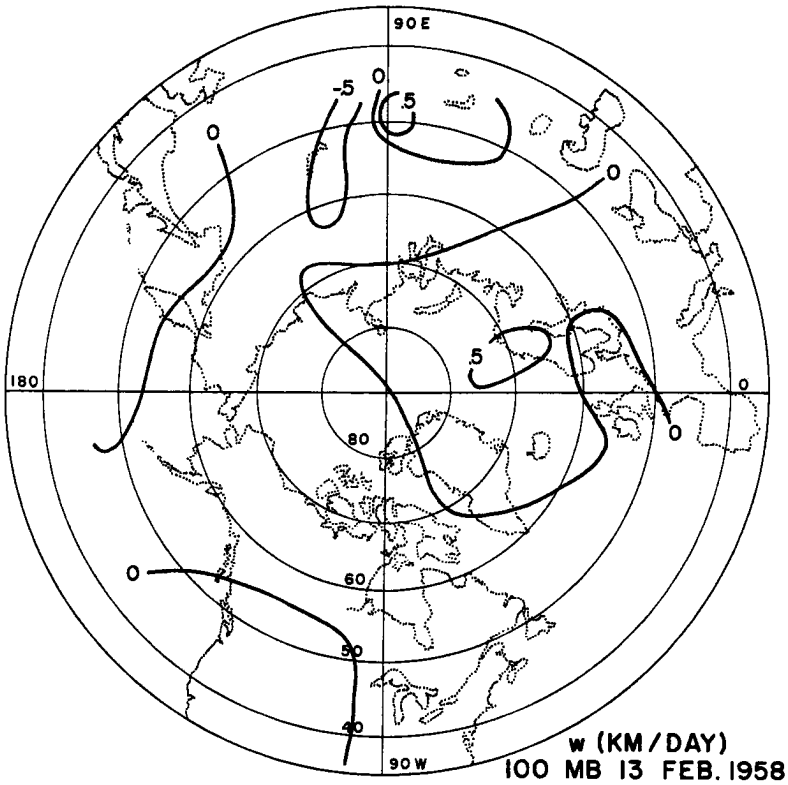
90E
180
0
80
60
50
40
90W
-5
0
.5
0
0
.5
0
0
w (KM/DAY)
100 MB 13 FEB. 1958

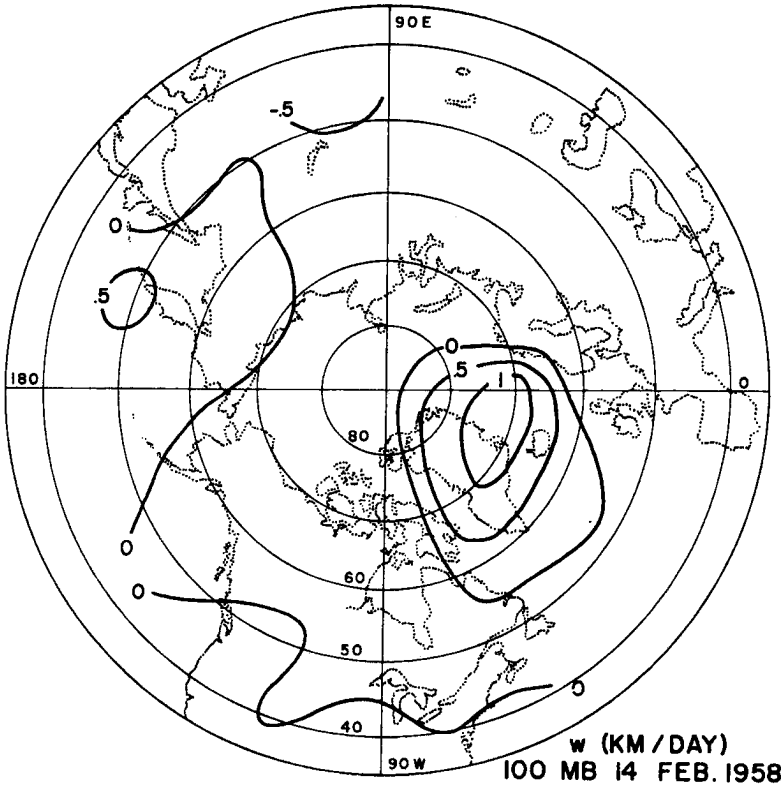
90E
180
0
80
60
50
40
90W
-5
0
.5
0
0
.5
1
0
0
0
w (KM/DAY)
100 MB 14 FEB. 1958

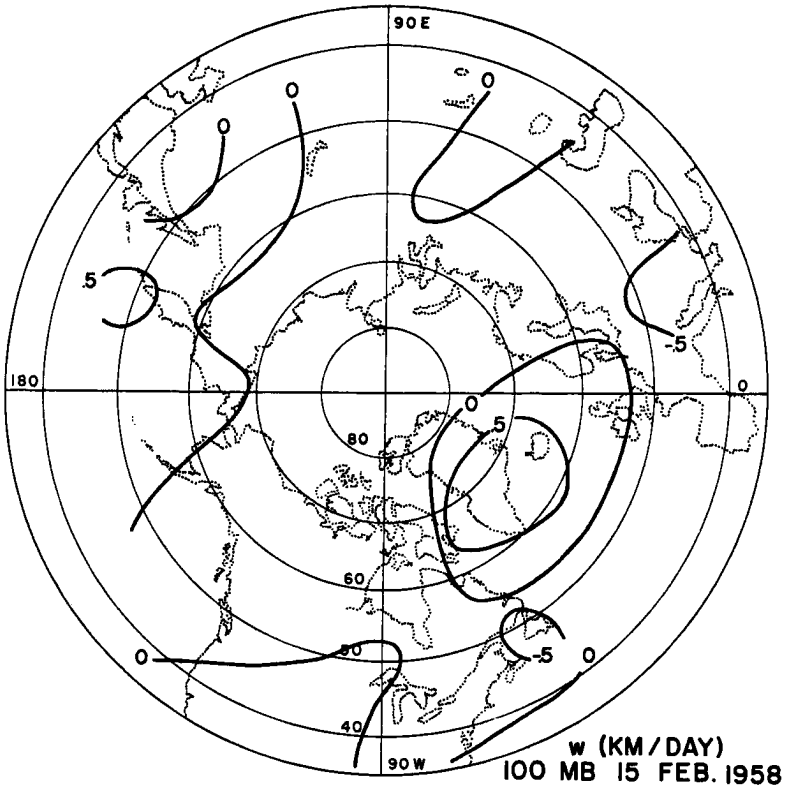

w (KM/DAY)
100 MB 15 FEB. 1958

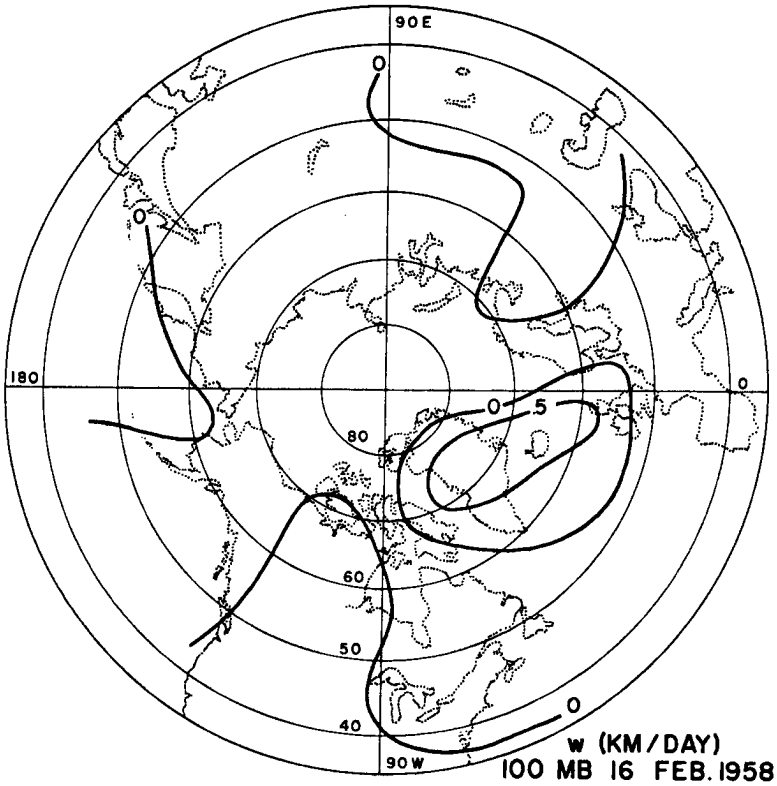

w (KM/DAY)
100 MB 16 FEB. 1958

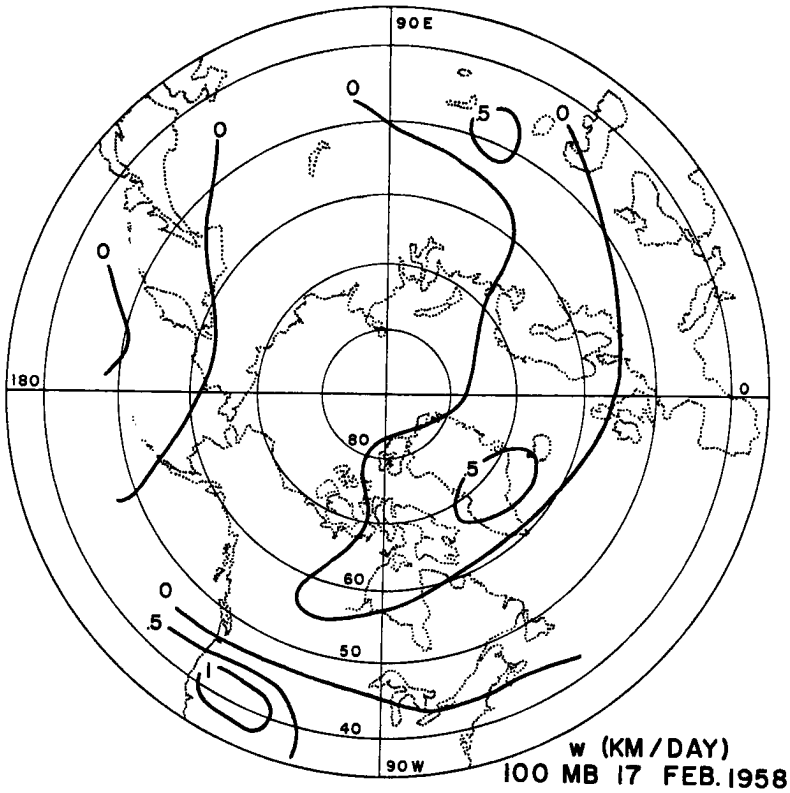

w (KM/DAY)
100 MB 17 FEB. 1958

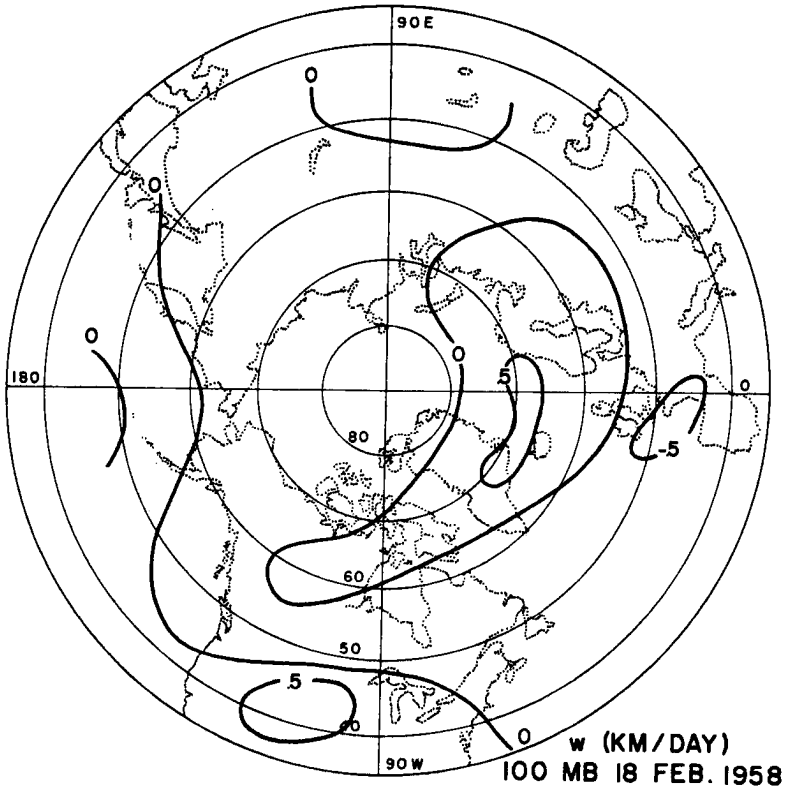

w (KM/DAY)
100 MB 18 FEB. 1958

ATMOSPHERIC SCIENCE PAPERS

(Beginning May 1966)

(Previous Numbers Refer to "Atmospheric Science Technical Papers")

101. On the Mechanics and Thermodynamics of a Low-Level Wave on the Easterlies by Russell Elsberry. Report prepared with support under Grant No. WBG-61, Environmental Science Services Administration. May 1966.

102. An Appraisal of TIROS III Radiation Data for Southeast Asia by U. Radok. Report prepared with support under Grant No. WBG-61, Environmental Science Services Administration. August 1966.

103. Atmospheric General Circulation and Transport of Radioactive Debris by J. D. Mahlman. Report prepared with support under Contract No. AT(11-1)-1340, U. S. Atomic Energy Commission. September 1966.